Can the whole life cost of railway track be reduced through the effective management of tangential wheel-rail loading?

Thesis submitted to the University of London for the degree of Doctor of Philosophy and for the Diploma of Imperial College

Gareth James Tucker

March 2009

Abstract

Railway vehicles running along rail tracks generate significant stresses and strains at the wheel-rail contact patch. These high stresses and strains cause degradation of the wheel and rail. In fact every passing of a rail vehicle is an irreversible event. Provision of railway track makes up approximately 20% of the annual cost of British mainline railways. In order to create a more cost efficient railway, and reduce the heavy reliance on government subsidy (currently £6 billion pa, 2006/2007 figures) it is necessary to identify areas where cost reductions can be achieved.

This research investigates the possibility of reducing the whole life cost of railway track through the effective management of tangential wheel-rail loading. This can be achieved by improving the 'track friendliness' of trains, possibly through the use of 'steering bogies' which can reduce tangential wheel-rail loading through curves.

To put this research into context the thesis begins with an introduction to the vehicle-track system, along with the loading environment and the causes of wheel-rail loading. How wheel-rail loading damages the track is reviewed, along with the cost of that damage in terms of maintenance and renewals, and methods of estimating that cost. Methods of modifying train design to reduce track damage (and therefore cost) are reviewed before a selection of three types of steering bogie are identified for further analysis.

The three types of steering bogie investigated are: active, 'cross braced' and 'hardening spring'. The loading caused by these bogies over a variety of track types is studied using a vehicle-track interaction simulator, looking at mainline, cross country and metro routes. Short test routes are created to represent the different route types. All types of bogie achieved load reductions over smooth, design case tracks, with better saving on the more curvaceous routes. However when taking into account track roughness the total load savings where reduced and the hardening spring bogie actually increased total track loading.

Further analysis calculates the cost savings achievable with steering bogies. Over a curvy cross country route, the cost of track maintenance and renewals can be reduced by 35 % as a result of using actively steered bogies. However, over a straighter mainline route, cost savings are negligible.

Acknowledgements

I would like to thank my supervisor Professor Roderick Smith, for giving me the opportunity to carry out this research work and for supporting me during my time at Imperial. I would also like to thank Robin Sharp from the Department of Electrical and Electronic Engineering at Imperial for kindly proof reading this thesis and giving helpful advice along the way.

I would also like to thank all of my colleagues at the Future Railway Research Centre who have given their support and encouragement through out my time with the centre, and helped make the PhD process considerably more interesting and fulfilling.

Thank you also to the Rail Safety and Standards Board, Serco Assurance, Delta Rail, Network Rail and Tubelines Ltd, for providing the necessary information, software and technical assistance to help make this research possible.

Table of Contents

Table of Figures

Nomenclature, glossary and common abbreviations

a – Major semi axis (of an ellipse)

Angle of attack – Yaw angle between a wheel and a tangent to the rail at that point

b – minor semi axis (of an ellipse)

Bogie – Rail vehicle structural component containing two or more wheelsets

BR – British Rail

DB – German railway operator (Deutsche Bahn)

Cant – (or superelevation) Difference in height between the two rails which is applied through curves

CWR – Continuously welded rail

DB – German railway operator (Deutsche Bahn)

da/dN – Extension of a crack per loading cycle (in mm)

DOT – Direction of Travel

DMU – Diesel Multiple Unit

EMU – Electric Multiple Unit

F_x – Longitudinal wheel-rail loading

F_y – Lateral wheel-rail loading

F_z – Vertical wheel-rail loading

Gauge – Lateral distance between the inside faces of the two running rails

ICE – German Inter City Express

JR Central and JR East – Japanese regional railway companies

K – Stress intensity factor

Maglev – Magnetic Levitation Vehicle

MGT – Mega gross tonnes

MGT pa – Mega gross tonnes per annum (a unit of traffic density)

N – Normal contact load

Network Rail – UK rail infrastructure owner

NMT – New measurement train

P_0 – Peak vertical stress at the centre of a wheel-rail contact area

P1 – High frequency vertical dynamic load

P2 – Low frequency vertical dynamic load

Permanent Way – Railway track including rails, chairs, sleepers, ballast and subgrade

RCF – Rolling contact fatigue

Rolling Stock – Whole or part of a rail vehicle

RSSB – Railway Safety & Standards Board

SNCF – French national railway company (Société Nationale des Chemins de fer Français)

T – Tangential wheel-rail load (i.e. the combination of F_x and F_y)

TAC – Track access charge

TGV – French High Speed Railway Operators (Train à Grande Vitesse)

TOC – Train operating company

TSI – Technical Specification for Interoperability (for the proposed trans-European high speed network)

T SPA - Track Strategic Planning Application

TU – Transport unit (1 passenger km, or 1 freight tonne km)

UIC – International Union of Railway (Union Internationale des Chemins des Fer)

VTISM - Vehicle Track Interaction Strategic Model (a costing tool owned and licensed by RSSB)

WLRM – Whole Life Rail Model (a model created by RSSB to predict rail wear and fatigue)

WSAC – Weighted System Average Cost (model)

Unsprung Mass – Total weight of all vehicle components that are positioned underneath the lowest suspension element

γ – Creep ratio (i.e. relative wheel rotational speed compared to vehicle speed)

μ – Coefficient of friction

σ – Normal stress

τ – Sheer stress

Chapter 1 : Introduction

1.1 Background

The passing of every rail vehicle has an irreversible effect on the 'permanent way'. The loading generated as a rail vehicle travels along the track causes a variety of degradation modes, including: wear, fatigue, and ballast settlement. Over time these degradation modes develop, and it becomes necessary for the infrastructure manager to intervene with maintenance and renewal activities.

In the 2006/07 financial year the total cost of the UK mainline railway system was in the order of £9 billion per annum[1-3]; £6 billion of this was provided as a government subsidy[1]. This is not a sustainable situation. In order to improve the cost effectiveness of the railway system it is important to identify areas where costs can be reduced. The maintenance and renewal of railway track contributes 21%[4] towards the total expenditure on the UK railways. There is significant opportunity to reduce this cost, by improving the interaction between trains and track.

Track costs can be reduced by improving the efficiency of maintenance activities or through the introduction of technology changes to reduce the damage caused by train-track interaction. If more 'track-friendly' trains can be introduced, this will reduce the rate of track damage, extending track life and reducing maintenance requirement.

1.2 The wheel-rail interface

The key to the success of railways as a mode of transport is the small, extremely stiff contact patch* between the wheel and rail. This small, stiff contact provides a very efficient method of transmitting tractive effort from the wheel to the rail, because very little energy is used in deforming the contact area. This means that

* A wheel-rail contact area can be as small as 1 cm^2 [5], with a vertical linear contact stiffness of 758 MN/m[6]; in comparison one tyre/road contact area on a typical passenger bus is 340 cm^2 [7] with a vertical linear contact stiffness of 1.2 kN/m[8].

high loads can be moved with a comparatively small tractive effort*. However, because of this small contact patch and heavy loading, high stresses and strains are developed at the wheel-rail interface.

As trains become faster, heavier, or more frequent, the track damage rate is increased along with the consequential maintenance and renewal costs.

Railway operators are starting to push towards the physical limits of the steel wheel on steel rail system. In 1991 Tatsuhiko Suga[10] predicted that the maximum speed possible, using conventional, steel wheel on steel rail trains is '*somewhere upward of 500 kph*'. There are already trains in Japan and France that are regularly running up to 300 kph in operational service. JR East are now developing a 360 kph train to be used in operational service on the new Hachinohe – Aomori line, planned to be ready by 2010[11]. In April 2007 SNCF achieved a new train speed record of 575 kph with a modified version of their TGV POS train, which is significantly higher than the theoretical maximum predicted by Suga in 1991. Other trains achieving very high speeds in recent times are: the JR East STAR 21 (425 kph, 1991); JR Central 300X (443 kph, 1996); and the SNCF TGV Atlantique (515 kph, 1990). All of these records were achieved with specially modified trains, running on specially prepared track; not running under service conditions.

The physical limit at which a train can still accelerate is dependent on the friction available at the wheel-rail interface and consequently the tractive force that can be transmitted to the rails. When this force is equal to the total train resistance, it is not possible to accelerate any further. The technology is already available to achieve very high speeds, as demonstrated by the train speed records mentioned above. After the SNCF TGV Atlantique achieved a new speed record in 1990, the head of TGV research, Francois Lacote remarked, *'It is one thing to know the limits of brand new equipment, but quite another to make it last 35 years with acceptable maintenance costs'*[12]. When attempting to run a faster train service,

---

* The wheel on rail contact gives a rolling resistance one fifth that of a tyre on road carrying the same load[9].

a speed is reached at which the maintenance cost for wheels and track will become so high, it will be financially unfeasible to run a regular service any quicker.

If more 'track-friendly' trains can be produced, high speed train operation can become more economical. Improving the 'track friendliness' of trains is becoming increasingly important on all railways (not just high speed rail), as higher frequencies of traffic* and heavier axle loads† are being introduced, particularly in the UK and mainland Europe.

The cost savings achievable through the use of more 'track-friendly' trains can be used to allow for improvements in train performance, in terms of: speed, density and carrying capacity, without increasing the track maintenance requirement; or to lower the cost of an existing service. This second option is perhaps more relevant to the UK market, as a method of reducing the current dependence on heavy government subsidy.

1.3 An ongoing problem

Since 1804 when the first steam railway began service in the Penydarren iron works, engineers have been struggling to minimise the damage caused by trains on the track. Early railways used cast iron track which was very brittle and prone to fatigue cracking. It was very expensive and inconvenient to be constantly maintaining the track, and the ongoing problem of rails breaking underneath the trains did not help inspire public confidence in the new technology‡. Before railways could be a large scale financially viable operation, it was necessary to solve this problem. Rail life was dramatically increased through the introduction of wrought iron rails in the 1820s[13]. This move was championed by George Stephenson, of whom it has been said that *'his rise to prominence was because he*

* In the UK timetabled train kilometres have increased from 376.3 million in 1997/98 to 463.5 in the 2006/07 financial year, an increase of 23 %[14].

† Train mass has risen by 20 – 40 % over the last 15 years, in part due to the widespread introduction of air-conditioning, increased requirements for structural crashworthiness and disabled access requirements[14].

‡ The public demonstration of Trevithick's 'Catch Me Who Can' locomotive in 1808 had continual problems with rails breaking under the train, often resulting in a derailment[15, 16].

understood better than his contemporaries the importance of track and vehicle technology advancing together'[13]. In modern terms we would say that he took a Systems Engineering approach.

Another significant improvement to the 'track friendliness' of rail vehicles achieved in the early years was the widespread adoption of the fixed axle, conical wheelset in the 1830s. Providing the axle's design allows sufficient lateral movement relative to the rail, this type of axle generates a rolling radius difference between two opposing wheels during curving. This difference in radii causes the axle to steer through curves with a significantly lower track loading than simple cylindrical wheels. This type of axle is now the standard on the majority of trains worldwide*.

These two early developments in railway technology demonstrate two alternative methods of reducing track maintenance requirement:

a) increase the durability of the track
b) improve the 'track friendliness' of the train

Both of these methods have been employed throughout the subsequent development of the railway system. Recent examples are:

a) the introduction of slab track, which is more durable than conventional ballasted track.
b) attempts to reduce vertical dynamic loading on the track by reducing the unsprung mass (the mass of all components below the primary suspension) of railway vehicles.

1.4 The next steps

The steel wheel on steel rail system is not the only option for ground based guided way transport. Many of the problems experienced by conventional railways may be overcome by removing the steel wheel on steel rail contact. This can be achieved using some form of levitating vehicle. There is already a commercially

* The conical axle wheelset is discussed further in section 2.3.3

operated Magnetic Levitation Vehicle (Maglev) running between the Pudong Airport and downtown Shanghai[17].

However, as conventional rail is so well established it appears highly unlikely that there will be a large scale move to Maglev in the near future. New Maglev trains can not interchange with existing track; requiring a high initial investment in new maglev tracks and also station infrastructure. Significant improvements can be made to the railway system by continuing to improve and optimise the steel wheel on steel rail system.

Over the past 30 years, significant research effort has gone into highlighting the damaging effects of vertical dynamic loading (wheel-rail loading is discussed further in Chapter 2) on the track, and methods of reducing those loads. The benefits of reducing vertical loading are already well documented[18-23]. Significant tangential rail loads are developed during curving and the benefits of reducing these loads are now also being recognised. A tangential load of 40 kN* can be generated at the high wheel of the front axle of a 'Class 91' locomotive travelling through a 600 m curve radius[24]. This loading will be higher for tighter radius curves, and can also vary depending on the characteristics of the vehicle (Track loading caused by various types of vehicle is shown in Chapter 7). Tangential loading is known to contribute strongly to the development of fatigue cracking and wear of rails [15, 25-27]. Existing research has proposed the use of various 'steering bogies' to reduce tangential rail loading through curves[28-31]. However, the rail industry has been slow to take up these proposals, possibly in part because no studies have been published that link the achievable loading reductions to a financial benefit for the railway operators.

1.5 Aims and objectives of this research

The purpose of this research is to investigate the financial benefits of reducing track loading through the introduction of 'steering bogies'.
This has been achieved by:

* Compared to the nominal vertical load of 105 kN per wheel, the effects of vertical and tangential track loading are discussed further in Chapters 2 and 3.

- Conducting a review of existing research into vehicle-track interaction, and the modelling of track damage.
- Predicting the reductions in track loading that can be achieved through the use of 'steering bogies' on a variety of railway types in the UK, including; intercity, cross country and suburban/metro.
- Linking these loading reductions to a decrease in track damage and the consequent savings in maintenance and renewals cost.

1.6 Discussion of thesis content

This thesis contains nine chapters that discuss the need for an investigation of this type, look at a variety of solutions, then discuss the study of 'steering bogies' carried out and the subsequent cost benefits analysis, and, finally, review the results.

Chapter 2: The vehicle-track system describes the vehicle-track system and the track loading environment. The purpose of this is to give a background to the area, and to present the need for work in the specific area of investigation.

Chapter 3: Track degradation goes on to examine the various track degradation modes and the factors affecting them. An overall review of track damage is introduced, followed by a further discussion of the degradation modes most relevant to this research.

Chapter 4: Maintenance and renewals spending looks at the maintenance and renewals activities on the UK railways. Areas covered include the cost of these activities and how they fit into the overall spending on railways. This is currently not an extensively researched area; the available information is presented and reviewed here. A brief international comparison is also included.

Chapter 5: Existing degradation and costing models reviews existing degradation models, their methods and inputs used, and suitability for use as part of a larger costing model that can be used to assess the effects of introducing new

technologies. Other costing models already developed are discussed, along with their uses and their suitability for a study of this nature.

Chapter 6: Methods of reducing track loading through train design discusses the various methods of modifying trains to improve their 'track friendliness', including existing solutions as well as current proposals. The various types of steering bogie are introduced here.

Chapter 7: Loading reductions achievable with steering bogies presents the methods used to investigate achievable loading reductions for different types of railway with various types of 'steering bogie'. The full results of all models are also presented here.

Chapter 8: Cost savings achievable with steering bogies builds on the investigation described in Chapter 7, taking the analysis to the next step to predict what cost savings can be achieved with the various types of steering bogie under investigation.

Chapter 9: Discussion and Conclusion reviews the findings of the track loading and cost saving studies, and how the proposed ideas can be applied to the rail industry. Suggested further work is also discussed.

References

1. Department for Transport, Railway Finance, http://www.dft.gov.uk/?view=Filter&h=m&m=4552&s=5196&pg=1, [Accessed, 5/5/07]
2. *Strategic Plan*. 2003, Strategic Rail Authority.
3. *Railtrack's expenditure needs 2001 - 2006*. 1999, Booz Allen & Hamilton.
4. Tucker, G. and R.A. Smith, *Examining the cost of train/track interaction*. Railway Strategies, 2007. **43**: p. 91 - 93.
5. Esveld, C., *Modern Railway Track*. 2001: MRT-Productions.
6. Remington, P. and J. Webb, *Estimation of wheel/rail interaction forces in the contact area due to roughness*. Journal of Sound and Vibration, 1996. **193**(1): p. 83 - 102.
7. Mastinu, G., et al., *A Semi-Analytical Tyre Model for Steady - and Transient - State Simulations*. Vehicle System Dynamics, 1997. **27**(Supplement): p. 2 - 21.
8. Rustighi, E. and S.J. Elliot, *Stochastic road excitation and control feasibility in a 2D linear tyre model*. Journal of Sound and Vibration, 2005. **300**(3 - 5): p. 490 - 501.
9. Hardy, D.J., *Can railways compete with roads?* Proceedings of the IMechE Part F: Journal of Rail and Rapid Transit, 1997. **211**(1): p. 1 - 10.
10. Suga, T., *How fast can a train go?* Impact of Science on Society, 1991. **162**: p. 149 - 163.
11. Higashi, T., *Rival concepts in advanced train design*. Railway Gazette International, 2004. **160**(10): p. 682 - 684.
12. Tillier, C., *The TGV world speed record*, www.trainweb.otg/tgvpages/rec-intro.html, [Accessed, 10/8/2006]
13. Bailey, M.M., *The history of tracks and trains: a lesson in joined-up thinking*. ICE Proceedings, Civil Engineering, 2005. **158**(3): p. 134-142.
14. Brown, C. and S. Cussons, Rail *Evidence and Research Strategy 2007/08*. 2007, Department for Transport, Technical and Professional Directorate.
15. Cannon, D.F., et al., *Rail defects: an overview*. Fatigue & Fracture of Engineering Materials and Structures, 2003. **26**(10): p. 865-886.
16. Burton, A., *Richard Trevithick: Giant of Steam*. 2000: Aurum Press.
17. *Shanghai maglev train*, http://en.wikipedia.org/wiki/Shanghai_Transrapid, [Accessed, 3/5/08]
18. Li, D. and E. Selig, *Wheel/track dynamic interaction: Track substructure perspective*. Vehicle System Dynamics, 1995. **24**(Supplement): p. 183 - 196.
19. Jenkins, H.H., et al., *Effect of track and vehicle parameters on wheel/rail vertical dynamic forces*. Railway Engineering Journal, 1974. **3**(1): p. 2-16.
20. Rochard, B.P. and F. Schmid, *Benefits of lower-mass trains for high speed rail operations*. ICE Proceedings, Transport, 2004. **157**(1): p. 51-64.
21. Smith, R.A., *Railway fatigue failures: an overview of a long standing problem*. Materialwissenshaft und Werkstofftechnik (Materials Science and Engineering Technology), 2005. **36**(11): p. 697 - 705.

22. Barke, D.W., *A review of the effects of out-of-round wheels on track and vehicle components*. Proceedings of the IMechE Part F, Journal of Rail and Rapid Transit, 2005. **219**(3): p. 151-175.
23. Office of the Rail Regulator, *Final Report - Railway infrastructure cost causation. R/00202*, http://www.networkrail.co.uk/browse%20documents/regulatory%20documents/access%20charges%20reviews/previous%20access%20charge%20reviews/periodic%20review%202000/consultant%20reports/railwayinfrastcostcausationfinalreportboozallennov1999.pdf, [Accessed, 1/12/07]
24. Grassie, S.L. and J.A. Elkins, *Tractive effort, curving and surface damage of rails. Part 1. Forces exerted on the rails*. Wear, 2005. **258**(7 - 8): p. 1235 - 1244.
25. Burstow, M.C. *Rolling contact fatigue crack initiation prediction methods*. in Proceedings of 7th International Conference on Engineering Structural Integrity Assessment. 2004. Manchester. p. 385 - 393
26. Watson, A.S., *Whole life rail model: Initial investigations into traffic pattern effects*, AEATR-T&S-2002-038. 2002, AEA Technology.
27. Franklin, F.J. and A. Kapoor, *Modelling wear and crack initiation in rails*. Proceedings of the IMechE Part F: Journal of Rail and Rapid Transit, 2007. **221**(1): p. 23 - 33.
28. Brickle, B.V., *Railway Vehicle Dynamics*. Physics Technology, 1986. **17**(4): p. 181 - 186.
29. Mei, T.X. and R.M. Goodall, *Recent development in active steering of railway vehicles*. Vehicle System Dynamics, 2003. **39**(6): p. 415 - 436.
30. Scheffel, H., *Self-steering wheelsets will reduce wear and permit higher speeds*. Railway Gazette International, 1976. **132**(1): p. 453 - 456.
31. Okamoto, I., *Railway technology today 5: How bogies work*. Japan Railway & Transport Review, 1998. **18**: p. 52 - 61.

Chapter 2: The vehicle-track system

In order to provide a background to this research, this chapter introduces the vehicle-track system and the complex interaction at the wheel-rail interface. The various subsystems are discussed along with the loading generated between the wheel and rail.

The vehicle-track system can be represented as a series of masses, springs and dampers (see Figure 2 - 1 for a general schematic). There are various inputs to this system, such as the surface roughness experienced at the wheel-rail interface, route curvature and gradient, along with passengers boarding and disembarking from the train (or the loading and unloading of freight). Depending on the design and condition of the vehicle and track, the system will respond to these inputs in a variety of manners. Any loads passing between the vehicle and track must be transmitted through the small contact area* at the wheel-rail interface.

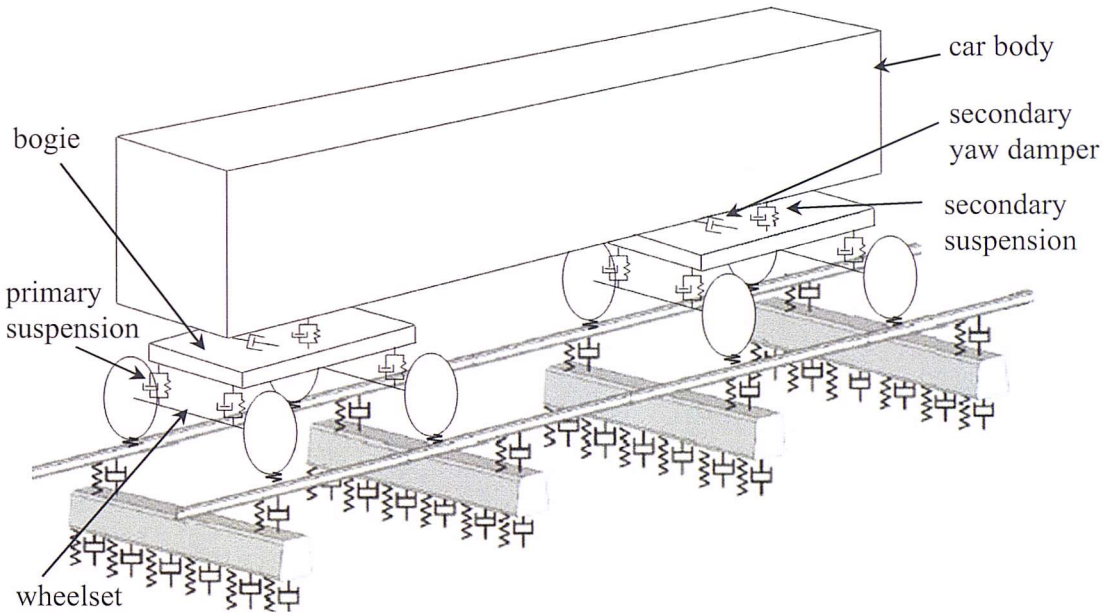

Figure 2 - 1 A mass, spring, damper schematic representing the vehicle-track system

2.1 A typical passenger train

A typical rail car (including locomotives, trailers and multiple unit cars) has four axles which are paired into bogies (or trucks). The two axles per bogie are

* As mentioned in section 1.2 the contact area between a railway wheel and rail can be as small as 1 cm^2.

attached through a primary suspension, the bogies in turn support the car body through a secondary suspension. The primary and secondary suspensions act not only in the vertical direction but also contain stiffness and damping in the longitudinal and lateral directions.

Bogies were first used in a locomotive manufactured by Jervis and Allen in 1832[1, 2], they were originally developed to improve curving performance. Curving is improved because bogies can rotate relative to the car body in order to follow the track curvature (curving is discussed further in section 2.3.3).

After the initial developments a variety of other benefits were discovered which have led to the current widespread use of the bogie arrangement for passenger vehicles. Vertical dynamics can also be improved through the use of a bogie, as shown in Figure 2 - 2; the geometry means the effect of any bumps (or dips) in the rail can be significantly reduced. With a two axle bogie, only half of the change in height due to a bump in the rail is passed on to the secondary suspension.

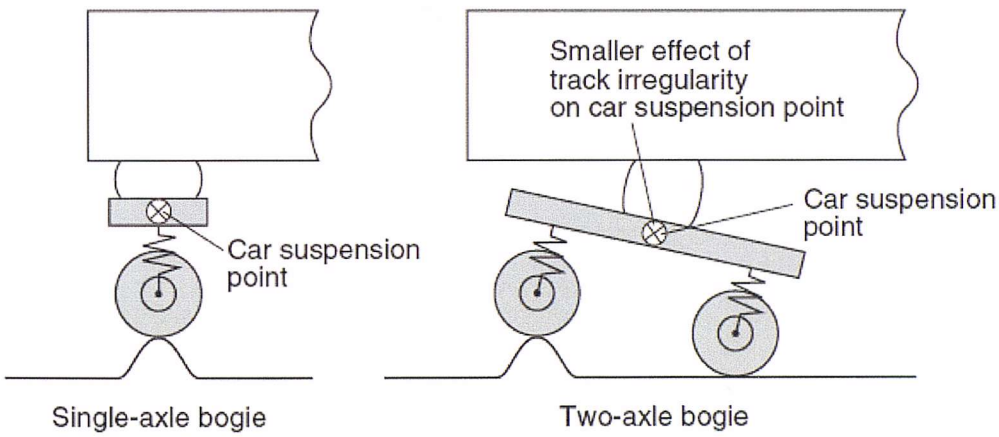

Figure 2 - 2 The use of bogie geometry to filter out effects of bumps in the rail[3]

The two stage suspension also has an isolation effect. Any vertical movement of the wheels will result in damped vibration of the bogie frame, which when damped again by the second suspension stage, results in a much reduced input to the car body. When a well designed train negotiates an uneven section of track, the car body height remains virtually constant, whilst the bogie oscillates up and down in response to track irregularities. The amount of force and movement

transmitted to the car body due to periodic track inputs is largely dependent on: the relative stiffnesses of the two suspension stages (and hence their comparative natural frequencies), the frequency and severity of the input from the wheel-rail interface and masses of the components involved (such as the wheels, axles, bogie frame and car body).

Forcing frequencies close to the natural frequency of the vehicle or its components result in resonant motion. Designers avoid using components that will result in resonant frequencies coinciding with common forcing frequencies. Figure 2 - 3 shows a range of possible forcing frequencies and typical component resonances.

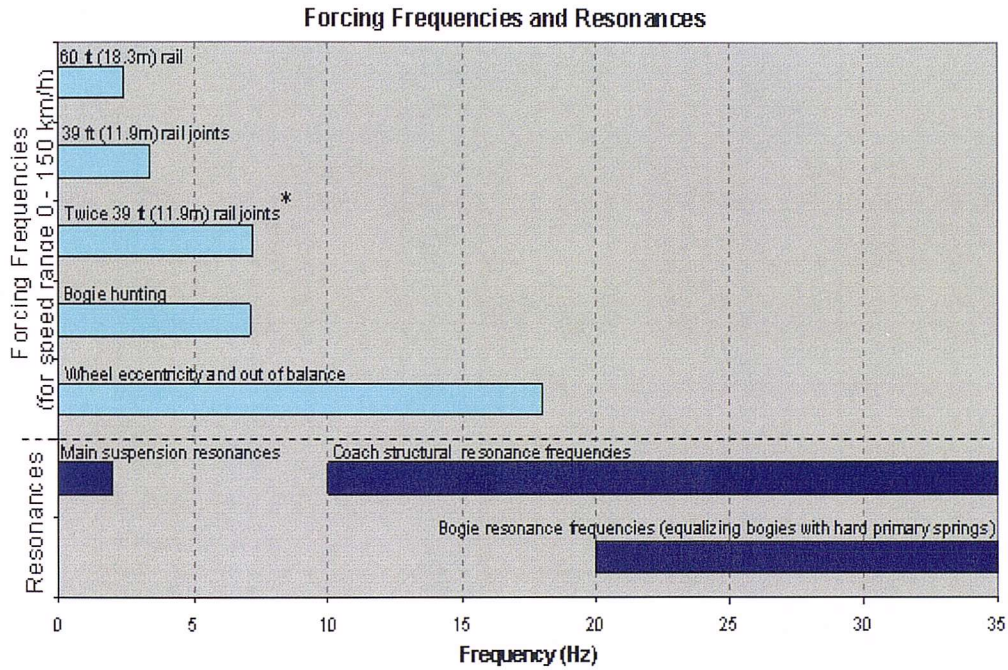

Figure 2 - 3 Forcing frequencies and resonances[4]

Rail joints are not necessarily such a problem for the current UK railways as they were 20 years ago because of the move to continuously welded rail†. However, cyclical loading due to wheel imbalance and eccentricity is still an issue. The primary suspension needs to be designed with a relatively high stiffness in order to achieve a resonant frequency high enough to avoid these cyclical inputs. The

* Twice 39 ft rail joints, means that the rail joints are staggered on each rail so the train hits a joint twice as often but only one side at a time; historically this setup has been more popular in North America rather than Europe.

† 75 % of the UK mainline network is now made up of continuously welded rail[5]

primary suspension effectively acts as a high pass filter. A much lower secondary suspension (or main suspension as it is sometime called) stiffness will result in a lower resonant frequency in the secondary suspension; this is necessary to keep the two resonances well separated to avoid instability. The secondary suspension acts as a low pass filter.

Resonant frequencies are approximated by:

Primary suspension (bogie frame vibrations): $\omega_1 = \sqrt{(k_1/m)}$ **(eqn 2 - 1)**

Secondary suspension (car body vibrations): $\omega_2 = \sqrt{(k_2/M)}$ **(eqn 2 - 2)**

Where, m = bogie mass, M = car body mass, k_1 = primary suspension stiffness, and k_2 = secondary suspension stiffness.

Thus from equation 2 - 1, a lower mass bogie will increase the resonant frequency of the bogie, moving it further away from the frequency of any likely inputs. However, reducing the mass of the car body will also increase the resonant frequency of the car body, bringing it closer to the bogie resonant frequency. This needs to be counteracted by modifying the secondary suspension stiffness accordingly. Damping must be chosen to sufficiently stabilise the system throughout the range of experienced frequencies (typical damping ratios are 0.05 for primary suspension and 0.2 for secondary suspension[4]).

2.2 Railway track

The purpose of railway track is to support and guide railway vehicles. The high pressures experienced at the wheel-rail interface must be distributed and transmitted down to the subgrade. In addition Wenty[6] suggests that, *'the function of track is to allow trains to run with the lowest possible and most uniform levels of force'*. In order to achieve this, track must be as straight as possible, and the geometry maintained to a high degree of precision.

The track is made up of a variety of components, a shown in Figure 2 – 4. Each component has its own function:

- Rails support and guide the train wheels.

- Sleepers (or ties) hold the rails at a constant gauge, and distribute the loads applied through the rails.
- The ballast distributes the loads further down to the subgrade, damps out dynamic loads from the rails, holds the sleepers in place laterally and longitudinally and allows water to drain away from the track surface.

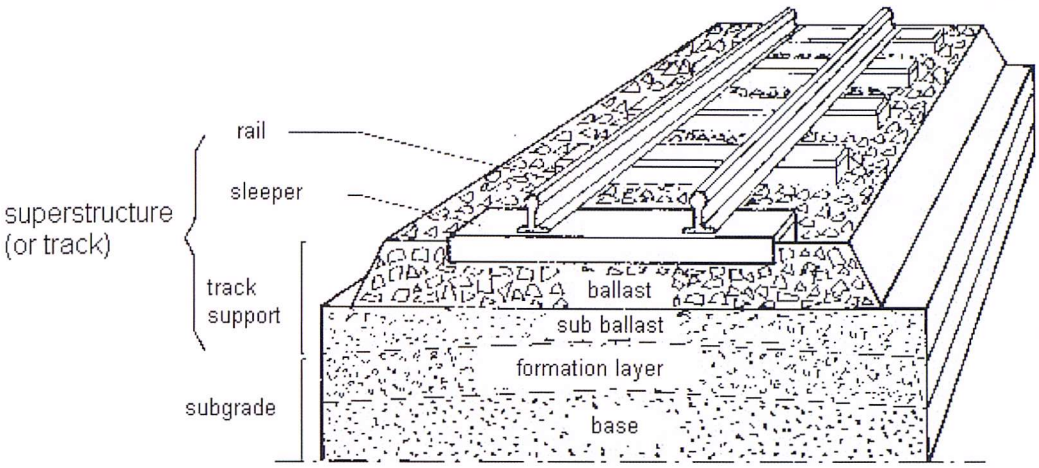

Figure 2 - 4 Structure of railway track[7]

The track formation is designed to reduce the mean contact stress with every layer, this is achieved by making the contact area larger with every step into the formation. Figure 2 – 5 shows the distribution of a 1000 MPa mean contact pressure at the rail into the track structure.

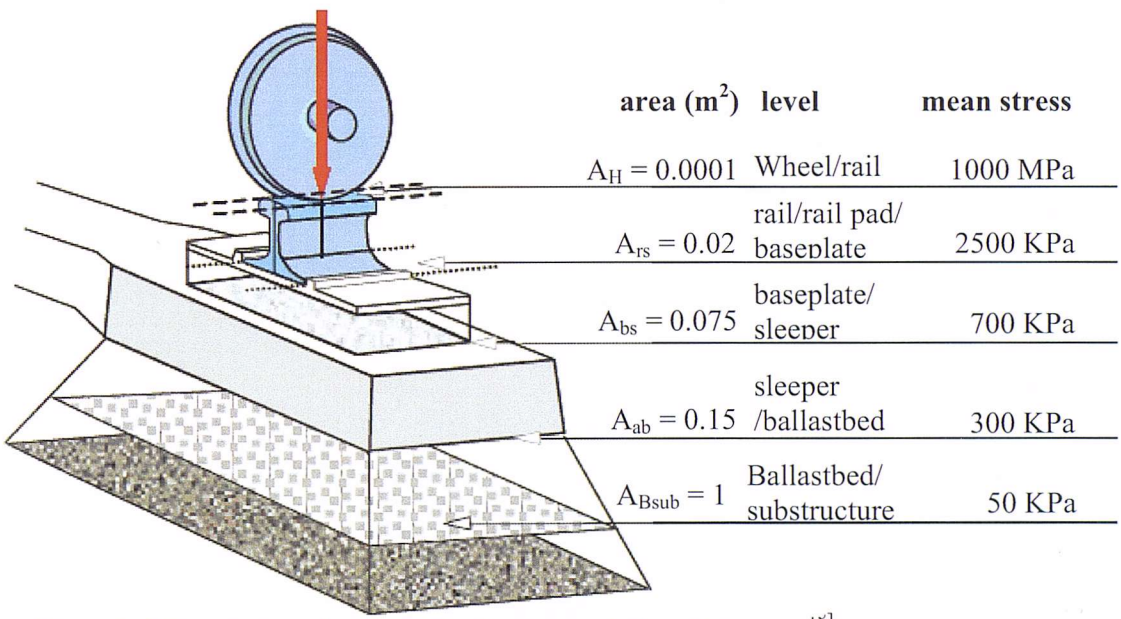

Figure 2 - 5 Distribution of vertical wheel load down to the substructure[8]

2.3 Rail loading

Railway rails are subjected to a range of loading, as shown in Figure 2 – 6. In the contact area, longitudinal (F_x), lateral (F_y) and vertical loads (F_z) are generated. In addition to these loads, bending stresses are generated in the rail, due to the vertical loads. There are also residual stresses in the rail as a result of manufacturing processes. For continuously welded rail, thermally induced stresses are also present.

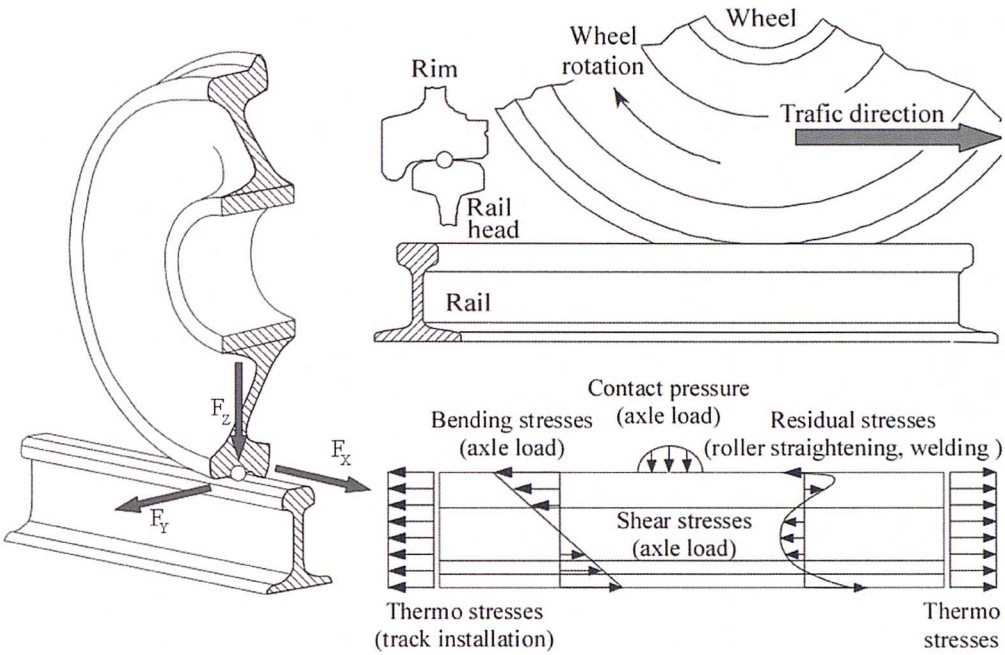

Figure 2 - 6 Rail loading[9]

For the purpose of this investigation we are primarily interested in the contact loads, F_X, F_Y and F_Z.

The vertical load is made up of a static and dynamic components. The static load is the fraction of vehicle weight carried by each wheel. Vertical dynamic loads are generated as the wheel travels over changes in rail height, due to: surface roughness, poor geometry, high welds, rail joints, points and crossings and applied cant* through curves.

Longitudinal forces are caused by tractive effort and braking and by steering through curves.

* Cant (or superelevation) is a difference in height between the two rails which is applied through curves, this is explained further in section 2.3.2.

Lateral loading is caused by curving, gauge discontinuities and travelling through points and crossings.

Residual stresses are present in the rail as a result of the manufacturing process, these are static loads which do not vary as a result of traffic. The sum of the residual stress through the rail cross section is zero, with tension at the top and bottom of the rail and compression at the middle of the section (shown in Figure 2 – 7).

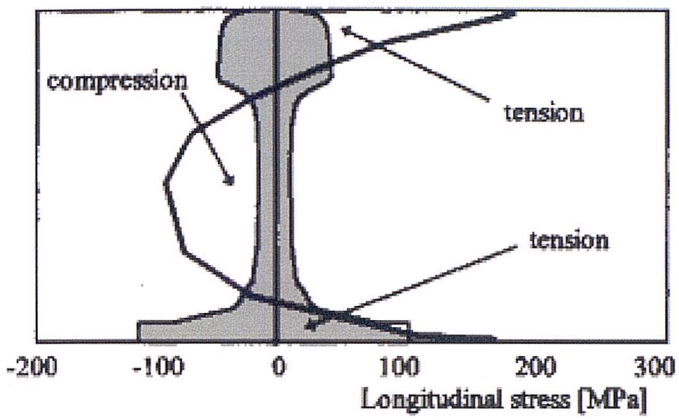

Figure 2 - 7 Residual stress in a rail due to straightening during manufacture[10]

Thermally induced stresses are also present in continuously welded rail. Higher temperatures would normally cause the rails to expand longitudinally; however, because they are longitudinally constrained this creates a stress in the rail material. This load will change over time depending on ambient temperature, but relative to the passing of rail vehicles it can be considered as a static load. When rails are installed, they are pre stressed to achieve a specific 'stress free temperature'. This is a temperature where there will be no thermally induced stresses. The operator must select a suitable 'stress free temperature' (SFT) somewhere in the mid range of temperature conditions the rails will likely experience, usually somewhere between 18 and 30 °C[10]. For every 1 °C change in rail temperature away from the SFT, a longitudinal stress of 2.5 MPa[10] is created in the rail. On sunny days the rail temperature can be much higher than ambient conditions, and can reach as high as 70 °C. For a SFT of 20 °C, this would cause a compressive longitudinal stress of 125 MPa. So at the top of the rail this would give a resultant tensile stress of 75 MPa (when superimposed on

the 200 MPa tension from the residual stress). A temperature of -5 °C would give a resultant tensile stress at the rail head of 262 MPa. This is why there are significantly more rail breaks during cold weather.

2.3.1 Vertical loading

As already mentioned in section 2.3, vertical loading is made up of static and dynamic components. A typical Electric Multiple Unit (EMU) passenger train such as the Electrostar (Class 375) has a gross weight of approximately 50 tonnes per car[11], which gives a static axle load of 12.5 tonnes, equivalent to 61 kN per wheel. The heaviest locomotives in the UK have axle loads up to 25 tonnes (or 125 kN[12] per wheel). Dynamic loading can increase the total to 4 or 5 times the static wheel load[13].

The dynamic response of a vehicle due to a vertical displacement at the wheel occurs in two stages. Firstly a high frequency 'impact' (P1) is experienced, which is typically damped within one oscillation, followed by a lower frequency (P2) damped oscillation. A commonly studied case is the loading created as a vehicle travels over a dipped rail joint; a typical response is shown in Figure 2 - 8.

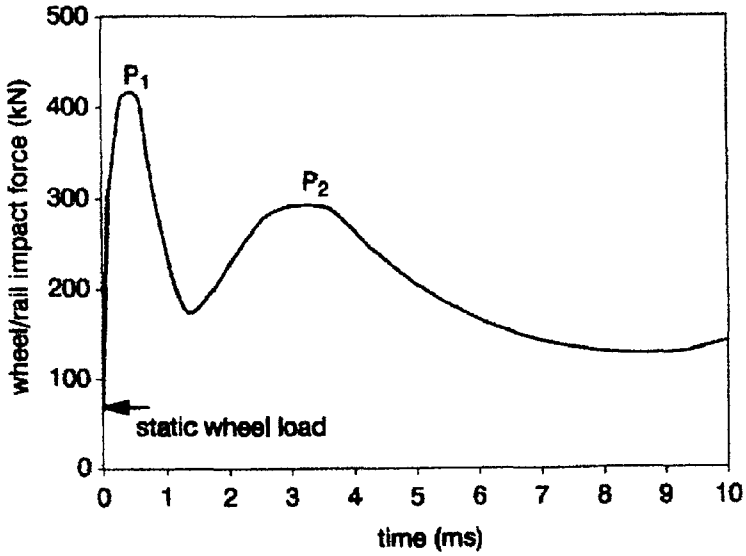

Figure 2 - 8 Response to a theoretical train travelling over a 0.02 rad dipped rail joint at 250 kph taken from the Zhai & Chai model[14]

Jenkins[13] first characterised P1 and P2 loading and carried out an investigation into the factors affecting the severity of these loads. As shown in Figure 2 – 9 the main factor affecting P1 and P2 loading is the unsprung mass.

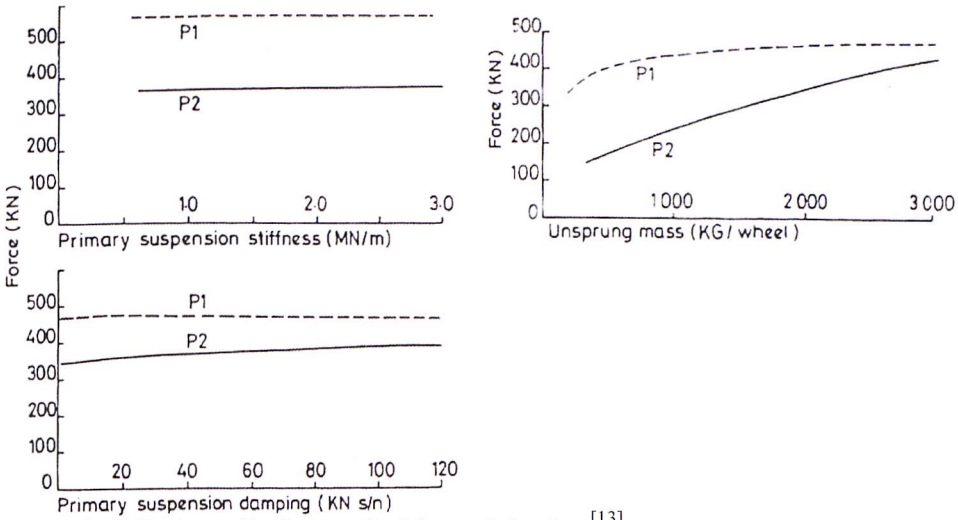

Figure 2 - 9 Factors affecting vertical dynamic loading[13]

Since Jenkins published this research in 1974, the need to reduce unsprung mass of rail vehicles has generally been accepted throughout the rail industry. See Figure 2 – 10 for an overview of axle load and unsprung mass of UK rail vehicles built since 1950.

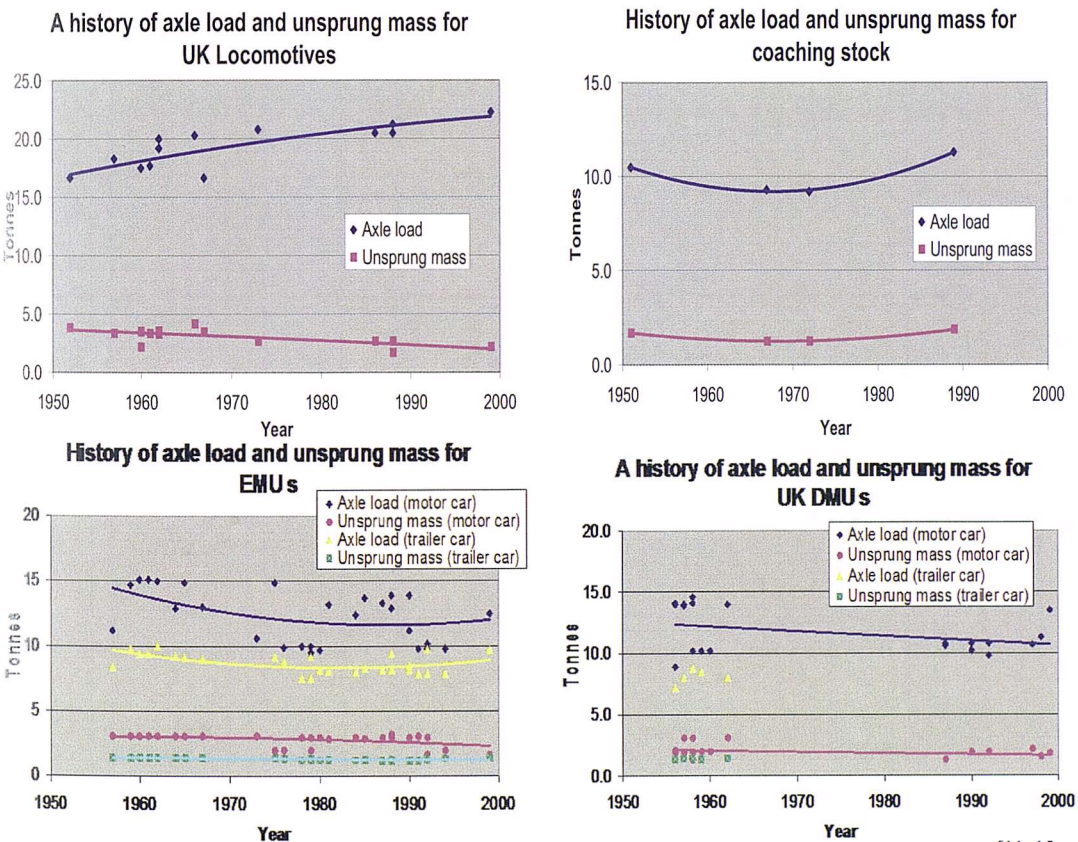

Figure 2 - 10 Change in axle load and unsprung mass for new build trains, data from [11, 15, 16]

There has been a general downward trend in unsprung mass, particularly for locomotives. This has been achieved through the use of hollow axles and the move from axle hung to bogie mounted motors. EMUs show a general downward trend in unsprung mass; motor cars built in the 90s showing a significant reduction in unsprung mass compared to their predecessors, due to the introduction of bogie mounted traction motors. For Diesel Multiple Units (DMUs) there has been no significant reduction in unsprung mass, though the overall axle load has been reduced. Coaching stock has actually shown an increase in unsprung mass; this is mainly due to the introduction of disc brakes. Disc brakes are required to produce the necessary braking power for high speed trains; unfortunately this improved braking capacity comes with a weight penalty. Locomotives and multiple unit power cars have not had the same increase in unsprung mass because of the increased use of rheostatic (motor) braking which minimises the required disc brake capacity.

Damage to the track is caused by the total loading, including static and dynamic. The static wheel load will act at every point along the track visited by a vehicle, while higher dynamic loading will only occur as the vehicle passes vertical discontinuities in the track. For the UK railways the infrastructure provider, Network Rail, calculates an access charge* for every vehicle running over their track, depending on a relative damage index for each vehicle type. The calculation takes into account axle load and unsprung mass. This should incentivise train manufacturers and operators to build and use vehicles which generate lower vertical loading. Tangential track loading is currently not included in the calculation.

Vertical dynamic loading can also be reduced by improving the track. For a perfectly smooth, straight piece of track there would be no dynamic loading, the only vertical load would be the weight of the vehicle. Network Rail (and their predecessors) have started working towards this by removing jointed track and replacing it with continuously welded track.

* This is discussed further in Chapter 5

2.3.2 Lateral loading

Because of the geometry of the wheels and rails, there is always a lateral element to the wheel-rail loading. The rails are inclined towards the centre of the track*, and the wheels are coned to match this†. Due to the weight carried by each wheelset, there is a normal reaction at the rail, and a tangential component due to friction. If these forces are resolved in the vertical and lateral directions, the vertical loads will match the weight of the vehicle. When the wheelset is in a central position on straight track the lateral loads on opposing wheels are equal and opposite, transmitting no resultant lateral force up to the vehicle.

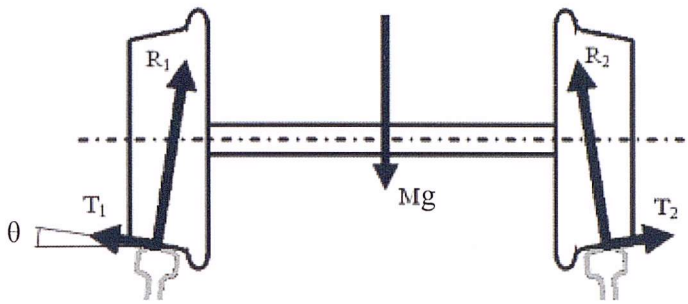

Figure 2 - 11 Wheel loading normal and tangential to the rail surface

where: Mg = component of vehicle weight carried by one axle, R_1 and R_2 are the reactions at the left and right wheel respectively, $T_1$and T_2 are the corresponding tangential (frictional) loads, θ = rail incline, e.g. 1:20 = 2.86°

For this case the forces on each rail are equal ($R_1 = R_2$ and $T_1 = T_2$), the reaction forces can be calculated by:

$$R_1 = R_2 = \frac{Mg - 2T_1 \sin\theta}{2\cos\theta} \quad \textbf{(eqn 2 – 3)}$$

T_1 and T_2 are friction loads with a limiting value of: $T_{1\max} = T_{2\max} = \mu R_1$ **(eqn 2 – 4)**

where μ = coefficient of friction, a typical value for a clean dry rail is 0.3

As the wheelset travels through a curve it shifts laterally, which causes the contact angle between the wheel and rail to change. Both direction and severity of the

* Typically a rail inclination of 1:20 is used in the UK

† NB Over time the conicity of the wheels will change due to uneven wear, this changes the comparative vertical and lateral loading

normal reaction are affected, see Figure 2 - 12. NB loads shown here are the loads acting on the wheelset; rail loadings are equal and opposite.

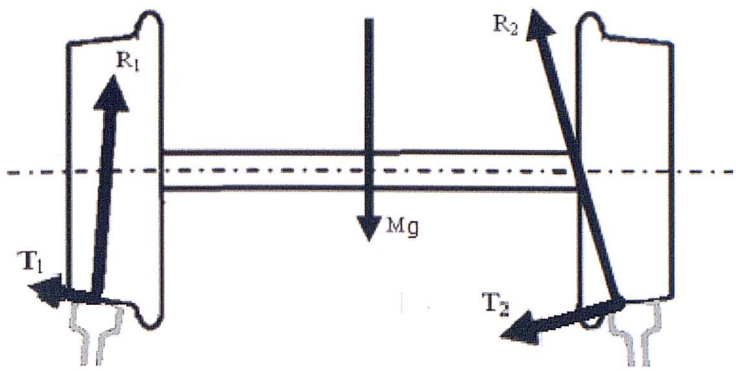

Figure 2 - 12 Normal and tangential wheel loading though a curve

In this case the wheelset has moved to the right, due to a left hand curve. At both rails the frictional force is acting towards the right, i.e. the outside of the curve. T_1 and T_2 are limited by the friction available at the rail, in very tight curves (below 500 m radius of curvature) the flange of the outer (i.e. right hand) wheel can also hit the gauge face of the rail creating even higher lateral loads.

The magnitude and direction of R_1 and R_2, has changed because the wheel-rail contact angles change with lateral shift of the axle. This change in the reaction loads is known as the 'quasi-static' curving load.

A cant is applied to the track, in order to avoid passing on a perceived centrifugal acceleration to the passengers*, as shown in Figure 2 – 13.

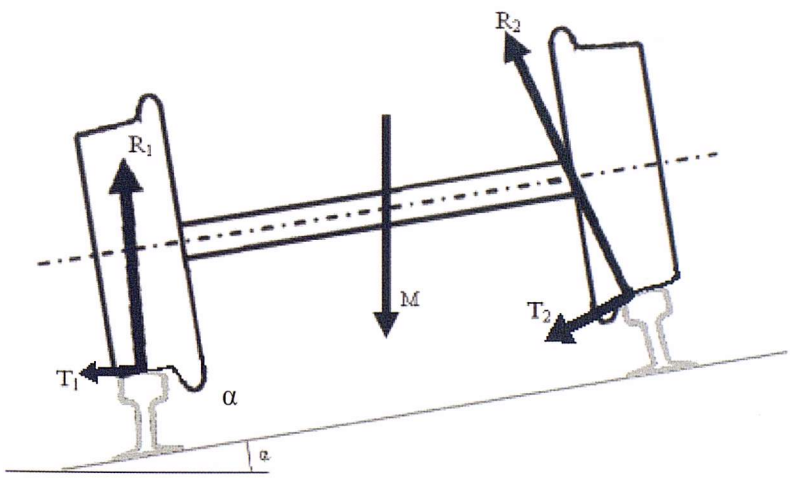

* As this would cause an uncomfortable ride for the passengers, this cant provides no significant contribution towards 'steering' as this is dominated by the effect of the rolling radius difference as described in the following section

Figure 2 - 13 Effect of cant

If the perfect balancing cant is applied:

$$\frac{Mv^2}{R} = Mg\cos\alpha \quad \textbf{(eqn 2 – 5)}$$

In practice a range of values either side of the balancing cant are used, depending on the different speeds of trains using the same track.

2.3.3 Longitudinal creep loading due to curving

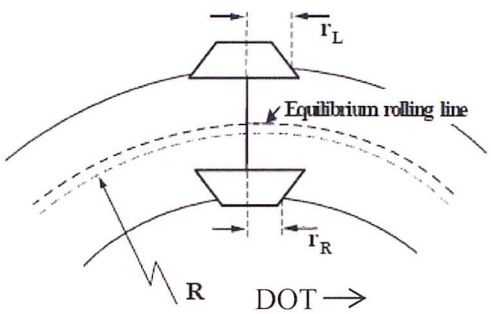

Figure 2 - 14 Single wheelset negotiating a curve[17]

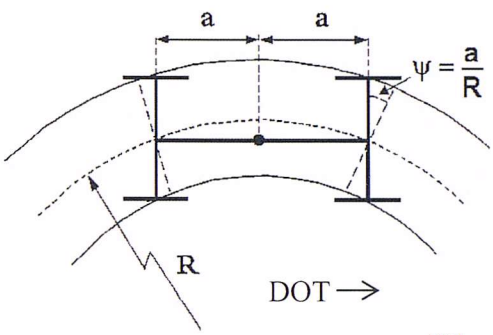

Figure 2 - 15 Bogie negotiating a curve[17]

A standard wheelset is made up of two conical wheels connected by a rigid axle. The coning of the wheel creates a steering effect through curves, and also centres the wheelset on straight track. The wheels are flanged to limit the lateral displacement of the wheels.

Figure 2 – 14 shows a single wheelset negotiating a curve of radius, R. The wheelset has moved laterally towards the outside of the curve, which means the outside wheel has a larger rolling radius (marked r_L) than the inside wheel (r_R). Because both wheels have the same rotational speed, the outside wheel will roll through a longer distance. This creates a steering effect, pulling the outside wheel around the curve. The wheelset can travel through the curve, remaining at an angle normal to the rails; neither wheel will slip.

Figure 2 – 15 shows a bogie or two axle vehicle negotiating a curve; because the two axles are constrained to remain parallel, neither axle can stay normal to the rails. This creates an 'angle of attack', marked Ψ. As shown in the diagram this angle of attack is equal to a/R, where a = half the axle spacing. Because of this

angle of attack, the conical steering can not create the desired effect to drive the vehicle through the curve. This means that the wheels need to partially slip in order to get round the curve; this partial slip is known as creep. Larger angles of attack lead to larger creepage. This creepage causes longitudinal track loading. As stated in section 1.4, a 'Class 91' locomotive travelling around a curve of 600 m can generate a longitudinal creep load of 40 kN.

As mentioned in section 2.1, bogies were first introduced to improve curving performance of rail vehicles. For a given carriage length, the use of a bogie, compared with two fixed axles at either end of the carriage, gives a much reduced space between the axles. This reduces the angle of attack, and reduces the rail loading. However, even with the use of a bogie, significant creep loading can still be generated through curves.

ıere is an added complication when bogies are attached to the car body, the yaw stiffness in the secondary suspension acts against the rolling radius difference steering, increasing the angle of attack for the front axle, see Figure 2 – 16.

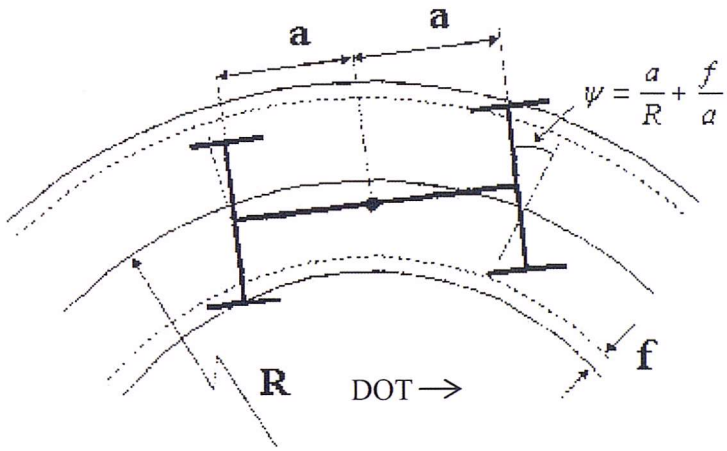

Figure 2 - 16 Bogie negotiating a curve with increased angle of attack due to secondary yaw stiffness[17]

The front wheel has an increased angle of attack, as the bogie rotates away from the neutral curving angle. The increased angle is dependent on the flangeway clearance*, f, and the length of the bogie. The increased angle of attack leads to

* This is the distance between the front face of the wheel flange and the gauge face of the rail, when the wheelset is positioned centrally to the track.

higher levels of creep and consequentially larger longitudinal rail loading at the front axle.

In reality bogies have a certain degree of flexibility and the rolling radius steering effect can force the axles towards a position normal to the rails, as shown in Figure 2 – 17. The degree of flexibility of the bogie frame and axle connection is known as the primary yaw stiffness, k_ψ. A more flexible bogie, with a lower primary yaw stiffness, allows the axles to move closer toward a neutral angle. As yaw stiffness moves towards zero, the angle of attack approaches zero, meaning the wheelset can traverse the curve with no creep and zero longitudinal load.

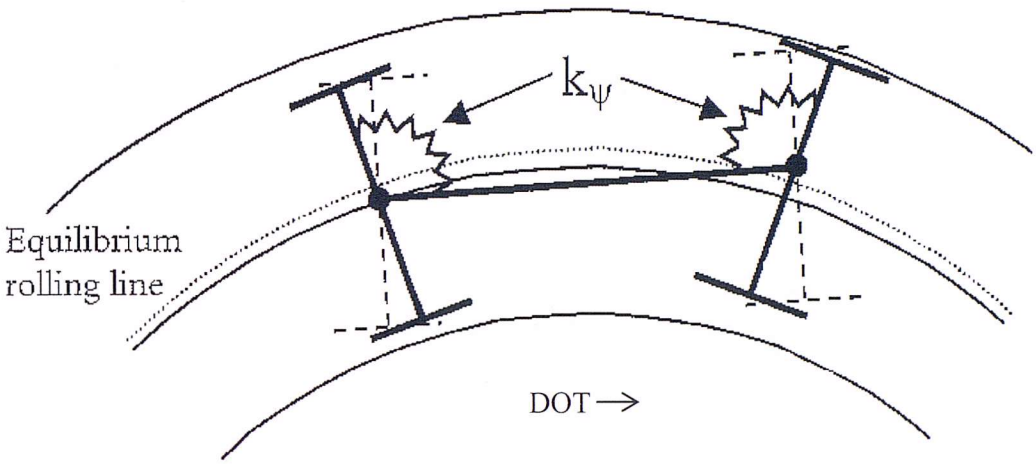

Figure 2 - 17 A flexible bogie negotiating a curve[17]

2.3.4 Bogie hunting

Another effect of the conical wheelset is to centre the wheelset on straight track. If the wheelset becomes displaced laterally* the conical steering effect steers it back to a central position. However, the wheelset can overshoot the central position and become too far displaced in the opposite direction. This in turn causes a steering action back toward the centre; an oscillation about the centre position is set up, known as hunting. If unconstrained, the path of the wheelset will describe a sine wave, as shown in Figure 2 – 18. The longitudinal primary suspension connections create a yaw stiffness between the wheelsets and bogie. As the wheelset yaws relative to the bogie, the longitudinal stiffness elements at

* This can occur due to geometry defects, such as twists in the track or minor changes of gauge; travelling through points and crossings, or as the vehicle exits a curve onto a straight section

each axle box connection create a yaw torque, opposing the hunting motion. This in turn creates a creep force at the wheel-rail contact, damping out the hunting oscillations. However, this is only effective up to a certain speed limit, know as the critical speed, after which the hunting motion begins. This instability problem has long been a barrier to increasing train speed.

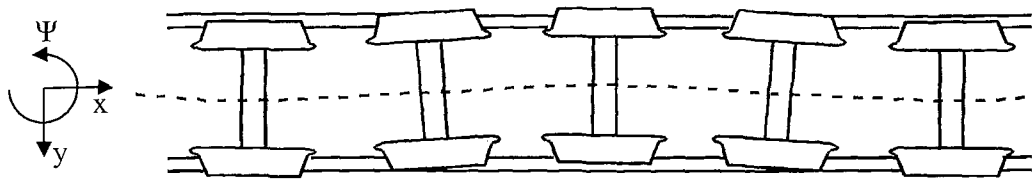

Figure 2 - 18 Unconstrained wheelset hunting[17]

The mechanism of hunting and its relationship to creep, were first identified by Carter[18], with his ideas developed further by Matsudaira[19, 20]. Wickens'[21] later work in this area resulted in the current understanding of hunting and vehicle stability.

The lateral motion of the wheelset is described by the following equations[17]:

$$m\ddot{y} + 2f_{22}\left(\frac{\dot{y}}{V} - \psi\right) + k_y y = 0 \qquad \textbf{(eqn 2 - 6)}$$

$$I\ddot{\psi} + 2f_{11}\left(\frac{l_0\lambda}{r} y + \frac{l_0^2}{V}\dot{\psi}\right) + k_\psi \psi = 0 \qquad \textbf{(eqn 2 -7)}$$

where; m = wheelset mass, f_{22} and f_{11} = Kalker coefficients* (dependent on contact patch geometry), y = lateral displacement, ψ = yaw angle, V = train velocity, k_y = primary suspension lateral stiffness, k_ψ = primary yaw stiffness, λ = wheel cone angle, l_0 = the nominal contact separation, i.e. the effective axle width, r_0 = the nominal wheel radius

These equations have a solution of the form:

$$y = Ye^{\alpha t}$$
$$\psi = \Psi e^{\alpha t}$$

where Y = initial lateral displacement, Ψ = initial yaw angle

* Kalker coefficients[22] are linear elastic coefficients used to describe the relationship between shear force and creep at the contact

α is dependent on the speed, wheel conicity and the lateral and yaw stiffness. Negative values of α result in a damped oscillation. Positive values of α result in negative damping and therefore hunting.

Hunting leads to poor ride quality and severe lateral track loading as the wheel flanges continually hit the rails, and can lead to derailment.

For a given wheel conicity and suspension stiffness, a critical speed can be identified where hunting begins. Wickens suggests, for an elastically constrained wheelset, the critical speed[21]:

$$V_C = \sqrt{\frac{2r_0 l[W(\delta_0\zeta + \in -\delta_0)l + 2k_x l^2 + 2k_y b^2]}{\lambda(C + ml^2)}} \qquad \textbf{(eqn 2 – 8)}$$

where; l = contact separation, r_0 = wheel radius, W = axle load, δ_0 = contact angle, ζ and $\in$ = parameters dependent on wheelset geometry, k_x = primary suspension longitudinal stiffness, b = contact area half length, C = wheelset yaw inertia, m = wheelset mass.

Looking at this equation we can see that increasing the longitudinal and lateral stiffnesses gives a higher critical speed.

The critical speed of an empty freight wagon can be as low as 61.2 kph (38 mph)[23], whilst there are high-speed trains, such as the Shinkansen in Japan that have critical speeds over 500 kph[24].

2.3.5 Compromise between curving and straight line stability

As described in sections 2.3.3 and 2.3.4 the requirement for good curving and straight line stability are conflicting. For a vehicle to negotiate curves with minimum track loading, low primary stiffnesses are required. However, low primary yaw stiffness means the suspension is not capable of creating enough damping force to prevent hunting at high speeds. To increase the vehicle's critical speed and avoid hunting, the primary stiffnesses must be increased, but this leads to high track loading through curves.

When selecting an appropriate primary yaw stiffness, vehicle designers need to make a compromise, depending on: known routes the vehicle will be used for, range of operating speed and required comfort levels.

For a vehicle operating over a wide range of routes under a variety of speeds, it is very difficult to optimise the design appropriately.

The vehicle design needs to be modified to fundamentally change the steering mechanism; if this can be achieved it will be possible to reduce longitudinal creep loads through curves, without compromising straight line stability. The options available in order to achieve this need to be investigated further.

2.4 Contact patch mechanics

2.4.1 Vertical stress distribution

The wheel and rail are two curved surfaces which come into contact. The stress distribution can be described by Hertzian contact theory, giving a stress distribution as shown in Figure 2 – 19.

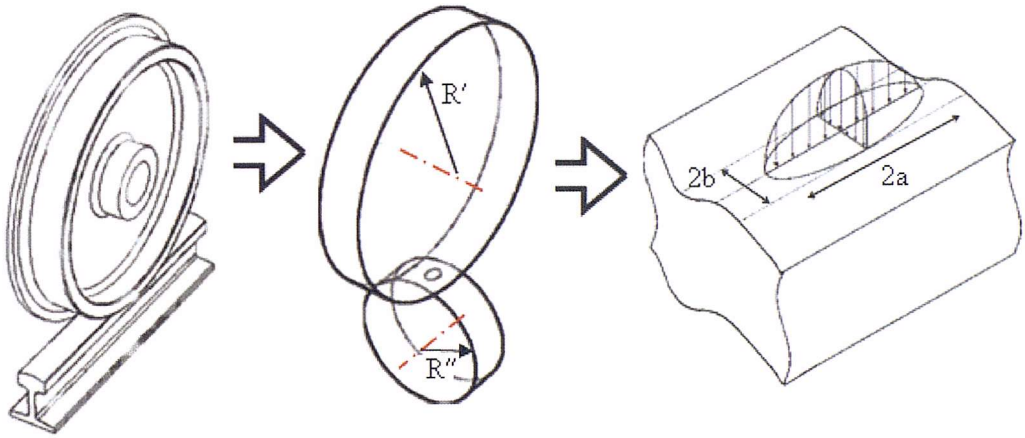

Figure 2 - 19 Wheel/rail Hertzian contact[25, 26]

Hertz defined the following equations[27], which are now widely accepted and used for wheel-rail contact mechanics calculations.

The shape of the contact patch is dependent on the relative curvature of the two bodies in contact (i.e. the wheel and rail).

$$\frac{a}{b} = \left(\frac{R'}{R''}\right)^{2/3} \qquad \textbf{(eqn 2 – 9)}$$

Whilst the area of the contact is dependent on the applied vertical load:

$$A = \pi\left(\frac{3PR_e}{4E^*}\right)^{2/3} F_1\left(R'/R''\right) \quad \textbf{(eqn 2 – 10)}$$

where,

$E^* = \frac{E_1}{1-\nu_1^2} - \frac{E_2}{1-\nu_2^2}$, E_1 and E_2 are the Young's modulus of the two materials, ν_1 and ν_2 are the respective Poisson's ratios, $R_e = (R'R'')^{1/2}$, P is the total vertical load and F_1 is a function, defined in Appendix A.

The peak load at the centre of the contact patch can be calculated from:

$$p_0 = \frac{3P}{2\pi ab} \qquad \textbf{(eqn 2 – 11)}$$

The pressure distribution along the major semi axis (x = 0 to x = 2a), can be described by:

$$P(x) = p_0\left\{1-\left[\frac{2x}{2a}\right]^2\right\}^{1/2} \quad \textbf{(eqn 2 – 12)}$$

Because the curvature of the rail top varies across the rail profile, as the wheelset moves laterally on the rail the contact patch shape can vary considerably. See Appendix B for examples.

Hertzian contact mechanics assumes two perfectly smooth surfaces. Steel wheels and rails appear smooth to the naked eye. However, as with all materials, there is a microscopic roughness. The real area of contact between a wheel and rail is the total area of contact between asperities on the wheel and rail surfaces, which can

be a small fraction of the perceived area of contact*. The width of each asperity contact is in the order of a few microns[28].

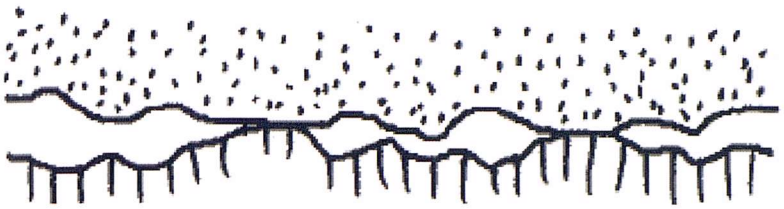

Figure 2 - 20 Asperity contact between two rough surfaces[29]

Depending on the level of roughness, the real pressure levels at the microscopic contact areas at the wheel-rail interface can be up to ten times the peak pressure predicted by Hertzian theory[30, 31], see Figure 2 - 21.

These peak pressures cause highly concentrated stresses at the asperity contact, penetrating only microns into the rail. The microscopic stress concentrations are often not considered in larger scale studies of wheel-rail interaction. However, they do have a significant affect on the properties of a very thin layer at the top of the rail; this is discussed further in section 3.2.2.3.

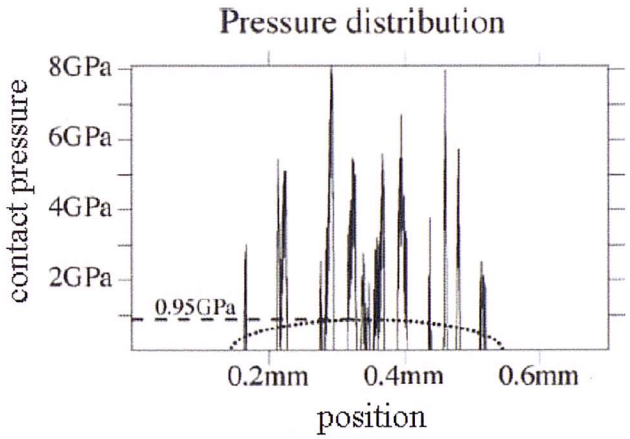

Figure 2 - 21 Contact pressure due to surface roughness compared to Hertzian theory[30]

2.4.2 Tangential stress distribution

As described in sections 2.3.2 and 2.3.3, curving causes lateral and longitudinal loads that are generated at the wheel-rail interface. Longitudinal loads are also caused by traction and braking. These loads are generated as the wheel, partially

* Bucher suggests the real contact area can be as small as 0.02 of the apparent contact area[29]

slips, i.e. creeps along or across the rail. Creep is the ratio of wheel contact point speed to rolling or vehicle speed, i.e.:

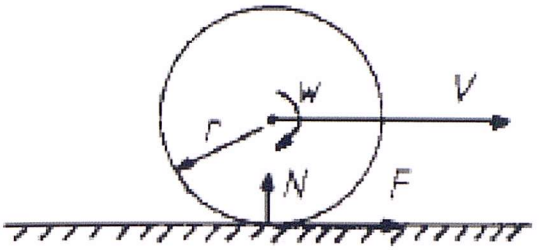

$$\text{creep, } \gamma = \frac{\omega r - V}{\omega r} \quad \textbf{(eqn 2 – 13)}$$

Figure 2 - 22 Longitudinal wheel creep[32]

Creep also occurs in the lateral direction, see Figure 2 – 23, and equation 2 – 14.

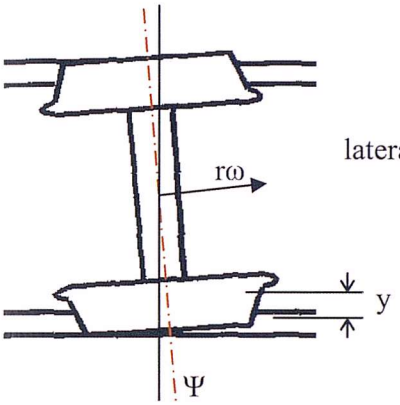

$$\text{lateral creep, } \gamma_y = \frac{\omega r \cos\Psi - \dot{y}}{\omega r \cos\Psi} \quad \textbf{(eqn 2 -14)}$$

Figure 2 - 23 Lateral wheel creep

The magnitude of the creep load is dependent on the creep ratio, limited by the frictional force available at the wheel-rail interface, as shown in Figure 2 – 24.

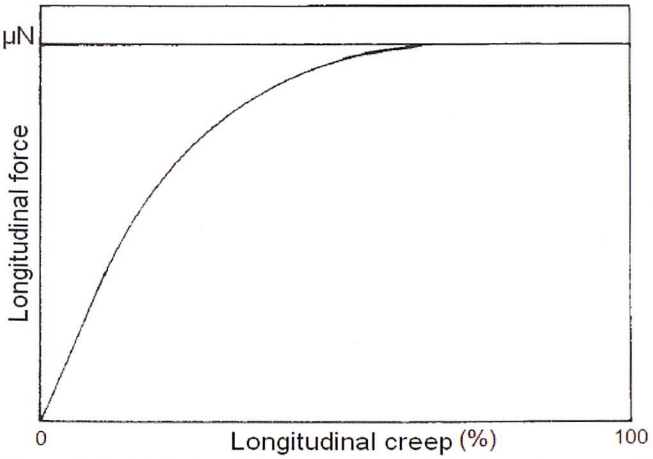

Figure 2 - 24 Relationship between creep force and creep ratio, based on Kalker's creep model[32]

It is possible to limit the creep forces through curves by limiting the friction at the wheel-rail interface. Many operators achieve this by applying friction modifiers, such as vehicle or track based lubricators. However, the use of these friction modifiers are only mitigating the problem of poor wheel-rail interaction. The lubricators themselves require maintenance, and need to be filled with lubricant at regular intervals. A more appropriate solution might be to fundamentally remove the problem, by improving train steering, thus reducing wheel-rail creep.

Within the contact area there are regions of stick and slip. In the stick region there is pure rolling, while in the slip region pure sliding. The exact details of what is happening in the contact area when a wheel is subject to creep loading are still unknown. However, a significant research effort has gone into this area, resulting in some models which are widely agreed to show a good representation of reality.

Figure 2 – 25 shows the shape of the slip and stick regions as defined by Haines & Ollerton[33], along with the consequential tangential load distribution along the major semi axis. The dotted line, q′(x) shows the maximum possible tangential load for full slip condition (= μP). NB The stick region typically occurs at the front of the contact area, in the direction of travel.

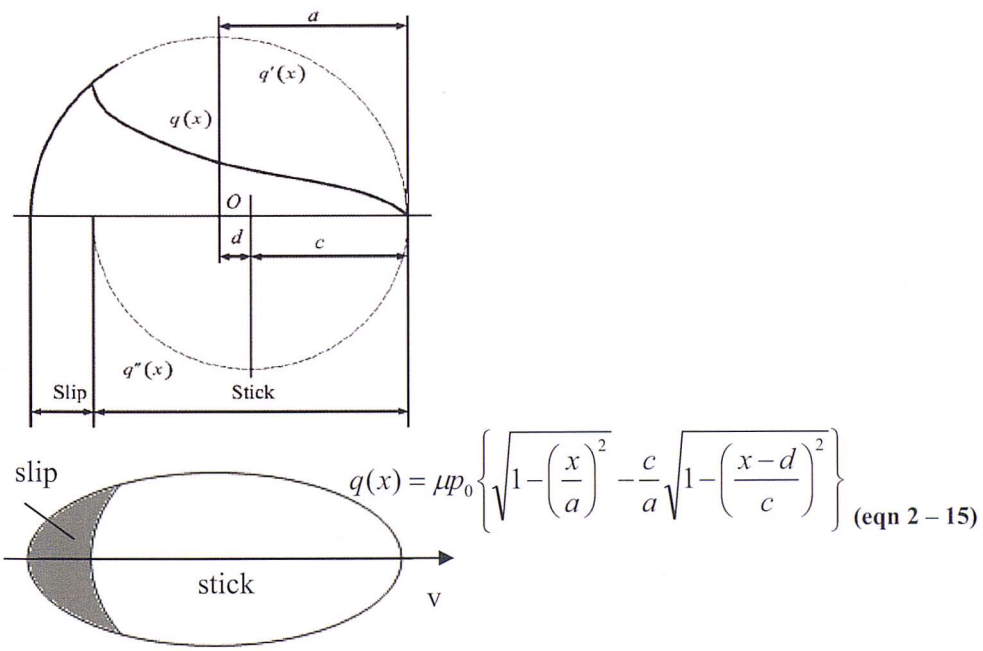

$$q(x) = \mu p_0 \left\{ \sqrt{1-\left(\frac{x}{a}\right)^2} - \frac{c}{a}\sqrt{1-\left(\frac{x-d}{c}\right)^2} \right\} \quad \textbf{(eqn 2 – 15)}$$

Figure 2 - 25 Distribution of tangential load in the slip and stick regions[33]

Equation 2 – 15 shows the tangential load distribution along the centre line of the contact patch.

Johnson[34] suggested an alternative distribution, with a completely elliptical stick zone; however, his later work[35] also reverted to the layout shown in Figure 2 – 25. Kalker's[22] creep equations are based on the Haines and Ollerton distribution; Kalker's equations are now widely accepted, and form the basis of the creep calculation used in many of the most popular vehicle dynamics software packages.

2.5 Discussion

There is a complex interaction between the vehicle and track, with forces concentrated in the small, stiff contact patch between the wheel and rail. Vertical loads are caused not only due to the weight of vehicle, but also because of dynamic loading as the vehicle negotiates any changes in height at the rail surface. Vertical dynamic loading can be reduced, by reducing the unsprung mass. There has already been a significant contribution towards this through the use of hollow axles, bogie mounted motors and smaller wheels. However, significant tangential loads are also generated at the wheel-rail interface. Some progress has been made to reduce these by attempting to select primary yaw stiffnesses that will create some compromise between the need for low force curving and straight line stability; and through the use of track based lubrication. For the UK railways, the track access charge gives no penalty for high tangential loading, so there is not the same incentive for train manufacturers to improve tangential loading (compared to vertical loading). However, the damage caused by high tangential loads is still causing an overall system cost*. This can be reduced by changing the steering mechanism used for rolling stock, a method of achieving this is to introduce 'steering' bogies. The aim of this research is to quantify the benefits that can be achieved by reducing these loads.

* Maintenance and renewal costs are discussed further in Chapter 4

The following chapter goes on to discuss the damage caused by the track loading discussed in this chapter, and the various damage mechanisms caused by loads in the different directions (lateral, longitudinal and vertical).

References

1. Wickens, A.H., *Fundamentals of Rail Vehicle Dynamics - Guidance and Stability, Chapter 6: The bogie vehicle*. 2003: Taylor & Francis.
2. Stover, J.F., American Railroads. University of Chicago Press, 1961: p. 25.
3. Okamoto, I., *Railway technology today 5: How bogies work. Japan Railway & Transport Review*, 1998. **18**: p. 52 - 61.
4. Newland, D.E. and R.J. Cassidy, *Suspension and Structure: Some fundamental design considerations for railway vehicles*. Proceedings of the IMechE, Railway Division, 1975. **4**(2): p. 4-34.
5. Cannon, D.F., et al., *Rail defects: an overview*. Fatigue & Fracture of Engineering Materials and Structures, 2003. **26**(10): p. 865-886.
6. Wenty, R., *High-capacity, precision and reliability in track maintenance*. Railway Technical Review, 2006. **46**(3).
7. Profillidis, V.A., *Railway Engineering*. 2nd ed. 2000, Aldershot: Ashgate. p 33.
8. Esveld, C., *Modern Railway Track*. 2nd ed. 2001, Zaltbommel: MRT-Productions.
9. Zerbst, U., M. Schodel, and R. Heyder, *Damage tolerance investigations on rails*. Engineering Fracture Mechanics, [in press].
10. Szelazek, J. *Monitoring of thermal stresses in continuously welded rails with ultrasonic technique*. in German Society for Non-Destructive Testing Annual Conference. 1997. Dresden.
11. *Structure of costs and charges review: Emerging views on key Issues, Annex C: Vehicle characteristics for usage charge model*, http://www.rail-reg.gov.uk/upload/pdf/229.pdf, [Accessed, 5/10/07]
12. *GM/TT0088, Permissible Track Forces for Railway Vehicles*, Railway Group Standard, British Railways Board, 1993
13. Jenkins, H.H., et al., *Effect of track and vehicle parameters on wheel/rail vertical dynamic forces*. Railway Engineering Journal, 1974. **3**(1): p. 2-16.
14. Zhai, W. and Z. Cai, *Dynamic interaction between a lumped mass vehicle and a discretely supported continuous rail track*. Computers and Structures, 1997. **63**(5): p. 987-997.
15. The Junction, www.thejunction.org.uk, [Accessed, 4/9/06]
16. Southern E-Group, www.semg.org.uk, [Accessed, 4/9/06]
17. DeltaRail. Course notes from: Introduction to Railway Vehicle Dynamics. 2006. Derby.
18. Carter, F.W., *The electric locomotive*. ICE Proceedings, 1916. **201**: p. 221 - 252.
19. Matsudaira, T., *Shimmy of axle with pair of wheels*. Journal of Railway Engineering Research, Japan, 1952(November): p. 16 - 26. *(Original in Japanese - referred to in [20])*
20. Gilchrist, A., *The long road to solution of the railway hunting and curving problems*. Proceedings of the IMechE Part F: Journal of Rail and Rapid Transit, 1998. **212**(3): p. 219-226.

21. Wickens, A.H., *The dynamics of railway vehicles on straight track: fundamental considerations of lateral stability*. Proceedings of the IMechE, 1965. **180**(3): p. 1 - 16.
22. Kalker, J.J., *On the rolling contact of two elastic bodies in the presence of dry friction*. 1967, PhD Thesis, Delft University of Technology.
23. Molatefi, H., M. Hecht, and M.H. Kadivar, *Critical speed and limit cycles in the empty Y25-freight wagon*. Proceedings of the IMechE Part F, Journal of Rail and Rapid Transit, 2006. **220**(4): p. 347 - 359.
24. Kondo, K., K. Yoroizaka, and Y. Sato, *Cause, increase, diagnosis, countermeasures and elimination of Shinkansen shelling*. Wear, 1996. **191**(1 - 2): p. 199 - 203.
25. Gauagliano, M. and M. Pau, *Analysis of internal cracks in railway wheels under experimentally determined pressure distributions*. Tribology International, 2007. **40**(7): p. 1147 - 1160.
26. Fletcher, D.I., P. Hyde, and A. Kapoor, *Investigating fluid penetration of rolling contact fatigue cracks in rails using a newly developed full-scale test facility*. Proceeding of the IMechE Part F: Journal of Rail and Rapid Transit, 2006. **221**(1): p. 35 - 44.
27. Hertz, H., *Ueber die Beruehrung elastischer Koerper (On Contact Between Elastic Bodies)*. Gesammelte Werke (Collected Works), 1895.
28. Kapoor, A., et al., Surface roughness and plastic flow in rail wheel contact. Wear, 2002. 253(1-2): p. 257-264.
29. Persson, B., F. Bucher, and B. Chiaia, *Elastic contact between randomly rough surfaces: Comparison of theory with numerical results*. Physical Review B, 2002. **65**(184106): p. 1 - 7.
30. Franklin, F.J. and A. Kapoor, *Modelling wear and crack initiation in rails*. Proceedings of the IMechE Part F: Journal of Rail and Rapid Transit, 2007. **221**(1): p. 23 - 33.
31. Bucher, F., K. Knothe, and A. Theiler, *Normal and tangential contact problem of surfaces with measured roughness*. Wear, 2002. **253**(1 - 2): p. 205 - 218.
32. Brickle, B.V., *Railway Vehicle Dynamics*. Physics Technology, 1986. **17**(4): p. 181 - 186.
33. Haines, D.J. and E. Ollerton, *Contact stress distributions on elliptical contact surfaces subject to radial and tangential forces*. Proceedings of the IMechE, 1963. **177**(4): p. 95 - 114.
34. Johnson, K.L., *The effect of a tangential contact force upon the rolling motion of an elastic sphere on a place*. Transactions of the ASME: Journal of Applied Mechanics, 1958. **25**: p. 339 – 346.
35. Johnson, K.L., *Contact Mechanics*. 1985: Cambridge University Press.

Chapter 3: Track degradation

This chapter introduces the various modes of degradation experienced by railway track, and the factors affecting them. The purpose of this research is to reduce the cost of track maintenance and renewals through the use of steering bogies. Before this can be achieved it is necessary to first understand how the track degrades and what causes it to degrade.

3.1 Environmental and traffic based degradation

Railway track can degrade in a variety of manners, either due to the passage of trains or as a consequence of the environment it is placed in. Figure 3 - 1 shows the main degradation modes, both environmental and traffic dependent, or a combination of both.

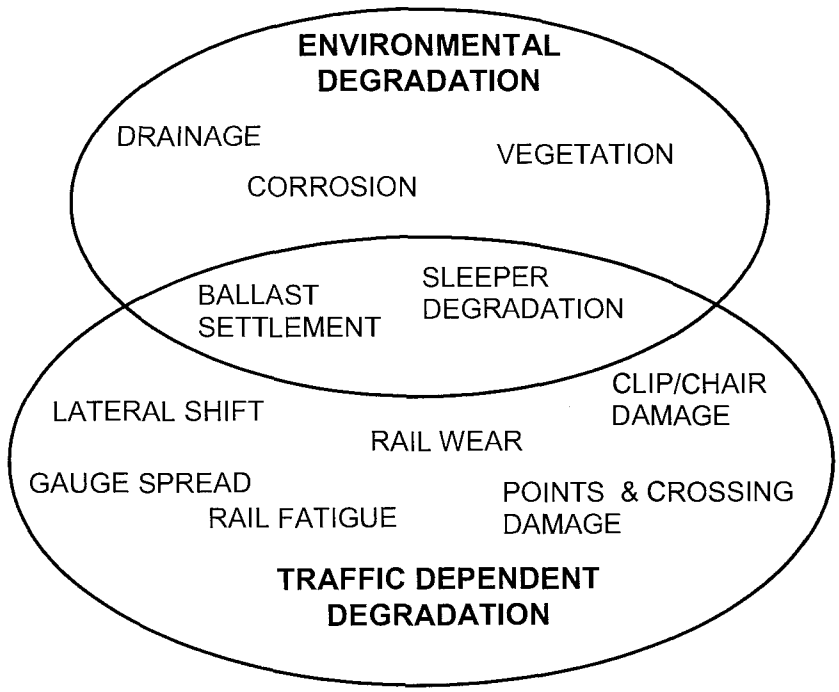

Figure 3 - 1 Railway track degradation modes

The degradation rate of the traffic dependent modes is proportional to the amount of traffic being carried by the track, and is also heavily dependent on the dynamic performance of the vehicles being used. As traffic densities increase, the traffic dependent modes will come to dominate the maintenance and renewals costs (this

is discussed further in Chapter 4). The rate of traffic dependent track degradation can be reduced by:

1. modifying service patterns;
2. reducing train mass;
3. improving the dynamic performance of the train;
4. changing the track design.

This research concentrates on option three, specifically looking at improving tangential loading. Before the financial benefits of this can be investigated, it is necessary to identify and understand the degradation modes that will be affected.

The purely environmental degradation modes will occur irrespective of the amount of traffic. It is possible to reduce the cost of track degradation by modifying the maintenance programme; however this is outside the scope of this study.

3.2 Traffic based degradation

The traffic dependent modes which have the biggest impact on maintenance and renewals requirement are: ballast settlement/degradation, rail wear and rail fatigue.

Wear and surface initiated fatigue damage of the rail are caused by contact forces generated at the wheel-rail interface. The two modes are interdependent, and have a complex relationship. Wear is the removal of material from the rail surface, and fatigue damage is the development of cracks due to cyclic loading. At low rates of fatigue cracking, the wear of the surface can 'rub out' small cracks before they propagate and therefore arrest their progress. Fatigue cracking can also cause a severe form of wear if cracks in the rail turn up towards the surface resulting in the removal of chunks of rail material; this is sometimes known as 'shelling' or 'spalling'.

Ballast is compressed due to the vertical loading caused by passing rail vehicles. This loading also causes ballast stones to wear or even break up, resulting in the

ballast losing its elasticity and ability to distribute load. Lateral shift of the track and sleepers, due to high lateral loads can also lead to further ballast settlement. Lateral movement of sleepers can disturb the settlement of the stones underneath, possibly leading to further ballast compression or wear.

The presence of water has an effect on all three degradation modes listed above. In future, climate change could have a significant impact on track maintenance regimes as the rates of these degradation modes changes with rainfall. Water acts as a lubricator at the rail head, changing the wear and fatigue properties, whilst flooding of the ballast can increase the rate of settlement by reducing the friction holding the stones together.

3.2.1 Wear

The Encyclopaedia of Science and Technology[1] defines wear as; *'The removal of material from a solid surface as a result of sliding action'*. There are a number of different mechanisms that cause wear, many different researchers have defined various types of wear, or groups of wear mechanisms. For example Vingsbo[2] defined forty different wear mechanisms, while Archard and Hirst[3] allocated wear into two groups, either mild or severe.

Much of the well recognised historical research into wear was conducted using experimental data from pin on disc, sliding contact machines (i.e. under pure sliding conditions). At the wheel-rail interface there is a sliding/rolling contact, which has slightly different characteristics. Theories developed for sliding contact can be drawn upon and modified as necessary for rolling/sliding contact; however care needs to be taken to ensure results are converted correctly. In their study of wheel-rail interaction, Nielsen et al[4] list four wear types experienced at the rail head:

Abrasive wear - hard particles are forced against the contact surface and moved along it, effectively machining grooves in the contact surface, for example, wear of wheels and rails due to the presence of sand in the contact area.

Adhesive wear – wear due to local bonding between contacting solid surfaces leading to microscopic failures of asperities on the two bodies. Very small pieces of material from the rail surface effectively stick to the wheel and are plucked away from the rail.

Delamination wear – shear forces at the contact surface cause thin layers of material to shear away from the surface. These thin layers then subsequently break off.

Oxidation (or corrosive wear) – removal of reaction products from chemical (or electrochemical) reaction between the contact surface and the environment.

The type of wear and the wear rate are dependent on the loading characteristics. Various formulae have been developed in an attempt to predict wear rates (a selection of these are discussed in Chapter 5). There are a range of factors affecting wear rate; various models are available based on differing parameters. Some factors which may affect wear rate of the rail head due to the passing of trains are:

- Vertical load
- Tangential load
- Creep ratio
- Surface roughness
- Wheel and rail hardness
- Contact area

3.2.2 Fatigue

Fatigue is the development and propagation of cracks caused by time varying loads, which, even if globally small, are magnified (concentrated) in the vicinity of the crack such that local stresses exceed the yield limit of the material.

The rail is exposed to time varying loads due to the passing of rail vehicles; because of the nature of the contact, fatigue caused by these loads is known as rolling contact fatigue (RCF). RCF rail damage resulted in a major railway accident at Hatfield in 2000[5]. This was caused by the break up of the rail

underneath a train due to multiple RCF cracking. Because of this accident, the rest of the rail network was thoroughly inspected for RCF; a major re-railing project was initiated in order to ensure the problem would not lead to any further accidents. By studying removed rails, Dutton et al[6] made a major contribution towards characterising RCF cracks. Several other researchers have also characterised the process of crack initiation and propagation. It has been shown that cracks initially develop at an angle of 5 – 15 ° to the rail surface, and continue to do so, to a depth of 5 – 6 mm[6-8]. At this point the crack can either: turn down into the rail, resulting in a rail break; or turn up towards the rail surface causing shelling or spalling (i.e. removal of a section of material from the rail surface, this is a severe type of delamination wear). Neither of these results is particularly favourable; however if the crack does turn down into the rail causing a break, the effects can be catastrophic (as was unfortunately demonstrated at Hatfield*).

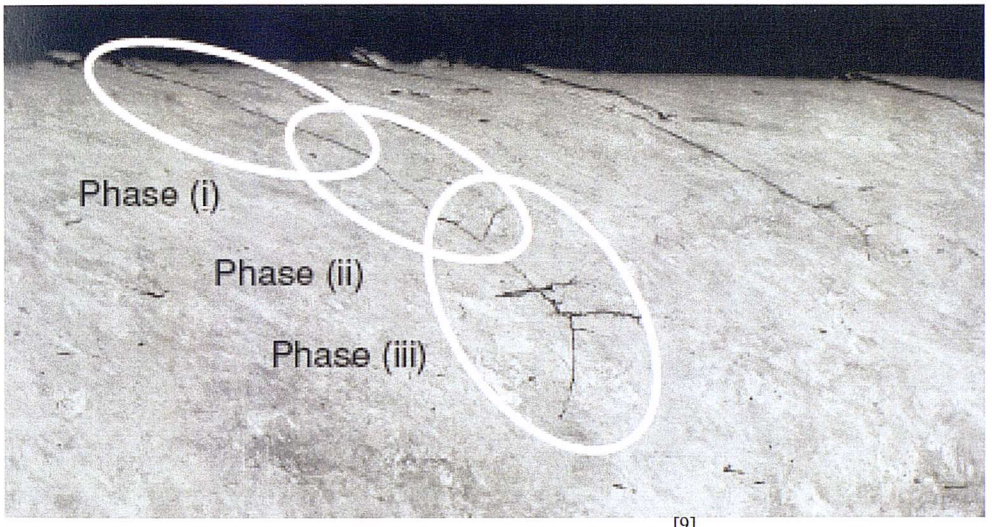

Figure 3 - 2 Surface initiated RCF crack, from a twin disc test[9]

Figure 3 – 2 shows a surface initiated RCF crack created during a twin disc roller rig experiment; as shown in the figure, Ringsberg[9] defines three phases of crack growth. The first phase being initiation and growth under shear loading, phase two is transient crack growth (i.e. a combination of phase one and phase three), and phase three is growth under rail body stress. In this case the phase three

* NB The Hatfield accident was due to multiple cracking which led to the catastrophic break up of the rail underneath the train. A single crack turning down into the rail causing a rail break would not necessarily have the same severe consequences. It is possible for a train to travel over a single break in the rail without derailing, and even if the train does derail it is also more likely to stay upright.

growth is down into the rail. RCF damage can be split into a variety of categories, such as: head checking, gauge corner cracking, spalling, squats, and shelling.

Gauge corner cracking normally occurs through curves when the wheel is running in contact with the gauge corner.

Head checking is a series of RCF initiated cracks in close succession along the rail surface (most typically these will be a series of gauge corner cracks)

Spalling is the removal of material as a result of short cracks turning up to the rail surface.

Squats are RCF damage typically witnessed on straight rail, with a group of cracks centred about a point at the top of the rail. These are usually caused by the initiation of subsurface cracking.

Shelling is the removal of bigger sections of rail material as a result of deep cracks turning up to the rail surface.

A comprehensive list of rail damage definitions along with pictures can be found in the 'International Cross Reference of Rail Defects'[10].

3.2.2.1 Shakedown

Loads are concentrated in the wheel-rail contact area, often causing stresses in excess of the yield limit. This does not however, lead to immediate catastrophic failure, but rather to the accumulation of fatigue damage. This is due to a process called shakedown, which creates a higher effective yield limit at the rail surface, known as the shakedown limit. When a new piece of rail is installed, the passing of every wheel causes plastic shear strain of the rail surface (because the loading is above the yield limit). This accumulated plastic strain leads to work hardening which increases the shakedown limit. Only loading above this new shakedown limit can cause further plastic deformation. The shakedown limit will continue to

increase with every cycle, but only up to a certain asymptotic value. Jones et al[11] suggests the shakedown limit for BS11 rail steel will reach approximately 1.9 times the original yield limit, see Figure 3 – 3.

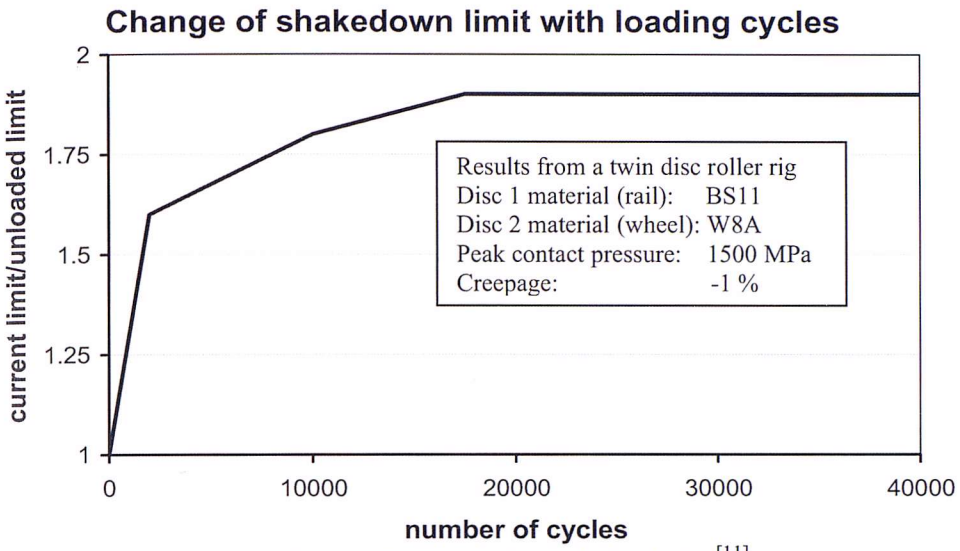

Figure 3 - 3 Change in shakedown limit cause by strain hardening[11]

This limiting value has been found to vary with the traction coefficient (F_x/F_z)[11-13], as shown in Figure 3 – 4.

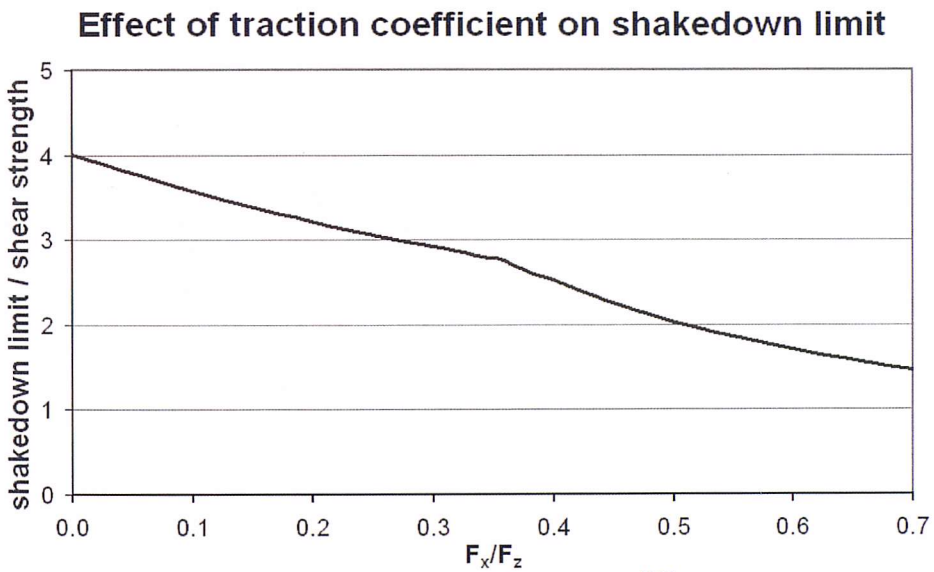

Figure 3 - 4 Shakedown map for a strain hardening material[11]

3.2.2.2 Stress distribution in the contact patch

As discussed in section 2.3, the rail is subjected to a complex loading environment. The stress distribution as a result of the contact loads is shown in Figure 3 – 5.

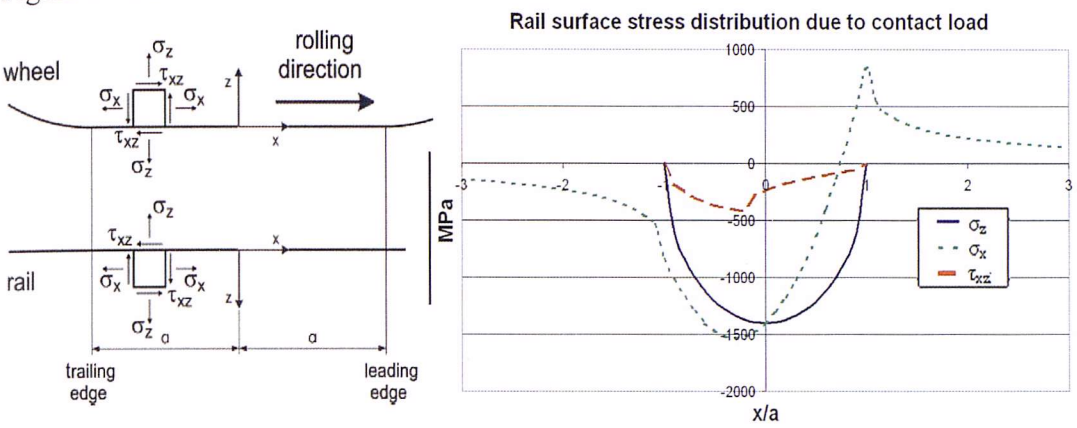

Figure 3 - 5 Stress distribution acting on the rail due to a passing wheel

3.2.2.3 Modes of crack growth

There are three modes of crack growth, driven by different loading characteristics, shown in Figure 3 - 6.

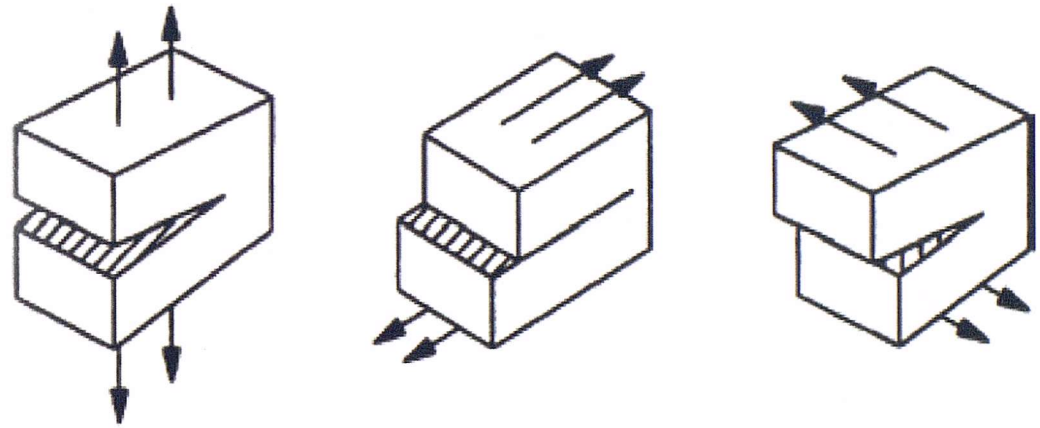

Mode I, tensile Mode II, in-plane shear Mode III, out-of-plane shear

Figure 3 - 6 Crack growth modes

At the rail surface there is typically a combination of mode I and mode II crack propagation[14], caused by stresses acting normally and tangentially to the cracks.

Crack initiation and early growth is dominated by mode II cracking due to the high shear loads at the rail surface. As the crack tip gets deeper into the rail material the bending and vertical shear stresses will start to drive crack growth.

3.2.2.4 Taking a closer look at RCF and tribological layers

Figure 3 – 5 shows the stress in the rail based on smooth wheel-rail contact, as already mentioned in section 2.4.1 highly localised stress at asperity contacts can be far in advance of the stress distributions given here. The localised high stresses act in a very thin, highly sheared layer at the top surface of the rail. The microstructure of the steel is this layer is dramatically changed due to the severe contact conditions (a distinct surface layer can be seen in see Figure 3 – 8). This layer is typically in the order of 50 μm, experiencing localised stress in the order of GPa. Below the highly sheared layer is a plastically deformed zone (Figure 3 – 8, clearly shows the microstructure has been sheared to the left, with a strong texture aligned at an angle to the rail surface). This zone will penetrate to a depth in the order of 5 mm; stresses here are in the order of hundreds of MPa. For a crack to develop it must break through the top highly sheared layer, driven by the highly localised contact stresses. The crack tip will then enter the plastically deformed zone where it will experience a different microstructure and may propagate under the Hertzian contact loads (as the highly localised asperity stresses will have been dissipated in the highly sheared layer). It is in this layer that the crack grows at an angle of 5 – 15 °, following the angle of shear. When the crack tip reaches the bottom of the plastically deformed zone, it can propagate under the influence of the elastic contact stress. However the contact stress decreases rapidly with depth. It is possible the crack stops growing at this point, however if the bulk stresses in the rail are significantly high, propagation can continue into the rail.

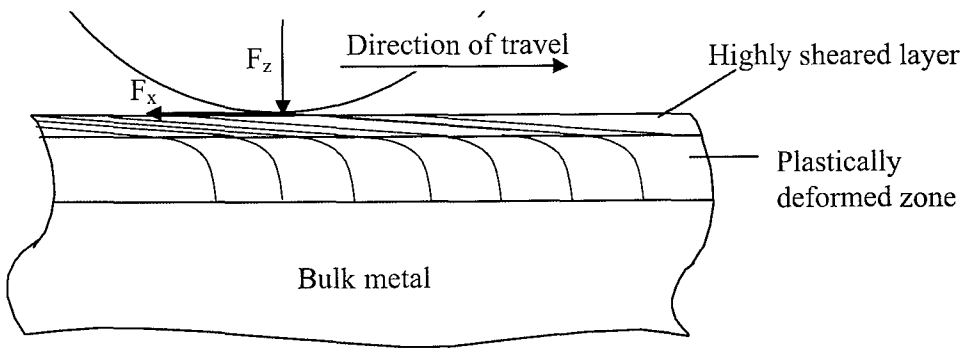

Figure 3 - 7 Tribological layers of the rail

In each layer of the rail, the crack is subject to a different stress profile and a different structure with different material properties. These three layers cause three different phases of crack growth, matching up to the three phases described

by Ringsberg and Bergkvist[15]. As a crack grows, when it reaches the boundary of a new layer (e.g. highly sheared layer to plastically deformed zone) its growth may be arrested, or if stress conditions in the new layer are adequate it may continue to grow. The exact mechanics behind this process are still not well understood.

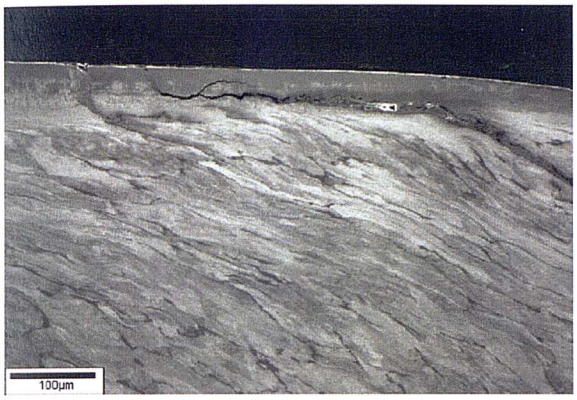

Figure 3 - 8 Highly sheared layer, and plastically deformed zone at the top of a BS EN 13674-1 grade 200 rail steel roller rig testing using 1% slip[16]

3.2.2.5 RCF and wear interaction

If material is being removed from the rail surface at a faster rate than cracks can be initiated, the crack can not propagate into the rail material. If just enough material is removed to prevent cracking, this is the so called 'Magic Wear Rate' of Kalousek and Magel[17]. This wear rate can either be achieved naturally through traffic, or introduced artificially by grinding, as discussed in Chapter 4.

In tight curves, the wear rate is higher than the crack propagation rate, because the contact loads are so severe there are high wear rates, which 'rub out' any cracks before they can propagate; this means RCF is commonly not experienced in these tighter curves. In higher radius curves the shear stresses are lower, so RCF is not initiated. This leaves mid range curves where RCF is currently most common. Curve radii of around 1500 m are the most likely to experience RCF crack damage[18].

3.2.2.6 RCF - Background

Since the Hatfield disaster, RCF has been highlighted as a problem for the UK railways and worldwide; significant spending has gone into attempting to

understand the problem. Suitable maintenance programmes, including controlled grinding, have been put in place, which along with track based lubrication are helping to control RCF. A number of major investigations into RCF have been carried out in recent years, and a variety of models have been developed to predict initiation sites and crack growth rates (although the exact process is still not completely understood). A selection of these are discussed further in Chapter 5. The factors affecting RCF are generally very similar to those affecting wear rate discussed in the previous section (unsurprisingly considering the close interaction between the two degradation modes). Some examples are:

- Vertical load
- Tangential load
- Creep ratio
- Wheel and rail hardness
- Contact area
- Sleeper spacing
- Rail cross section

3.2.3 Ballast settlement

As described in Chapter 2, one of the functions of ballast is to transmit vertical loads from the sleepers to the substructure. The contact pressures between sleeper and ballast will be in the order of 700 kPa. After an initial settling in period, new ballast is a relatively elastic foundation, transmitting vertical loads from the sleepers down to the substructure. However, over time the ballast is compacted and the contact surfaces of the stones can break off, resulting in the accumulation of 'fines' in the ballast. These 'fines' are wear material from the broken up ballast stones. As the ballast stones are compressed and small 'fines' build up in the gaps between the stones, the ballast loses its flexibility and becomes less effective at distributing the loads applied through the sleepers. Figure 3 - 9 shows the various types of ballast deterioration (as defined by Dalhberg[19]).

The rate of ballast settlement is dependent on the vertical load experienced by the ballast. If the ballast settled at a constant rate along the whole route, this in itself would not be a major problem. However, due to its nature, ballast is not a

homogenous material, and the vertical loads generated along the track are also not constant. This means certain parts of the ballast are compressed more than others, resulting in vertical geometry deficiencies. This deterioration can be self perpetuating, as the geometry deficiencies cause further dynamic loading, which results in uneven rail wear and further uneven ballast settlement.

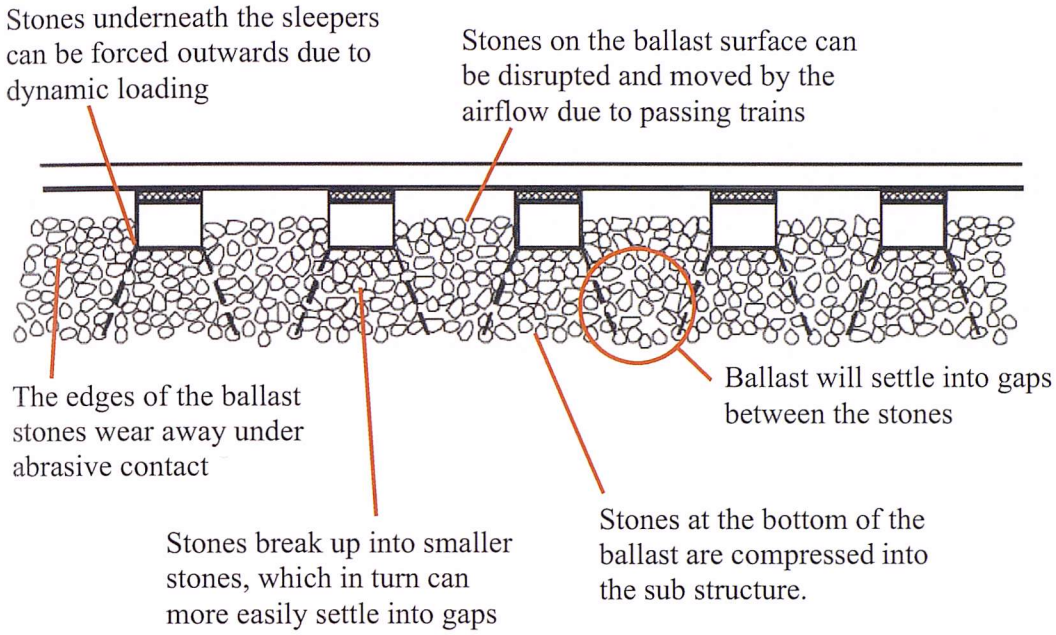

Figure 3 - 9 Degradation of ballast

The settlement rate is not constant over time, and will occur in 3 phases. When new ballast is first installed, it will go through a phase of rapid settlement as the ballast is consolidated, with the stones rearranging to reduce the gaps between them. After this the settlement is slower with a more direct relationship to cumulative loading. During this second phase the ballast continues to be rearranged, reducing gaps between the stones, small particles are worn away where the stones meet, and stones start to break up[19]. At some point the ballast will lose its elasticity, meaning it can not be compressed any further. This can lead to rapid failure of the ballast, causing the stones to break up and become further compressed into the subgrade.

The rate of ballast settlement and useful ballast life are dependent on a number of factors, listed below. In the example used for Figure 3 – 10, rapid ballast

settlement starts to occur after 10^5 loading cycles*. In practice ballast lasts much longer than this because tamping is carried out to return the ballast to a suitable working condition before it reaches this state (discussed further in Chapter 4). However the ballast can only be tamped a limited number of times before it is life-expired. After a certain time the average stone size will have reduced, and the accumulated 'fines' will clog up the ballast; tamping will no longer return the ballast to an acceptable condition. Depending on the operating conditions the time this takes can vary considerably†.

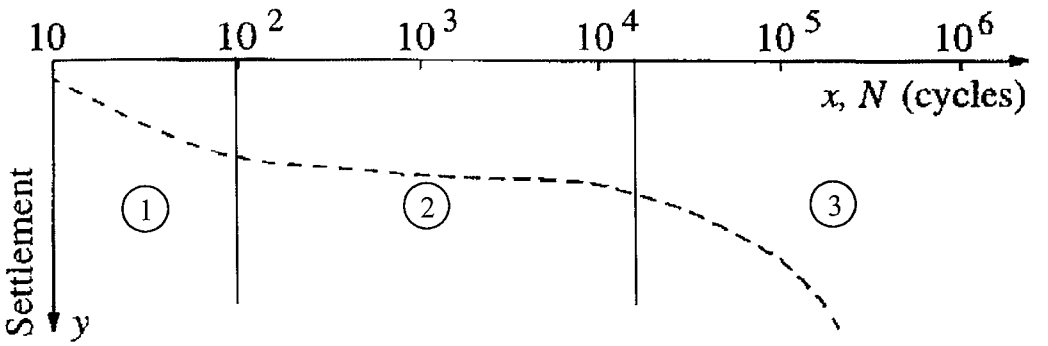

Figure 3 - 10 Example stages of ballast settlement, modified from[19]

As with the other degradation modes, various ballast settlement models have been proposed, which are discussed further in Chapter 5. Factors affecting ballast settlement are:

- Sleeper/ballast pressure
    - which is affected by:
        - Vertical rail loading
        - Sleeper size
        - Rail pad characteristics
- Average stone size
- Subgrade stiffness
- Number of times already tamped
- Presence of water

* Based on the curve in Figure 3 - 10 a piece of track carrying three, nine car IC125 trains per hour, for 20 hours a day, this ballast would last roughly 1.5 years.

† An example ballast life of 60 mega gross tonnes, with that ballast having been tamped 3 times is given in [20].

3.3 Discussion

In this chapter the three main traffic based degradation modes have been identified; their characteristics and causes have been discussed. The introduction of 'steering bogies' should reduce the degradation rate of some of these modes. All modes can also be reduced through other methods, as we can see by looking at the factors which cause them, listed at the end of each section.

The tangential load reductions achieved with the use of 'steering bogies' should help to reduce the rates of wear and fatigue damage. To completely evaluate the benefits (or disbenefits) of using steering bogies, track settlement also needs to be understood. This is because some types of steering bogie may be heavier (or in some cases possibly lighter), which will affect the rates of ballast settlement. Methods of calculating the rate of degradation of the three modes included in this chapter are discussed further in Chapter 5.

The benefits of reducing track degradation rates will be the savings that can be made on maintenance and renewals spending. The following chapter discusses the current maintenance and renewal strategies, spending on these activities and how this fits into the overall cost of the UK railways.

References

1. Trefil, J., *Concise Encyclopedia of Science and Technology*. Fifth ed. 2004: McGraw-Hill.
2. Vingsbo, O. *Wear and wear mechanisms*. in International Conference on Wear of Materials. 1979. Dearborn, Michigan: American Society of Mechanical Engineers.
3. Archard, J.F. and W. Hirst, *The wear of metals under unlubricated conditions*. Proceedings of the Royal Society of London, Series A, 1956. **236**: p. 397 - 410.
4. Nielsen, J.C.O., et al., *Train-track interaction and mechanisms of Irregular wear on wheel and rail surfaces*. Vehicle System Dynamics, 2003. **40**(1 - 3): p. 3 - 54.
5. ORR, *Hatfield Derailment Investigation: Interim Recommendations of the Investigation Board*, http://www.rail-reg.gov.uk/upload/pdf/incident-hatfield-investigationb1.pdf#search=%22hatfield%20rail%20disaster%20rcf%22, [Accessed, 6/9/06]
6. Dutton, J.T., et al., *Measurement of crack depths in a section of head hardened rail, in Post Hatfield rolling contact fatigue*. 2005, Office of Rail Regulation: Health & Safety Laboratory.
7. Bhangale, V., A. Kumar, and S.O. Dwivedi, Indian Railways Institute of Civil Engineering, *Development of rolling contact fatigue and its prevention*, http://www.iricen.gov.in/projects/725/rcf.pdf, [Accessed, 13/12/07]
8. Smith, R.A., *Railway fatigue failures: an overview of a long standing problem*. Materialwissenshaft und Werkstofftechnik (Materials Science and Engineering Technology), 2005. **36**(11): p. 697 - 705.
9. Ringsberg, J.W., *Life prediction of rolling contact fatigue crack initiation*. Interational Journal of Fatigue, 2001. **23**(7): p. 575 - 586.
10. Cannon, D.F., *UIC D229/RP3, An international cross reference of rail defects*. 2001, International Union of Railways.
11. Jones, C.P., et al., *The effect of strain hardening on shakedown limits of a pearlitic rail steel*. Proceedings of the IMechE Part F: Journal of Rail and Rapid Transit, 1997. **211**(2): p. 131-140.
12. Bohmer, A., M. Ertz, and K. Knothe, *Shakedown limit of rail surfaces including material hardening and thermal stresses*. Fatigue & Fracture of Engineering Materials and Structures, 2003. **26**(10): p. 985-998.
13. Ekberg, A. and E. Kabo, *Fatigue of railway wheels and rails under rolling contact and thermal loading-an overview*. Wear, 2005. **258**(8): p. 1288 - 1300.
14. Bogdanski, S. and M.W. Brown, *Modelling the three-dimensional behaviour of shallow rolling contact fatigue cracks in rails*. Wear, 2002. **253**(1 - 2): p. 17-25.
15. Ringsberg, J.W. and A. Bergkvist, *On propagation of short rolling contact fatigue cracks*. Fatigue & Fracture of Engineering Materials & Structures, 2003. **26**(10): p. 969 - 983.

16. Carroll, R.I. and J.H. Beynon, *Rolling contact fatigue of white etching layer: Part 1 crack morphology.* Wear, 2007. **262**(9 - 10): p. 1253 - 1266.
17. Kalousek, J. and M. Magel, *Achieving a balance: The 'magic wear rate'*, Railway Track and Structures, March 1997, p. 50 - 52
18. Doherty, A., et al., *Why rails crack.* Ingenia, 2005. **23**: p. 23 - 28.
19. Dalhberg, T., *Some railroad settlement models - a critical review.* Proceedings of the IMechE Part F: Journal of Rail and Rapid Transit, 2001. **215**(4): p. 289 - 300.
20. Jovanovic, S. and M. Pearce, *ECOTRACK: An overview of the system's functionality and implementation to date*, in AREMA 2000 Annual Conference. 2000: Dallas.

Chapter 4: Maintenance and renewals spending

When attempting to reduce the operating cost of a system, it is first necessary to understand how money is currently being spent on the system; what are the fixed costs? and where are the opportunities for savings? By introducing more 'track-friendly' trains, it should be possible to reduce spending on maintenance and renewal of track. This chapter reviews the existing spending on railway track and how this fits into the overall system cost.

4.1 Railway spending

Provision of railway infrastructure accounts for 30 - 50 % of total costs in rail transport[1]*. Western European railways currently operate more than 200,000 km of track, with annual spending on renewal and maintenance in the order of €10 – 15 billion[1] (£7 – 10 billion). The Union Internationale des Chemins de fer (UIC)† has suggested that there is a significant opportunity to reduce infrastructure cost; it has proposed the 'factor 3 formula'[1], which means doubling capacity whilst simultaneously halving infrastructure cost. Achieving this would make a significant contribution towards the economic success of the railways.

To achieve this 'factor 3 formula', improvements need to be made across a range of areas, including: efficiency of the maintenance and renewal task; planning and management of maintenance; and also reducing traffic-dependent track degradation as discussed in section 3.1. Improving the track friendliness of trains may not achieve the UIC objective on its own, but should make a significant contribution.

4.1.1 UK spending breakdown

As stated in section 1.1 the UK railway industry is currently spending £9 billion per year. £6 billion of this is provided as a government subsidy (based on

* i.e. The cost of maintaining and renewing existing infrastructure (not including the cost of building new infrastructure)
† International Union of Railways

2006/07 figures), while the remainder is generated as income through passenger fares and other activities. See Figure 4.1 for a spending breakdown*.

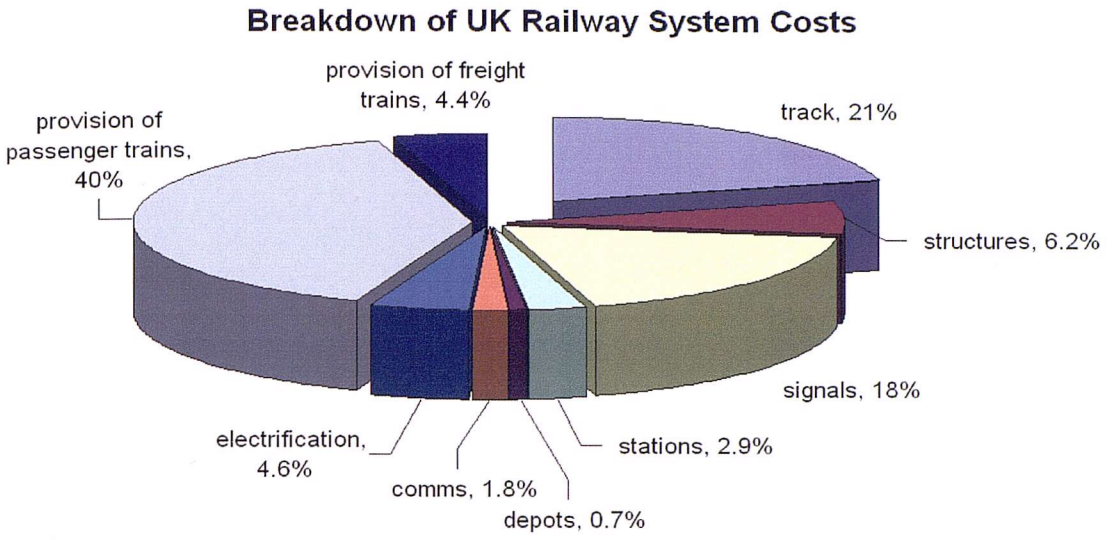

Figure 4 - 1 UK Railway System Costs, data from [2-4]

In line with Bente's European wide figures[1], roughly 50 % of spending is on the provision of infrastructure. This is split up into, track, structures, signals, stations, depots, communications and electrification equipment. The provision of track (maintenance and renewals)† contributes 21 % toward the total cost of the system. How much this can be reduced, by introducing more 'track-friendly' trains still needs to be assessed.

4.1.2 Accounting and availability of information

It can be difficult to assess the economic performance of the UK railway system as a whole to any level of detail. The rail system does not exist as a single economic entity, but a variety of companies working in their own areas. Infrastructure is owned and maintained by Network Rail, with a number of Train Operating Companies (TOCs) managing the trains and stations under franchise agreements. Network Rail is a "not-for-profit" company, while all of the TOCs

* NB all staff costs are allocated to the appropriate asset area, so the cost of employing a train driver/maintainer is included on the provision of trains, and the cost of employing track maintainers is included in track, etc.

† i.e. Not including the cost of building new routes

are private companies. All the railway companies publish a certain amount of financial information in their annual reviews. However, they typically do not publish, in any significant level of detail, how much is being spent on specific maintenance and renewal activities. For example, the data for Figure 4 - 1 has been collated from three different sources and extrapolated as necessary to give an approximation of the overall picture. Detailed budget sheets showing where the money is being spent are not generally available, partially because this type of record is not always kept, but also because of the secrecy of the various companies involved in the rail industry. For example, of the 21 % total being spent on track, exactly how much is spent on the different types of maintenance activity is not specified.

The costing information presented in this chapter is drawn from a variety of sources, in an attempt to give an overall picture of the system and how different areas contribute towards the total costs. The railways industry, particularly in the UK, still has a long way to go to fully understand its costs, this really needs to be achieved before any significant efficiency savings can be recognised.

4.2 Fixed and variable costs

As stated in section 3.1, railway track degrades because of the environment it is placed in*, and also due to the passing of traffic. Once a section of rail is installed, even if no trains operate on that section, there will be a fixed cost to the infrastructure manager to maintain the rail condition in response to environmental degradation. As more trains are run an additional variable cost will be incurred (see Figure 4 - 2).

The numbers presented here are averages for a typical railway. In reality each route has its own characteristics, with a different route profile, line speed and rolling stock mix. However, the relationships presented here can be used to give an overall picture of the trend in track cost, depending on traffic density.

* Including the effects of corrosion, ingress of vegetation and drainage problems

Service densities on UK mainline routes are typically up to 10 mega gross tonnes per annum (MGT pa)* [5]; this is relatively low compared to a high density mass transit system, or a heavy haul freight railway. For the lowest density lines, the traffic-dependent (variable) cost is only a small proportion of the overall spend on track maintenance and renewals. For these lines, the benefits of improving 'track friendliness' of trains would have a minimal impact on the overall operating costs. It may be more effective for these lower density railways to achieve cost savings through other methods.

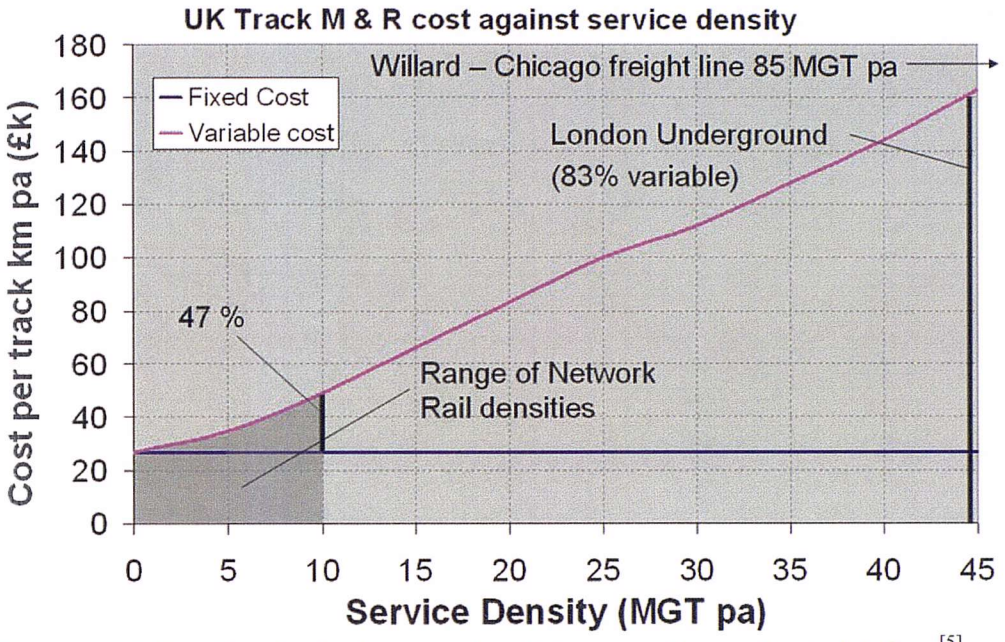

Figure 4 - 2 Effect of service density on track maintenance and renewal cost, data from[5]

For London Underground routes operating at 44 MGT pa†, track cost is 83% traffic-dependent, according to this analysis. For heavy haul freight railways, such as the Willard – Chicago line, service densities can reach 85 MGT pa[6]; the traffic-dependent costs will dominate for a route of this nature. For these types of railway it is important for the operators to ensure each of their trains is causing the minimum damage possible; there is significant opportunity for cost savings by improving the 'track friendliness' of their rolling stock. At the top end of the Network Rail service densities, track costs are 47 % traffic-dependent. For these lines it should also be possible to make significant reductions to the overall cost

* i.e. The total mass of trains travelling over any position on the track is up to 10 million tonnes per year, or roughly 250,000 rail cars.

† Figure based on 30 trains per hour, 18 hours a day, 8 car trains weighing 22 tonnes per car

by using 'track-friendly' trains. Further analysis is required to estimate what is achievable.

4.3 Track maintenance and renewal activities

As described in section 2.2, railway track is made up of a variety of components, including rails, sleepers and ballast. Each of these components have their own life cycle, they need to be replaced as they become life-expired and maintained during their life to continually provide the necessary function.

Rails have a typical service life of 500 – 600 MGT[7]*, while ballast has a service life of 60 MGT[8]. So for a 10 MGT pa railway, rails would last approximately 50 years, while the ballast needs to be replaced every 6 years, and sleepers typically need to be replaced every 40 years[9].

However, rails in curved sections have a considerably lower service life (see Figure 4 – 3), introducing steering bogies should extend the replacement interval for these sections.

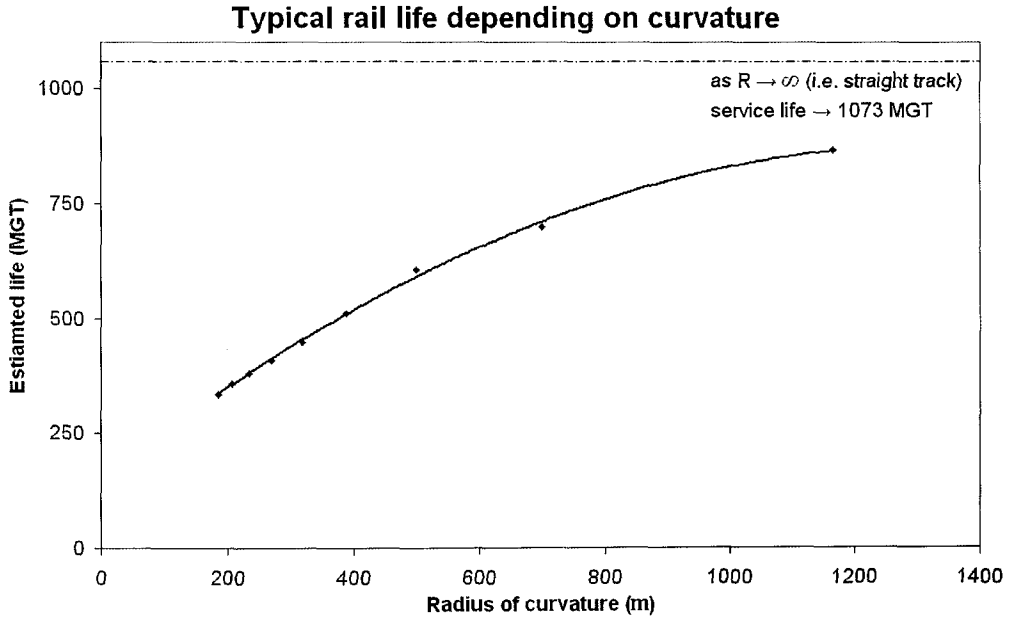

Figure 4 - 3 Estimated rail life against curvature, data from [10]

* Various sources suggest a range of different rail lives, presumably because it can vary significantly depending on service conditions. As shown in Figure 4 – 3, an alternative source suggests a service life of 1073 MGT for straight rail.

As well as periodically replacing the various track components, regular maintenance activities are carried out.

The principal track maintenance activities for railway track are[11-14]:

Rail Grinding is a method of removing the top layer of the rail, primarily to remove material containing fatigue cracks, in order to prevent them from propagating further into the rail; it is also used to remove corrugations and to restore the rail profile after uneven wear. Grinding is normally automated with the grinding stones mounted on engineering trains. Manual grinding is also carried out over short sections to locally restore track conditions or around points and crossings.

Track based lubrication is used in tight curves, to reduce wheel and rail wear. This is achieved by lowering the coefficient of friction between wheel and rail, limiting the maximum creep loading*.

Tamping is conducted to correct alignment and level of the ballast after settlement caused by the passing of traffic. Again, this is an automated process conducted using specialised engineering trains. Groups of adjacent sleepers are lifted and the ballast is vibrated mechanically to return the formation to the correct level.

Track Stabilisation restores the lateral resistance of track to suitable levels (tamping and ballast settlement can lead to loss of lateral resistance, which needs to be corrected). The track is vibrated in a lateral direction whilst a vertical load is applied to ensure sleepers are well located in the ballast; this can be carried out at the same time as tamping

Ballast Injection (Stoneblowing) is a method of adding extra ballast to the formation after settlement.

* As stated in section 2.4.2, this method can be used to reduce rail damage through curves, rather than the use of 'steering bogies'. However, steering bogies should give more consistent results and are not expected to require the same maintenance effort. Also maintaining remote track based equipment is typically more expensive than maintaining train mounted equipment at the depot.

Ballast cleaning is used to remove 'fines' from the ballast, this is carried out with a specialised engineering train that excavates ballast from under the track, passes it through a series of sieves to remove the smallest particles and then returns the larger stones to the ballast bed. New ballast is added to make up for the material removed by the process.

4.3.1 Programmed or condition based maintenance

Traditionally railways have built up programmes of maintenance through trial and error over the years, finally coming up with a programme of maintenance and renewal based on fixed time intervals or cumulative traffic. For an established railway system, with known risks and well understood failure mechanisms, this approach can provide a suitably low-risk strategy. However, problems can arise when unexpected failure modes start to occur, such as the RCF damage that led to the Hatfield disaster mentioned in section 3.2.2. Conversely, infrastructure companies can easily over maintain their track, if they continue to use fixed interval maintenance and renewals without fully understanding the degradation modes they are attempting to prevent.

Condition based maintenance relies on thorough, up to date knowledge of all assets within the infrastructure. This can be achieved through regular inspection, either manual/visual or mechanised.

Many railways are still using fixed interval maintenance; however, there has been a shift towards the condition based approach. On the UK mainline routes, track geometry (largely dependent on ballast settlement) is monitored using the 'New Measurement Train' (NMT) [15], and fatigue damage is monitored using an ultrasonic test vehicle, UTU2[16]. Data from these vehicles can be used to develop maintenance and renewal plans for ballast and rails.

4.3.2 Track maintenance and renewal spending

It is difficult to obtain a detailed breakdown of spending for the different track maintenance and renewal activities; however, a study has recently been published by BSL Management Consultants[17]. Total Network Rail expenditure on track in

2007/08 was £1,356 million (£42,000 per track km pa*), split 33%:67% between maintenance and renewals[17].

NB This figure is lower than the £1.8 billion presented in Figure 4 – 1, which is based on the previous financial year (2006/07). The estimates for Figure 4 – 1 include Network Rails overheads which were not included in the BSL study. Because of the lack of available economic information and accounting transparency, it is difficult to explain the differences any further.

In the BSL study, there is no further breakdown of the renewals activities beyond rail, sleeper and ballast. Ballast maintenance is shown as 6% of the total, which is made up of tamping, stone blowing, ballast re-profiling and geometry correction. Rail maintenance includes, ultrasonic inspections, weld repairs and rail changing†. Rail grinding and track-based lubrication are not included in the rail maintenance cost; presumably, they are part of 'other track maintenance'.

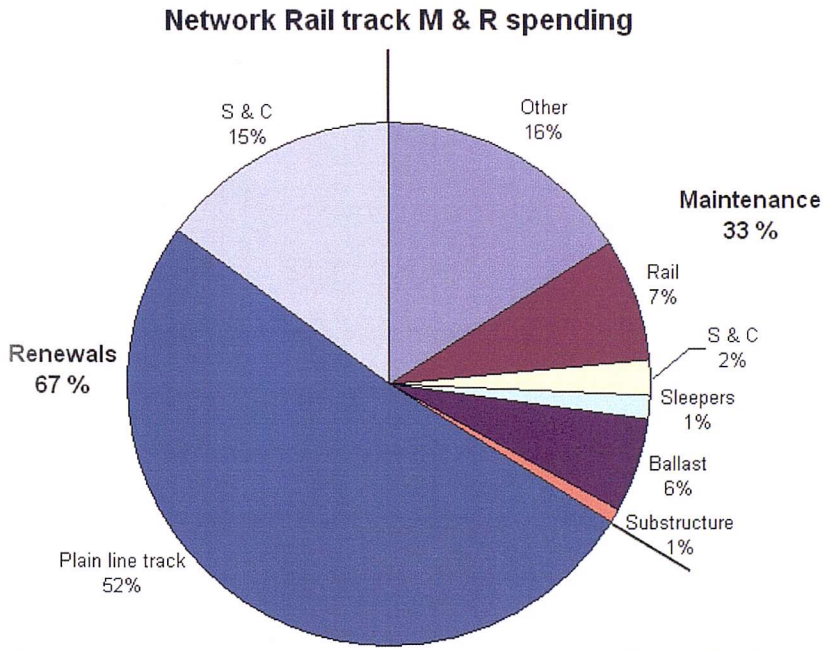

Figure 4 - 4 Breakdown of track maintenance and renewals spending based on 2007/08 figures, data from[17]

This research is focused on the achievable cost benefits of reducing tangential track loading through the use of steering bogies. This should reduce rail damage

* As the network is made up of 32,000 track kms[18]
† Changing short sections of rail because of localised damage

through curves, so there should be reductions in the necessary track renewals, rail changing, grinding and track based lubrication.

4.4 How does RCF damage contribute towards the overall costs?

Tunna et al[19] suggest that the total contribution of traffic dependent degradation causes £242.4 million worth of track maintenance and renewals work. This makes up 18% of the total track maintenance cost given by BSL[17]. This correlates well with the EWS study[5] which suggests that, at average Network Rail service densities (of 5 MGT), the traffic dependent degradation will be approximately 20% of total track cost.

Tunna suggests 30 % of the traffic dependent track maintenance cost (£73 million pa) is due to 'rail surface damage', which is defined as RCF, squats and wear. Reducing tangential wheel-rail loading should reduce these degradation modes, consequently reducing the contribution they make to the overall maintenance and renewals spending. Exactly what saving can be achieved still needs to be quantified.

Tunna suggests that the total cost of 'rail surface damage' (as defined above) is £106.9 million, but only £73 million of this is 'assumed to be variable with traffic'. RCF, wear and squats do not occur because of environmental factors, the justification for suggesting only a portion of the total is due to traffic remains unclear.

As already mentioned in Chapter 2, the tangential wheel-rail loading caused by a rail vehicle currently has no bearing on how much a train operator has to pay the infrastructure company to operate vehicles over its tracks; however, Tunna et al[19] suggest a method to include this, which is discussed further in section 5.5.3.

4.5 International comparison of maintenance and renewal spending

According to the UIC Lasting Infrastructure Cost Benchmarking (LICB) exercise, carried out by BSL Management Consultants in 2008[17], Network Rail is currently the most inefficient infrastructure manager in Europe*. The LICB compared infrastructure spending across Europe and also included the Amtrack North-East Corridor. Network Rail's expenditure per mile is more than double the average, as shown in Figure 4 – 5.

It is difficult to compare railway economics across a variety of countries operating completely different types of railways across greatly differing geographies. Further to this, there are many factors that will affect spending, such as: local labour markets, availability of resources, network complexity, asset age and passenger density. Most of these factors are largely outside the control of the current asset managers.

The LICB claims to have accounted for some of these differences by *'applying normalisation based on: comparative price levels, network complexity and network utilisation'*[17]. How effective this normalisation has been, and whether the numbers presented here are truly a fair comparison remains unclear. However, due to the magnitude of difference in the cost, it certainly suggests that Network Rail has significant room for improvement in its cost management.

Network Rail is already planning to reduce this spending gap, by improving the efficiency of its maintenance and renewals operations[20]. To make further improvement in order to work towards the UIC factor 3 formula†, all infrastructure managers will have to work with train operators to ensure the whole system is working together in an effective and efficient manner. This requires an increased understanding of train-track interaction, and the damage caused to all components during the operation of a train service.

---

* Based on spending per track mile
† As mention in section 4.1

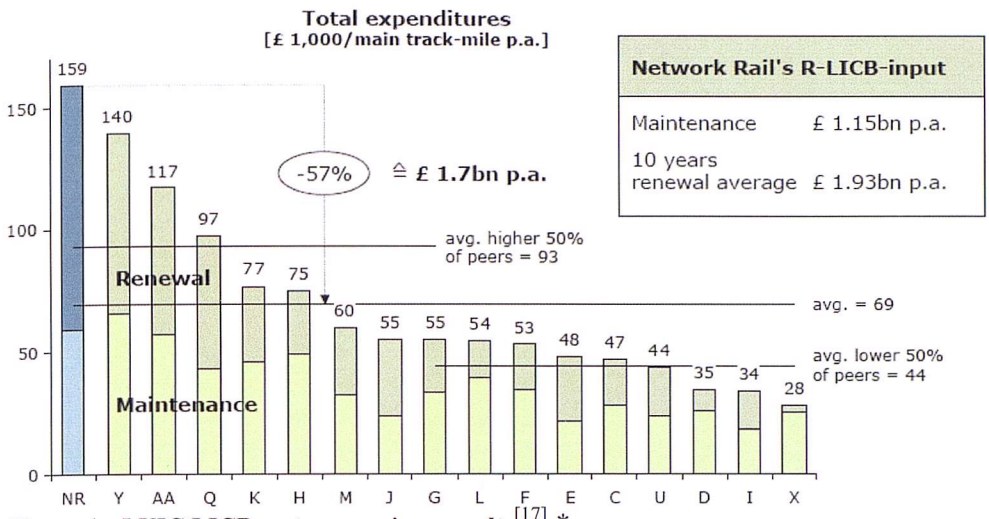

Figure 4 - 5 UIC LICB cost comparison results[17] *

4.5.1 Other cost comparison studies

A variety of other international comparisons have also been published, all using different comparison metrics, showing a range of different results. For example Thompson and Perkins[21] compared the infrastructure cost per train km, which is perhaps a more useful comparison (than £/track-mile), and suggests the UK railways are spending an average amount compared to the rest of Europe (see Figure 4 – 6).

These results give a very different picture to the LICB study, Thompson and Perkins are comparing cost per train mile rather than cost per mile of track; however, the LICB study claims to have normalised their data, taking into account network utilisation. It is difficult to say which study is more accurate; however, the large discrepancy in comparative results highlights the need for further work in this area, with comprehensively defined comparison metrics and a clear understanding of how the results can be applied.

* The numbers presented here are total infrastructure spend, track is suggested to contribute 40 % of this total, which matches up with the data presented in Figure 4 – 1.

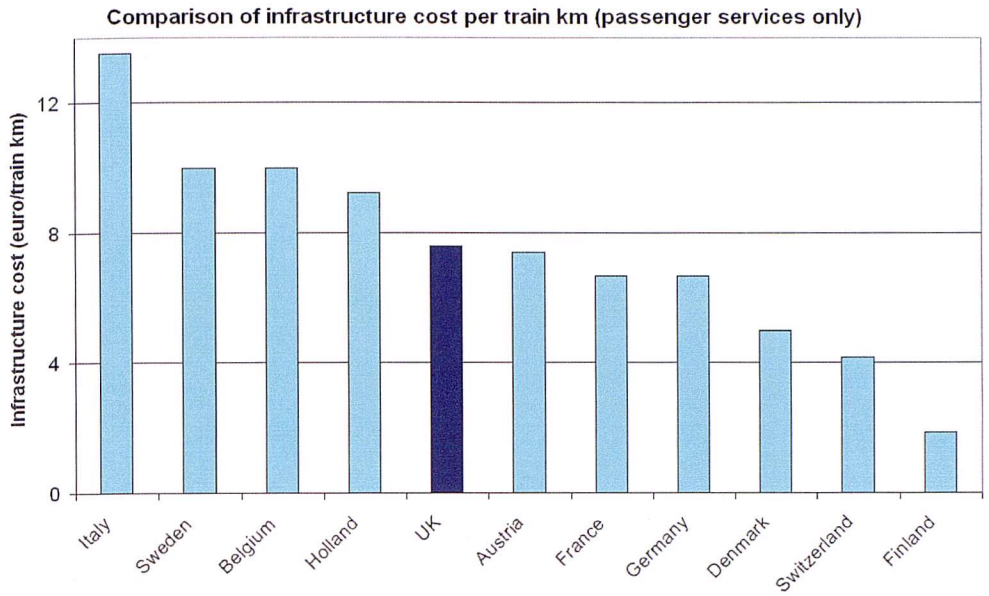

Figure 4 - 6 European railways infrastructure cost comparison[21]

4.6 Vehicle life cycle cost

The purpose of this research is to reduce the cost of track maintenance and renewals, by introducing a design change to rail vehicles. From a vehicle perspective, the damage to track caused by a rail vehicle can be allocated to the vehicles life cycle cost. A brief analysis has been carried out to compare how this cost of damage compares with the other vehicle costs. The UK class 170, three car DMU has been taken as an example; train purchase price, train maintenance, track damage cost and fuel cost have been reviewed and compared. Over a 30 year service life a total cost of £16 million is estimated, divided between the four areas as shown in Figure 4 – 7.

As already stated in section 4.1.2, it is difficult to obtain detailed costing statistics for the UK railways; data for the costing analysis shown in Figure 4 – 7 was obtained from a variety of sources in order to build up an estimate of the overall picture. This is based on a three car class 170 DMU, which travels 250,000 miles per annum over a service life of 30 years. Train purchase price is taken from 'The comprehensive guide to Britain's Railways'[24]; train maintenance cost is based on an average maintenance cost per car, derived from figures presented in Central Trains 2005 annual accounts[23]; track damage cost is based on the track access charge for this type of train[22]; while fuel usage is based on the average fuel

consumption for this type of train as suggested by Hinde and Larsson[26] and a diesel cost of 46 pence/litre[25]*.

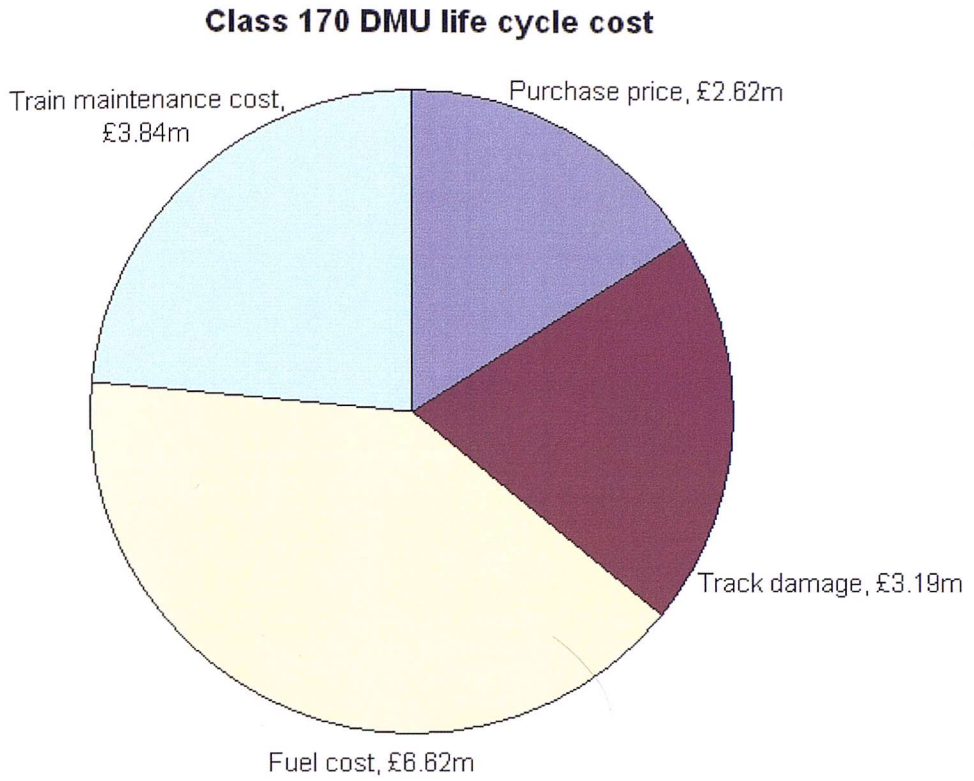

Figure 4 - 7 Life cycle cost of a three car class 170 DMU, data from [22-26]

NB For this analysis no adjustments have been made for inflation now or in the future, and no factors have been included to modify future spending in terms of net present value (NPV).

As demonstrated in Figure 4 – 7 the major cost component over the life of this rail vehicle is the fuel cost, while the original purchase price makes up only 16% of the whole life cost. Track damage is 20% of the total, whilst train maintenance is 24 % of the total.

Any benefits in reduced track damage, achieved through the use of 'track-friendly' trains, must not be completely negated by an increased cost of manufacturing those 'track-friendly' trains. A complete cost-benefit analysis needs to be carried out, including increased manufacturing costs, in order to make

* This is the 2008, quarter one diesel cost.

a fully informed decision on the benefits of 'track-friendly' trains. This research will makes steps towards that by estimating the cost benefits of various types of steering bogie, in terms of track maintenance and renewals (as detailed in the following chapters).

4.7 Discussion

The cost of providing track makes up a significant proportion of the overall system cost of a railway. By reducing the cost of infrastructure a notable reduction in the overall system cost of the railway can be achieved.

Cost can be reduced by improving the planning of maintenance and renewal activities, and operational efficiency. Better understanding of the component degradation modes can lead to a more effective condition-based maintenance scheme. With more knowledge of how components degrade, the most effective intervention point can be identified. Degradation models are discussed further in Chapter 5.

To achieve significant reduction in the cost of maintaining infrastructure, the interaction between trains and track needs to be optimised. Degradation of the ballast can be reduced by light-weighting of trains, specifically of the unsprung mass; whilst rail wear and fatigue can be reduced by decreasing tangential and vertical rail loading. This research focuses on attempting to reduce tangential track loading through curves through the use of steering bogies, in order to reduce wear and fatigue. The cost benefits of this are analysed and discussed further in Chapter 8.

The cost of rail wear and fatigue is £107 million per annum across the UK rail network, roughly 40% of the traffic dependent track damage cost. If this can be halved through the use of trains with reduced tangential loading, a significant reduction in traffic based track damage can be achieved. This is small compared to the total railway expenditure of £9 billion per annum, and will certainly not cause a step change in the economic position of the railways. However, all efficiency improvements can make a contribution to the larger system.

References

1. Bente, H. and J. Luking, *The Cost of Railway Infrastructure: Status quo and ways ahead*, Innovations for a cost effective Railway Track, November 2001, p. 22 - 27
2. *Railtrack's expenditure needs 2001 - 2006*. 1999, Booz Allen & Hamilton.
3. Strategic Plan. 2003, Strategic Rail Authority.
4. Department for Transport, *Railway Finance*, http://www.dft.gov.uk/?view=Filter&h=m&m=4552&s=5196&pg=1, [Accessed, 5/5/07]
5. Smith, G., *Detailed comments by English Welsh & Scottish Railway on the periodic review 2008 consultation on caps for freight track access charges*, http://www.ews-railway.co.uk/news/downloads/EWS%20-%20ORR%20letter%20to%20Tim%20Griffiths%2029%2001%2007.pdf, [Accessed, 5/4/07]
6. Madelin, K., et al., *A Prototype Expert System for Railway Track Renewal and Maintenance*, http://www.railway.bham.ac.uk/expert.htm, [Accessed, 21/11/06]
7. Profillidis, V.A., *Railway Engineering*. 2nd ed. 2000, Aldershot: Ashgate. p 33.
8. Jovanovic, S. and M. Pearce, *ECOTRACK: An overview of the system's functionality and implementation to date*, in AREMA 2000 Annual Conference. 2000: Dallas.
9. *Technical plan, Section 9: Plans by asset type*. 2003, Network Rail.
10. Cannon, D.F., et al., *Rail defects: an overview*. Fatigue & Fracture of Engineering Materials and Structures, 2003. **26**(10): p. 865-886.
11. Higgins, A., L. Ferreira, and M. Lake, *Scheduling rail track maintenance to minimise overall delays*, in The 14th International Symposium on Transportation and Traffic Theory. 1999: Jerusalem.
12. Esveld, C., *Modern Railway Track*. 2nd ed. 2001, Zaltbommel: MRT-Productions.
13. *Network Rail's rock solid investment in new ballast cleaner*, http://www.networkrailmediacentre.co.uk/Content/Detail.asp?ReleaseID=3569&NewsAreaID=2&SearchCategoryID=2, [Accessed, 15/5/08]
14. Cope, G., *British Railway Track*. 6th ed. 1993: The Permanent Way Institution.
15. Hughes, M., *Intensive inspection at high speed*. Railway Gazette International, 2003. **158**(7): p. 441 - 442.
16. Clark, R., *Rail flaw detection: overview and needs for future developments*. NDT & E International, 2004. **37**(2): p. 111 - 118.
17. Bente, H., T. Kindler, and K. Wittmeier, BSL management Consultants GmbH & Co. KG, *Rail Infrastructure Cost Benchmarking: Brief LICB-gap analysis and cost driver assessment*, http://www.networkrail.co.uk/browse%20documents/StrategicBusinessPlan/Update/Cost%20benchmarking%20assessment%20(BSL).pdf, [Accessed, 19/5/08]

18. Transport Watch UK, The *case of rail by Railfuture - A critique by Transport-Watch*, http://transwatch.co.uk/transport-case-for-rail.htm, [Accessed, 1/6/08]
19. Tunna, J. and R. Joy, TTCI(UK), *Methodology to calculate variable usage charges for control period 4, UK NR report No. 08-002*, www.networkrail.co.uk/browse%20documents/StrategicBusinessPlan/Update/TTCI%20(UK)%variablecharges%methodology.pdf, [Accessed, 25/6/08]
20. Network Rail, *Strategic business plan update control period 4*, http://www.networkrail.co.uk/browse%20documents/StrategicBusinessPlan/Update/Strategic%20Business%20Plan%20April%20update.pdf, [Accessed, 18/5/08]
21. Thompson, L. and S. Perkins, *Mixed signals on access charges*. Railway Gazette International, 2006. **162**(1): p. 27 - 29.
22. Office of the Rail Regulator, *Track usage price list*, http://www.rail-reg.gov.uk/upload/pdf/arev-price_list1_19dec.pdf, [Accessed, 8/8/08]
23. *Rail Industry Monitor*, ed. C. Cheek. 2005, Skipton: TAS Publications & Events Limited.
24. *The Comprehensive Guide to Britain's Railways*. Ninth ed, ed. P. Dunn. 2006, Peterborough: EMAP Active Limited.
25. *Energy Prices and Taxes (Quarterly)*. 2008 (Q1), International Energy Agency: IEA Statistics.
26. Hinde, P. and C. Larsson, *The energy consumption of rail vehicles in Britain*. October 2006, A joint study by ATOC, Bombardier Transportation & National Express Group, with support of IMechE & Network Rail.

Chapter 5: Existing degradation and costing models

The purpose of this research is to investigate the financial benefits of reducing tangential track loading through the introduction of steering bogies. Once the load reductions that can be achieved with steered bogies have been calculated, it is necessary to predict the possible reduction in track degradation; the consequent savings in maintenance and/or extension of component lives can then be estimated. This chapter discusses methods of calculating track degradation based on wheel-rail loading, as well as introducing some existing costing models.

The benefit of introducing steering bogies should be the reductions in wear and surface fatigue of the rail, as these degradation modes are the most dependent on tangential loading. Some of the steering bogies may be heavier than a conventional bogie which will influence the rate of ballast settlement, so it is also necessary to consider this degradation mode.

This chapter identifies and discusses degradation models for wear, fatigue and ballast settlement*. The modelling techniques and required inputs are discussed along with their suitability for use as part of a study looking at the effect of introducing new technology to modify wheel-rail loading.

In order to be useful for an investigation of this nature, degradation models must:

- Give a suitable output that can be linked to the physical progress of degradation (i.e. a damage index is not useful unless that index can be linked to a real rate of damage in suitable units, or in some way linked to the maintenance requirement generated by that damage).
- Show a reasonable relationship between outputs and measured results from in-service data or physical models.

* NB This research focuses on the degradation of the track caused by traffic, degradation of rolling stock components such as wheels and suspension elements are outside the scope of this study.

Providing the above criteria are achieved, simple models requiring minimum calculation time are also beneficial.

Existing costing models are also discussed, including: the costing algorithms; if they are based on physical degradation models or simply on historical data; what they are currently being used for; their suitability for assessing the cost benefits of new types of rolling stock (specifically for steering bogies).

5.1 Wear

5.1.1 Archard's Law

Archard's Law[1] is a simple and well established wear model. The premise behind this model is that the wear rate is directly proportional to the normal contact load. This model was originally developed for sliding contact between two solid objects, rather than rolling contact. As discussed in Chapters 2 and 3 the contact between a wheel and rail is part rolling and part sliding. A creep ratio can be added into the Archard's Law equation in order to model the wear rate caused by the wheel/rail contact.

Generic Case

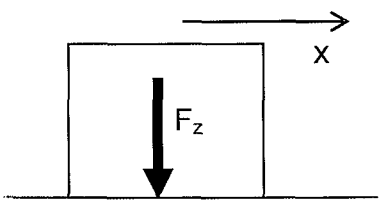

$$W = \frac{k \cdot F_z \cdot x}{H} \quad \textbf{(eqn 5 – 1)}$$

Rolling/Sliding Case

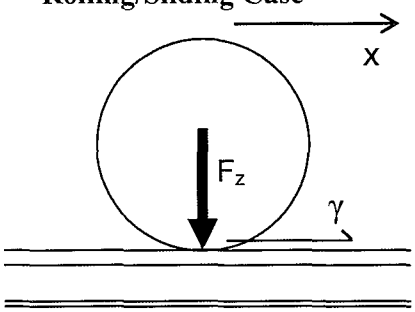

$$W = \frac{k \cdot F_z \cdot \gamma \cdot x}{H} \quad \textbf{(eqn 5 - 2)}$$

Figure 5 - 1 Archard's Law

W is the wear volume, F_z the vertical contact load, x the distance travelled, k is the wear constant and H is the material hardness, γ is the creep in the rolling/sliding contact.

This simple model has been used in a number of studies, including Jendel's study of wheel and rail wear on the Stockholm commuter network[2], and Telliskivi & Olofsson's research into wheel and rail wear simulation[3]. Jendel has shown a good correlation between calculated and measured wear rates, as demonstrated in Figure 5 – 2; in this case the model has been used for wheel wear predictions.

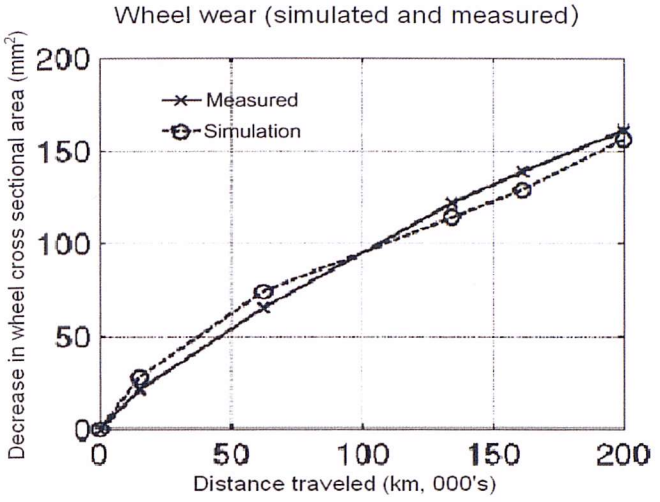

Figure 5 – 2 Wear rate calculated with Archard's law compared with measured data[2]

5.1.2 Critical normal load

The basic assumption behind Archard's research into wear[1, 4] is that wear rate is proportional to the normal load. Later research has shown that this is only the case up to a limiting value of vertical load. Singh and Kumar[5] carried out extensive laboratory based experiments to identify this limiting value for wheel and rail steels and what happens to the wear rate at higher loads (see Figure 5 – 3).

At a vertical contact stress of 1400 MPa, the wear rate is dramatically increased. The maximum allowable static load per wheel on the UK railways is 112 kN, producing a 1680 MPa peak stress at the centre of the contact patch (based on a 1 cm^2 circular contact area*). Lighter trains will produce a peak contact stress below 1400 MPa. Vertical dynamic loading also increases the contact stress. The effect of this increased wear rate at higher contact stresses really needs to be taken into account for a more accurate representation of track degradation.

* See equation 2 – 11 for a method of calculating peak contact pressure passed on vertical load and contact geometry

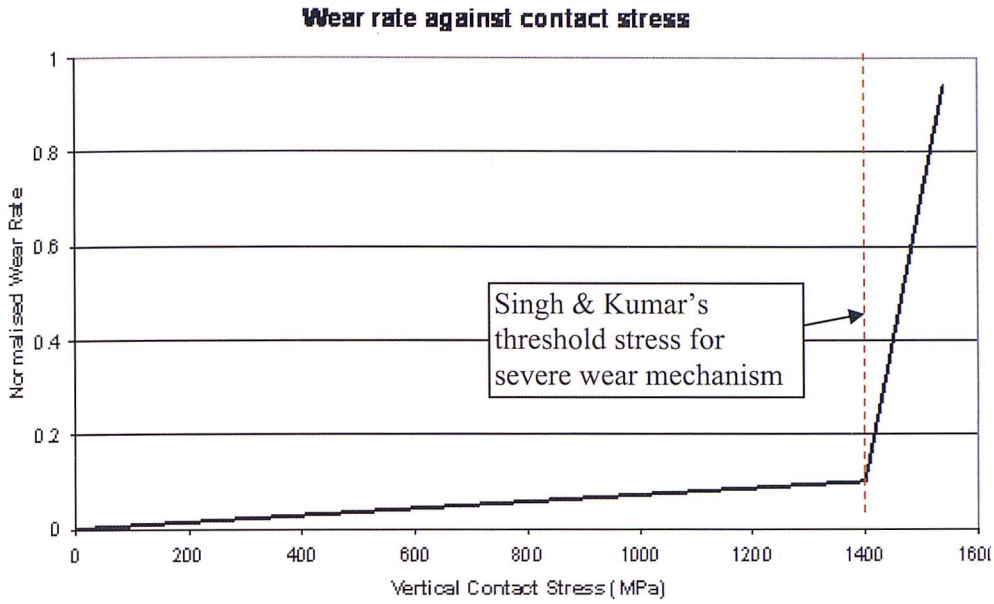

Figure 5 – 3 Wear rate against vertical contact stress[5]

5.1.3 Wear maps

Wear mechanism and an estimated wear rate can also be identified using a 'wear map'. Lim and Ashby[6] created a wear map for steel under dry sliding (see Figure 5 - 4). This map is based on experimental results for a steel pin on steel wheel sliding experiment. The wear mechanisms caused by the sliding velocity and normalised pressure are identified, along with the wear rate.

In the diagram, normalised pressure, $\tilde{F} = \frac{F_z}{A \cdot H}$ **(eqn 5 – 4)**

where, F_z is the vertical contact load, A is the contact area and H is the material hardness. This corresponds to the relationship proposed in Archard's Law, that wear rate is proportional to 1/H. The normalised pressure used in the diagram means that wear mechanism and wear rate can be looked up for a variety of steels, of different hardnesses on this same graph. Contours of normalised wear rate are shown on the graph; the units of this are m (i.e. wear depth per cycle). Because of the log scales used, it is difficult to accurately estimate wear rate using this 'map' alone, Lim & Ashby also suggest wear rate equations for each wear mechanism.

The area marked zone A shows the loading range expected at the wheel/rail interface. The maximum sliding velocity shown is 62.5 m/s, which is based on a

wheel lock up, i.e. full sliding at 225 kph, which is the maximum line speed in the UK. The range of normalised contact pressures, 0.11 to 1.07 is based on a contact area of 1 cm^2, a rail hardness of 30 GPa and a vertical load ranging from 32* to 322† kN/wheel. Based on this, we would expect to see predominantly oxidation wear with delamination in some severe cases.

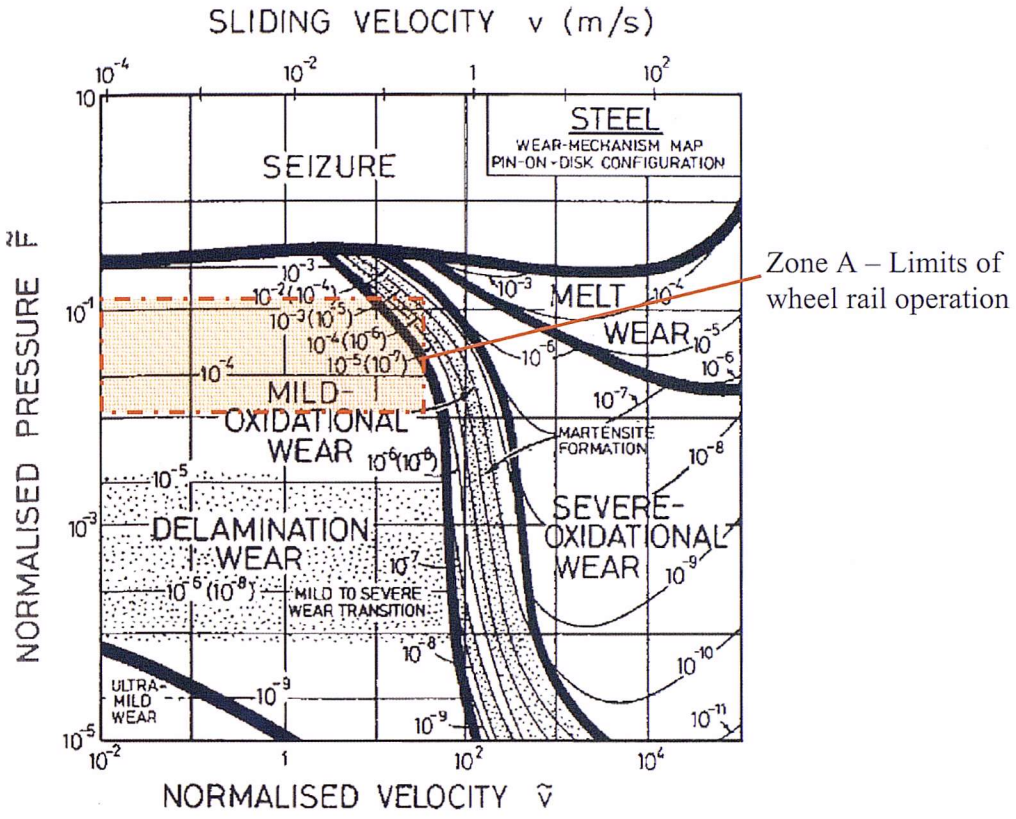

Zone A – Limits of wheel rail operation

Figure 5 - 4 Wear map[6]

This wear map is based on a considerable amount of physical testing with a variety of hardnesses of steel; however, as mentioned above all experimental work was carried out for sliding contact. It is currently not known how well results can be equated to rolling/sliding contact. Before this model can be used in a wheel-rail analysis, further work needs to be carried out to test the validity of the relationships for rolling/sliding contact.

* the class 507 trailer car has an unladen axle load of 6.4 tonnes[6], i.e. 32 kN per wheel, this is currently one of the lightest rail vehicle in operation in the UK

† The maximum permitted P2 loading allowable under Railway Group Standard GM/TT0088[7] is 322 kN/wheel

5.1.4 Energy approach

An alternative method to calculate wear is to assume the wear rate is proportional to the tangential contact load multiplied by the creep ratio, as suggested by Elkins & Eickhoff[9]. A wear index can be calculated:

$$W_i = k_i(F_x\gamma_x + F_y\gamma_y) \quad \textbf{(eqn 5 – 4)}$$

Where F_x and F_y are the longitudinal and lateral contact loads, γ_x and γ_y are the longitudinal and lateral creepages, k_i is a constant dependent on material properties.

An alternative equation is:

$$W_i = k_i(T\gamma) \quad \textbf{(eqn 5 – 5)}$$

Where T is the tangential load (i.e. $T = \sqrt{F_x^2 + F_y^2}$) and γ is the combined creepage ($\gamma = \sqrt{\gamma_x^2 + \gamma_y^2}$).

The $T\gamma$ relationship is used as the basis of the Whole Life Rail Model (WLRM), created by the Railway Safety and Standards Board. The WLRM is discussed further in section 5.3.2. This approach has also been expanded by Lewis[10, 11], as discussed in section 5.1.5.

5.1.5 Energy approach taking into account wear mechanism

The work of Elkins & Eickhoff discussed above suggested that wear rate under rolling contact is linearly proportional to $T\gamma$, know as the wear number. Wheel and rail wear rates have been investigated further by Lewis et al[12], and Ward et al[13]. They define three wear phases based on the severity of the contact, see Figure 5 - 5. A different wear mechanism occurs in each phase, resulting in the different wear rates. Oxidation, mild delamination and severe delamination are the wear mechanisms listed (Also referred to as: mild, severe and catastrophic).

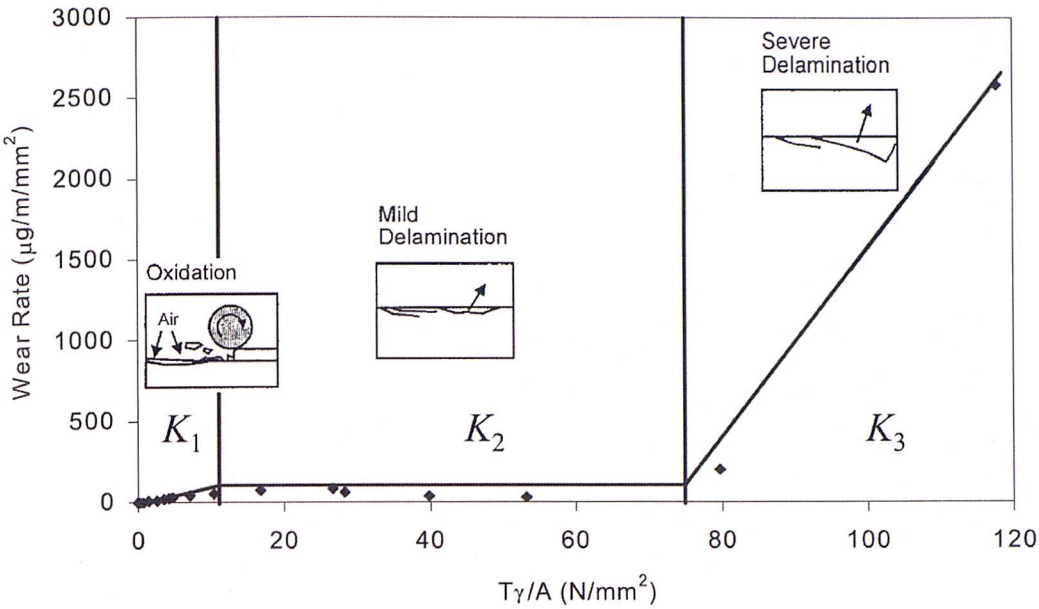

Figure 5 – 5 Three phase wear rate, data from[10, 13]

The wear rates described by the studies of Lewis and Ward were based on a variety of investigations over the previous two decades, including: laboratory based 'roller rig' experiments and measured data from a test track. Their various sources of data have been verified against each other and the wear rates given above derived from this data.

5.2 Fatigue

A variety of models have been created to predict RCF damage. Some can be used to predict initiation sites only, while other more comprehensive models can also be used to calculate crack propagation rates.

5.2.1 Shakedown limit based models

The basic premise behind shakedown based models is that providing the track loading doesn't exceed the shake down limit, there will be no RCF initiation (see Chapter 3 for a definition of shakedown limit). Shakedown maps were first used as a tool for predicting RCF by Johnson[14]. Various researchers have applied this approach to wheel and rail RCF[15-17]. A shakedown map created by Ekberg and Kabo[17] is shown in Figure 5 – 6.

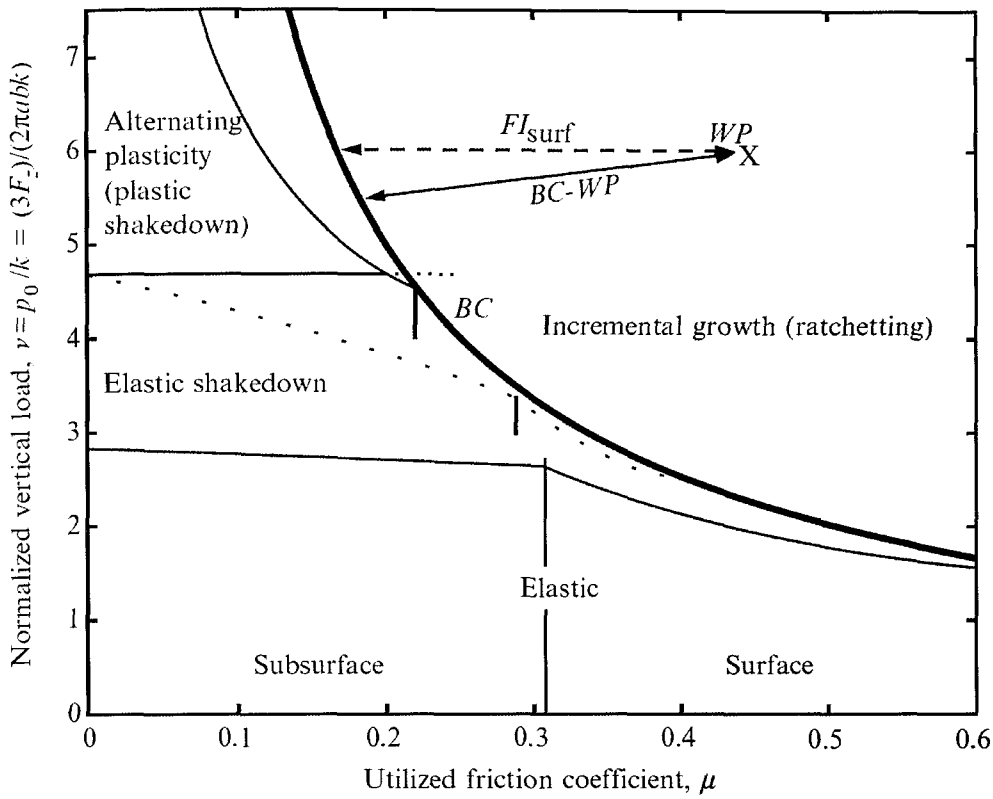

Figure 5 – 6 Shakedown map[17]

Ekberg and Kabo also define a fatigue index:

$$FI_{surf} = \mu - \frac{k}{p_0} = \mu - \frac{2\pi abk}{3F_z} \qquad \textbf{(eqn 5 – 6)}$$

Where μ, is the 'utilised traction coefficient' (= T/F_z), p_0 is the peak vertical contact pressure, a and b are the contact semi axis lengths, F_z is the vertical contact force, and k is the yield limit in shear.

In the diagram any loading combination which creates a point to the right of the shakedown limit line (or any positive fatigue index) will lead to fatigue initiation. The peak vertical pressure (p_0) is used in the shakedown map, as this value will represent the peak vertical stress applied to the rail surface. Equation 5 – 6 uses Hertzian theory to estimate this peak contact pressure based on the vertical force and contact geometry.

Afferrante et al[18] present values for the shear yield limit (k) for various rail steels, yield stress for BS11* steel is given as 289 MPa (which is significantly lower than the 400 MPa shear loading calculated in Chapter 3, for a class 91 loco travelling through a 600 m radius curve).

This fatigue index can be related to the 'likelihood of fatigue initiation'; the larger the index (or the further to the top right on the graph), the higher the likelihood of fatigue. This method can not be used for predicting rates of crack growth; a higher fatigue index does not necessarily mean faster crack propagation.

The shakedown map was originally developed by Johnson through laboratory based experimental work using twin disc rolling contact machines[14]. Further experimental work was carried out by Tyfour et al[19] who also used twin disc machines with a range of railway track and wheel steels. Many of the more recent studies[15-17] are largely numerical, referring back to these earlier experiments for their theoretical basis. The Wheel Rail Interface System Authority (WRISA)† carried out two major investigations into RCF initiation using the shakedown approach, 'Great Western RCF Study' and 'C2C RCF Study'. In both cases RCF sites were located on the operational railway, measured results were used to validate the theoretical calculations[20].

5.2.2 Fracture mechanics based approach

Fracture mechanics is another method of modelling fatigue behaviour, using equations developed to predict crack growth rates. The basic premise behind this type of model is that stress intensity factors at the crack tip can be estimated, and from these factors the crack growth rate is calculated. Various researchers have proposed different permutations on this approach with different factors included, depending on their experimental data and the type (mode) of crack growth considered.

* NB BS11 is a standard type of steel used for rails in the UK

† A group formed of various industrial bodies, no longer in existence but replaced by the Vehicle Track System Interface Committee (VT SIC)

The crack growth rate per cycle can be calculated using the Paris equation:

$$\frac{da}{dN} = C(\Delta K)^m \quad \textbf{(eqn 5 – 7)}\ [21]$$

Where: a is the crack half length; N is the number of cycles; C and m are material constants; and ΔK is the change in stress intensity factor per cycle (i.e. $K_{max} - K_{min}$).

For in plane mode I and mode II cracking, the stress intensity factors can be calculated by[22]:

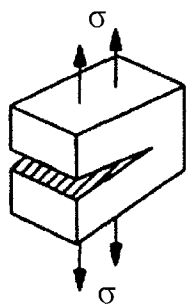

$$K_I = \sigma\sqrt{\pi \cdot a} \quad \textbf{(eqn 5 – 8)}$$

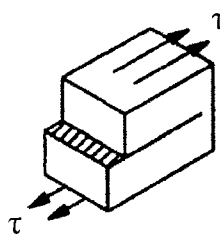

$$K_{II} = \tau\sqrt{\pi \cdot a} \quad \textbf{(eqn 5 – 9)}$$

Where σ is a uniformly distributed normal stress applied remotely from the crack surface, τ is a uniformly distributed tangential shear stress applied remotely from the crack surface.

As discussed in section 3.2.2 unfortunately the stresses driving crack propagation in rails are a lot more complicated than this. When calculating initial crack growth, the contact stresses can be used, as these will dominate the stresses experienced on the crack surfaces. However, these stresses are not uniformly distributed and the loads move relative to the crack tip as the wheel passes over the crack. Also to add another degree of complexity, because the cracks grow at an angle to the rail surface, the applied stresses are out of plane.

It is possible to calculate the stress intensity factor at a crack tip in the rail using finite element analysis. Given an assumed initial crack length, crack growth rates can then be calculated. Several studies have been published based on finite element models using a fracture mechanics approach[23-25]. In these studies a variety of loading conditions have been used to predict mode I and mode II stress intensity factors at the crack tip. They have made progress in understanding crack

growth rates and the relationship to loading characteristics. However, to calculate a range of stress intensity factors over the length of a railway network (or even a shortened representative route) would be very time consuming using a finite element model for each section.

In order to calculate stress intensity factors for an inclined crack in a surface subject to vertical and longitudinal loading, Rooke et al[26] give the equations:

$$K_N^{\sigma} = \frac{1}{\sqrt{\pi a}} \int_{b_1}^{b_2} \sigma(b) G_N^{P}(b) db \quad \textbf{(eqn 5 – 10)}$$

$$K_N^{\tau} = \frac{1}{\sqrt{\pi a}} \int_{b_1}^{b_2} \tau(b) G_N^{Q}(b) db \quad \textbf{(eqn 5 – 11)}$$

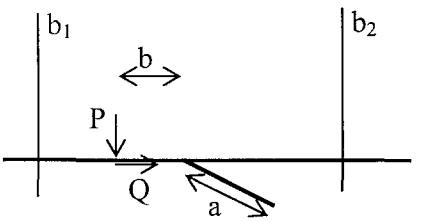

Where N is mode (I or II), σ is the vertical stress due to the applied vertical load, P (=F_z), τ is the shear stress due to the applied tangential load Q (=F_x), and b is the distance from the mouth of the crack.

As discussed in section 3.2.2.1 RCF cracks typically start to grow at an angle of 5 – 15 ° to the rail surface. If we assume a crack angle of 15 °, all of the necessary values of G are provided by Rooke et al. Based on equations 5 – 10 and 5 – 11 values for K_I and K_{II} can be calculated. The necessary values of σ and τ can be calculated using a vehicle-track dynamics model.

When K_I and K_{II} have been calculated by FEA methods or using Rooke et al's[26] 'Greens' function, their effects need to be combined to calculate the crack extension rate, da/dN. Various researchers have produced their own equations in order to do this, a selection of these are shown below. Ishida et al[27] suggest the relationship:

$$\frac{da}{dN} = 3.47 \times 10^{-11} \left[\Delta K_I \times \left\{ 1 + \left(\Delta K_{II} / \Delta K_I \right)^{1.2} \right\} \right]^{2.17} \quad \textbf{(eqn 5 – 12)}$$

Bogdanski and Brown[28] suggest an alternative relationship:

$$\frac{da}{dN} = 5.07 \times 10^{-13} \left(\Delta K_{eq}^{3.21} - 4^{3.21} \right) \quad \textbf{(eqn 5 – 13)}$$

$$\text{where } \Delta K_{eq} = \sqrt{\Delta K_I^2 + \left[\left(\frac{614}{507}\Delta K_{II}^{3.21}\right)\right]^{2/3.74}} \qquad \textbf{(eqn 5 – 14)}$$

da/dN is given in mm/cycle and ΔK in MPa $m^{½}$. Both of the above equations were developed from experimental data produced by Wong et al[29]. In equation 5 – 13, the '-4' term, is used to allow for the fatigue threshold limit of 4 MPa $m^{1/2}$. This means that loadings giving a stress intensity below 4 MPa $m^{1/2}$ will not result in any crack growth.

Zerbst et al[30] suggest three 'ranges' of crack growth (see Figure 5 – 7) which match up to the 'phases' of crack propagation suggested by Ringsberg and Bergkvist[31] as discussed in section 3.2.2.1. Range 2, known as the Paris range, is described by equations 5 – 12 and 5 – 13. Zerbst also gives his own equation for this range:

$$\frac{da}{dN} = 1.65 \times 10^{-11}\left[\Delta K_{eff}\right]^3 \qquad \textbf{(eqn 5 – 15)}$$

A fatigue threshold ΔK_0 is suggested, below which cracks will not propagate, a value of 2 MPa $m^{1/2}$ is given. This threshold links back to the shakedown limit discussed in the previous section. The value of 4 MPa $m^{1/2}$ given by Bogdanski and Brown is for the beginning of the Paris range.

The Bogdanski and Brown equation appears to be the most used version of this calculation, with Kapoor and Fletcher suggesting it in one of their post Hatfield investigative reports[32].

No research has been published showing large investigations using this approach compared against measured crack growth in rails. Using the fracture mechanics approach it may be possible to create a more accurate crack growth model, which will differentiate between dangerous cracks that may lead to catastrophic failure, and more benign, non propagating cracks that will 'run out of steam' before they reach a dangerous length. For the method to be completely verified, further large scale experimentation needs to be carried out.

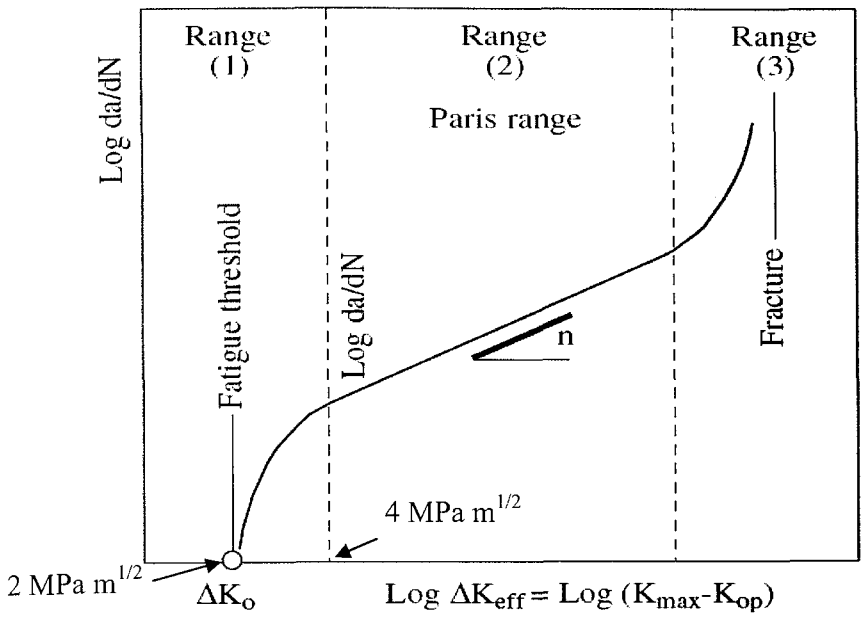

Figure 5 – 7 Crack growth against stress intensity[30]

5.3 Integrated wear and fatigue models

As the wear and fatigue damage mechanisms are so closely linked, it may be beneficial to use an integrated wear and fatigue damage model when assessing rail damage. Otherwise it is necessary to superimpose the wear rate onto a fatigue model to allow for the effects of wear 'rubbing out' the fatigue damaged material at the rail head, before a crack propagates into the rail. Because of this, some researchers have attempted to create integrated models, two of which are discussed below.

5.3.1 The brick model

Franklin and Kapoor[33] suggest a 'Brick Model' that can be used for evaluating both wear and fatigue. Their model takes slices longitudinally through the depth of the rail. These slices are divided into a number of very small elements (or bricks), and the accumulated plastic shear strain in each element is calculated. When the strain reaches a certain limiting value, that element is defined as a weak (fatigue damaged) brick.

The accumulated plastic shear strain for a given element is defined as:

$$\gamma_i = \gamma_{i-1} + \Delta\gamma \text{, where } \Delta\gamma = C\left[\left(\frac{\tau_{max}}{k_{eff}}\right) - 1\right] \quad \textbf{(eqn 5 – 16)}$$

γ is the shear strain, τ_{max} is the maximum shear stress at the element depth, k_{eff} is the effective yield stress, C is a numerical constant.

Because of plastic hardening due to shear strain accumulation, the effective yield stress increases as the total shear strain in the element increases.

$$k_{eff} = k_0 \cdot \max\left\{1, \beta\sqrt{1 - e^{-\alpha\gamma}}\right\} \quad \textbf{(eqn 5 – 17)}$$

where k_0 is the original yield stress, with values between 450 and 500 MPa[34]. .

The track loading per cycle is required as an input, which can be obtained from a vehicle dynamics program. The shear stress against depth into the track also needs to be calculated. Each element builds up plastic shear strain until it reaches a critical value, known as the shear strain for failure. After this limit the element is marked as failed, and deemed to no longer be capable of carrying any load.

This model can output a wear rate at every position along the rail and also a depth of fatigue damage. As elements on the surface fail, an algorithm is used to predict which elements will be removed as wear debris; from this a wear rate can be derived.

Individual cracks are not modelled; fatigue damage is assessed by calculating the percentage of failed elements against depth. From this an output of 1 % and 10 % damage depth is given*. See Figure 5 – 8 for an example.

Using this damage depth prediction it would be possible to develop a rail grinding strategy.

This brick model would require a high degree of computing power to calculate damage along a sample route of any significant length. Franklin and Kapoor use

* The 1 % damage depth is the depth into the rail head whereby 1 % of bricks above this depth are defined as damaged.

element sizes as small as 1 x 1 μm, which would be impractical for calculations over long routes. However, it does allow them to model the microstructure of the rail steel, by applying different material properties to necessary elements in order to model them as either ferrite or pearlite.

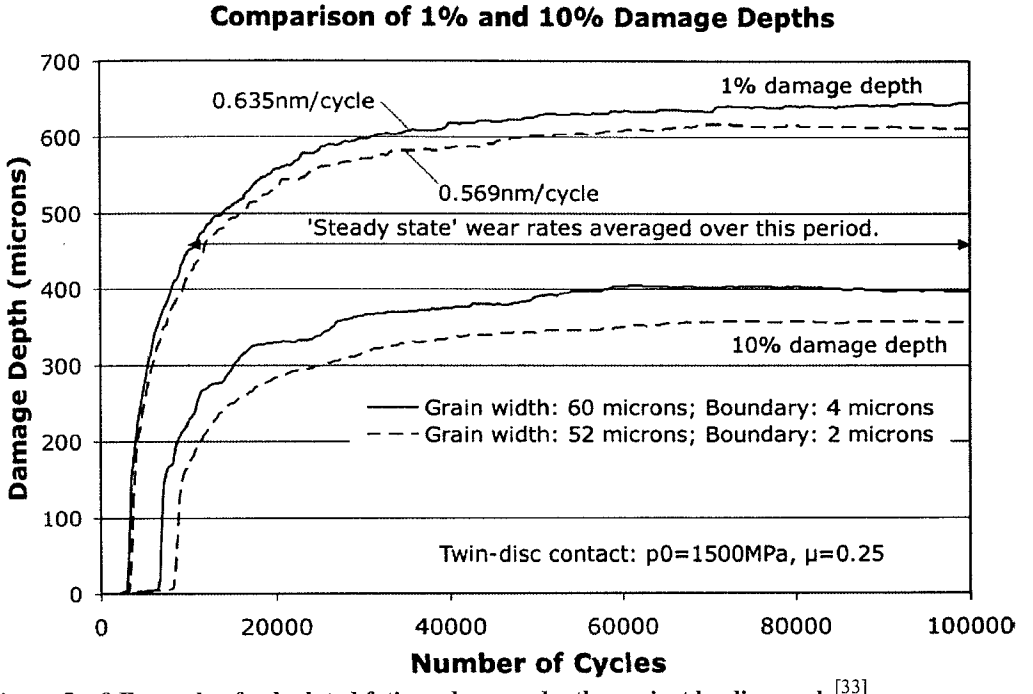

Figure 5 – 8 Example of calculated fatigue damage depths against loading cycle[33]

As with many of the other theoretical models discussed in this chapter, no large scale validation of this model against measured data from in service track appears to have been published. Kapoor et al[34] state that the model does not adequately predict wear rate; however, it is possible to calculate wear rate using an alternative model and use this brick model to calculate fatigue damage. To a certain extent this would negate the benefits of having an integrated wear and fatigue model.

5.3.2 The RSSB Whole Life Rail Model

The Whole Life Rail Model (WLRM) is an integrated wear and fatigue prediction tool. The WLRM has been developed by the Railway Safety and Standards Board (RSSB), in collaboration with AEA Technology (now Delta Rail) and Sheffield University, along with input from Network Rail.

The WLRM is based on the wear number, Tγ (as used in the wear model suggested by Elkins & Eickhoff[9] discussed in section 5.1.4), where T is the tangential load at the rail head, and γ is the creepage between wheel and rail. Burstow[35] suggests that the Tγ relationship can be used to predict crack initiation as well as wear rate. A damage function has been developed which is the core of the WLRM (see Figure 5 – 9).

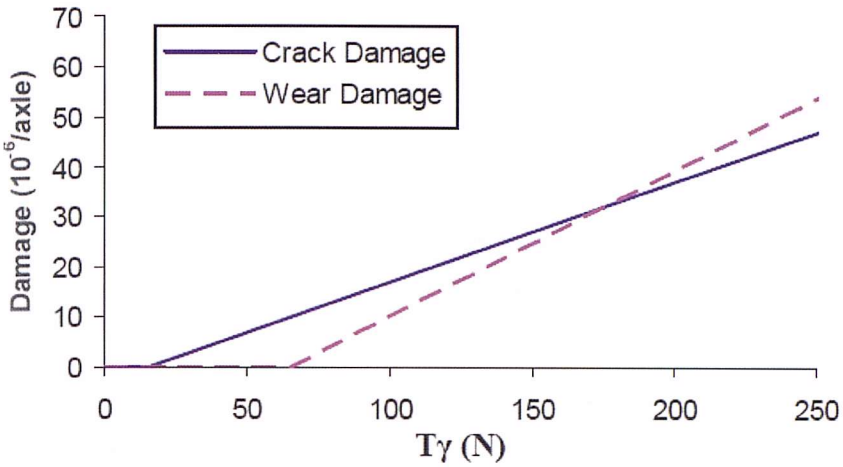

Figure 5 – 9 WLRM Crack damage and wear damage indices[35]

NB The outputs of these models are relative damage indices and not directly linked to a physical value. Using empirical relationships the indicies can be linked to physical damage rates, they are most useful for assessing the interaction between wear and fatigue. Kalousek and Magel's 'magic wear rate'[36] (as described in section 3.2.2.3) occurs at the point where the wear and crack damage lines cross. For higher values of Tγ there is no RCF. A RCF index taking this into account is shown in Figure 5 – 10.

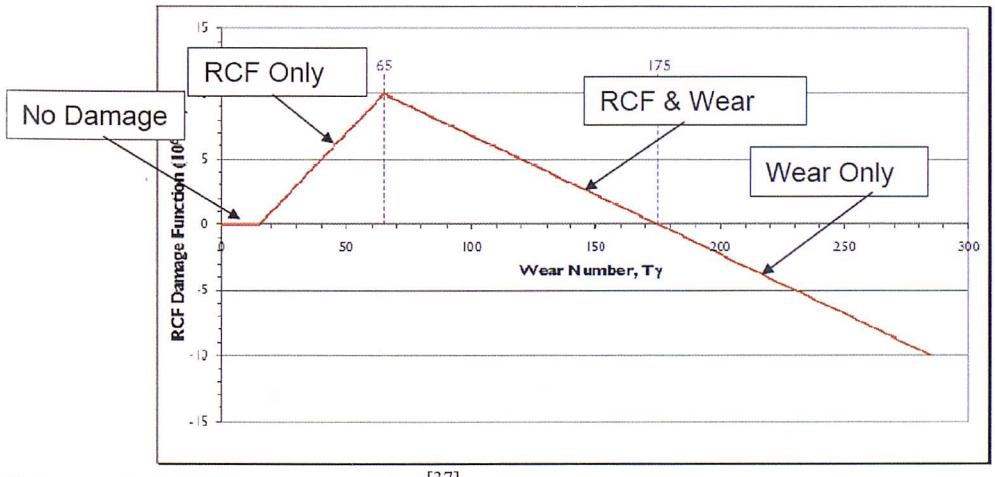

Figure 5 – 10 WLRM Damage function[37]

As shown in Figure 5 – 10, a positive damage index leads to RCF, and a negative index to wear only. This is because at higher loads, wear dominates and 'rubs out' RCF cracks, as discussed earlier in this chapter.

For the passing of every wheel, a damage index is created. Damage indices are summed so the effect of traffic over a period of time can be assessed. This has the benefit that a range of $T\gamma$ can be calculated for various types of rail vehicle that use a particular route and the cumulative effect of those vehicles can be calculated (depending on the total number of each vehicle using the piece of track in question).

Using the cumulative damage index over a period of time, the wear rate can be calculated. The WLRM can be used to predict RCF initiation, but not rate of crack growth following that initiation. When the cumulative damage index reaches a certain cut off value, RCF is deemed to have been initiated.

The developers of the WLRM have carried out various studies in order to calibrate the damage index against measured data. They have shown a good correlation between predicted RCF sites and measured data[35, 38, 39]. Burstow[35] compared the shakedown criteria method against the $T\gamma$ approach, and suggests the $T\gamma$ approach gives a closer correlation to measured data from in-service tracks.

5.4 Ballast settlement

There are a range of ballast settlement models available, with varying outputs. Some models give the average increase in geometry deviation over a given length of track based on the traffic levels and various vehicle parameters; while other models can be used to calculate the change in height of the rail due to ballast settlement. All of the ballast settlement equations shown below were derived as a result of long term studies of measured ballast settlement, with the equations developed to empirically fit the measured data. There are a number of factors affecting ballast settlement rate, as listed in section 3.2.3. The equations shown below are useful to give an indication of settlement rate; however, they are all

based on studies from different rails with varying operational conditions. It is not necessarily wise to link these empirically derived formulae with completely different railways operating under their own unique conditions. However, these empirical equations are the best models available at the present time.

As discussed in section 3.2.3, if the rail along an entire route were to settle into the ballast at a uniform rate this would not necessarily be a major problem. The need for maintenance intervention typically arises from uneven settlement; as the ballast is a non-homogenous material, different sections will settle at different rates. Varying dynamic loads experienced along the track are also a cause of uneven settlement. A selection of ballast settlement models are discussed below.

5.4.1 The Shenton model

Shenton[40] suggested a model based on the equation:

Ballast settlement, $y = K_1 N^{0.2} + K_2 N$ **(eqn 5 – 18)**

As shown in Equation 5 – 18, Shenton suggests that ballast will initially settle at a rate proportional to the 5th root of N (number of loading cycles); at higher loading cycles settlement is linearly proportional to the number of loading cycles. K_1 and K_2 are constants selected based on a number of factors, with axle load being the main consideration. It is suggested that the $N^{0.2}$ term will dominate up to 10^6 cycles, and the constants are calculated accordingly. Shenton recognised that the track settlement was not necessarily directly proportional to axle weight (i.e. an 80 tonne vehicle does not necessarily cause twice the settlement of a 40 tonne vehicle). An 'equivalent axle load' calculation was used to consider a section of track carrying a variety of trains with different axle loads.

$$F_{eq} = \left(\frac{\sum_{1}^{I} F_i^{\,5}}{I} \right)^{0.2} \quad \textbf{(eqn 5 – 21)}$$

where F_i is the weight of the ith axle, and I is the total number of axle passes.

These equations were based on a range of experimental and field measurements, and should therefore show a good relationship to real settlement rates. However, no account is made for vertical dynamic loading or for uneven settlement due to the inhomogeneous nature of ballast.

5.4.2 The Ishida model

Ishida's model, which is included in a Japanese track design standard[41], is based on the equation:

Ballast settlement, $y_b = a(P_t - b)^2 c$ **(eqn 5 – 22)**

P_t is the peak sleeper base pressure (in kPa), and y_b is the settlement rate (in mm/axle pass). a, b and c are constants. This equation can be used to calculate the settlement at each individual sleeper, based on peak sleeper base pressure (which can be derived from the rail loading obtained using a vehicle dynamics programme). By evaluating the comparative settlement at adjacent sleepers the development of track irregularities can be simulated. Ishida's model[42] also includes the effect of tamping, and allows the constants (a, b, and c) to be varied to allow for the rate of settlement increasing after each tamp.

5.4.3 Fröhling model

Fröhling[43] suggests the equation:

$$\varepsilon_N = \left[\left(c_1 + c_2 \frac{k_0}{c_3}\right)\frac{P_{dyn}}{P_{ref}}\right]^w \log N \quad \textbf{(eqn 5 – 23)}$$

where ε_N is the vertical settlement after N loading cycles (mm), k_0 is the vertical ballast stiffness (Pa), P_{ref} is the static axle load (kN), P_{dyn} is the total dynamic vertical axle load (kN). c_1, c_2, c_3 and w are constants..

As with the previous method, this equation can be used for calculating the settlement at each individual sleeper along a given route. k_0 can be varied along a simulated route in order to allow for random differences in ballast stiffness.

An equation for calculating P_{dyn} is suggested, based on a simplified 3 DOF vehicle model, adding three standard deviations of vertical load based on a given track irregularity function. However, it is also possible to use the outputs of a vehicle dynamics program to obtain the vertical dynamic loading along any given route and use this as the input to equation 5 – 23.

Fröhling used a variety of measured track settlements from a test track to validate the outputs of the model.

5.4.4 Sugiyama irregularity model

Sugiyama[44] suggests a model for predicting the growth of track irregularities*. The growth of irregularities over a 100 day cycle is calculated by:

$$S = 2.09x10^{-3} \cdot T^{0.31} \cdot V^{0.98} \cdot M^{1.1} \cdot L^{0.21} \cdot P^{0.26} \quad \textbf{(eqn 5 – 24)}$$

where S is the average growth in irregularity (mm/100 days), T is the annual tonnage (mega tonnes/year), V is the average running speed (kph), M is a structural factor, L is a factor for jointed rail or continuously welded rail (1 for continuously welded rail, or 10 for jointed rail), P is subgrade condition factor (1 for good 10 for bad).

No differentiation is given for the 'track friendliness' of the trains being used, the only measure of traffic being annual tonnage. In this model there is no factor included for the vertical dynamic performance of the rolling stock being used. Because of this, when attempting to compare the track friendliness of different train designs, this model may not be particularly useful. However, if this model is integrated with the equivalent gross tonne model[45], used as part of the Network Rail track access charge calculation (as discussed below in section 5.5.3) it may prove to be more useful. This would allow the model to differentiate between trains with better or worse vertical dynamic performance.

* NB the other models discussed above were used to predict track settlement at given locations and the difference in settlement rate could then be used to calculate track irregularity (i.e. the difference in height along the track); however, this model is used to directly calculate the track irregularity.

5.4.5 Track Strategic Planning Application

Network Rail uses a track maintenance planning tool called, Track Strategic Planning Application (T SPA)[46]. This includes a ballast settlement model which has been derived from the MARPAS[47] system (Maintenance And Renewal Planning Aid System) which was developed by British Rail in the late '80s. The output of this model is a standard deviation (i.e. track irregularity), which is calculated based on an estimated typical P2 force (as described in Chapter 2) for a given rolling stock, over the route being considered. This is then factored against ballast age, number of times already tamped, ballast settlement factor, sleeper type factor and sleeper load factor[48]. Ballast settlement rate is increased after each tamping cycle, and the ballast is termed life expired after a given number of taming cycles.

This model is now generally accepted by the UK rail industry and has been validated against measured data over a number of years. The exact calculations used are not published.

5.5 Costing models

Aside from the degradation models already discussed, there are a variety of models available that can be used to estimate cost of infrastructure maintenance and renewals. Some of these models are based on the calculated degradation rates, while others attempt to estimate cost, based on a variety of other inputs and parameters. They have been developed for a range of different purposes; some of them may be useful as tools to assess new rolling stock designs. In this section a number of the costing models are discussed. Their current uses and required inputs are identified. The possibility of using these models to calculate the effect of new rolling stock on infrastructure cost is examined.

5.5.1 Weighted System Average Cost model

The Weighted System Average Cost (WSAC) model was developed by the Association of American Railroads, largely based on historical data. Various parameters of the system are identified and given relative cost weightings.

Variables taken into account are[49, 50]:

- axle load
- speed
- type of bogie
- wheel diameter
- wheel profile
- number of axles per train
- track curvature
- rail grade and weight
- rail hardness
- rail lubrication
- type of sleeper and rail fastening system

Maintenance and renewal costs are not considered separately; the output of this model is an average cost per annum for a given section of track. This model can, to a certain extent, take into consideration the curving performance of the rail vehicles used (as the curvature of the track along with a factor for bogie type are included). However, as the model is largely based on historical data, further analysis would be necessary to calculate suitable factors for the influence of new types of bogie design.

5.5.2 UIC 715R cost comparison

The UIC have created an index that can be used for cost comparison (see Figure 5 – 11), again based on historical data; in this case the model is designed to be used for scaling up or down the infrastructure cost on a specific railway if that railway decides to modify its service*. Costs are based purely on traffic density; no vehicle and track parameters are taken into account.

This index takes no account of the dynamic performance of the rail vehicles being used, either vertically or tangentially (through curving). Also, no differentiation is made between a number of light trains or a single heavy train (i.e. two 10 tonne

* Either through using new lighter (or heavier) trains, or by changing service patterns

vehicles will cause the same track damage as one 20 tonne vehicle in this model), which is not necessarily a good representation of reality.

Comparing this UIC curve against costing figures presented by EWS[51], as discussed in section 4.2, the relationship between tonnage and cost looks very different (as shown in Figure 5 – 11).

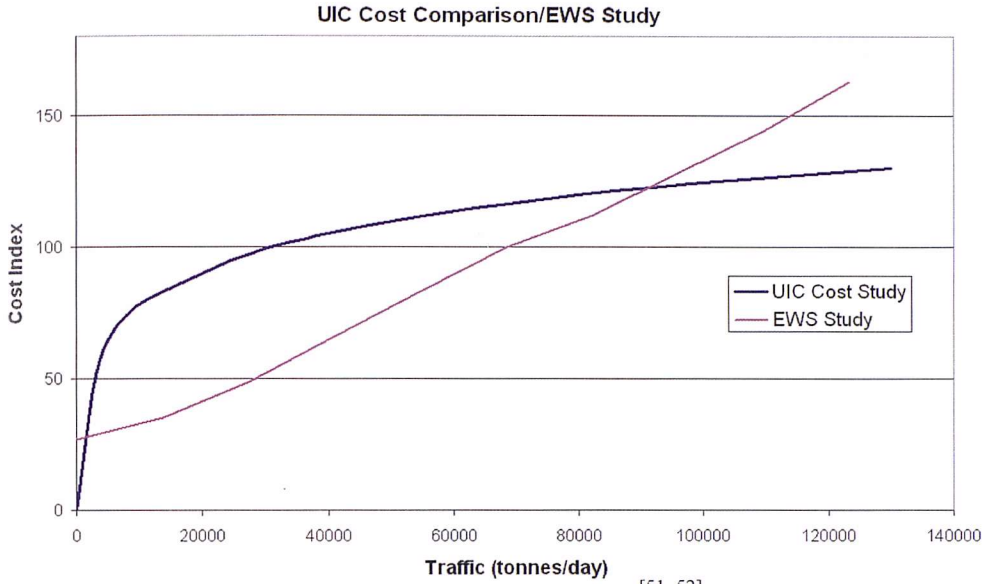

Figure 5 – 11 Comparison of UIC and EWS costing studies[51, 52]

The initial sharp rise in cost index with traffic in the UIC curve is not explained in the literature[52]; it appears to suggest improving the track friendliness of trains would be most effective for low service density railways which appears to be counter intuitive. The EWS study suggests there is a fixed cost of maintaining track because of the environmental track damage, then an additional almost linear increase with traffic. The EWS costing relationship appears to be more realistic, suggesting for higher service densities the variable (traffic dependent) cost is a larger proportion of the overall cost; meaning it is more beneficial to improve track friendliness of trains for these higher service density railways.

5.5.3 UK Track Access Charge model

Many track costing models/indices are based purely on gross tonne kilometres, with no account taken for the vehicle and rail characteristics. The UK Track Access Charge (TAC) model attempts to take into account the vehicle

characteristics by producing an Equivalent Gross Tonne Miles (EQTM) figure that is used to divide up the maintenance and renewal spend appropriately.

NB This factor is used to divide up a predetermined total budget, based on historical spending levels. The total used is not necessarily based on a maintenance and renewal programme optimised for today's train service.

Equivalent gross tonne miles $EGTM = K \cdot C_t \cdot A^{0.49} \cdot S^{0.64} \cdot USM^{0.19} \cdot GTM$ **(eqn 5 – 25)** [45]

Where K = a constant, C_t = train type constant, A = axle load, S = speed, USM = unsprung mass

This model allows for the effect of both train mass and vertical dynamic loading (as a factor for the unsprung mass of the vehicle is included, which is strongly related to vertical dynamic loading); however, the existing model has no factor included for curving performance of a rail vehicle. This means there is currently no incentive for train operators (and manufacturers) to use (or produce) trains with better curving performance.

5.5.3.1 Tunna's model to include tangential rail loading

Tunna's recent paper[53] (as already mentioned in section 4.4) suggests that 'rail surface damage' makes up 30 % of the traffic dependent rail damage, or 8 - 13 % of the overall traffic dependent infrastructure cost. A method of allocating 'rail surface damage' cost is suggested, and recommended for incorporation into the UK track access charge. Values of Tγ (wear number) are fed into the WLRM RCF and wear damage equations, as described in section 5.3.2. The resulting wear (WI) and RCF (RI) indices are multiplied by constants to give a 'rail surface damage' cost/mile*. This is a useful method of converting the WLRM indices into a meaningful output.

For $T\gamma < 15$, $C = 0$

For $15 < T\gamma \leq 175$, $C = 14500 \times RI + 12500 \times WI$ **(eqn 5 – 26)** [53]

* A full derivation of these equations in presented in Appendix C

For $T\gamma \geq 175$, $C = 12500 \times WI$ **(eqn 5 – 27)** [53]

where, C = surface damage cost (£/m)

Tunna suggests calculating Tγ caused by the steady state curving loads at the outer rail for every vehicle in operation*, over the range of curves experienced across the UK rail network. Then using Equations 5 – 26 to 5 – 28 to calculate the cost of surface damage caused by each vehicle, and to use this figure as part of the track access charge. The range of curves across the whole network is shown in table 5 – 1.

If this suggestion is taken up it may encourage train manufacturers and train operating companies to produce and use rail vehicles with reduced tangential wheel/rail loading.

Radius of curvature	Track kilometres
0 – 300	83
301 – 500	332
501 - 700	775
701 - 900	1872
901 - 1100	1187
1101	1187
1301	1187
1601 – 2000	1878
2001 – 2400	1712
2401 – 2800	1712
2801 – 3500	1712
3501 – 5000	4280
>5000	11088

Table 5 – 1 Curvature profile for UK rail network [53]

Under these current proposals rail vehicles would be assessed for their curving performance across this whole curvature spectrum. However, vehicles designed for specific routes may not travel across the whole range of curvature. Intercity trains, with stiff suspension designed for high speed stability, would give very high loading if they travelled through the tightest curves shown in the table above (however, they are unlikely to ever need to travel through curves of this type).

* This would mean the high peak loads caused by track roughness would not be included in the analysis (curving loads and the overlaid loads generated from track roughness are explained further in Chapter 7).

This would make their charges unfairly high; conversely trains designed for very curvy routes would also be evaluated for their performance over the straighter sections. This could encourage designers to produce trains which are not optimised for the routes they need to travel on. Route specific charging may be more appropriate, although this could be difficult to implement as rolling stock is often moved between franchises over the course of its life.

5.5.4 Ecotrack

Ecotrack[54, 55] is a maintenance planning tool developed by the European Rail Research Institute (ERRI), under the instruction of the UIC. The system is based on historical trends, and can be used to plan maintenance activities for existing railways. A scale of track condition is used, which is based on inputs from measurement trains. Based on the historical values of this measure and the effect of maintenance intervention, forward predictions are made for track condition. Various intervention levels are identified to allow for the planning of future maintenance activities. This plan of future activities is used to build up a cost of maintaining the track over the coming years, and to identify a suitable track replacement period. Figure 5 – 12 shows an example output from the Ecotrack system.

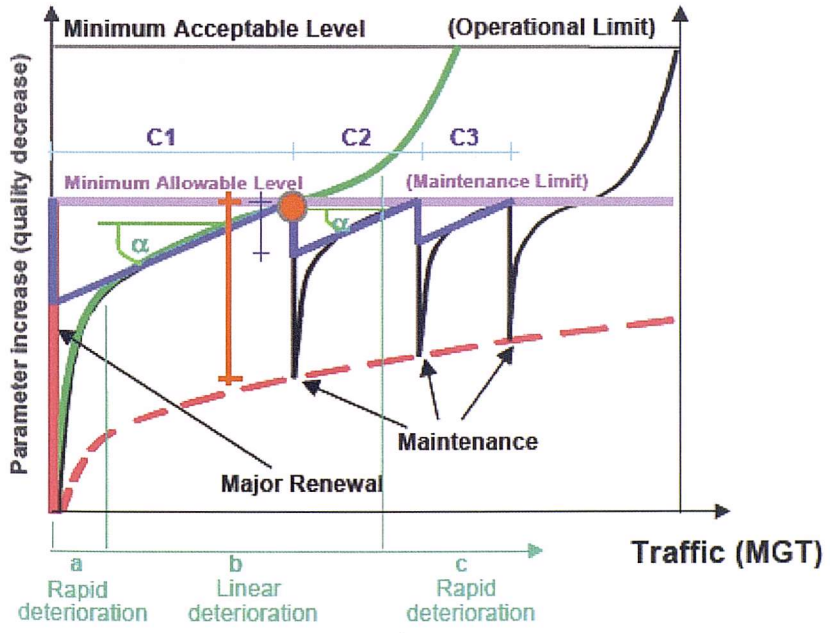

Figure 5 – 12 Ecotrack rail quality against accumulated tonnage[56]

This method has proved to be useful for optimising the maintenance and renewal costs of an existing system. However, due to its heavy dependence on historical data, the system is not necessarily particularly useful for predicting the effects of introducing new types of rolling stock.

5.5.5 Stochastic failure approach

Zhao et al[57] suggest a method of analysing rail life cycle cost (LCC)*. The cost of rail renewal, inspection and grinding are all included as with other models; however, this model also includes a factor for the risk of failure due to RCF cracking, and the cost of that failure. An equation for a unit LCC (£/MGT) is defined:

$$C(T) = \left\{ c_R + \frac{c_I T}{s_I} + \frac{c_g T}{s_g} + \left[(1-\varepsilon)c_f + \varepsilon c_x\right] N_f(T) + c_d N_d(T) \right\} \frac{1}{T} \quad \textbf{(eqn 5 – 28)}$$

where, C(T) is the cost per MGT per km per annum, T is the service density in MGT per annum, c_R is the cost of rail renewal, c_I is the cost of inspection, s_I the frequency of inspection (per MGT), c_g the cost of grinding, s_g the frequency of grinding, c_f the cost of functional failure, c_x the cost of a derailment, ε is the likelihood of a fatigue failure leading to an accident, N_f the expected number of failures per MGT, c_d the cost of repairing a defect that has been identified through inspection, and N_d the expected number of defects to be detected by inspection.

Some example values, given in the paper are shown in Table 5 - 2:

Activity/event	Cost
Rail renewal	£87,000 /km
Cost of functional failure	£4,850 /incident
Cost of repairing a defect	£680 /defect
Cost of inspection	£100 /km
Cost of a derailment	£2,700,000
Cost of grinding	£1,860 /km

Table 5 – 2 Activity costs[57]

* NB This model considers only rail, not sleepers and ballast etc.

Zhao's model specifically focuses on the effect of RCF on life cycle cost, which is particularly relevant to this thesis. Zhao's model is also the only model discussed here that includes a cost for the latent risk due to fatigue failures escaping maintenance procedures, and leading to an accident. Other models concentrate on the maintenance and renewals cost only. The rate of fatigue initiation and development, and the consequential risk of an accident occurring, can be lessened by reducing track loading through improving the 'track friendliness' of bogies. When considering the reductions in this risk as well as the reductions in maintenance requirement, it may be possible to give a more substantial business case for improving the 'track friendliness' of bogies.

This model on its own cannot be used for assessing the economic benefits of improved train/track interaction. Values for N_f (expected failures per MGT) need to be estimated, this number should be reduced by reducing track loading. It may well be possible to use one of the other models discussed above, to calculate suitable values for N_f based on loading outputs from a vehicle dynamics simulator.

As with many of the models discussed, further work needs to be carried out in order to fully validate this model against data from an operational railway.

5.5.6 VTISM

The Railway Safety and Standards Board has also instigated a project to create a track costing model, know as VTISM (the Vehicle Track Interaction Strategic Model). This model is being created by Serco Assurance and Delta Rail (formerly known as AEA Technology Rail), with support from Network Rail. This model is being produced specifically to calculate the effect of making changes to the vehicle track system[46], including physical design changes to the vehicles or track, or changes to the maintenance procedures. The system is based on two existing degradation models, WLRM and T SPA, which have already been discussed in sections 5.3.2 and 5.4.5 respectively. A vehicle dynamics

programme, VAMPIRE* is also used to calculate wheel/rail loadings which are then used as inputs to the degradation and costing models.

This system is being strongly promoted by RSSB and Network Rail, and is likely to become the standard industry costing model in the UK. The WLRM and T SPA which the system is based on are already well established and have both been validated against on-track measurements. The main benefit of this system is that the creators have access to the widest variety of information about the system and have been able to draw upon this data to develop a model strongly based on records of track degradation and real historical spending on the track.

A working version of this system has been made available to users throughout the rail industry; however, it is still under development with room for improvement in some areas†.

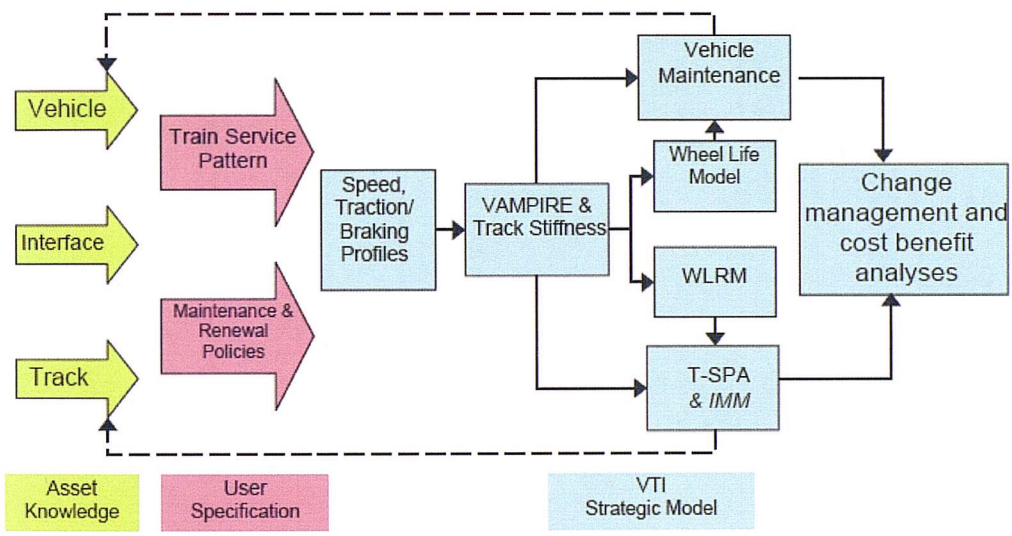

Figure 5 – 13 Schematic of VTISM system[59]

* NB VAMPIRE is a Train/Track dynamics programme[58], it is coming to be accepted as the industry standard dynamics package.

† See Chapter 8, for calculations using VTISM, and a further discussion of its functionality.

5.6 Discussion

There are a range of costing and damage prediction models available, containing varying levels of detail. The more wide-scale economic models are useful for evaluating overall cost implications of changing maintenance methods or introducing a new technology, while other models focus on the technical details of a specific degradation mode. When attempting to evaluate the cost impacts of introducing a new technology, such as the steering bogies under investigation in this study, a balance between the two is required with an approach containing an appropriate level of technical detail whilst giving suitable outputs for high level decision making.

There are a variety of models available looking at the details of: wear, fatigue and ballast settlement. Models have been developed through academic research, and also by industrial bodies. The industry based models tend to be more empirically based, and have a lot of measured data supporting them. The more academic models, for example the fracture mechanics based approach for predicting fatigue crack growth, are more theoretically sound, but are normally not validated to the same extent with measured data from an operational railway.

All three degradation modes discussed are complicated physical processes that are difficult to model, occurring in a variety of size scale where the life determining factors can be in the order of nanometres, which makes it difficult to carry out valid calculations on a macroscopic level. It is necessary to simplify the problem in order to create a useful model that can simulate the system based on the available inputs.

When modelling wear and fatigue at the rail surface care must be taken to ensure the calculated rates for each mode are closely correlated. When taking existing models from two different sources extra care needs to be taken to ensure the damage development rates are correctly superimposed.

Any maintenance regime will leave an inherent risk of failure (albeit a very small likelihood). This risk has an associated cost which really needs to be included for

a full cost assessment. Introducing technologies such as steering bogies that reduce the physical loading of the infrastructure will reduce this risk of failure as well as reducing maintenance requirement. The only model presented here that includes an element of latent risk, left over by a maintenance regime is the 'stochastic failure approach' described in section 5.5.5.
The industry model VTISM is a useful costing tool. The wear and fatigue elements of this are based on the $T\gamma$ relationship which has been shown to correlate well with fatigue initiation. However, no detailed model for crack growth rate after initiation is included. For the current maintenance planning technique this is suitable. In future, knowledge of crack growth rate may be beneficial for further optimising grinding strategy and assessing the risk of failure over time. If a crack length can be calculated to a reasonable degree of accuracy over time it would be possible to predict when the crack is starting to reach a critical length (i.e. when it is likely to turn down into the rail, leading to rapid failure), or to identify non-propagating cracks which will not require the same level of maintenance. This knowledge could be used to define more appropriate maintenance intervention criteria.

In spite of its limitations, which are discussed further in Chapter 8, VTISM is the most complete system available that can be used to assess the high level cost impact of introducing a design change to the train. Although other models can be used to give a more detailed simulation of the individual degradation rates, VTISM can be used to make high level decisions about the effect of design changes, using the empirical models WLRM and T SPA to calculate the various degradation rates.

Chapter 7 discusses the methodology used for assessing the loading reductions achievable with steering bogies and presents the results, and Chapter 8 goes on to investigate how these loading reductions will affect track damage and maintenance cost. VTISM is used to calculate these savings, and compared against the Tunna model for the cost of 'surface damage'.

References

1. Archard, J.F. and W. Hirst, *The wear of metals under unlubricated conditions*. Proceedings of the Royal Society of London, Series A, 1956. **236**: p. 397 - 410.
2. Jendel, T.T., *Prediction of wheel profile wear - Comparisons with field measurements*. Wear, 2002. **253**(1-2): p. 89-99.
3. Telliskivi, T. and U. Olofsson, *Wheel-rail wear simulation*. Wear, 2004. **257**(11): p. 1145 - 1153.
4. Archard, J.F., *Contact and rubbing of flat surfaces*. Journal of Applied Physics, 1953. **24**(8): p. 981 - 988.
5. Singh, S.P. and S. Kumar, *Laboratory investigation of threshold stress in wheel/rail interaction for heavy axle loads*. Journal of Engineering and Industry, 1992. **114**(1): p. 109 - 115.
6. Lim, S.C. and M.F. Ashby, *Wear-mechanism maps*. Acta Metallurgica, 1986. **35**(1): p. 1 - 24.
7. Fox, P., R. Pritchard, and P. Hall, *Locomotives & Coaching Stock*. 2004: Platform 5.
8. *GM/TT0088 Permissible track forces for railway vehicles*. 1993, Railway Group Standard, Railway Technical Centre.
9. Elkins, J.A. and B.M. Eickhoff, *Advances in non-linear wheel/rail force prediction methods and their validation*. Journal of Dynamic Systems, Measurement and Control, 1982. **104**(2): p. 133 - 142.
10. Lewis, R. and R.S. Dwyer-Joyce, *Wear mechanisms and transitions in railway wheel steels*. Proceedings of the IMechE Part J: Journal of Engineering Tribology, 2004. **218**(6): p. 467 - 478.
11. Lewis, R. and U. Olofsson. *Mapping rail wear transitions*. in 6th International Conference on Contact Mechanics and Wear of rail/Wheel Systems. 2003. Gothenburg.
12. Lewis, R., et al. *Wheel material wear mechanisms and transitions*. in 14th International Wheelset Congress. 2004. Orlando.
13. Ward, A., R. Lewis, and R.S. Dwyer-Joyce. *Incorporating a railway wheel wear model into multibody simulations on wheelset dynamics*. in 29th Leeds-Lyon Symposium on Tribology. 2002. Lyon.
14. Johnson, K.L., *The strength of surfaces in rolling contact*. Proceedings of the IMechE Part C; Journal of Mechanical Engineering Science, 1989. **203**(3): p. 151.
15. Jones, C.P., et al., *The effect of strain hardening on shakedown limits of a pearlitic rail steel*. Proceedings of the IMechE Part F: Journal of Rail and Rapid Transit, 1997. **211**(2): p. 131-140.
16. Bohmer, A., M. Ertz, and K. Knothe, *Shakedown limit of rail surfaces including material hardening and thermal stresses*. Fatigue & Fracture of Engineering Materials and Structures, 2003. **26**(10): p. 985-998.
17. Ekberg, A. and E. Kabo, *Fatigue of railway wheels and rails under rolling contact and thermal loading-an overview*. Wear, 2005. **258**(8): p. 1288 - 1300.

18. Afferrante, L., M. Ciavarella, and G. Demelio, *A re-examination of rolling contact fatigue experiments by Clayton and Su with suggestions for surface durability calculations*. Wear, 2004. **256**(3 - 4): p. 329 - 334.
19. Tyfour, W.R., J.H. Beynon, and A. Kapoor, *The steady state wear behaviour of pearlitic rail steel under dry rolling-sliding contact conditions*. Wear, 1995. **180**(1 - 2): p. 79 - 89.
20. Dembosky, M., et al., *Management of Rolling Contact Fatigue (RCF) in the UK Rail system: A systems solution*, in World Congress on Railway Research. 2005: Montreal.
21. Paris, P.C., *The fracture mechanics approach to fatigue*, in Fatigue - An Interdisciplinary Approach, J.J. Burke, N.E. Reed, and V. Weiss, Editors. 1964, Syracuse University Press. p. 107 - 132.
22. Ragab, A.R. and S.E. Bayoumi, *Engineering Solid Mechanics: Fundamentals and Applications*. 1998, Washington, D.C.: CRC Press.
23. Bogdanski, S., J. Olzak, and J. Stupnicki, *Numerical stress analysis of rail rolling contact fatigue cracks*. Wear, 1995. **191**(1 - 2): p. 14 - 24.
24. Chen, Y.C. and J.H. Kuang, *Partial slip rolling wheel-rail contact with a slant rail crack*. Transactions of the ASME, 2004. **124**: p. 450 - 458.
25. Kim, J.K. and C.S. Kim, *Fatigue crack growth behaviour of rail steel under mode 1 and mixed mode loadings*. Materials Science & Engineering, 2002. **A338**(1 - 2): p. 191 - 202.
26. Rooke, D.P., D.B. Rayaprolu, and M.H. Aliabadi, *Crack-line and edge greens functions for stress intensity factors of inclined edge cracks*. Fatigue & Fracture of Engineering Materials & Structures, 1992. **15**(5): p. 441 - 461.
27. Ishida, M., et al., *The current status of theory and practice on rail integrity in Japanese railways - rolling contact fatigue and corrugations*. Fatigue & Fracture of Engineering Materials & Structures, 2003. **26**(10): p. 909 - 919.
28. Bogdanski, S. and M.W. Brown, *Modelling the three-dimensional behaviour of shallow rolling contact fatigue cracks in rails*. Wear, 2002. **253**(1 - 2): p. 17-25.
29. Wong, S.L., et al., *A branch criterion for shallow angled rolling contact fatigue cracks in rails*. Wear, 1996. **191**(1 - 2): p. 45 - 53.
30. Zerbst, U., K. Madler, and H. Hintze, *Fracture mechanics in railway applications - an overview*. Wear, 2005. **72**(2): p. 163-194.
31. Ringsberg, J.W. and A. Bergkvist, *On propagation of short rolling contact fatigue cracks*. Fatigue & Fracture of Engineering Materials & Structures, 2003. **26**(10): p. 969 - 983.
32. Kapoor, A. and D.I. Fletcher, *The effect of residual stress on contact stress driven crack growth*, NewRail Report WR061106-3. 2006, Office of Rail Regulation.
33. Franklin, F.J. and A. Kapoor, *Modelling wear and crack initiation in rails*. Proceedings of the IMechE Part F: Journal of Rail and Rapid Transit, 2007. **221**(1): p. 23 - 33.
34. Kapoor, A., et al., *University of Sheffield and AEAT Whole life rail model Interim Report MEC/AK/AEAT/September02/*. 2002, Rail Safety & Standards Board.

35. Burstow, M., *Whole Life Rail Model application and development for RSSB - Development of a rolling contact fatigue damage parameter*. 2003, Railway Safety & Standard Board.
36. Kalousek, J. and M. Magel, *Achieving a balance: The 'magic wear rate'*, Railway Track and Structures, March 1997, p. 50 - 52
37. Doherty, A., Railway Safety & Standards Board, *Optimising the future railway: The work of the Vehicle / Track SIC*, http://www.rssb.co.uk/sysint/sic/2007_SIC_seminar_4_V-T_SIC.pdf, [Accessed, 9/12/07]
38. Carlisle, M. and G. Hunt, *Scoping and development of the vehicle track interaction strategic model: WP3 - Pre-stage 1 HST2 study*. 2005, Railway Safety and Standards Board.
39. Burstow, M., *Whole life rail model application and development for RSSB - Continued development of an RCF damage parameter*. 2004, Rail Safety & Standards Board.
40. Shenton, M.J. *Ballast deformation and track deterioration*. in 10th International conference on soil mechanics and foundation engineering. 1985. Stockholm, Sweden: Thomas Telford Ltd.
41. Design *standard of railway structures and others - track structures (Ballasted track)*. 1997, Railway Technical Research Institute (Japan).
42. Ishida, M., *Effect of rail grinding and/or ballast tamping on track deterioration caused by rail corrugations*, in Eighth International Conference on Maintenance & Renewal of Permanent Way; Power & Signalling; Structures & Earthworks'. 2005: London.
43. Fröhling, R., *Low frequency dynamic vehicle-track interaction: Modelling and simulation*. Proceedings of 15th IAVSD Symposium, Vehicle System Dynamics, 1997. 29((Supplement)): p. 30 - 46.
44. Sato, Y., *Japanese studies on deterioration of ballasted track*. Vehicle System Dynamics, 1995. **24**(Supplement): p. 197 - 208.
45. Nash, C., *Rail infrastructure charge in Europe*. Journal of Transport Economics and Policy, 2005. **39**(3): p. 259 - 278.
46. Jablonski, A., *Scoping and development of the vehicle-track interaction strategic model: Report on the scoping study*. 2004, Rail Safety & Standards Board.
47. Barber, S.J., N.H. Jones, and M.J. Shenton, *Causation and modelling of railway civil engineering costs*. ICE Proceedings, Transport, 1992. **95**: p. 263- 264.
48. Office of the Rail Regulator, *Final Report - Railway infrastructure cost causation*. R/00202, http://www.networkrail.co.uk/browse%20documents/regulatory%20documents/access%20charges%20reviews/previous%20access%20charge%20reviews/periodic%20review%202000/consultant%20reports/railwayinfrastcostcausationfinalreportboozallennov1999.pdf, [Accessed, 1/12/07]
49. Resor, R.R., *Meeting the need for accurate maintenance of way costing*, Railway Track & Structures, August 1994, p. 30 - 33
50. Zetatech, *Introduction to TrackShare*, http://www.zetatech.com/CORPQIII44.htm, [Accessed, 4/10/06]

51. Smith, G., *Detailed comments by English Welsh & Scottish Railway on the periodic review 2008 consultation on caps for freight track access charges*, http://www.ews-railway.co.uk/news/downloads/EWS%20-%20ORR%20letter%20to%20Tim%20Griffiths%2029%2001%2007.pdf, [Accessed, 5/4/07]

52. Rochard, B.P. and F. Schmid, *Benefits of lower-mass trains for high speed rail operations*. ICE Proceedings, Transport, 2004. **157**(1): p. 51-64.

53. Tunna, J. and R. Joy, TTCI(UK), *Methodology to calculate variable usage charges for control period 4, UK NR report No. 08-002*, www.networkrail.co.uk/browse%20documents/StrategicBusinessPlan/Update/TTCI%20(UK)%variablecharges%methodology.pdf, [Accessed, 25/6/08]

54. Jovanovic, S.S., *Condition-based decision-making minimises track costs*. Railway gazette international, 2003. **159**(5): p. 277-282.

55. Jovanovic, S. and A. Zoeteman, *Ecotrack and Life Cycle Management Plus: Towards Computer-Based Track Renewal Planning on the Dutch Rail Network*, in IQPC Asset Management In Railway Infrastructure. 2000: London.

56. Arcadis, http://www.arcadis-global.com/resources/ECOTRACK.pdf, [Accessed, 5/3/07]

57. Zhao, J., et al., *Assessing the economic life of rail using a stochastic analysis of failures*. Proceedings of the IMechE Part F: Journal of Rail and Rapid Transit, 2006. **220**(2): p. 103 - 111.

58. DeltaRail, *VAMPIRE - Rail Vehicle Dynamics Software*, http://www.vampire-dynamics.com/what-is-vampire.html, [Accessed, 3/4/07]

59. Lupton, J., Rail Safety & Standards Board, *Scoping and development of the Strategic Vehicle-Track Interaction Model*, http://www.rssb.co.uk/pdf/reports/research/T353%20Scoping%20and%20development%20of%20the%20Startegic%20Vehicle%20-%20Track%20Interaction%20Model%20-%20Research%20Brief.pdf, [Accessed, 9/5/07]

Chapter 6: Methods of Reducing Track Loading Through Train Design

In this chapter a review of methods used to improve 'track friendliness' of trains is presented; how they improve wheel-rail interaction; if the methods are already being used; where and if so how effective they are. Vertical and tangential loadings are considered, with the methods to reduce tangential loading discussed in more detail as that is the focus of this research.

6.1 How can track loading be reduced?

As described in Chapter 2, rail vehicles moving along a track create a complex loading system at the wheel-rail interface. Loads are generated in all three directions, longitudinal, lateral and vertical to the track. In addition to this, the size and shape of the contact patch between the wheels and rails varies, along with the amount of slip (or creep) at each wheel.

Vertical loads are made up of a static and dynamic components. The static load is the vertical reaction at each wheel due to the total vehicle mass. Dynamic vertical loads are additional forces created as the vehicle travels over changes in rail height. The static load can be decreased by reducing vehicle mass. Dynamic loads are strongly dependent on the unsprung mass*. NB If car body mass can be reduced, this can still have an effect on reducing not only static loading, but also dynamic loads; this is because if the car body weighs less, the components below it can be reduced in size as they have a lower load to carry, hence enabling a reduction in unsprung mass.

Longitudinal loads are caused by traction and braking and, along with lateral loading, due to curving and travelling through track irregularities. Tractive and braking loads can be optimised through improved driving styles, while curving loads can be improved by optimising suspension yaw stiffnesses or by changing the steering mechanism. Light-weighting of rail vehicles could also have an effect on reducing curving loads, which is discussed further in section 6.2.

* Dynamic loading can also be reduced, through improving track quality, but here we are only discussing how the track loading can be reduced through modifying train design.

6.2 Light-weighting of rail vehicles

There are various methods of reducing train mass, including: the use of new light weight car body materials; reducing weight of interior components such as passenger seats; reducing amount of cabling used for communications etc, and optimising interior layouts to maximise space utilisation and therefore reduce the size of the train without reducing carry capacity (or increase capacity and keep train size constant). All of these measures have been implemented successfully on the Japanese high speed trains, the Shinkansen. The newest rolling stock introduced in 2007, the Series N700 weighs 700 tonnes for a 16 car train, compared the Series 0 which weighed 970 tonnes, introduced in 1964.

Unfortunately, in recent years new trains introduced to the UK railways have generally not achieved any significant reduction in mass, compared to the trains they are replacing. In a lot of cases new trains are actually heaver than their predecessors*. The introduction of on-train air conditioning, disc brakes and, it is supposed, the use of heavy energy absorbing structures to meet crashworthiness legislation, has contributed to this. However, some improvements have been made in reducing unsprung mass, as mentioned in section 2.3.1.

As described in Chapter 2, light-weighting can reduce vertical loading; however, it can also reduce tangential load. This is because for the same value of creep, a lower tangential load will be produced. For example if the vehicle mass is reduced by 10 % this also reduces the maximum frictional force available at the wheel-rail interface (μN) by 10 %, which changes the creep/creep force relationship. See Figure 6 – 1.

Figure 6 – 2 shows how this would affect the tangential force at the wheel/rail interface when travelling through a curve, based on a sample section of curved track.

* For example, Voyager (class 220) DEMU trains introduced from 2001, have an unladen axle load of 13 tonnes, compared to the average unladen axle load of an IC125 (introduced in 1976), at 10.8 tonnes

The use of steering bogies or low yaw stiffness bogies should reduce the amount of creep, through curves; however, reducing the weight of the vehicles should reduce the force that a given creepage creates.

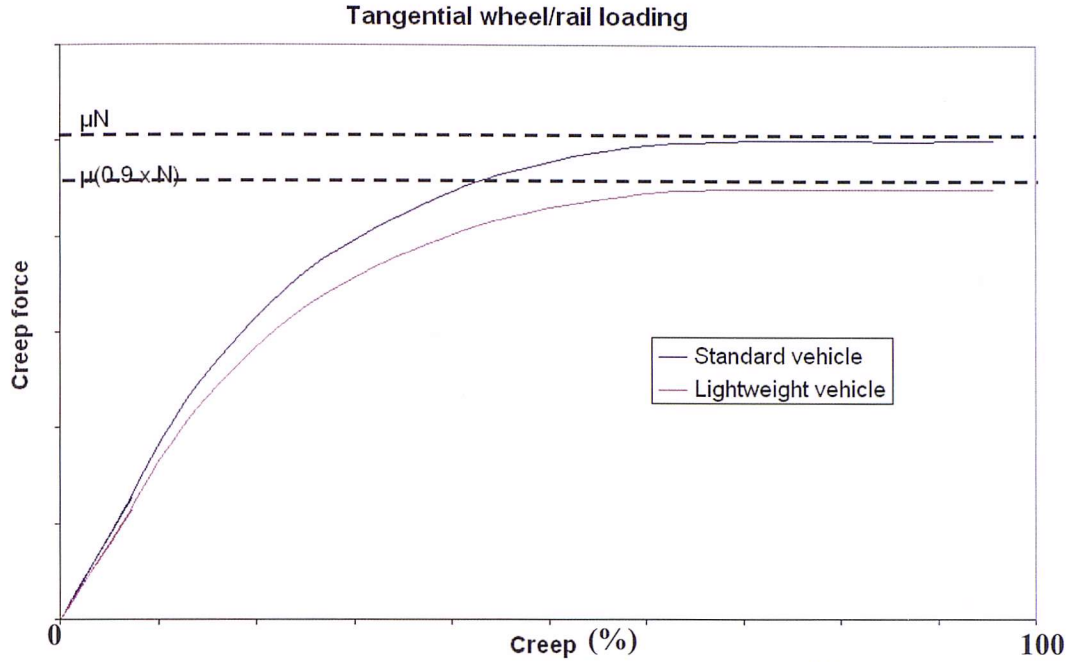

Figure 6 - 1 Comparison of creep curves (baseline curve based on data from [1])

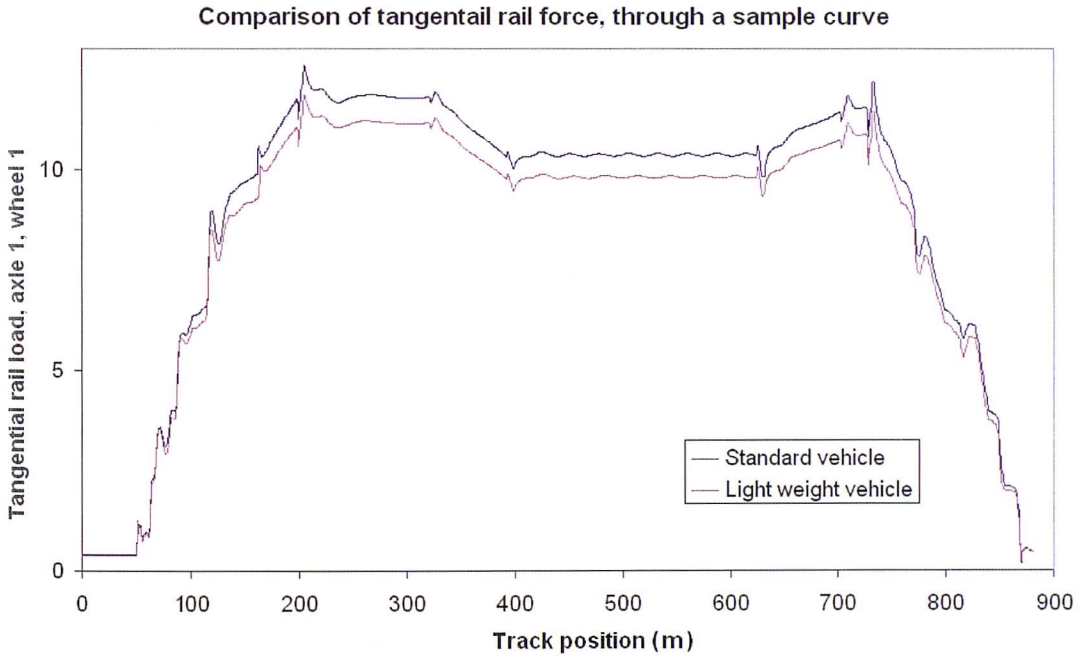

Figure 6 - 2 Comparison of tangential load caused by a standard and light weight vehicle

6.3 Optimised yaw stiffness

If train mass is not being reduced, whatever the reasons may be, other methods can be used to reduce wheel-rail loadings. As described in Chapter 2, designers can affect tangential track loading through curves by modifying the primary yaw stiffness of rail vehicles. This can only be reduced to a certain level, as the designer needs to keep yaw stiffness sufficiently high for the vehicle to remain stable up to its highest operational speed. Dembosky[2] suggests a relationship between a damage function (based on the WLRM fatigue index) and curve radius, for three rail carriages with different primary yaw stiffness, shown in Figure 6 – 3.

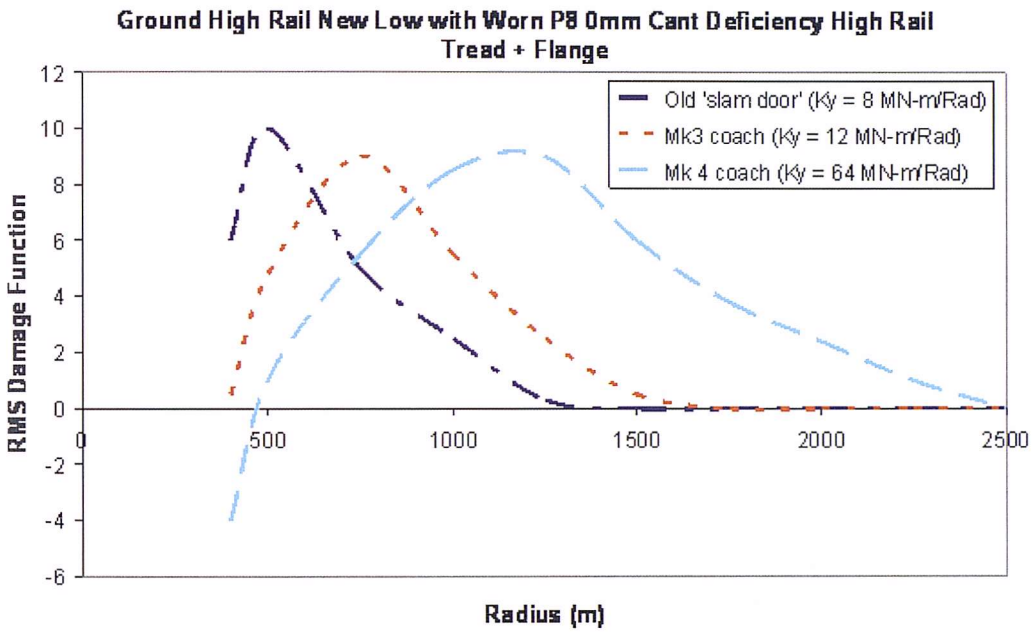

Figure 6 - 3 Effect of yaw stiffness on track damage through curves, redrawn from[2]

The vehicles with higher yaw stiffness have larger areas beneath the curve on this graph, indicating that across the full range of track curvatures they will cause more damage. However, for the tighter curves, the vehicle with higher stiffness causes less 'damage'. For the high yaw stiffness vehicle, high tangential loads are created through the tighter curves; however, this creates a low damage index as this would result in only rail wear and no resultant fatigue cracking. This is because the high wear rate removes material faster than cracks can develop, as described in Chapter 5.

The vehicles used for this study have different yaw stiffnesses, as shown in Figure 6 – 3; however, they also have different masses along with other varying characteristics. Whilst it may be safe to assume the overall results of this study are correct and lower yaw stiffness means less track damage, the exact shape of each line on the graph may also be influenced by other factors.

If a designer knows the range of curves a vehicle is likely to operate on, and the speeds a vehicle is likely to operate at, primary yaw stiffness can be selected appropriately in an attempt to minimise track damage. Unfortunately, across the range of speeds and curvatures a vehicle will operate on, it is generally not possible to create a vehicle that will cause low track loading along a whole route. The use of steering bogies may give a more appropriate solution.

6.4 Steering bogies

As stated in Chapter 2, there is a fundamental conflict with the suspension parameters required for good curving performance and high speed stability, in a conventional bogie. The purpose of a steering bogie is to modify the relationship between curving performance and stability; to improve curving performance, with out reducing vehicle stability.

There are various types of steering bogie, a limited number of which are already in use, and many further theoretical designs have been proposed by a number of engineers. The use of steering bogies has not been widely adopted by the rail industry. A small number of studies have been carried out looking at individual types of steering bogie and the load reductions they can achieve; a selection of these are described in the following sections. However, there do not appear to be any existing published studies which have comprehensively identified their benefits to train operators and infrastructure providers.

6.4.1 Steered or steering bogies?

A 'steer**ed** bogie' is a bogie that is controlled to remain tangential to the rails and hence reduce the angle of attack of the axles contained in the bogie, as shown in Figure 6 – 4.

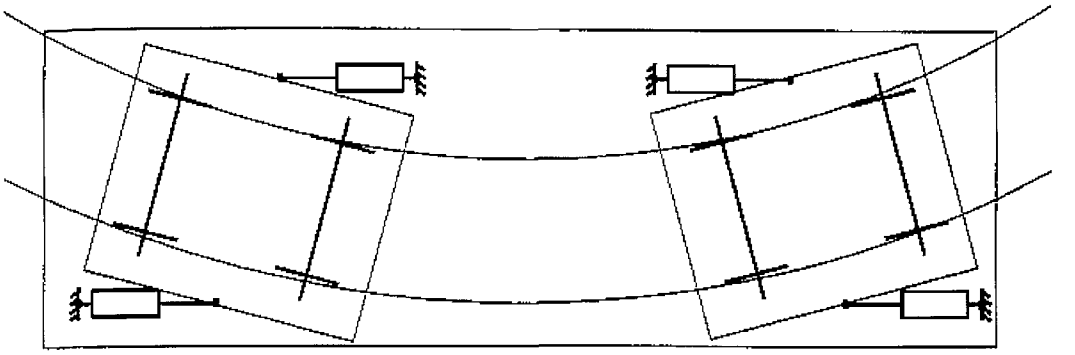

Figure 6 - 4 Steered bogies[3]

A 'steer**ing** bogie' is a bogie which controls the angle of attack of the axles it contains, moving them towards a tangential position to the rails, shown in Figure 6 – 5.

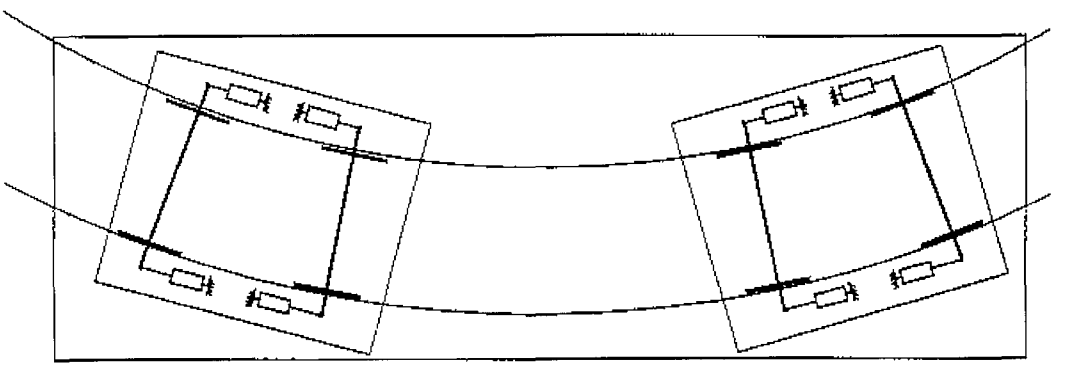

Figure 6 - 5 Steering bogies[3]

In both of the examples shown the yaw position of either the bogies or the axles is actively controlled with some form of actuator. It is difficult to implement steered bogies with a passive linkage system alone; active control systems are required. Steering bogies can be controlled passively or with active feedback control. Steering bogies should also be capable of producing lower track loading, as the axles can be moved closer to a tangential track position.

For this investigation only 'steering bogies' are being considered, as they should produce better load reductions because the individual axles can achieve a smaller angle of attack.

6.4.2 Passively controlled linkage steering

There are currently two main types of passively controlled linkage steering bogies, the 'cross-braced bogie' and the 'link type forced steering bogie'. Both are already being used, to varying extents, on a number of railways around the world. Another linkage type steering system, although not based on bogied vehicles, is the 'Talgo system'[4] which is used widely on the Spanish railways.

6.4.2.1 The cross braced bogie

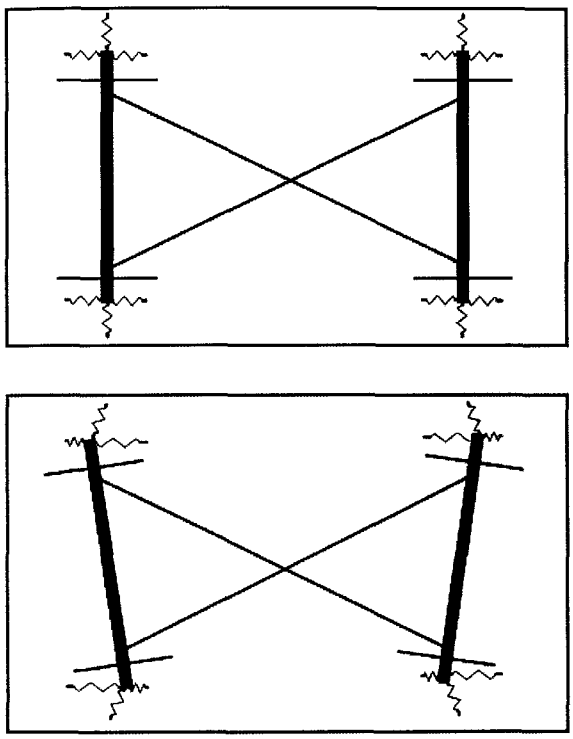

Figure 6 - 6 The cross braced bogie

The cross braced bogie, works by connecting the diagonally opposite axle boxes through a 'steering linkage'. The aim of this is to force both axles towards a neutral angle of attack through curves, a yaw displacement in one axle creates an equal and opposite yaw displacement in the other axle. This bogie should respond with a high yaw stiffness to high frequency/short wavelength track roughness (i.e. changes in track condition with a wavelength shorter than the axle separation), but with a low effective yaw stiffness through curves.

This type of bogie is generally used for heavy haul freight trucks, particularly in South Africa and North America. The class 66 locomotive in the UK also uses a

cross braced bogie. The class 66 has two, three-axle bogies, with the outer axles on each bogie connected using the cross bracing.

Figure 6 – 7 shows load reductions that can be achieved using a cross braced bogie, as predicted by Molyneux-Berry et al[5]. In this case the comparison is carried out using Tγ (Tangential load x creep), as described in sections 5.1.4 and 5.3.2. The figure suggests that load savings are only achieved for curve radii below 600m, when the wheels have made flange contact. A bogie achieving this loading reduction would not be particularly beneficial for mainline routes, which don't tend to have many curves below 600 m radius (see Figure 7 – 5, in section 7.3.1 for typical curvature profiles). Molyneux-Berry et al's[5] study used this bogie to assess the suitability of a cross braced bogie for a reasonably straight mainline route, comparing the outputs against an existing conventional train. Unsurprisingly, they showed no benefits for using a cross braced bogie. Although their design was not suitable for mainline applications, it is possible to tune the behaviour of a cross braced bogie by modifying the stiffness and damping values of the connections with the axles and between the two cross bracing links; which may have produced more favourable results in their study.

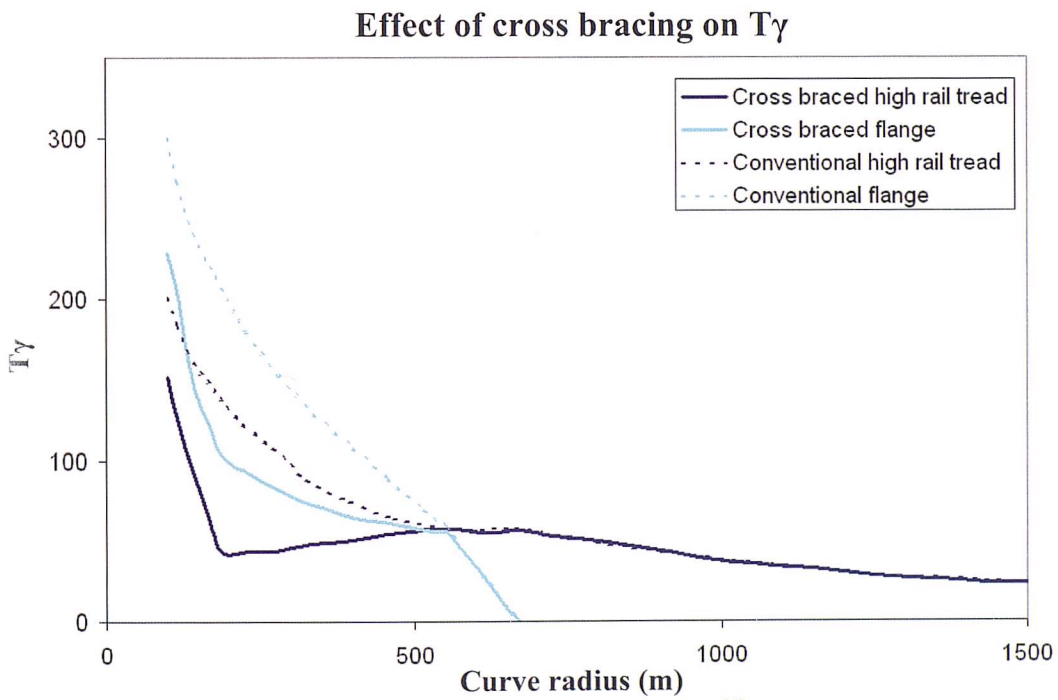

Figure 6 - 7 Effects of cross bracing on T-gamma, redrawn from[5]

6.4.2.2 The 'link type forced steering bogie'

An alternative arrangement is the 'link type forced steering bogie' which is already employed by the class 283 DMU operated by JR Hokkaido in northern Japan.

Okamoto's discussion of bogie design[6] includes a comparison of the lateral loading caused by this type of steering bogie, with that of a conventional bogie travelling through a 302 m radius curve. The output of this is shown in Figure 6 – 9.

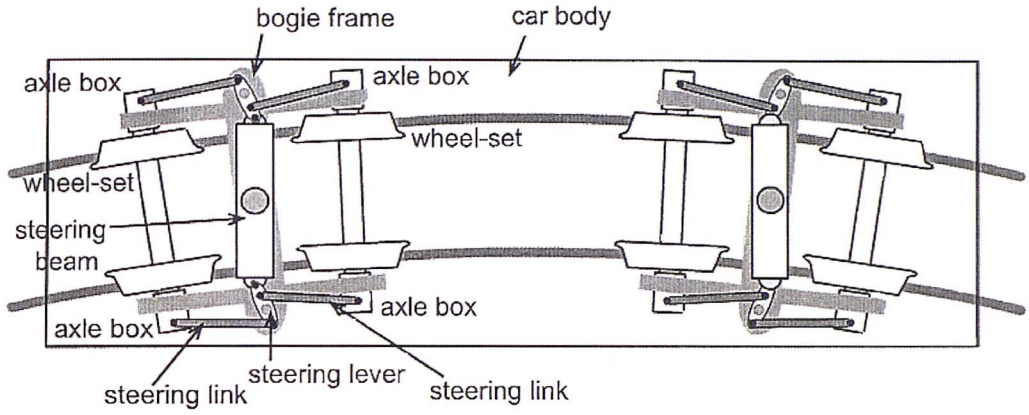

Figure 6 - 8 Link type forced steering system as used on the JR Hokkaido 283 DMU[7]

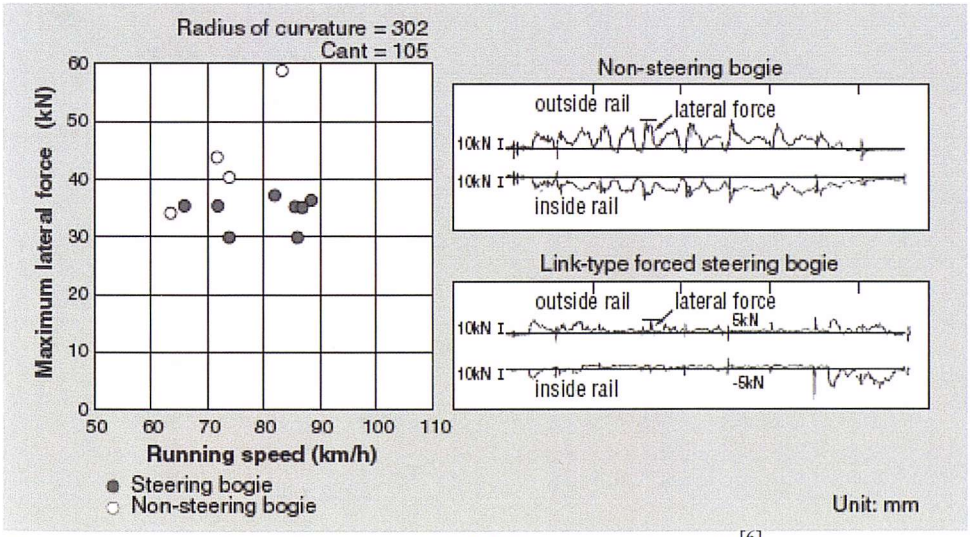

Figure 6 - 9 Achievable load reductions with link type steering bogie[6]

The combination of a train's speed through a curve and the applied cant, can have a significant effect on the lateral wheel/rail loading. Peak lateral loading for the conventional (non-steering) vehicle shown in Figure 6 – 9 increases

almost linearly with curving speed. However, the linkage steering bogie appears to have removed this relationship between speed and peak lateral force, showing a fairly constant peak loading as the speed is increased. This means the loading benefits are greater at higher speed; as shown in Figure 6 – 9, at 82 kph there is roughly a 40 % reduction in peak loading. This bogie was designed to allow vehicles to travel faster through the many curves on the JR Hokkaido lines (which travel through a very mountainous region).

For the lower speed shown in Figure 6 – 9, there appears to be little (or no) reduction in lateral loading.

Unfortunately the effects of this bogie on longitudinal load, which should also be significant, are not published.

6.4.3 Hardening spring bogie

The 'hardening spring bogie' contains a low primary yaw stiffness for small yaw movements of the axle. To avoid the instability normally associated with low yaw stiffness, primary yaw damping is introduced; and bump stops are included at the extremes of allowable yaw motion, effectively increasing the stiffness for larger yaw displacements. This type of bogie is being developed for use with freight, an example is the 'light and low noise LEILA bogie'[8, 9]. Hecht and Keudel[9] suggest this bogie can reduce the angle of attack through a 300 m radius curve by 90%. How the bogie performs on larger curve radii is not mentioned, and no specific details of the bogie design are published.

6.4.4 Independently rotating wheels

A method of reducing the longitudinal loading through curves is to decouple the pitch movement of parallel wheels on the same axles, i.e. to allow them to rotate independently of each other. This is not a new idea; it was first suggested by Robert Stephenson, who patented a design for a railway truck containing independently rotating wheels[10], using an arrangement called 'axle-trees', as shown in Figure 6 – 10. The purpose of this arrangement was *'to remedy the extra friction on curves'*.

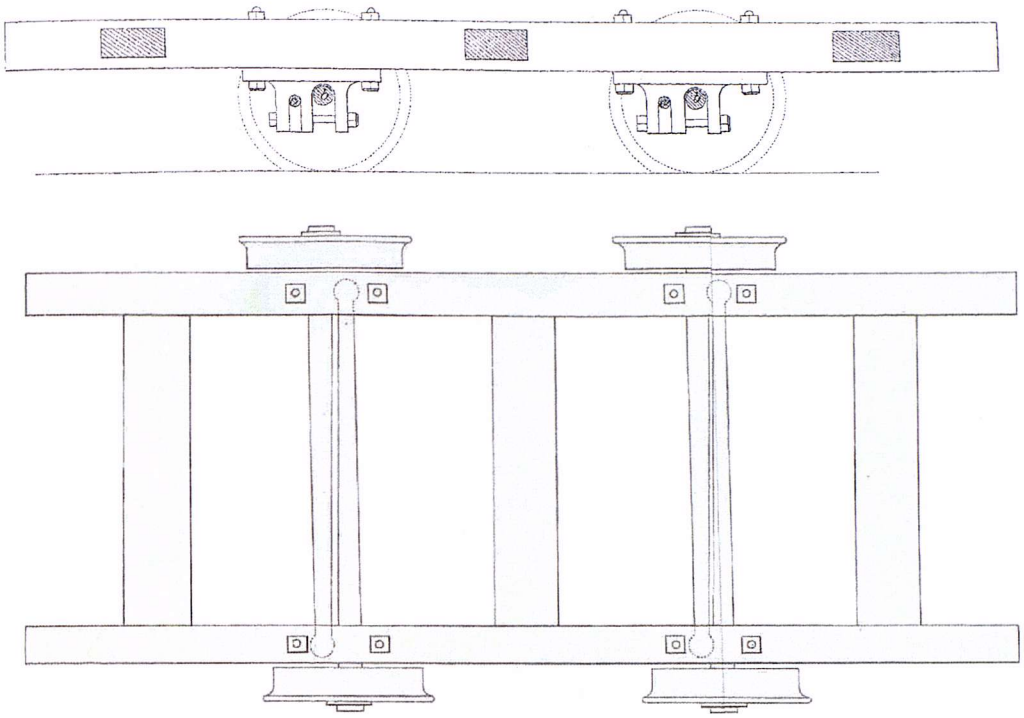

Figure 6 - 10 Robert Stephenson's Axle Trees[10]

In this design flanges are on the outside of the rails, and cylindrical wheels are used.

Independently rotating wheels, when used for hauled stock, can significantly reduce longitudinal loads; opposing wheels do not have to maintain the same rotational speed, so there is no longitudinal creep generated to keep both wheels moving at the same speed. The downside of this is that rolling radius difference steering will not work with independently rotating wheels. This means wheels will often run in flange contact through curves, creating high lateral loads. Independently rotating wheels are sometimes used for trams, such as the new Nottingham and Edinburgh trams.

For powered bogies, wheels can all be controlled independently. This means that through curves the outside wheels can turn faster, and replace the effect of the rolling radius steering. This would mean reducing longitudinal loads and still avoiding flange contact. A complicated active control system would be required to set the necessary rotational speed at each wheel.

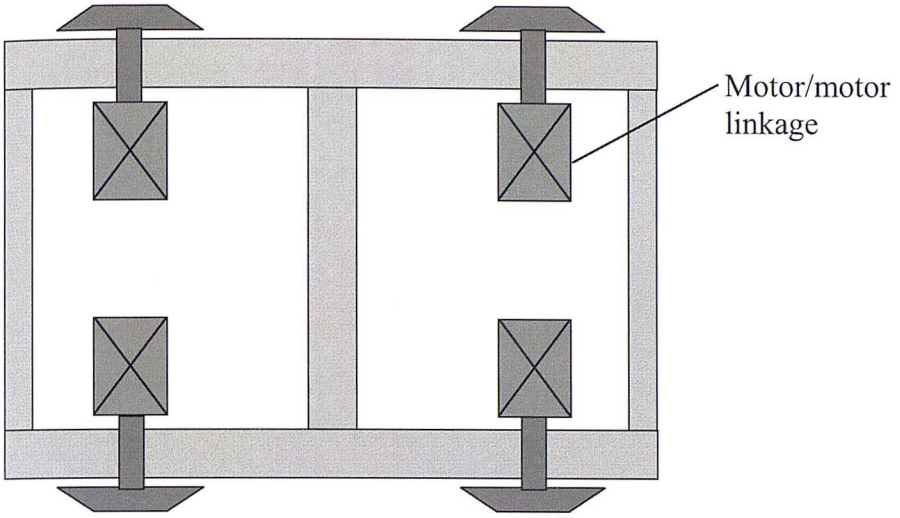

Figure 6 - 11 Independently controlled wheels

6.4.5 Active steering

The passive steering types already mentioned can be used to modify the relationship between curving performance and stability; however, a well designed active steering system can be used to completely isolate curving performance from stability through rough track.

There are a variety of wheel arrangements that can be used for actively controlled steering, including independently driven wheels which have already been mention in section 6.4.4. Another possibility is to control axle yaw relative to the bogie frame, either with a rotary actuator, or using linear actuators at either end of the wheelset as shown in Figure 6 – 12. This approach was first suggested by Shen and Goodall[11] as a means of reducing curving loads without compromising vehicle stability.

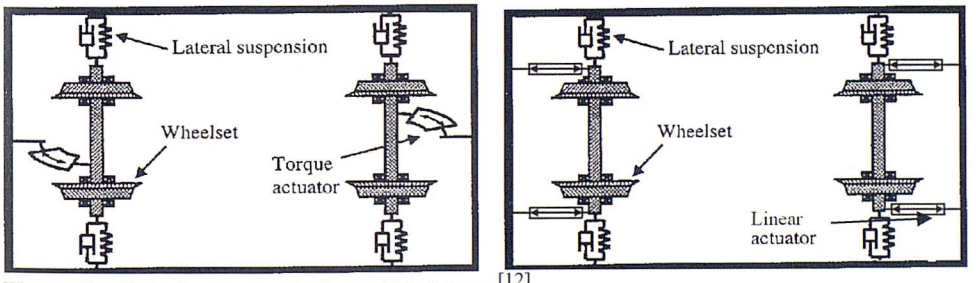

Figure 6 - 12 Axle yaw control, modified from[12]

These systems could be used either with independently rotating wheels, or conventional fixed axle wheelsets. For powered axles, bogie mounted motors

need to be mounted with either a flexible connection to the axle, or an arrangement to allow the motors to swing with the axle movement.

Another option is to steer each wheel relative to the bogie frame, as shown in Figure 6 – 13. This system will not be able to set both wheels to a perfectly tangential position relative to the rail, as the methods in Figure 6 – 12 could; however, actuator forces to move this steering system should be much lower. This arrangement would be more suitable for non-powered axles, but again flexible connections to traction motors could be arranged to provide power to the wheels.

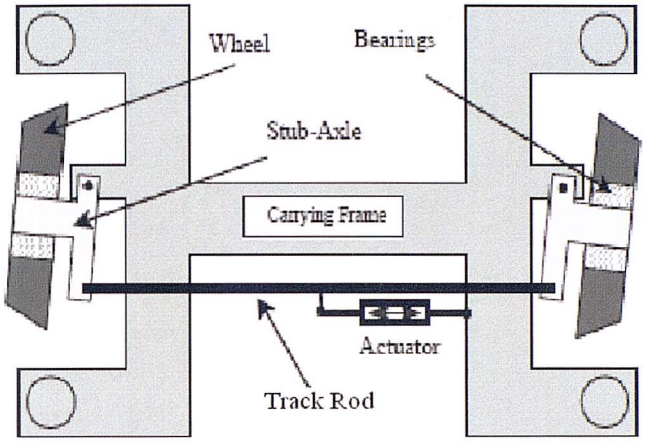

Figure 6 - 13 Steered wheels, using stub axles and track rod[13]

With all of these steering designs, their success in reducing tangential loads through curves will depend on the control systems, the measured inputs used for control, and the speed and accuracy of the control actuators. Care must be taken to ensure the active system does not interfere with the stability of the vehicle. As stated by Pérez et al[14] the use of actively controlled systems *'provides the designer with more freedom and flexibility than conventional design methods based on the exclusive use of mechanics, allowing achieving simultaneous different goals that have been traditionally considered contradictory'.*

Active steering bogies can be designed with limited bandwidth so the system only applies control forces as a response to low frequency changes in the track, i.e. curves; not responding to the higher frequency track roughness'. The system should be designed so that it does not attempt to 'steer' through high frequency track roughness, as this will exacerbate the problem of hunting. Using

bandwidth limited control the suspension can effectively be very stiff in response to track roughness, but flexible through curves; this can be achieved by placing the bandwidth limited actuators in parallel to a conventional suspension, as shown in Figure 6 – 14. The conventional suspension applied damping loads to prevent hunting through rough track, however through curves the active system applies a load to effectively 'hold off' the conventional suspension.

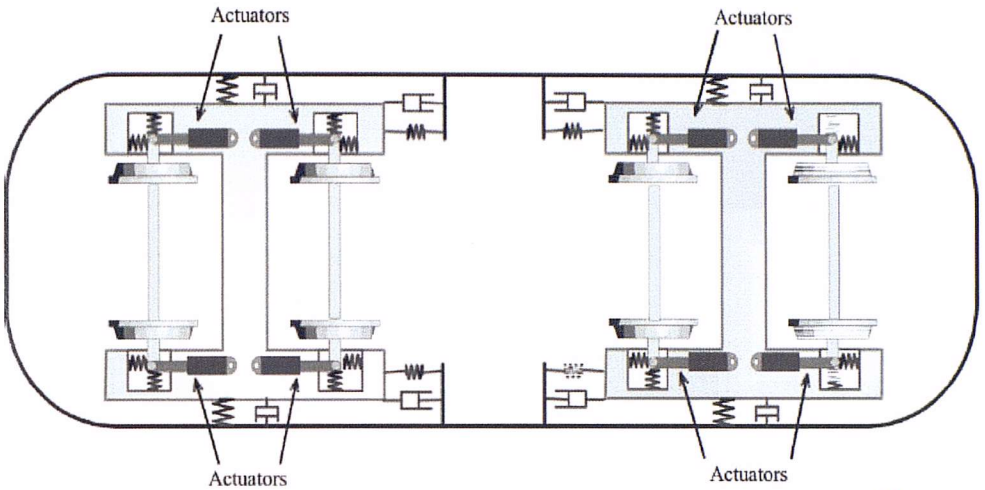

Figure 6 - 14 Steering actuators installed in parallel to a conventional suspension[15]

Mei and Goodall suggest a control algorithm for a torque actuated steering system, as shown in Figure 6 - 15, based on the two axle vehicle in Figure 6 -12.

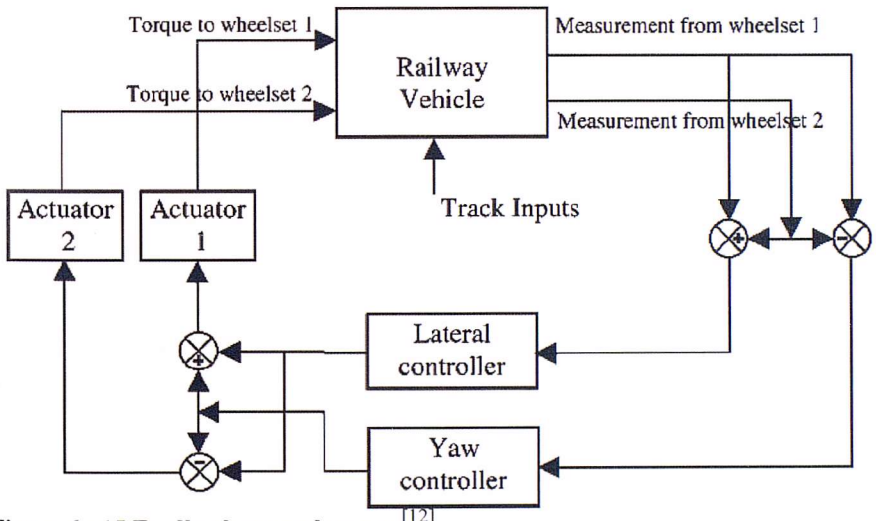

Figure 6 - 15 Feedback control system[12]

This control system requires knowledge of wheel lateral and yaw displacements, lateral and yaw velocities relative to the track; along with instantaneous radius of curvature. Using vehicle mounted sensors it is very difficult to measure all of these required inputs. However, Pérez et al[16] suggest a method of estimating

these inputs, based on measurements taken using accelerometers to measure the accelerations at the axle boxes, using their outputs to calculate the necessary velocities and displacements. Their approach is known as a 'Kalman filter'.

Based on computer simulations, Mei and Goodall give an indication of how this type of active bogie could reduce track damage, based on the wear number, Tγ (tangential force x creep). Load outputs for two curving cases are given:

A. A train travelling at 350 kph through a curve of radius 3500 m, with applied cant angle of 6°.
B. A train travelling at 90 kph through a curve of radius 300 m, the applied cant is not given for this example

The achieved reductions in wear index are shown in Figure 6 – 16.

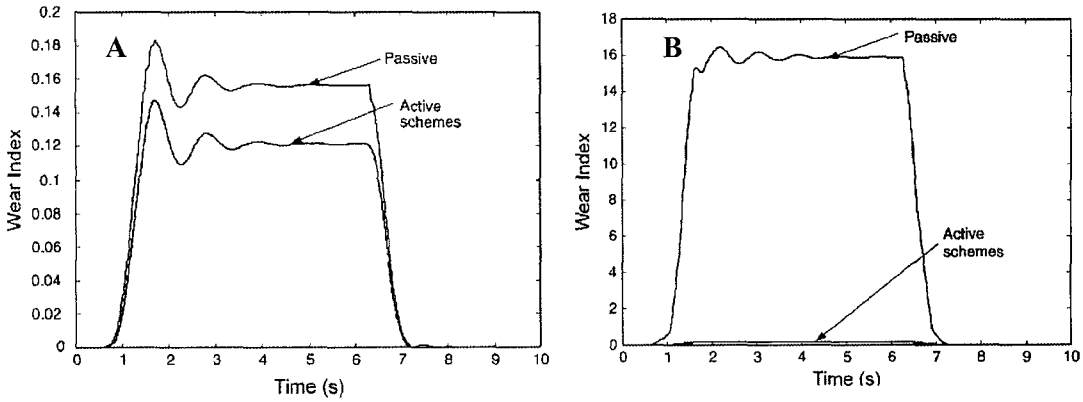

Figure 6 - 16 Reduction in wear number achieved with active steering[12]

For the low speed tight curve, the wear number has been reduced by almost 99 %, and approximately 25 % for the larger radius curve*. These numbers look very promising. At the moment there appears to be no published studies of practical testing for actively steered bogies to validate these results.
When designing the control system for any active bogie, the measured inputs required by the system need to be carefully considered; control inputs need to be easily measured using on-train sensors. An alternative is for steering inputs to be pre-calculated for every route a train will operate on, and applied appropriately using knowledge of the train position and speed. The problem

* NB The wheel load through the tighter curve is much higher, with the conventional vehicle giving a wear number 10 times higher than for the smoother curve.

with this method however, is that the train cannot be switched onto new routes until a new control routine has been programmed, and the train will not respond to changes in track condition over time.

6.4.5.1 Actuators

There are a range of actuators types that can be used for active suspension systems, Goodall & Mei[17] suggest possible options for steering actuators are:

- Servo-hydraulic
- Servo-pneumatic
- Electro-mechanical
- Electro-magnetic

Pneumatic and hydraulic actuators are both compact and easy to fit, giving good force capabilities. However when including a suitable compressor system this quickly adds to the required weight. As modern trains already contain a pneumatic system for the secondary 'air bag' suspension (and pneumatic door motors), there is an opportunity to integrate primary pneumatic actuators with existing on board pneumatic systems. Electro mechanical actuators such as servo motors would be efficient and easy to control, but the low speeds and high force requirements may be difficult to achieve. Adding a gear box to the system could create the suitable force outputs, however this would significantly increase the mass of the system. Electro magnetic actuators could create high forces with a quick response, but again they would likely use up a lot of room and add a lot of mass to the suspension system.

Pneumatic actuation appears to be the most promising. The compressibility of air, and flow rate restrictions can limit the response times of pneumatic actuators; however this should not limit their performance in low frequency applications.

6.5 Articulated bogies and the Talgo steering system

Another method of reducing tangential wheel loading is to place wheels at the ends of each car and share those wheels between two cars, either by sharing a bogie at each inter-car connection or a single wheelset. The arrangement of a train with articulated bogies is shown in Figure 6 – 17, and the Talgo wheel arrangement in Figure 6 – 18.

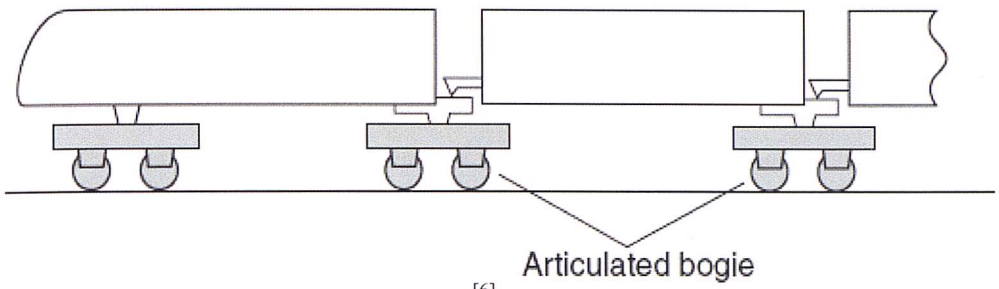

Figure 6 - 17 A train with articulated bogies[6]

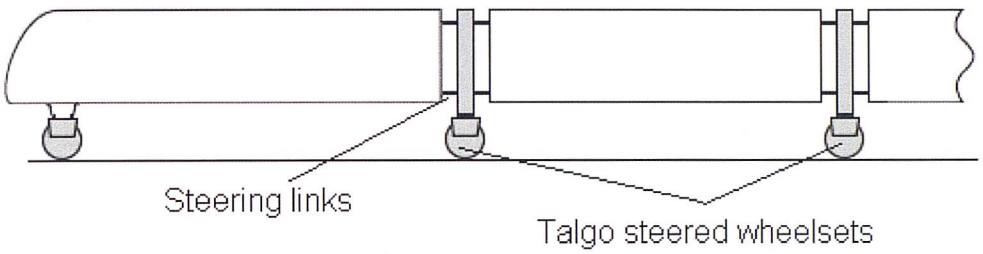

Figure 6 - 18 Talgo steering arrangement

For both of these train types, the total train mass should be lower than a conventional train of the same size, as there are less bogies (and axles); which contribute a significant proportion of train mass. However, the individual axle loads will be higher because the train mass is spread over fewer axles.

For the articulated bogies tangential load should be reduced. Because of the stiffness of the yaw connection between the bogie and each carriage, the bogie should move towards an angle half way between the two carriages, roughly normal to the track curvature. The Talgo system includes steering links that force the axle to an angle half way between the adjacent carriages, which should again be normal to the track curvature; hence developing minimal creep loading.

The benefits of both of these systems are largely anecdotal, as there have been no significant studies published giving the reductions in loading or track damages achieved by either arrangement.

6.6 Steering bogies in the UK

As already mentioned in section 6.4.2.1, the class 66 locomotive, which is used primarily for hauling freight, already has a cross braced (3 axle) bogie. This appears to be the only operational rail vehicle type in the UK that has a form of forced axle steering. However, Railway Group Standard, GM/GN2589, The Design and Construction of Freight Wagons[18], allocates bands of 'track friendliness' to freight wagons. With 1 being the least and 7 the most 'track friendly', as shown below in Table 6 – 1.

Band	Description
1	Four wheel (2-axle) wagon with pedestal type suspension
2	Four wheel (2-axle) wagon with leaf springs, friction damped
3	Wagon equipped with 3 piece bogie
4	Bogie wagon with enhanced 3 piece bogie (i.e. 'swing motion') of four wheel wagon with parabolic suspension
5	Bogie wagon with primary springs (e.g. Y25 suspension type)
6	Wagon equipped with enhanced primary springs(i.e. low track force bogies, TF25 types of 'axle motion'
7	Wagon equipped with enhanced primary springs and steering

Table 6 - 1 Freight wagon classifications

There are not yet any freight wagons in band 7. However, this does at least show the industry has some interest in reducing tangential loads and the possibility of using steering to achieve this.

The same classifications are not used for passenger wagons. However, a study recently carried out by TTCI(UK)[19] for Network rail, already mentioned in Chapter 4, suggests that tangential loading performance of rail vehicles should be included in the track access charge. If this is taken up, it may be an incentive for rail operators to consider the option of steering bogies more seriously.

6.7 Discussion

There are already a limited number of railway vehicles around the world using some form of steering, and a number of additional theoretical designs exist. A limited amount of data has been published showing the benefits that can be achieved in reducing track loading with these bogies. The limited information available shows very promising results for the different bogies. However, it is difficult to compare them against each other because every study has its own output metric. Molyneux-Berry et al's[5] study, which included the cross braced bogie, showed some load reductions in terms of wear number ($T\gamma$); Okamoto[6] shows reductions in lateral load achieved with 'link type forced steering bogie'; whilst Hecht and Keudel[9] suggest the benefits of a 'hardening spring' steering bogie in terms of angle of attack; Mei and Goodall[12] also used reductions in wear number to show the benefits of their active bogie design.

There are no comprehensive studies comparing the different steering types against each other using the same test condition and output scales; and many of the studies do not discuss the stability of the different bogie designs through rough track. There also does not appear to be any information currently available on how these bogies will benefit train operators and infrastructure providers, in terms of reducing operating cost by reducing maintenance requirement and extending track life.

The following chapter goes on to compare the reductions in tangential loading that can be achieved with three types of steering bogie, across different types of railway. Chapter 8 gives details of a further study looking at the cost savings that can be achieved with these types of bogie.

References

1. Brickle, B.V., *Railway Vehicle Dynamics.* Physics Technology, 1986. **17**(4): p. 181 - 186.
2. Dembosky, M., et al., *Management of Rolling Contact Fatigue (RCF) in the UK Rail system: A systems solution*, in *World Congress on Railway Research*. 2006: Montreal.
3. DeltaRail. *Course notes from: Introduction to Railway Vehicle Dynamics*. 2006. Derby.
4. Pascual, F. and J. Marcos. *Wheel wear management on high-speed passenger rail: A common playground for design and maintenance engineering in the TALGO engineering cycle.* in *ASME/IEEE Joint Rail Conference*. 2004. Baltimore, Maryland, USA.
5. Molyneus-Berry, P., *VTISM HST2 Study variation: parametric study and less conventional vehicles, AEATR-ES-2005-009 Issue 2*. 2006, AEAT.
6. Okamoto, I., *Railway technology today 5: How bogies work.* Japan Railway & Transport Review, 1998. **18**: p. 52 - 61.
7. Kamoshita, S., et al. *Development of assist steering bogie system for reducing the lateral force.* in *World Congress on Railway Research.* 2008. Seoul, Korea.
8. Briginshaw, D., *Leila: an innovative new freight bogie: a new disc-braked rail freight bogie is expected to offer greater functionality with lower life-cycle costs.* International Railway Journal, 2005. **45**(8): p. 13 - 14.
9. Hecht, M. and J. Keudel, TU Berlin, LEILA - a new cost-effective and environmentally friendly rail freight bogie, http://www.twanetwerk.nl/upl_documents/hecht-keudel.pdf, [Accessed, 7/1/08]
10. Stephenson, R., *Axle Trees, British Patent No. 5325* 1826
11. Shen, G. and R. Goodall, *Active yaw relaxation for improved bogie performance.* Vehicle System Dynamics, 1997. **28**(4 - 5): p. 273 - 289.
12. Mei, T.X. and R.M. Goodall, *Recent developments in active steering of railway vehicles.* Vehicle System Dynamics, 2003. **39**(6): p. 415 - 436.
13. Goodall, R.M. and W. Kortum, *Mechatronic developments for railway vehicles of the future.* Control Engineering Practice, 2002. **10**(8): p. 887-898.
14. Pérez, J., et al., *Combined active steering and traction for mechatronic bogie vehicles with independently rotating wheels.* Annual Reviews in Control, 2004. **28**(2).
15. Perez, J., J.M. Stow, and S.D. Iwnicki, *Application of active steering systems for the reduction of rolling contact fatigue on rails.* Vehicle System Dynamics, 2006. **44**(Supplement): p. 730 - 740.
16. Pérez, J., J.M. Busturia, and R. Goodall, *Control strategies for active steering of bogie-based railway vehicles.* Control Engineering Practice, 2002. **10**(9): p. 1005 - 1012.
17. Goodall, R. and T.X. Mei, *Chapter 11 Active Suspensions*, in *Handbook of Railway Vehicle Dynamics*. 2006, Taylor & Francis. p. 327 - 357.
18. *GM/GN2589 The design and construction of freight wagons*. 2004, Rail Safety and Standards Board.

19. Tunna, J. and R. Joy, TTCI(UK), Methodology to calculate variable usage charges for control period 4, UK NR report No. 08-002, www.networkrail.co.uk/browse%20documents/StrategicBusinessPlan/Update/TTCI%20(UK)%variablecharges%methodology.pdf, [Accessed, 25/6/08]

Chapter 7: Loading Reductions Achievable With Steering Bogies

In the previous chapter several methods of reducing track loading were discussed, including the use of steering bogies. In this chapter the track loading caused by three types of steering bogie is assessed and compared with that of conventional bogies. The possible reductions in curving forces are studied, including an assessment of the stability of the different bogie types through rough track. The scope of this study, methodology and results are all presented here.

7.1 Scope

The use of steering bogies should reduce the tangential (lateral and longitudinal) wheel-rail loading as a train travels through curves. The benefits to the railway will depend on the number, length and severity of the curves in a given route, and on how rough the track is and how the bogies respond to this. NB In this case track roughness refers to local changes in rail height, twist, lateral position, gauge and curvature over a matter of metres (not the surface roughness mentioned in section 2.4.1).

The speed of the trains and the applied cant will also have an effect on the loading generated through curves.

The advantages of steering will vary for different railways, depending on the combination of factors above. The aim of this investigation is to calculate the load reduction that could be achieved using various types of steering bogie on different types of railway.

The types of steering bogie being evaluated are: cross braced, hardening spring and active steering (see Figure 7 – 1). How they perform on different types of railway has been evaluated using a vehicle/track software package, VAMPIRE*.

* Vehicle dynAmics Modelling Package In a Railway Environment, produced by Delta Rail[1]

Four different test routes have been used, two based on mainline railways, one on a cross country route and one on a metro route.

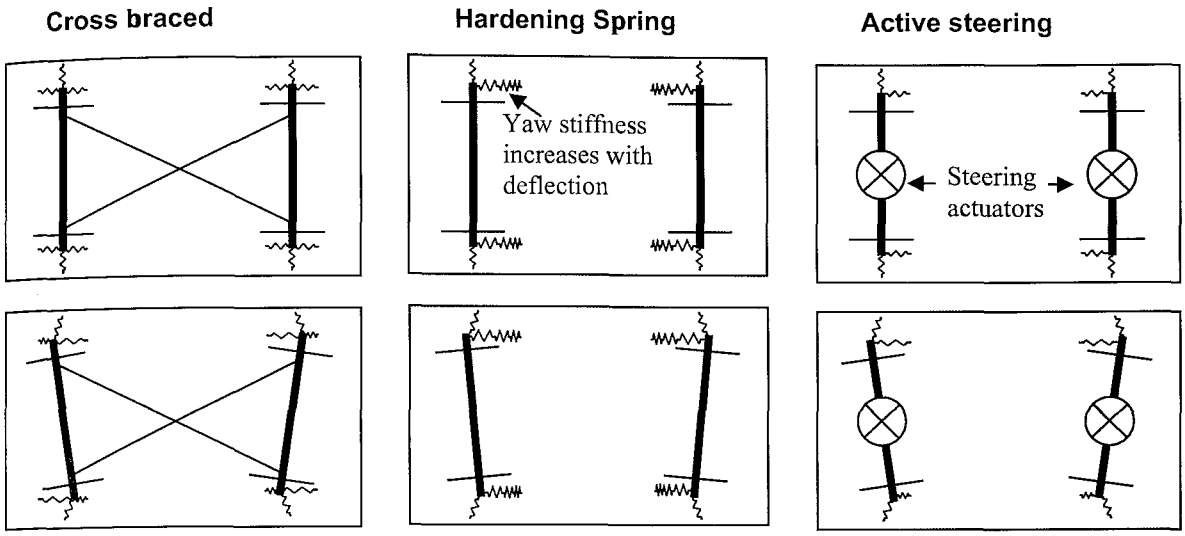

Figure 7 - 1 Types of steering bogie included in this investigation

7.2 Vehicle-track interaction modelling

At the core of this analysis is a vehicle-track interaction model. There are already a variety of commercially available vehicle-track interaction models, used widely throughout the rail industry. Some of the most popular packages are:

- VAMPIRE
- GENSYS
- SIMPACK
- ADAMS/Rail
- NUCARS

As it is difficult to carry out full scale experimentation to completely validate new vehicle-track interaction models, it is sensible to use one of these existing packages as the platform for this investigation. Results will still depend on the validity of the inputs used and the assumptions made during the modelling processes; however, the underlying calculations and methodologies have been validated against measured results for certain test cases and also compared against each other[2, 3].

7.2.1 The simulation process

In all of the dynamics packages listed, the vehicle is represented as a mass-spring-damper system. Each mass in the system has six degrees of freedom: longitudinal, lateral, vertical, yaw, pitch and roll (explained further in section 7.3.2). Degrees of freedom can be locked out as required, or controlled through the connections between masses. Vehicle suspension systems can be built up with the required stiffness and damping values. Tracks can be modelled to various levels of detail, with information on the curvature, applied cant, and track roughness (as described in section 7.1).

Equations of motion are defined for every mass in the system, a time step iteration is used to simulate the vehicle model moving along a predefined track. At every time step, the force in all springs and dampers along with the force at the wheel-rail contact is calculated. From this the position, speed and acceleration of every mass in all of the appropriate degrees of freedom can be derived.

The simulations tend to have a fixed time step, although the speed of the vehicle can be changed over the course of a simulation run (meaning the distance step will vary). It is very important to select an appropriate time step. If high frequency track roughness is being included, the time step must be small enough to include this detail and calculate the vehicle response appropriately. If the time step is too big, the calculation can become unstable. Conversely a shorter time step means longer calculation time; a balance must be found to take this into account.

The main differences between the available dynamics packages is the method used to calculate wheel-rail contact conditions and the level of detail included in the track foundation.

All of the systems mentioned use a derivative of Kalker's contact equations (as discussed in Chapter 2) for calculating wheel-rail tangential loads. Kalker developed a variety of wheel-rail contact codes, with methods of simplifying the contact problem to quickly calculate creep coefficients. Kalker's FASTSIM

code[4] is used by ADAMS/Rail and GENSYS. SIMPACK has a pre-processor to calculate a table of Kalker coefficients which are referred back to later in the main calculation, whilst NUCARS and VAMPIRE both contain pre-calculated look up tables of Kalker coefficients[5].

7.2.2 The Manchester benchmarks for rail vehicle simulation

The five vehicle dynamics packages mentioned above were all benchmarked against each other in an exercise led by Manchester Metropolitan University, known as the 'Manchester Benchmarks'. Full results of this study were published in 1999[3].

The benchmarking exercise involved using all five packages to simulate a range of test cases, involving two different types of rail vehicle, running over four different types of track. The two vehicles used were a bogied passenger car based on a standard benchmark vehicle, the ERRI B176; and a simplified two axle freight car. The different track types were used to test the systems' ability to calculate curving performance of rail vehicles, critical speed (for hunting) and response to track roughness/irregularities.

'The Results of the Manchester Benchmarks'[6], states that *'the number and range of results makes it difficult to draw clear conclusions. The overall impression, however, when looking through the tabulated and plotted results is that there is generally good agreement between the packages'*. Some examples given are: a 10% error for values of calculated critical speed across all packages, values for the vertical displacement of the car body within 1 %, and lateral displacement within 5 %.

The 'Manchester Benchmarks' also gave an indication of the calculation speed for each of the simulation packages, shown in Table 7 – 1.

This was not really a fair comparison because the same speed of computer was not used for every package. However, it does appear that VAMPIRE is generally the fastest system. This is because of the pre-calculated look up tables for creep

coefficients, which save processor time during the dynamics analysis. The tables store data for a range of creep coefficients and contact patch sizes; for contact conditions falling in-between data points, the values are interpolated. This simplification may lose some level of detail compared to the full creep calculation used by the more time consuming models.

	VAMPIRE	GENSYS	SIMPACK	ADAMS	NUCARS
	time /s	time /s	time /s	time /s	time /s
vehicle 1					
eigenvalues	1				2
case 1	62	3591	95	2470	93
case 2	3	204	28	520 / 910	8
case 3	4	258	373		15
vehicle 2					
eigenvalues					0.1
case 2	3	205	14	152 / 170	7
case 3	3	91	70	516	9
case 4	2	245	182	170	8
computer	Pentium II	Pentium	Pentium II	Pentium II	Pentium
	300 MHz	200 MHz	300 MHz	300 MHz	200 MHz

Table 7 - 1 Comparison of times to carry out a range of calculations

This investigation requires a range of calculations considering many different combinations of variables; because of this, processing time is very important. VAMPIRE was chosen to carry out the vehicle-track interaction modelling for this study; it is also readily available and widely used by the UK rail industry, which is another benefit.

7.2.3 VAMPIRE validation

The underlying calculations used by VAMPIRE were developed based on a range of measured data from on train testing. Evans[7] carried out a comparison of VAMPIRE outputs against measured data, including studies of curving performance, response to track irregularities and derailment risk. The important outputs relevant to this study are the wheel-rail loads generated due to curving and track roughness; examples of Evans' output for these types of calculations are shown in Figures 7 – 2 and 7 – 3, which demonstrate measured results correlating closely with outputs from VAMPIRE.

Evans' study demonstrated that VAMPIRE can produce results that closely correlate with measured data. However, in order to achieve this, the user needs a good knowledge of the vehicle characteristics and track conditions. When attempting to quantify the effects of theoretical vehicles across a large network

with varying track conditions, it is necessary to make a range of assumptions, and the quality of these assumptions has a significant effect on the accuracy of the model outputs.

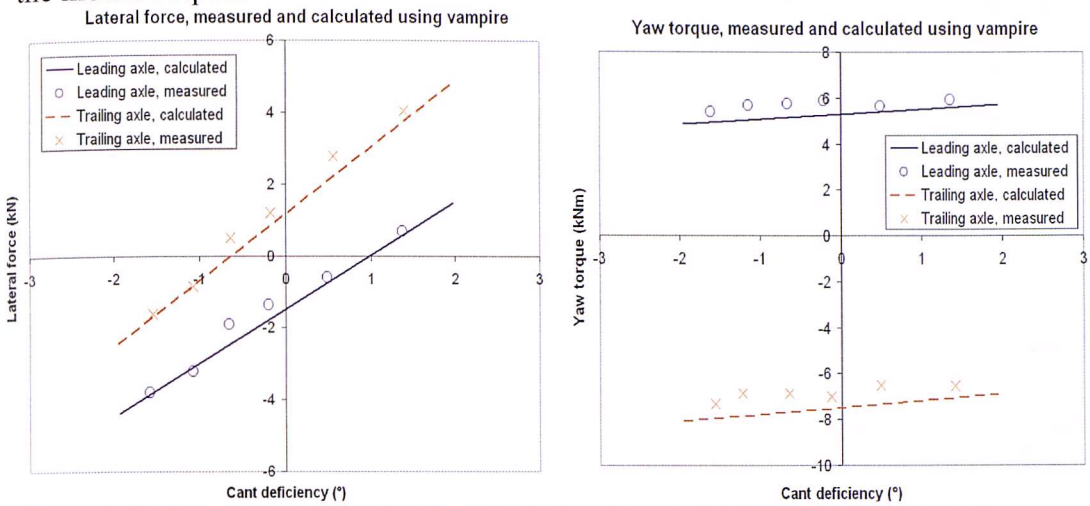

Figure 7 - 2 Comparison of curving forces calculated using VAMPIRE and measured results, across a range of cant deficiencies for a 580 m curve radius and soft suspension vehicle. Redrawn from[7]

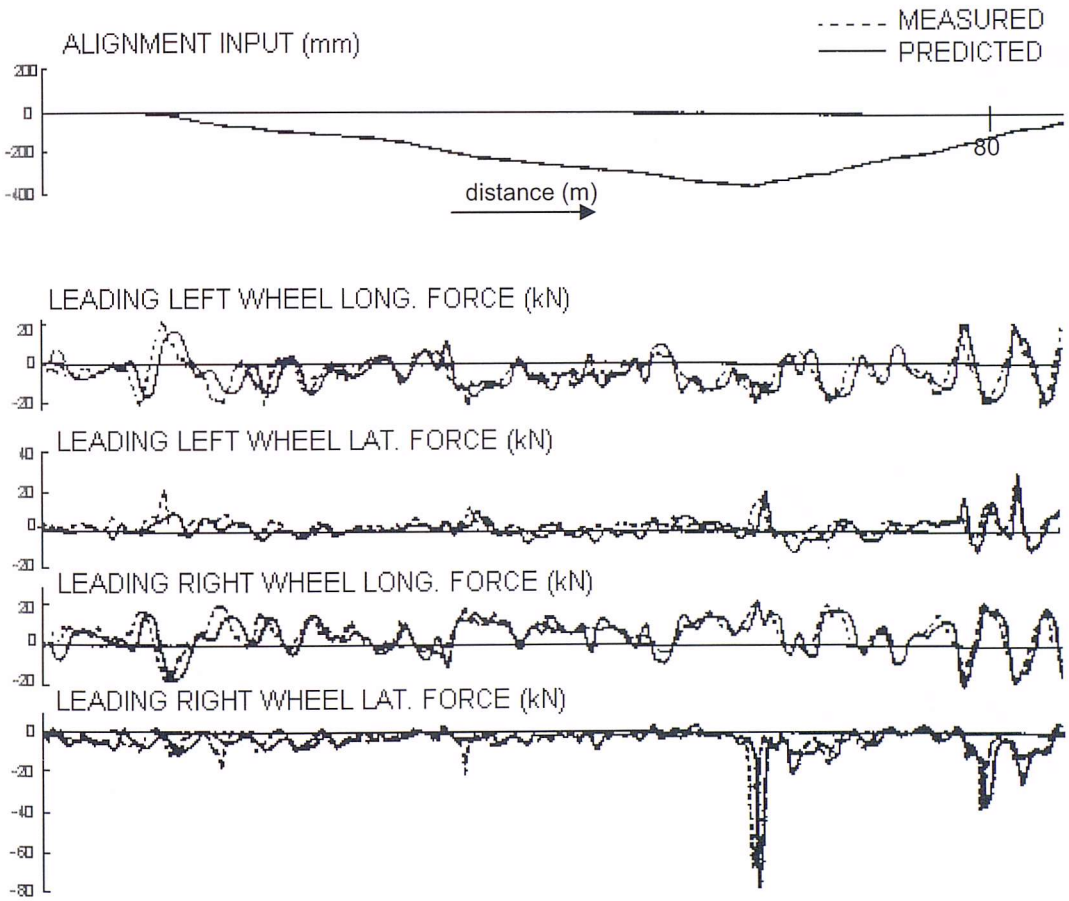

Figure 7 - 3 Comparison of calculated and measured tangential loading for a Class 56 locomotive travelling over a horizontal kink in the track[7]

7.3 Methodology

As described in section 7.1, the purpose of this study is to calculate the reductions in tangential loading that can be achieved with three types of steering bogie (cross braced, hardening spring and active), when used on: mainline, cross country and metro railways.

The benefit of using steering bogies should be the reduction in tangential loading that can be achieved through curving. Steering bogies will also have different dynamic behaviour when travelling through rough track. This needs to be taken into account when attempting to quantify their benefits (or disbenefits).

The first step in this analysis was to model test tracks containing suitable characteristics, to represent the types of railway under consideration. Test routes were created for newly installed (design case) track, and also with extra irregularities (or roughness) to simulate typical track conditions for each type of railway. Development of these test tracks is discussed further in section 7.3.1.

Two sets of vehicle models were also created, the first set based on the ERRI B176 benchmark vehicle, as used in the 'Manchester Benchmarks'. This vehicle was chosen because there is an existing model available in VAMPIRE and it has already been validated through comparison with other vehicle dynamics packages. The base case B176 model was first used to represent a conventional bogied passenger vehicle, and then modified as necessary to produce vehicles containing: cross braced, hardening spring and active steering bogies. Using this same set of vehicles across all test tracks means the only variables under investigation are the type of steering and type of route.

In reality, different types of railway use different types of rolling stock, with different mass and suspension designs. A second set of vehicles, which are more representative of real trains used on the different railways, was also created.

		Conventional steering		Cross braced bogie		Hardening spring bogie		Active steering	
		B176	Rep	B176	Rep	B176	Rep	B176	Rep
Mainline 1	Design								
	Rough								
Mainline 2	Design								
	Rough								
Cross country 1	Design								
	Rough								
Metro 1	Design								
	Rough								

B176 = Benchmark vehicle Rep = Representative vehicle for each route

Table 7 - 2 All test cases included in this study

Running a dynamic vehicle-track interaction model of each vehicle across every test track gave a total of 64 sets of results; see Table 7 – 2 for the full set of test cases.

Figure 7 – 4 shows a diagram of the simulation process for this investigation. VAMPIRE gives the option for many different outputs; for this analysis single rail vehicles are modelled and the outputs used are the three dimensional loadings at each wheel-rail contact patch, over time.

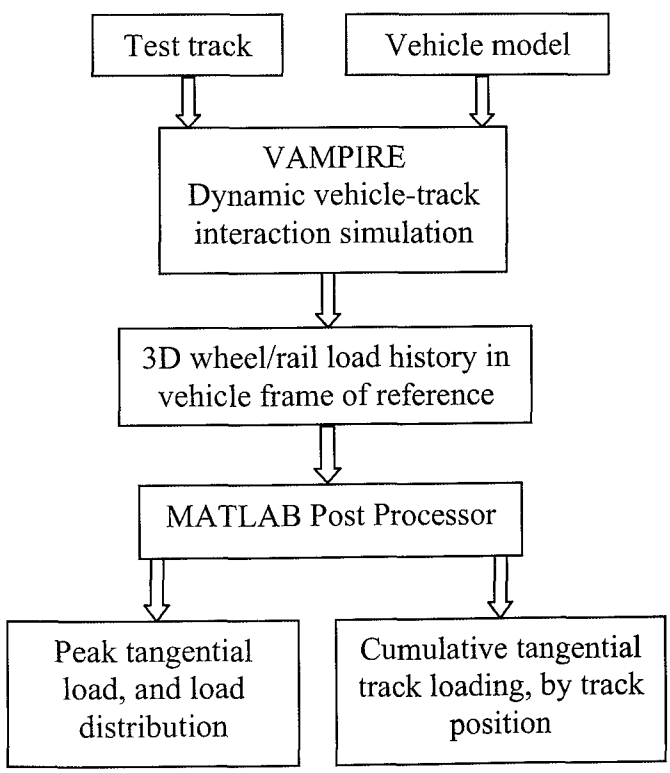

Figure 7 - 4 Simulation process

The track and vehicle input data are fed into the program by creating text files containing all of the relevant information. Vehicle files contain details of the mass and rotational inertias of all structural components (car body, bogies and wheelsets), as well as the stiffness and damping values of the suspension components connecting them. Track data is entered in two separate files, a design file containing design curvature and cant, and the vehicle speed along the track; and an irregularity file containing all of the track roughness data.

7.3.1 Test routes

As mentioned in section 7.1 there are four test routes. These routes have been developed based on measured data from UK railways, provided by Network Rail, Serco Assurance, and Tubelines Ltd. Each route has a different curvature profile, as shown in Figure 7 – 5.

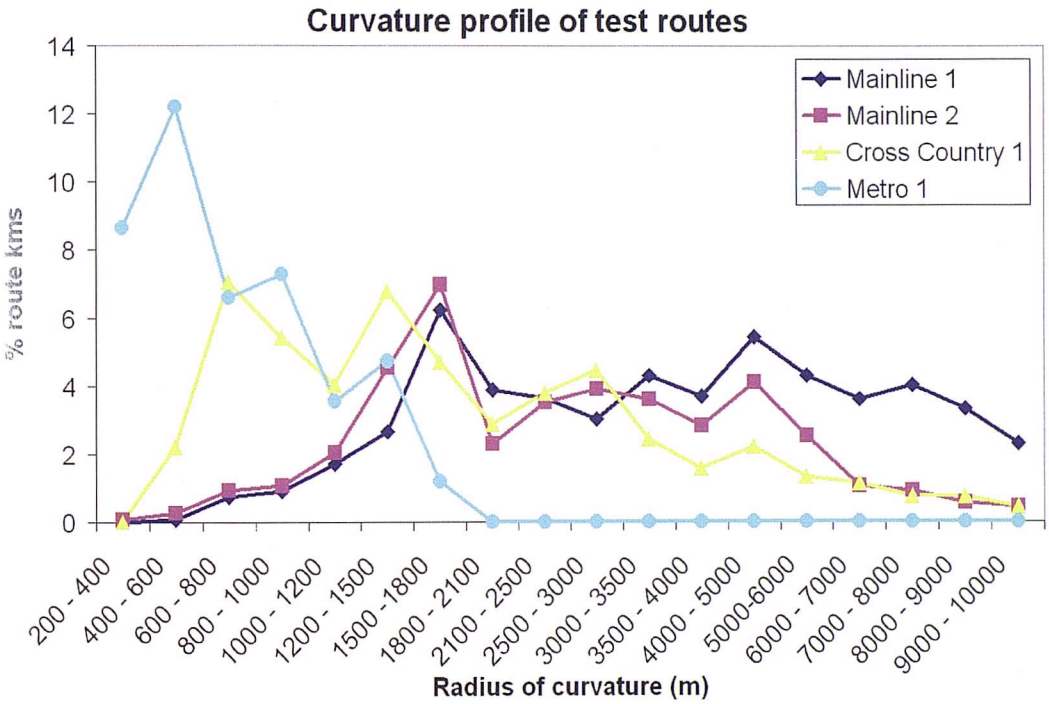

Figure 7 - 5 Comparison of curvature profiles across test routes

The metro route contains the lowest radius curves; as railways operating in urban environments are often built later than other infrastructure, meaning they have to curve around existing structures. The cross country route also contains a lot of curves, though it has less of the extremely tight curves (below 800 m radius). However, the line speed on this route is higher than for the metro route. The two mainline routes are generally straighter in comparison; both show reasonably similar curvature profiles. Mainline 1 has more curves in the higher 5000 –

10000 m range, while Mainline 2 has slightly more tighter curves in the 600 – 1800 m range. For the purpose of this study, track with a curve radius greater than 10000 m was considered to be straight. The curvatures alone do not give the full picture; it is the total combination of radius of curvature, applied cant and vehicle speed that gives the severity of each curve.

The curvature profiles shown in Figure 7 – 5 are based on measured data over hundreds of km of track. In order to reduce simulation time, and to allow testing of a variety of vehicle designs, shorter 5 km representative routes were developed to match these curvature profiles (i.e. the same percentage of track, by length, in each of the curvature ranges). The representative routes were built up from sections of the real track data (using the measured cant and curvature) and fitted together appropriately. Where necessary sections were 'smoothed' in an attempt to simulate 'design case' test tracks (i.e. there is no track roughness) and the only inputs to the system are the curvature and cant of the track. Speed limits along the test routes were set at the appropriate line speed, or the maximum allowable speed through curves, based on the UK maximum cant deficiency of 110 mm[8]. The exception to this is the Metro 1 route, where speed limit information was supplied by the operator.

Figures 7 – 6 to 7 – 9 show a summary of the design case track data for each test route.

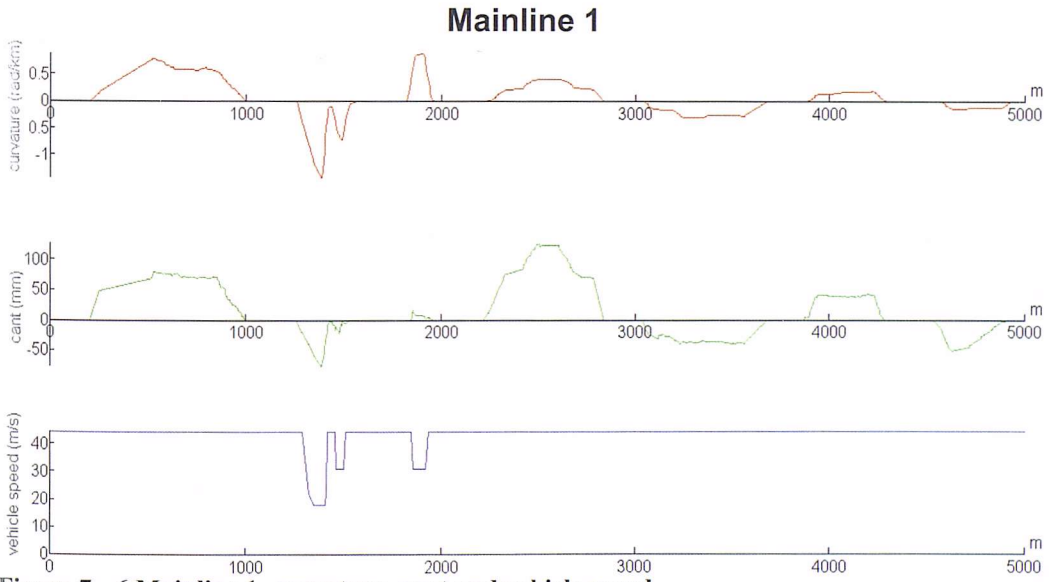

Figure 7 - 6 Mainline 1, curvature, cant and vehicle speed

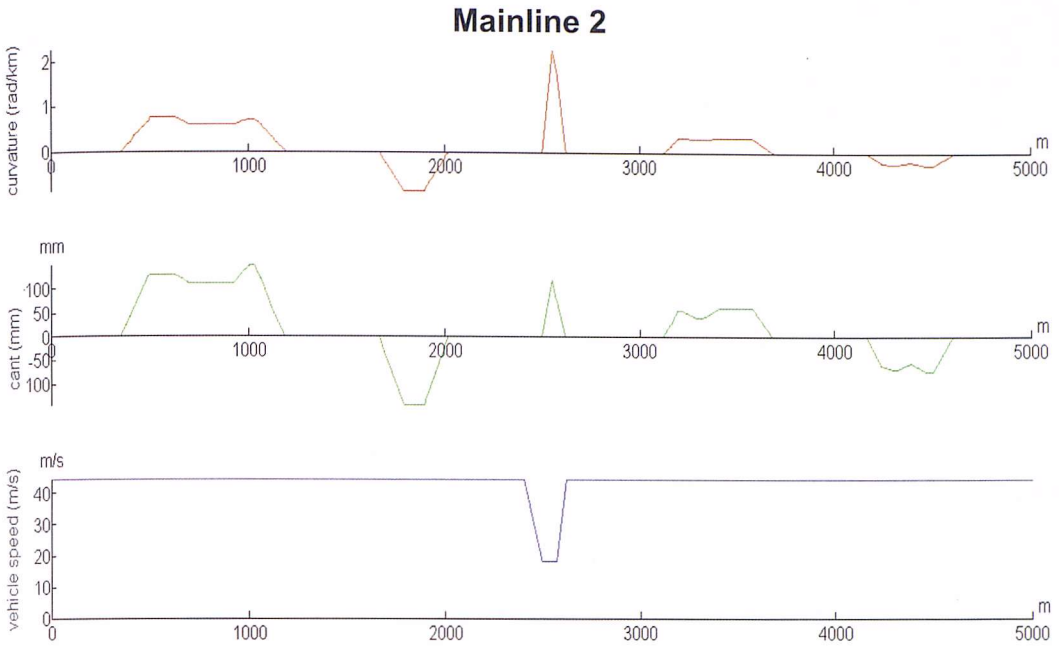

Figure 7 - 7 Mainline 2, curvature, cant and vehicle speed

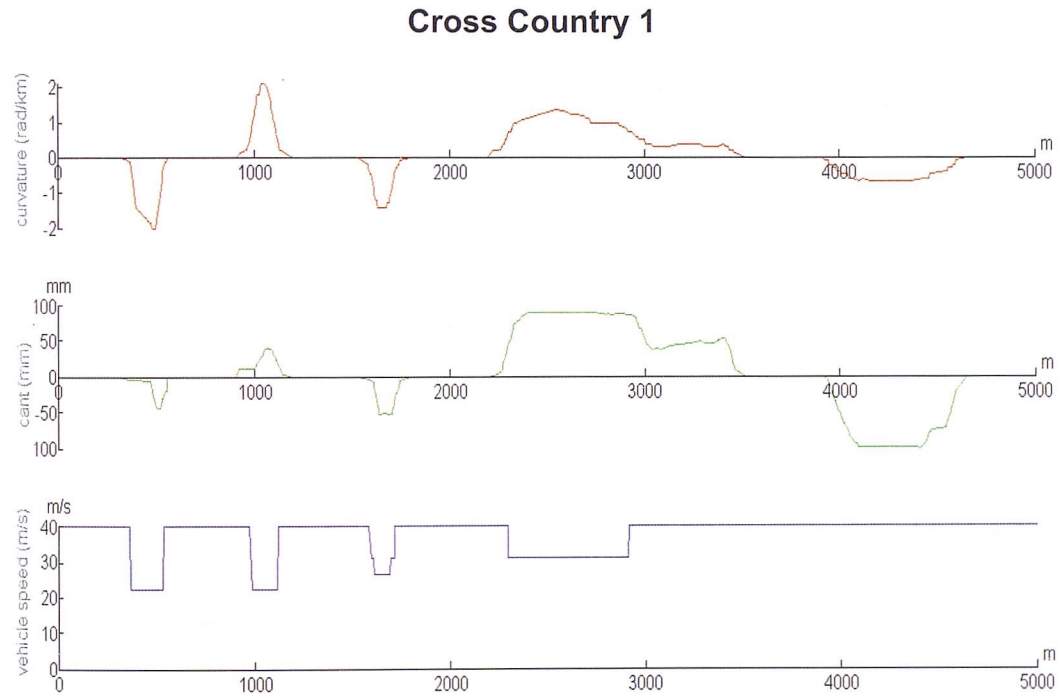

Figure 7 - 8 Cross Country 1, curvature, cant and vehicle speed

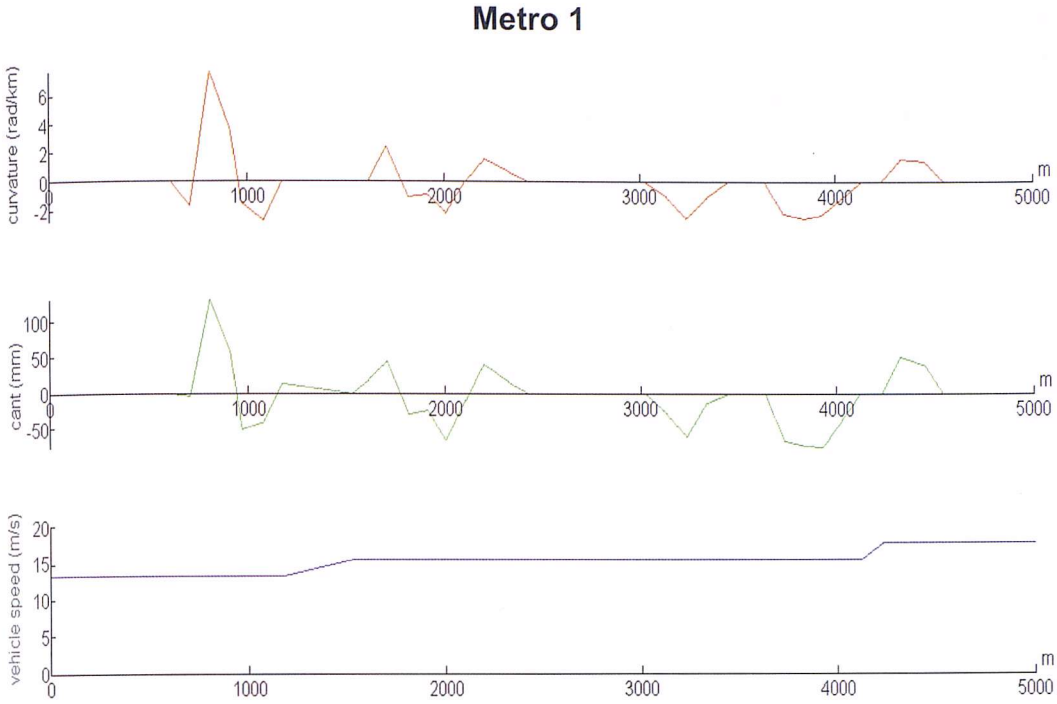

Figure 7 - 9 Metro 1, curvature, cant and vehicle speed

7.3.1.1 Track roughness

Figures 7 – 6 to 7 – 9 show the characteristics of the 'design case' smoothed routes; in addition to this, roughness profiles have been created for each route. For the vehicle-track simulations, track roughness can be overlaid onto the design case track. This should give a more realistic representation of track conditions. The track roughness profiles include: cross level, curvature, lateral and vertical irregularities. Railway Group Standard, GC/RT5021[8] defines track roughness limits for UK railways, depending on the line speed. These roughnesses are defined by the allowable standard deviations in rail height and lateral position (Appendix D shows a table of allowable roughnesses against line speed). Data for typical roughness profiles were supplied by Delta Rail as library files with VAMPIRE. The roughness profiles were prepared depending on the line speed of the route being modelled. In this case the library files track200 (i.e. for routes operating up to 200 kph) has been used for the mainline routes; track160 for the cross country route; and track110 for the metro route. The track roughnesses for the three types of railway are shown in Figures 7 – 10 to 7 – 12.

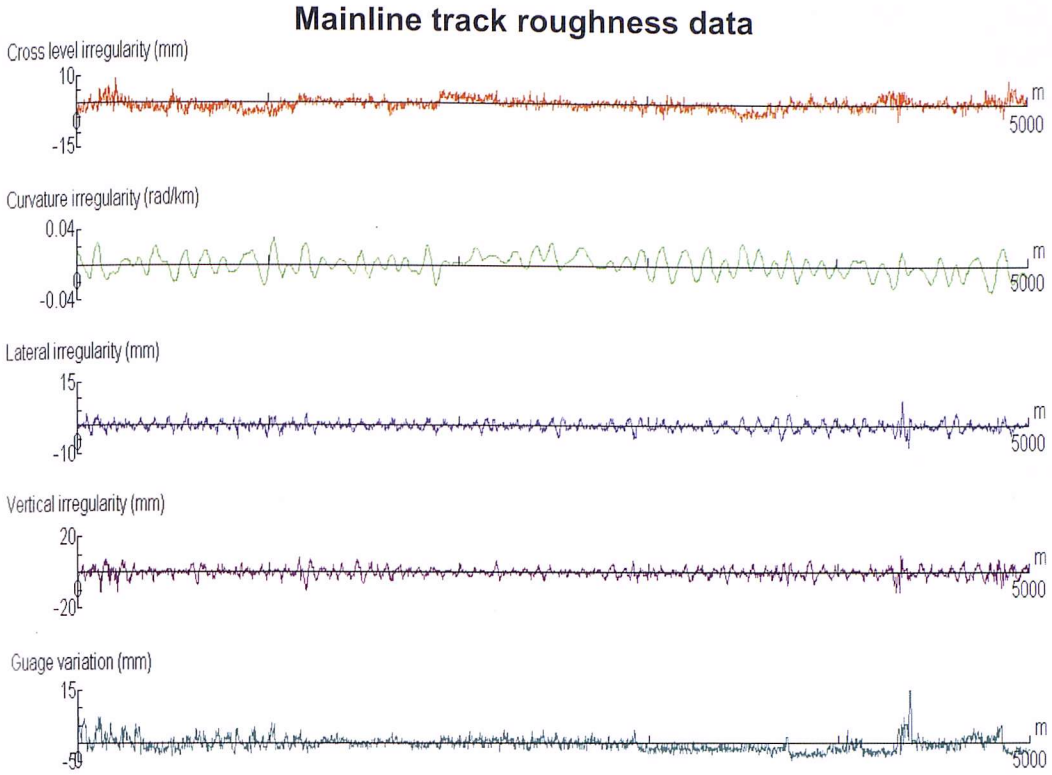

Figure 7 – 10 Mainline track roughness

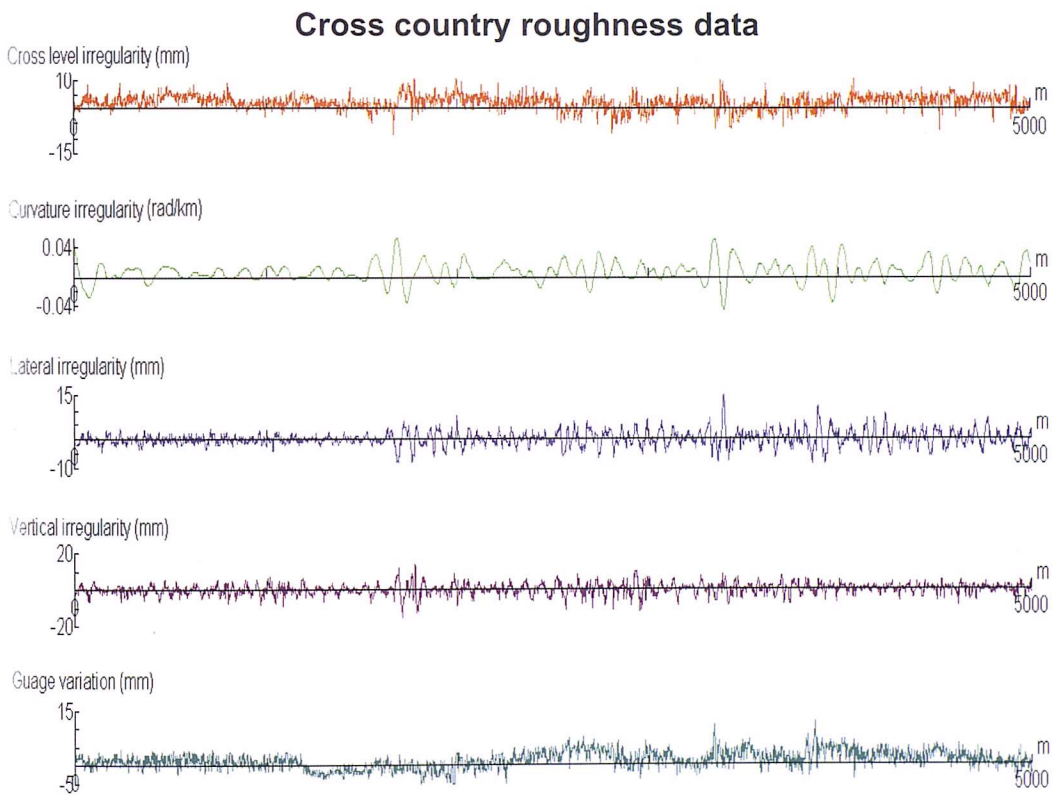

Figure 7 – 11 Cross country track roughness

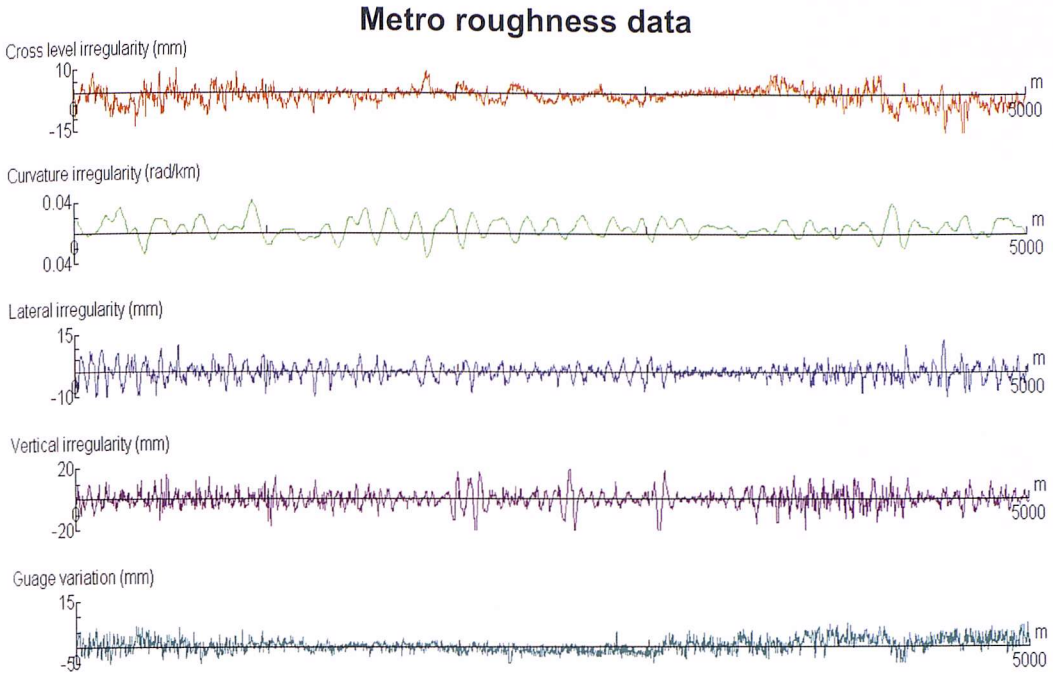

Figure 7 – 12 Metro track roughness

This method of producing design case track models and overlaying the roughness models from Delta Rail was chosen rather than using the measured roughness from the sections of track which make up the 5 km test routes. This is because these roughness models should represent the overall track irregularities for a route of each type, rather than including the roughness from a disparate set of track sections from random positions along the route.

For all simulations a uniform coefficient of friction between the wheel and rail has been taken as 0.3, which is a typical value for clean, dry rail[9].

7.3.2 Vehicle models

Each simulation is carried out with a single carriage running over a specific test route. Single carriage models have been chosen, rather than whole train models, to simplify and speed up the modelling process and also because the characteristics of the inter-car connections have a significant effect on the loading outputs for following carriages. Small changes in stiffness and damping values for the inter-car connections could have a big effect on the calculated wheel loads†.

† This could be an interesting area for further investigation, modifying the inter-car connection may be an alternative method of reducing tangential rail loading, possibly through the use of active damping.

Each vehicle is represented by a mass/spring/damper system with 36 degrees of freedom (shown in Figure 7 – 13), where X, Y, and Z are displacements in longitudinal, lateral and vertical directions, T is rotation about the X axis (roll), P is rotation about the Y axis (pitch), and W is rotation about the Z axis (yaw).

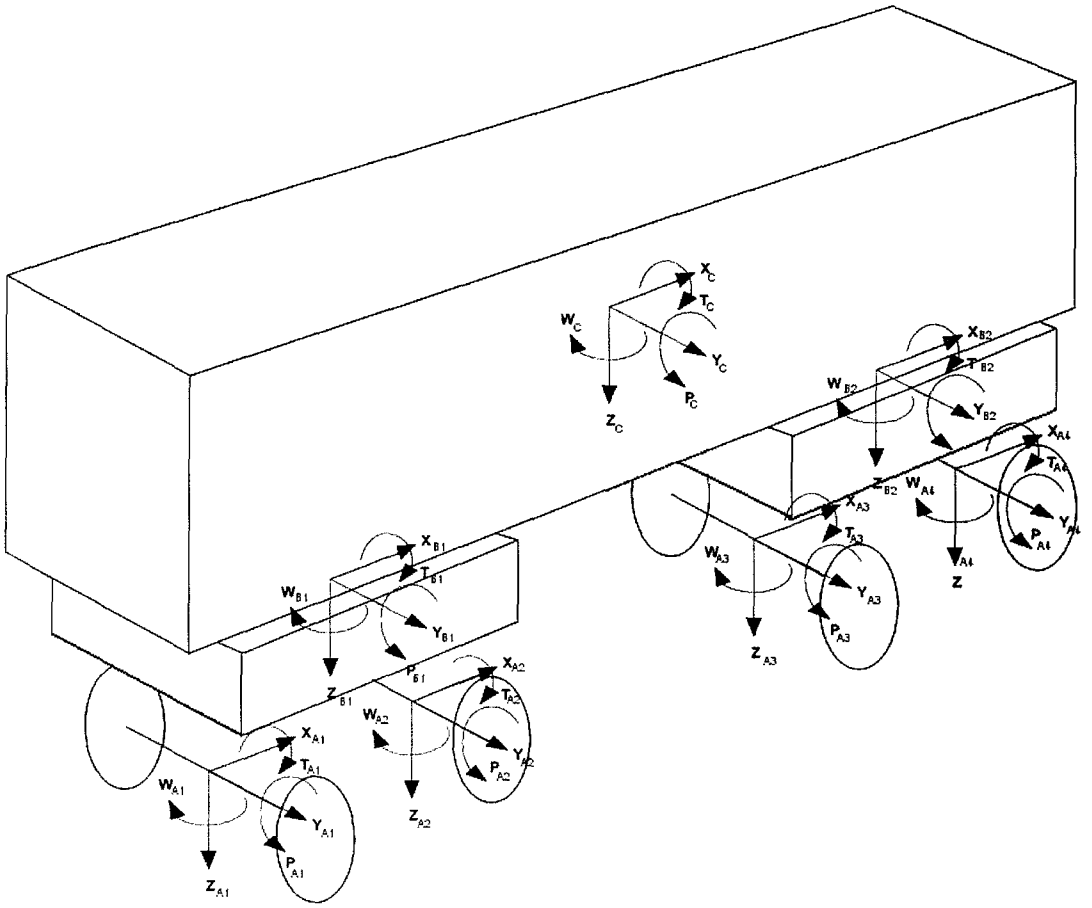

Figure 7 – 13 Vehicle model, degrees of freedom

An overview of the vehicle models is shown in Table 7 – 3.

	B176	Mainline locomotive	Mainline carriage	Cross country DMU	Metro motor car	Metro trailer car
Carbody mass (tonnes)	32	52.5	25.0	34.2	22.3	16.3
Bogie mass (tonnes)	2.6	5.7	2.1	2.9	1.9	1.4
Wheelset mass (tonnes)	1.8	1.5	0.9	1.3	0.8	0.6
Wheel radius (mm)	460	500	450	450	385	385
Powered axles?	No	4	No	4	4	No
Bogie wheel base (m)	2.56	3.00	2.60	2.60	2.05	2.05
Primary Yaw stiffness (MNm/rad)	41	30	15	15	15	15

Table 7 – 3 Basic vehicle model characteristics

The more realistic vehicle models were developed from template files, provided by Serco Assurance as part of the VTISM library, using as much data as possible from real vehicles[10-14]. For each route, different car types (i.e. carriage, locomotive, trailer car, motor car) were simulated separately, with their loading summed together appropriately to make up a whole train. The two mainline routes were simulated with a high speed train, made up of six coaches being hauled by two locomotives at each end of the train, loosely based on an IC125 train. A three car DMU was operated on the cross country route, loosely based on a class 170 DMU. For the metro route, a train made up of four motor cars and two trailer cars, based on London Underground tube stock, was used.

The data presented in Table 7 – 3 is for the conventional vehicles only. For each of the vehicles shown, there are a further three variants containing the different types of steering bogie. The only difference between the steering vehicles and their conventional counterparts is in the tangential aspects of the primary suspension. All component weights; secondary suspension characteristics; and vertical primary suspension values remain constant. All vehicle models have been created for a high level comparison of the various steering options; no attempt has been made to carry out any detailed design of each vehicle type.

7.3.2.1 Cross braced bogie

The cross braced bogie used for this study works by adding in two additional steering links between diagonally opposite axle boxes, as shown in Figure 7 – 1. The aim of this arrangement is to force both axles in a bogie towards a more neutral curving position, with a reduced angle of attack. A yaw movement in one axle creates an equal and opposite yaw movement in the other axle.

7.3.2.2 Hardening spring bogie

The aim of the hardening spring bogie is to give low primary yaw stiffness for small yaw displacements of the axle, to allow them to move towards a radial track position. The stiffness is increased with displacement to limit the range of movement, with the aim of avoiding the instability normally associated with low yaw stiffness.

As shown in Figure 7 – 1, at the end of each axle there is a variable stiffness longitudinal connection to the bogie, with the characteristics shown in Figure 7 – 14.

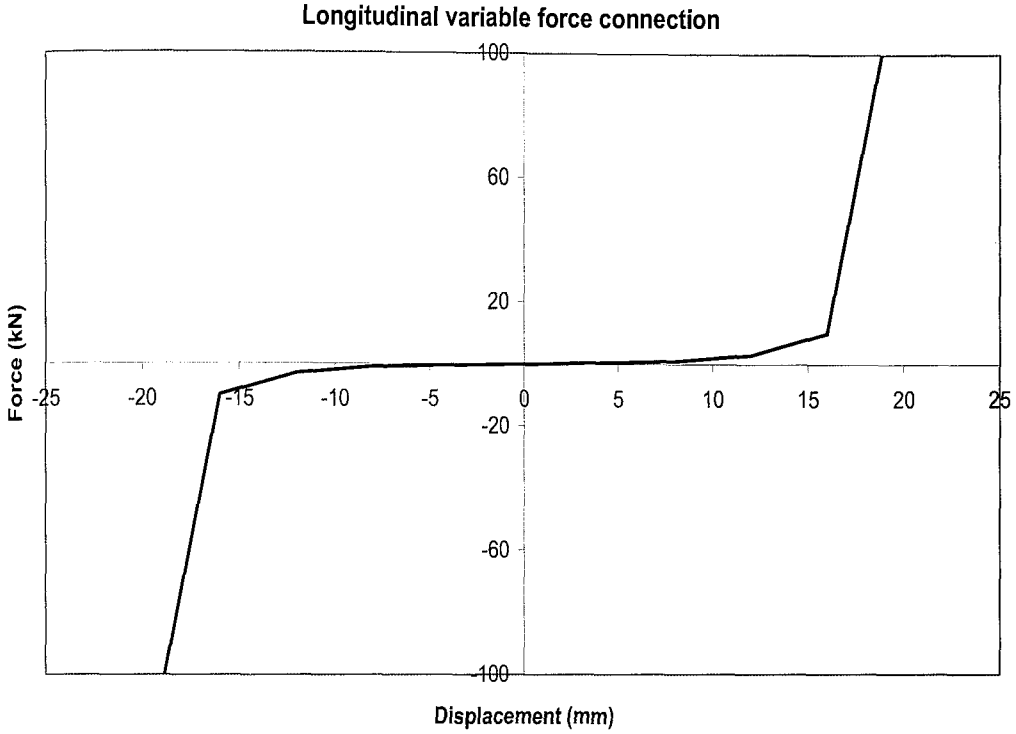

Figure 7 - 14 Force/displacement for longitudinal connections at the ends of each axle

7.3.2.3 Active steering bogie

A simple and robust control system is required for the active steering bogie; the feedback system must be based on measurements that can easily be obtained from vehicle mounted sensors.

Active bogies proposed by existing research tend to rely on knowledge of every wheelset position in the track frame of reference, as well as the instantaneous curvature and applied cant[15, 16]. As discussed in Chapter 6 these inputs can be calculated, based on accelerometer measurements taken at the axle boxes[17]. An alternative, simpler control system, based on force feedback is proposed for this study. At every time step the longitudinal force in the primary suspension at each axle box is measured; from this the yaw torque applied by the primary

suspension is calculated. Figure 7 – 15 shows the feedback control system for each bogie.

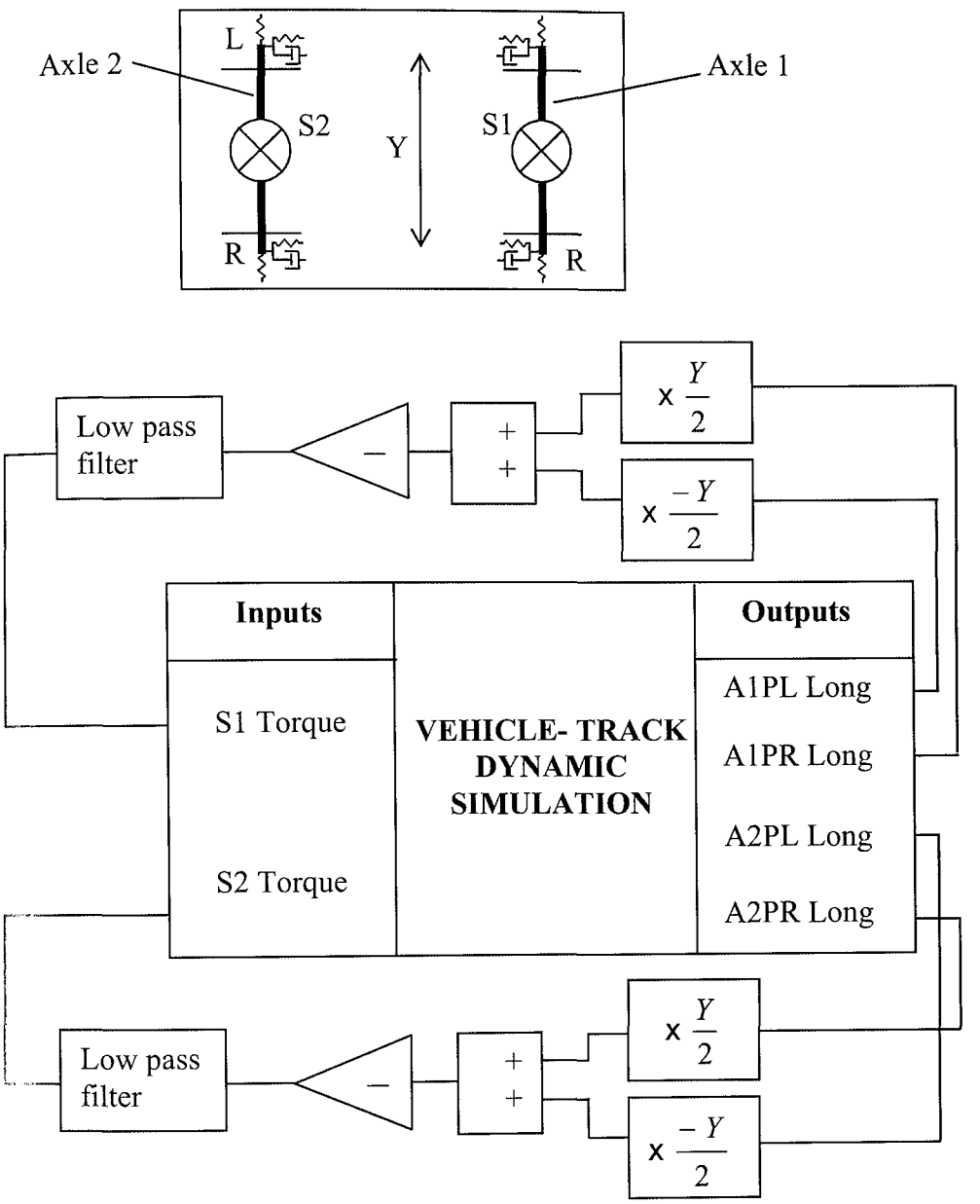

Where G = wheel gauge; A1PL Long = axle 1, primary suspension left wheel longitudinal force etc; S1 and S2 are the steering actuators

Figure 7 - 15 Active steering feedback system

The active system works in parallel with the conventional suspension (similar to the design suggested by Perez et al[17]), effectively 'holding off' the yaw stiffness through curves. A low pass filter is applied to the control system, which limits the bandwidth of the torque actuators. This means the active system only responds to the low frequency loads due to curving, leaving the conventional

suspension to maintain vehicle stability through the higher frequency track irregularities.

This gives a simpler control system than position based feedback, and should be easier to implement on a real rail vehicle. The aim of this system is not to force the wheelset through curves, but to allow the natural rolling radius steering of the wheelset to work fully. The wheelsets naturally move towards a neutral angle of attack, but the conventional elements of the suspension prevent this from being fully realised; causing creep loading as discussed in Chapter 2. The active system attempts to cancel out this creep loading and allow the wheelset to move through curves at a neutral angle.

This system has been simulated using a VAMPIRE/SIMULINK interface. The control system is modelled in SIMULINK which is used to feedback into the VAMPIRE dynamics calculation.

In the simulation the control system uses a torque actuator to apply the necessary torque to each wheelset. In practice this could also be achieved with a linear force actuator connected at the axle boxes (as described in Chapter 6).

To identify an appropriate cut off frequency for the control system, it is first necessary to identify the frequency components of the longitudinal wheel-rail loading.

Figures 7 – 16 and 7 – 17 show the amplitude spectrum of the longitudinal wheel-rail loads from simulations of a DMU train travelling over the cross country 1 test route, and a locomotive train travelling over the mainline 1 test route. In both cases the longitudinal wheel-rail load histories from the simulation output, for every wheel, have been recorded at a frequency of 1000 Hz (i.e. an output time step of 0.001 seconds). From these time steps the amplitude spectrum has been calculated in each case using a Fast Fourier Transform (FFT) analysis. By comparing the FFT outputs for the design case tracks against the outputs for tracks including roughness, the frequency components due to roughness only can be identified.

As demonstrated in Figures 7 – 16 and 7 – 17 the longitudinal loading due to curving is primarily at a frequency below 1 Hz, with the stabilising damping loads generated in response to track roughness mostly within the 1 to 10 Hz range.

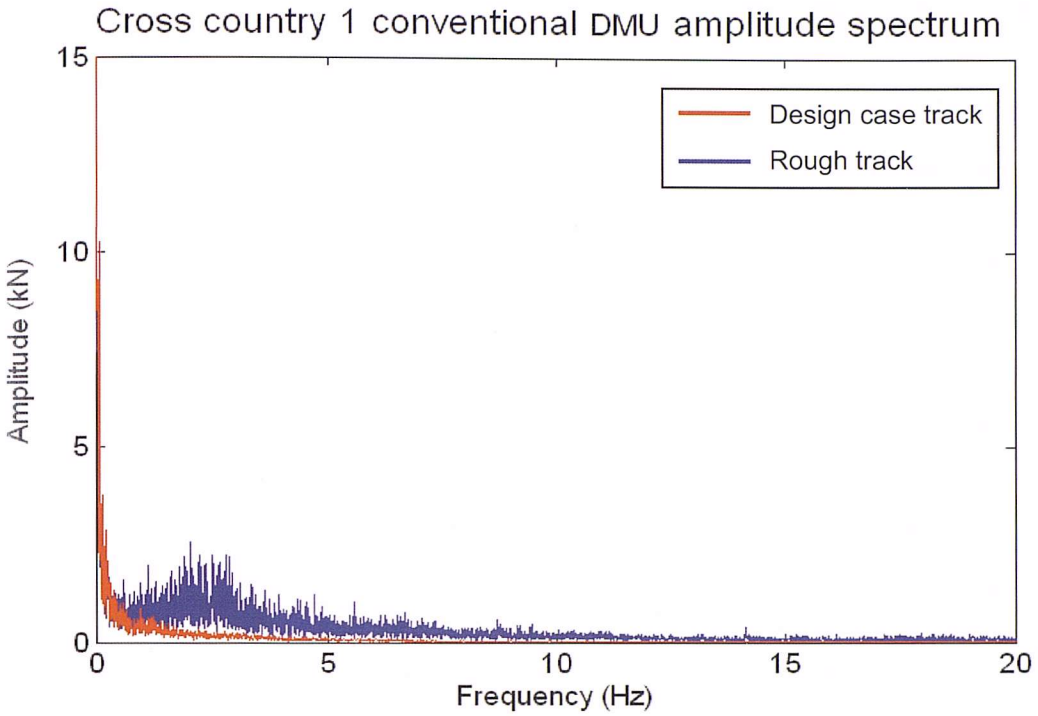

Figure 7 – 16 Longitudinal wheel-rail load amplitude spectrum, for a DMU train travelling on cross country 1

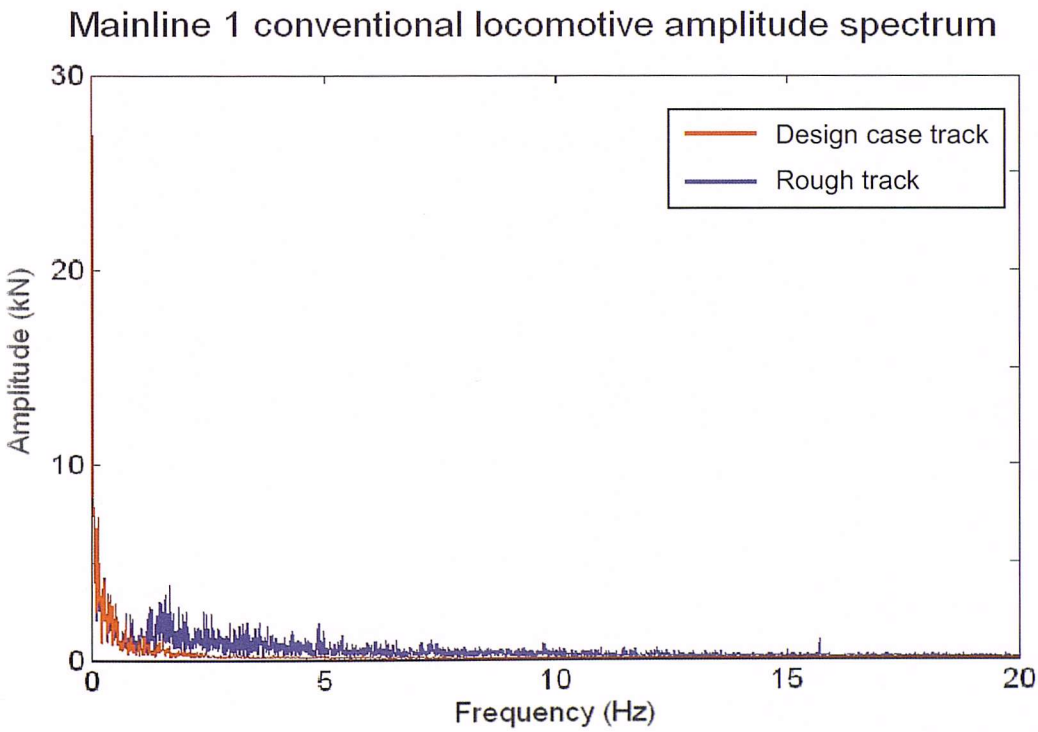

Figure 7 – 17 Longitudinal wheel-rail load amplitude spectrum, for a locomotive travelling on cross country 1

To ensure the active system only responds to the loading through curves, without interfering with the bogies' stability through rough track, a 1 Hz cut off frequency is applied to the actuators. This matches the 1 Hz cut off suggested by Perez et al[18].

In the simulations this is achieved by using a Butterworth filter to apply a low pass filter with a 1 Hz cut-off frequency to the feedback control signal.

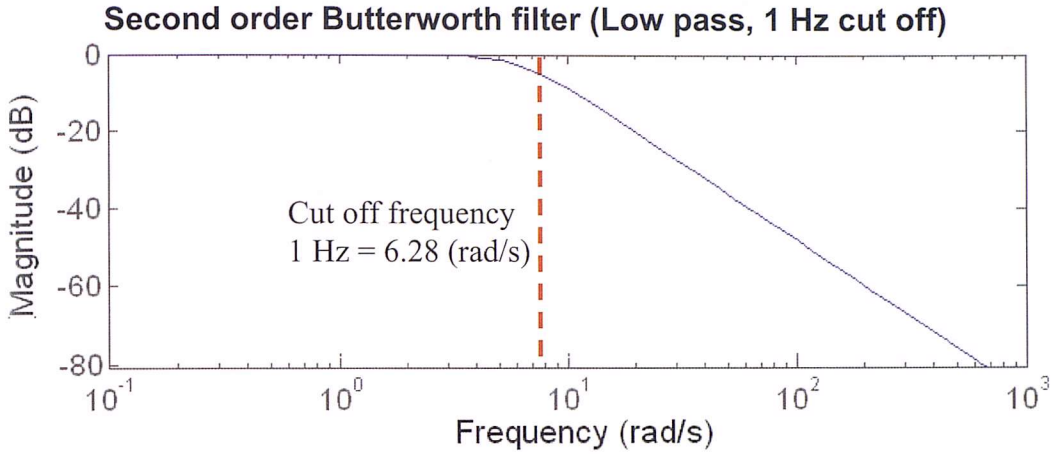

Figure 7 – 18 Low pass filter applied to the force feedback signal

7.4 Results from B176 vehicle derivatives

7.4.1 Design case tracks

There are a significant number of output channels available from the dynamic simulation. For every wheel, a three dimensional loading is calculated, along with creepage, contact patch size and geometry, wheel position, angle of attack, and forces in all suspension components.

Figure 7 – 19 shows all tangential load outputs produced by a simulation of vehicle B176 running over Mainline 1. It is difficult to make a quick and meaningful comparison of vehicle performance when evaluating all of these outputs. Because of this, it is necessary to summarise the outputs from each simulation in a suitable format for easy comparison. This has been carried out using two different methods.

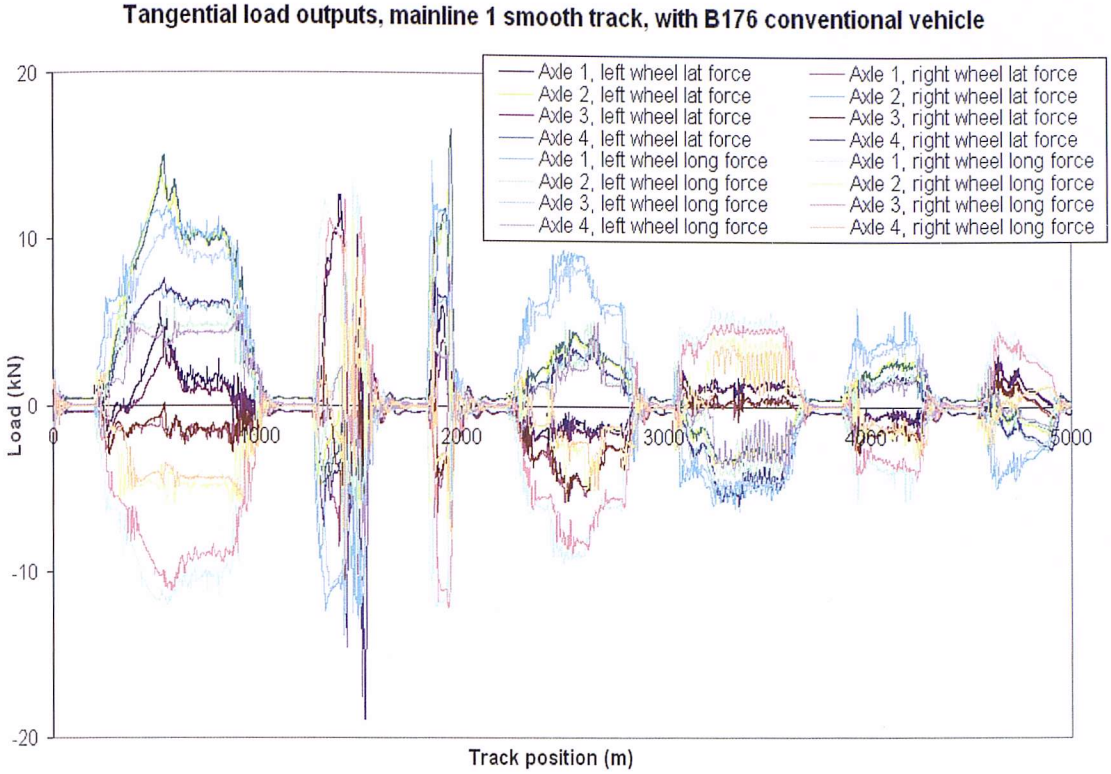

Figure 7 - 19 Tangential load outputs for conventional B176/Mainline 1 dynamic simulation

7.4.1.1 Comparison of cumulative load by track position

The first method used is to find the cumulative tangential load experienced at each point along the track due to the passing of one car, and compare this for all four types of vehicle. Figure 7 – 20 shows the cumulative tangential loading comparison for the Mainline 1 test route.

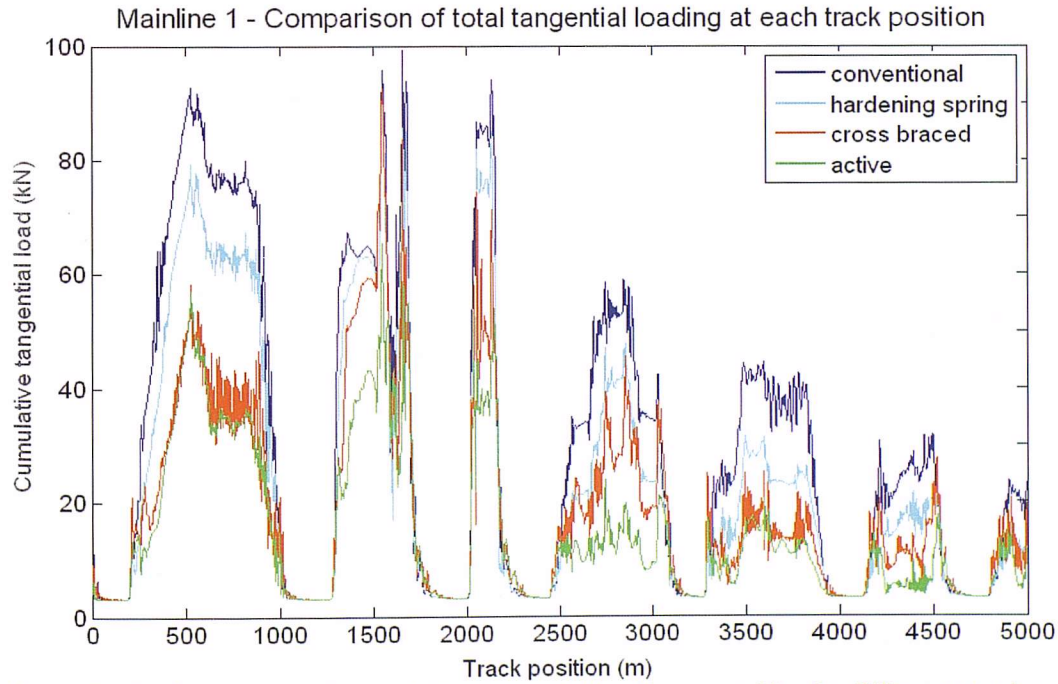

Figure 7 – 20 Comparison of cumulative tangential loading caused by the different steering mechanisms on the Mainline 1 test route

In this case the 5 km test route has been split up into 8514 sections[‡], the outputs show some high frequency oscillations, particularly through curves, because the wheels tend to oscillate around their ideal position as radius of curvature changes. As can be seen in Figure 7 – 20, the mechanical steering train gives the highest levels of hunting; however, the overall tangential loading passed down into the track by this type of train is still considerably lower than the conventional and passively steered vehicles.

In order to simplify the outputs, and to more easily compare the steering mechanisms graphically, the track has been split up into 10 metre sections; the maximum tangential load in each section has been identified. Figures 7 – 21 to 7 – 24 show comparisons of all types of steering across the four test routes using this smoothed data.

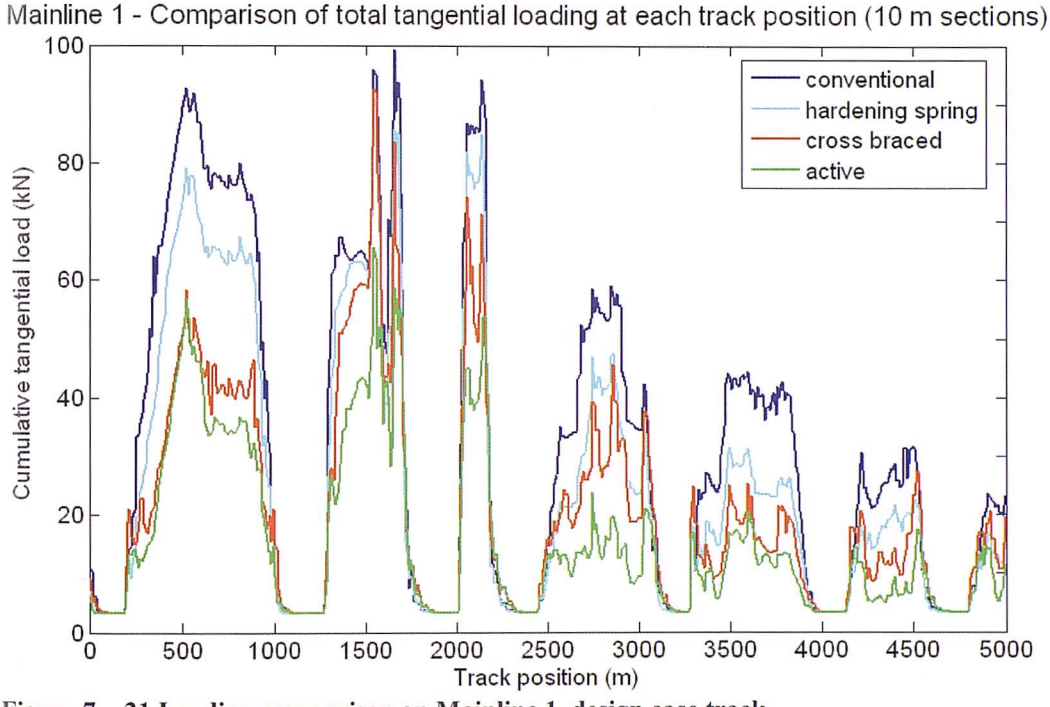

Figure 7 – 21 Loading comparison on Mainline 1, design case track

[‡] which is due to the time step of 0.013 seconds used for the VAMPIRE output signal

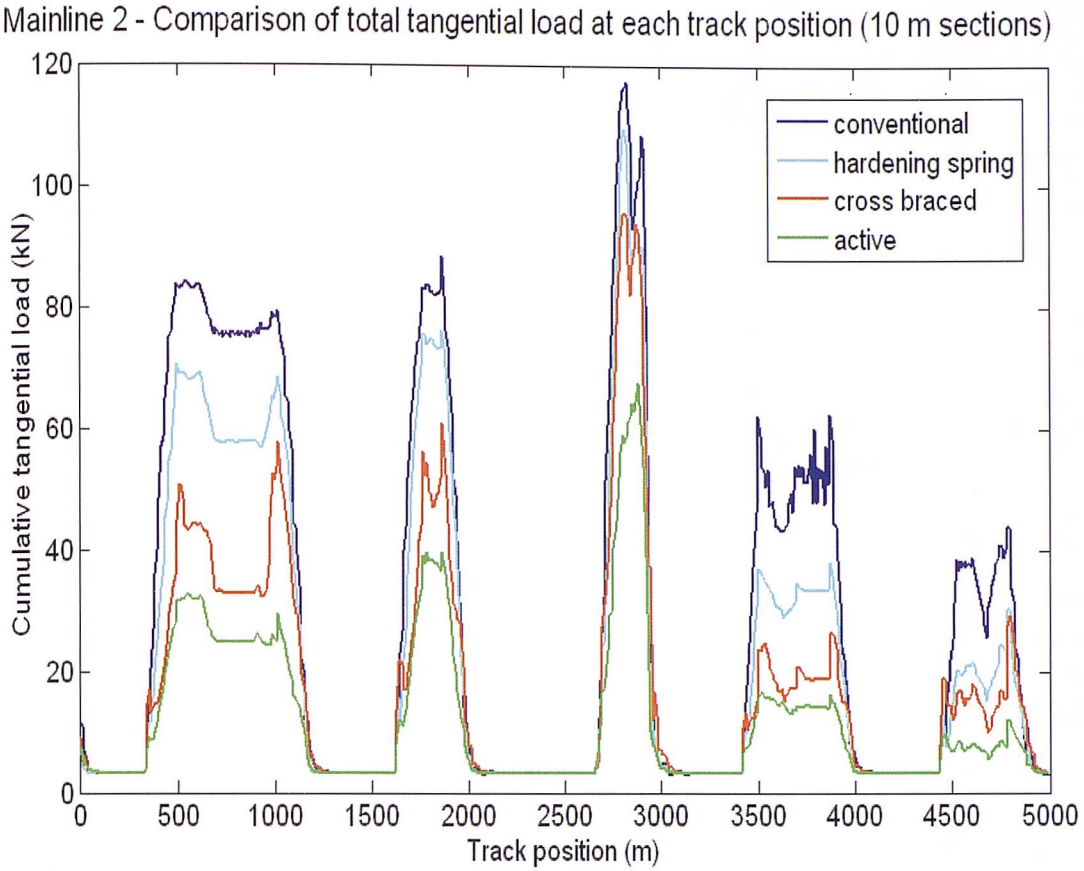

Figure 7 – 22 Loading comparison on Mainline 2, design case track

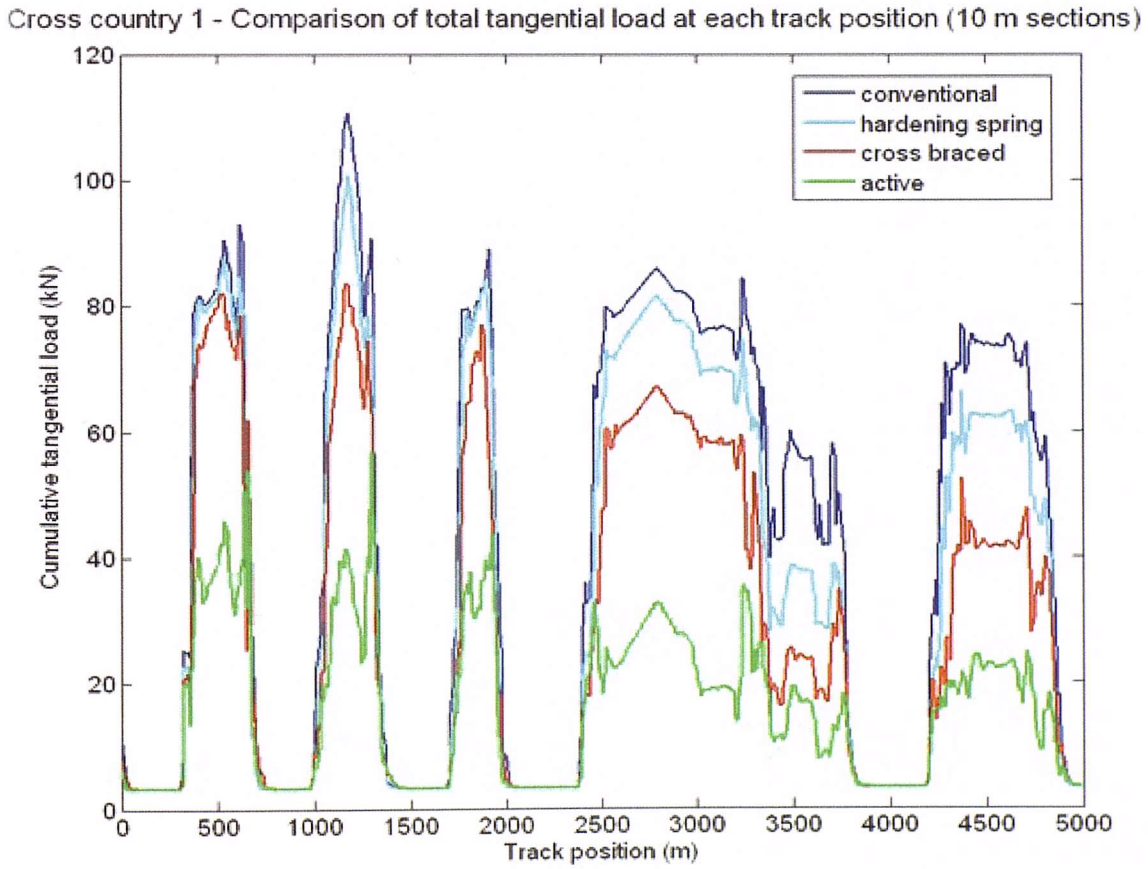

Figure 7 – 23 Loading comparison on Cross country 1, design case track

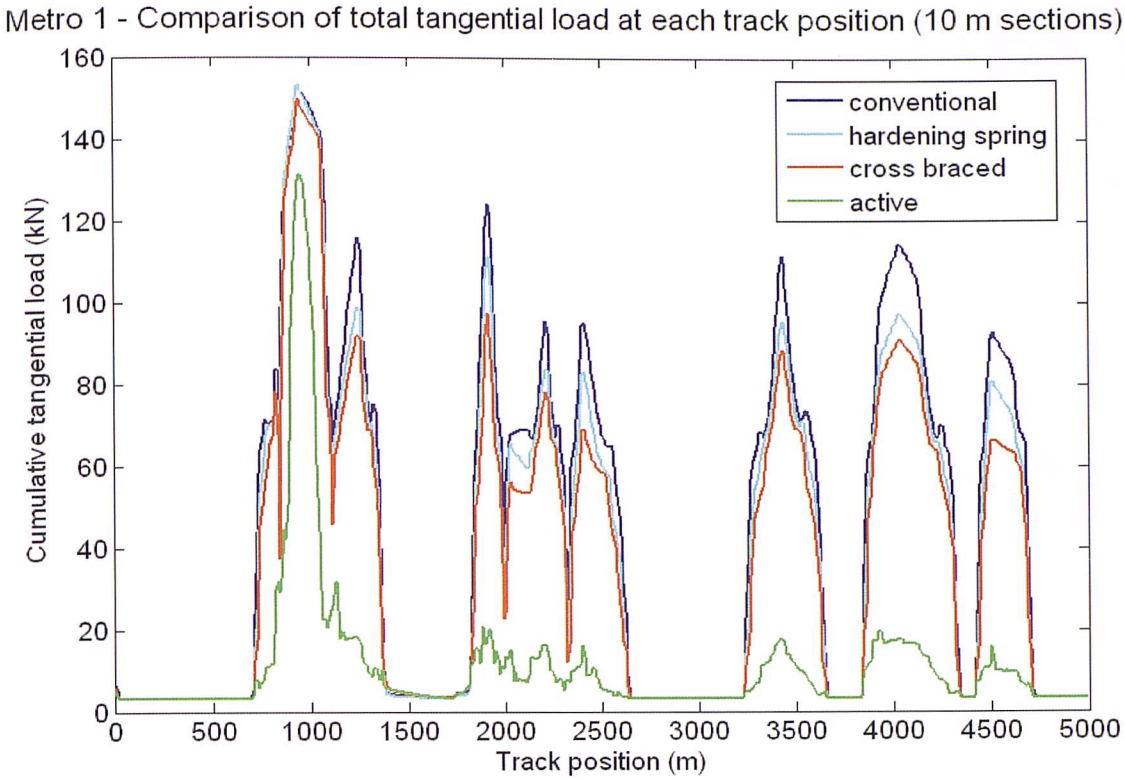

Figure 7 – 24 Loading comparison on Metro 1, design case track

Looking at Figures 7 – 21 to 7 – 24, across all routes the steering bogies achieve a loading reduction, with the active bogie giving significantly higher benefits than the other two designs. For the routes containing more severe curves, such as Cross Country 1 and Metro 1, the total loading is generally higher and the steering bogies give a higher percentage loading reduction. For the very tight curves on the metro route, the passive and mechanical steering bogies show a smaller load reduction than they have achieved on larger radius curves. However, the active bogie is showing the greatest load reductions for the metro route, and appears to perform well in these tighter curves.

7.4.1.2 Comparison of tangential load distribution

Comparing the total loading experienced by each track section does not necessarily give the whole picture. The peak wheel-rail loads are the most damaging; for example looking at Figure 7 – 21 the total load passing through the track at 500m due to the conventional vehicle is 90 kN. However, this output could be due to four axles passing, each generating a load of 22.5 kN, or one axle causing 60 kN and the following three 10 kN per axle. The second case would be more damaging to the track. Because of this a further analysis was carried

out, taking the tangential load at each wheel at every time step to create a distribution of loads. These load distributions for each train type were then compared. Figure 7 – 25 shows a comparison of load distributions for the different vehicle types on Mainline 1.

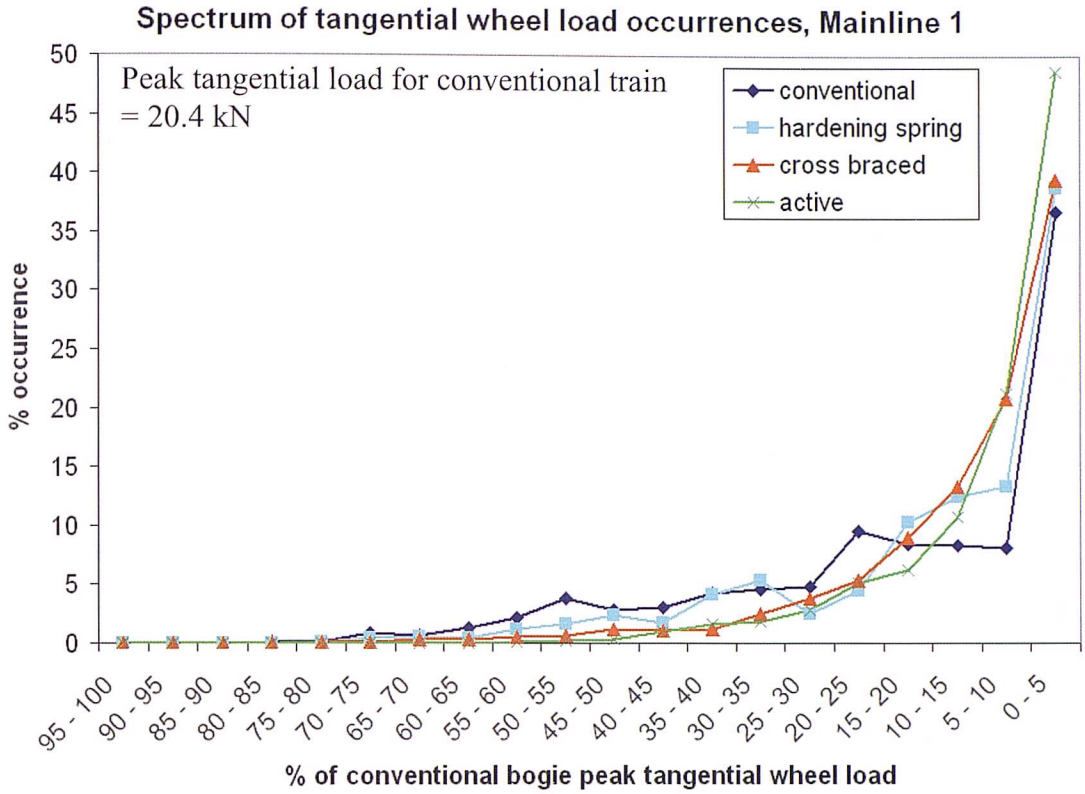

Figure 7 – 25 Comparison of loading distributions caused by the different steering mechanisms on Mainline 1 (design case track)

In the figure, the maximum tangential wheel load caused by the conventional bogies is taken as 100 %; the other load distributions are all calculated relative to this peak load in bands of five percent. All the steering bogies move the load distribution towards the right of the graph. The active bogie was shown to have the greatest effect on overall loading in the previous section; this graph shows that it also has the greatest effect on reducing high peak loads. Where the line for each steering bogie crosses the conventional distribution line is a good measure of how effective each steering bogie has been at reducing load. In this case, the active bogie distribution crosses the conventional distribution at around 10 % of peak loading. For all loads higher than this the active bogie has considerably lower occurrences, and the distribution has been shifted to the right, meaning more loads below 10 % of maximum are experienced.

On the scale shown in Figure 7 – 25, it is difficult to see what is happening in the higher loading spectrum, 50 – 100 % of maximum. This is shown more clearly in Figure 7 – 26.

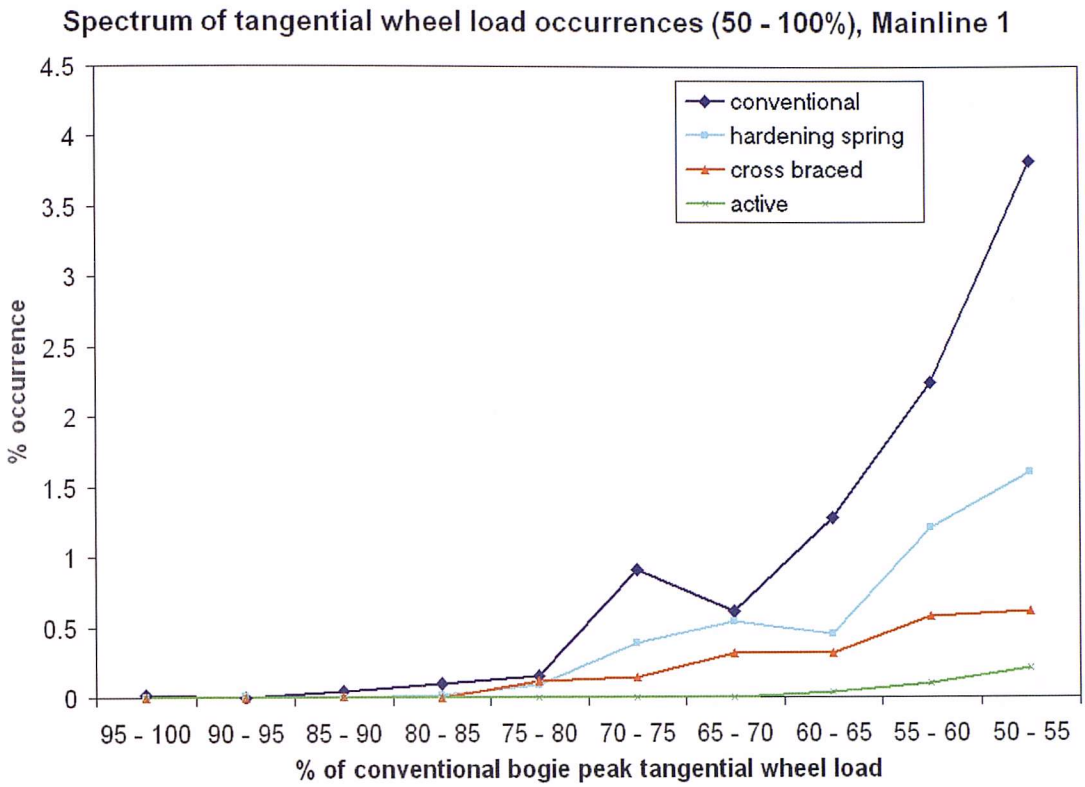

Figure 7 – 26 Comparison of higher loads caused by the different steering mechanisms on Mainline 1 (design case track)

It is these higher loads that will cause the most damage to track. Figure 7 – 26 shows that the active steering has been able to remove all loading over 65 % of the conventional peak load, whilst the maximum load from the passive and mechanical bogies is roughly 85 % of the conventional peak load. This reduction of top end peak loading may well be just as important as the total reduction in loading achieved with the steering bogies.

Figures 7 – 27 to 7 – 32 show the comparative load distributions for the different steering bogies across the remaining test tracks.

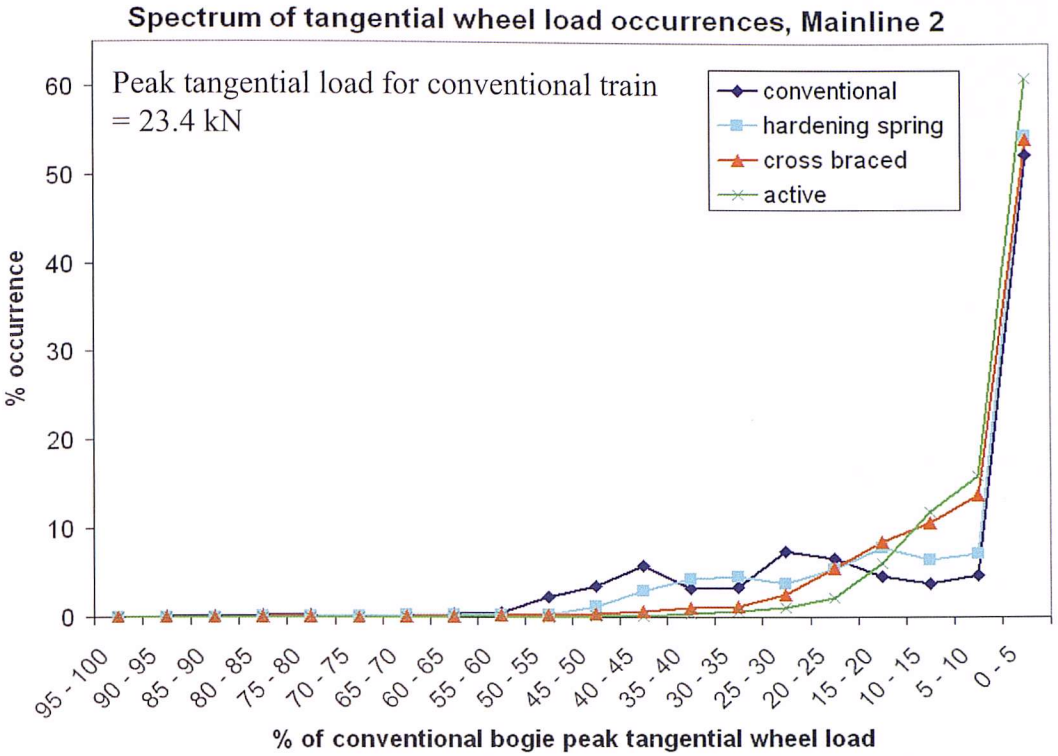

Figure 7 – 27 Comparison of loading distributions caused by the different steering mechanisms on Mainline 2 (design case track)

This distribution is largely similar to the output for Mainline 1, the steering bogies have shifted the distribution to the right significantly, with the active bogie again significantly more effective than the other two options. Again the active bogie has significantly reduced peak loading, which is shown more effectively in Figure 7 – 28.

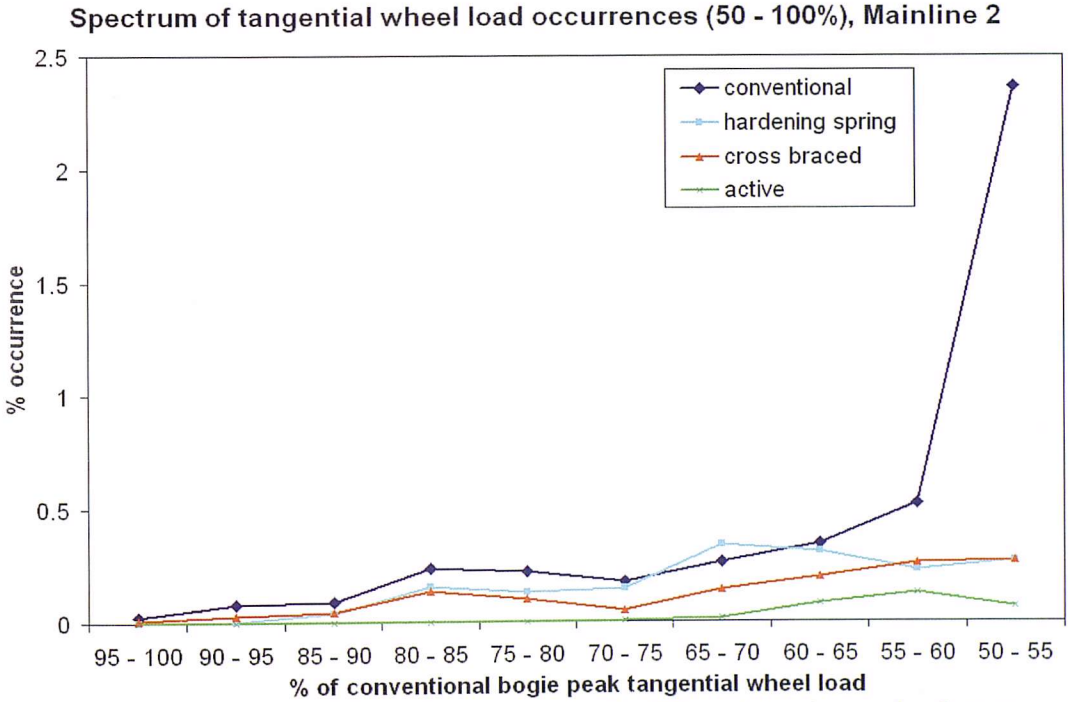

Figure 7 – 28 Comparison of higher loads caused by the different steering mechanisms on Mainline 2 (design case track)

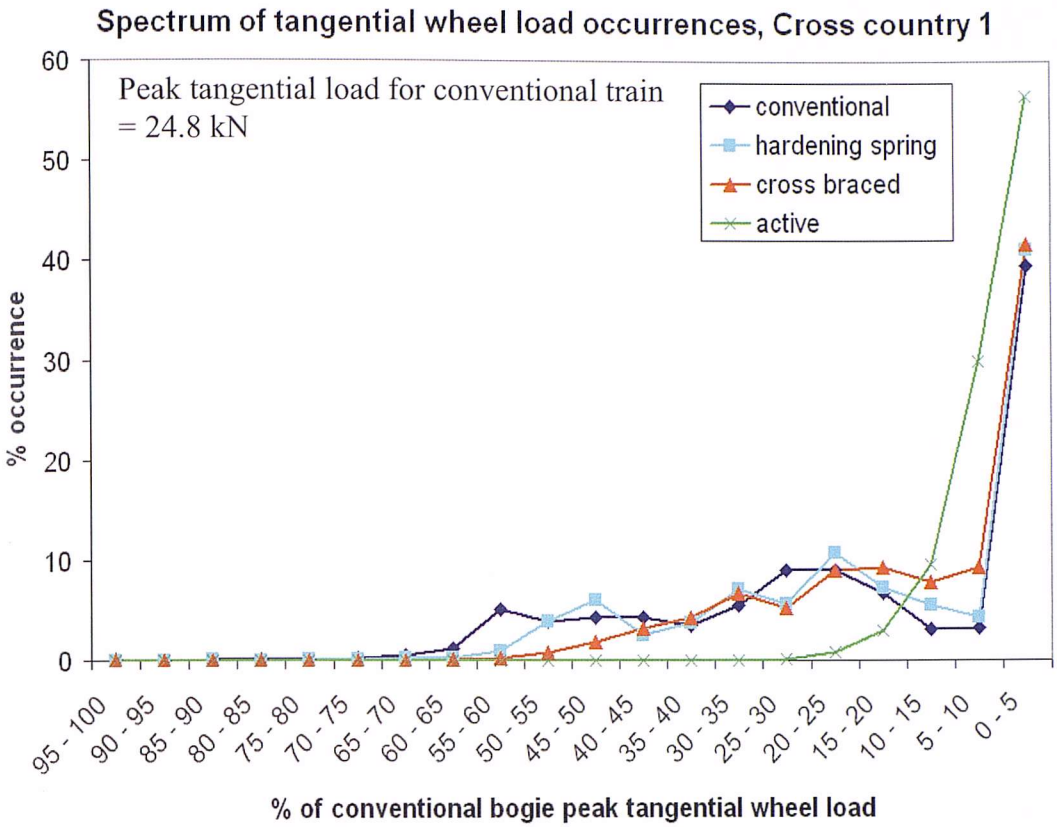

Figure 7 – 29 Comparison of loading distribution caused by the different steering mechanisms on Cross country 1 (design case track)

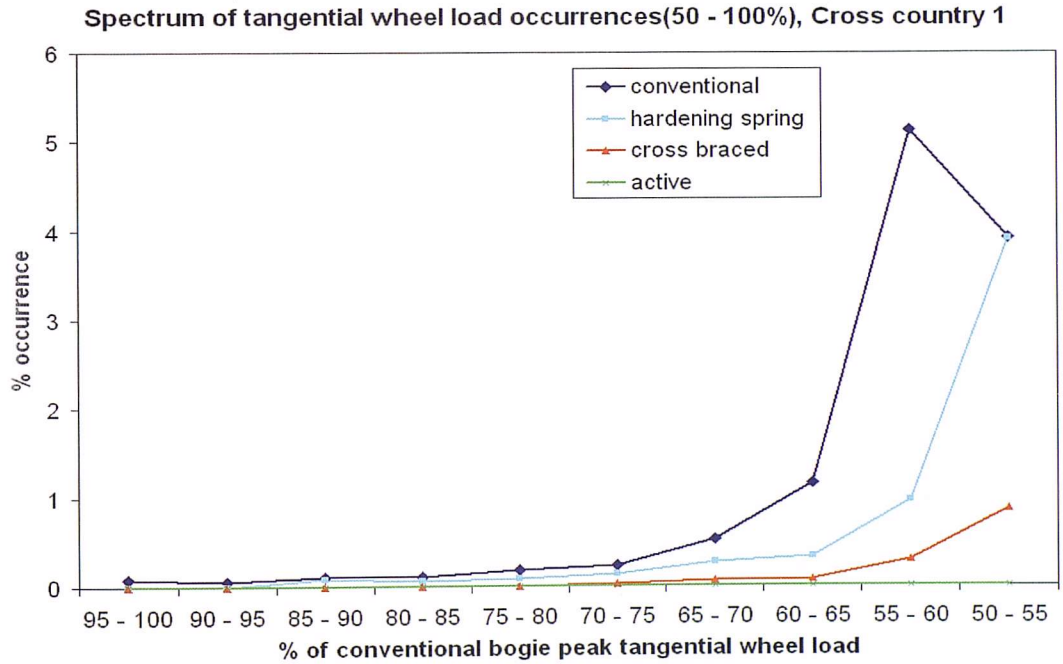

Figure 7 – 30 Comparison of higher loads caused by the different steering mechanisms on Cross country 1 (design case track)

This cross country route shows a generally flatter distribution for the conventional vehicle, compared to the mainline routes, with more loads in the mid range 10 – 65 %. The steering bogies also appear to have a larger impact on

the distribution, more successfully moving the loading spectrum to the right of the graph. In the case of active steering, there are no loads experienced over 50 % of the conventional maximum.

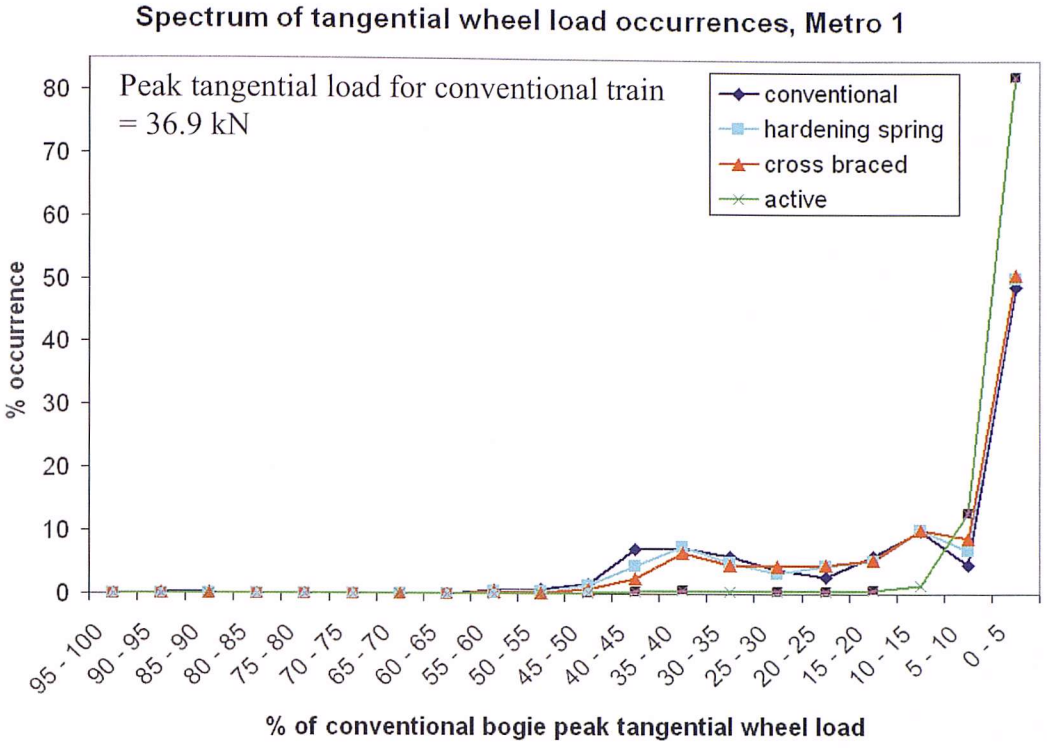

Figure 7 – 31 Comparison of loading distribution caused by the different steering mechanisms on Metro 1 (design case track)

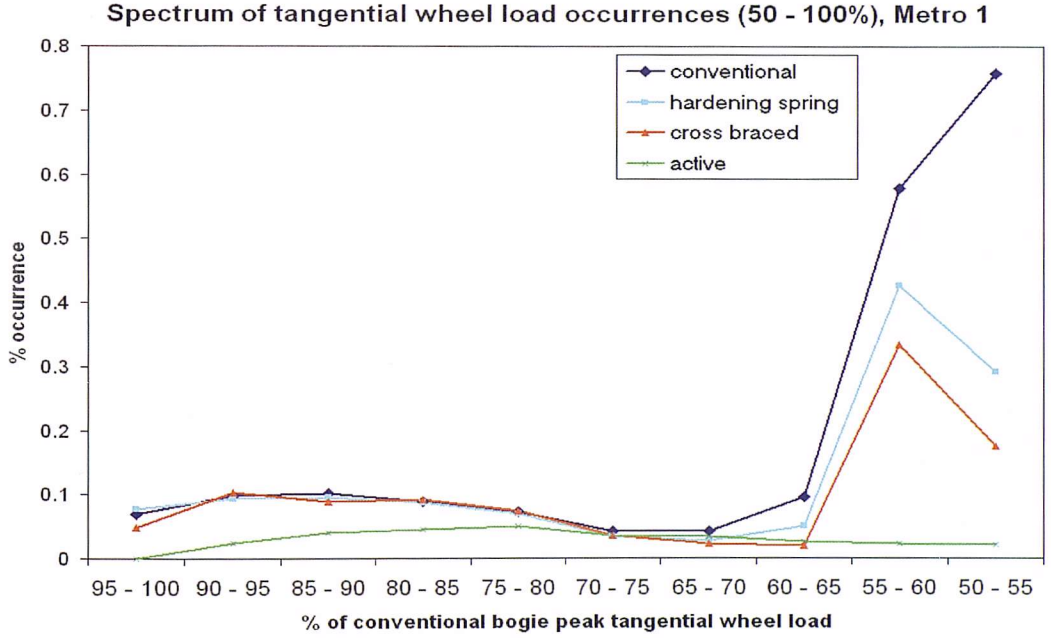

Figure 7 – 32 Comparison of higher loads caused by the different steering mechanisms on Cross country 1 (design case track)

The metro route shows the highest peak tangential load, because it contains higher severity curves. However, the load distribution is different from those of all of the other routes; the highest tangential loads (50 – 100 % of peak loading)

make up a much smaller proportion of the distribution. These loads occur at the peak of the most severe curve, at 800 m along the track (see Figure 7 – 9). Again, the active steering significantly outperforms the two other steering types, with the greatest load reductions in the 10 – 50 % loading range.

7.4.1.3 How have these savings been achieved?

The steering mechanisms, particularly the active system, have shown significant load reduction, but how has this been achieved? All of the steering systems have changed the dynamics of a vehicle travelling through curves. In every case the angle of attack has been reduced and consequently the lateral shift of the wheelsets relative to the rails. By turning the wheelsets towards a more neutral curving angle, this allows the rolling radius difference steering to have its proper effect, reducing the wheel-rail creep loading. Figures 7 – 34 and 7 – 35 show the angle of attack and lateral shift of the front wheelset of a train travelling over the Cross Country 1 test route, for each different type of bogie. The conventional bogie generates the largest angles of attack through curves. This means the rolling radius difference steering cannot work properly and the wheelset shifts even further to the outside of the curve in an attempt to create a larger radius difference and steer through the curve (as shown in Figure 7 – 34). The two passive steering systems (cross braced and hardening spring) reduce the angle of attack, achieving minor reductions in lateral shift, whilst the active system creates a small opposite angle of attack compared to the other systems, giving big reductions in lateral shift. This is small positive angle of attack is in fact the 'perfect curving position' which results in curving negotiation with zero longitudinal creep loading (due to curving) at each wheel, as shown in Figure 7 - 33.

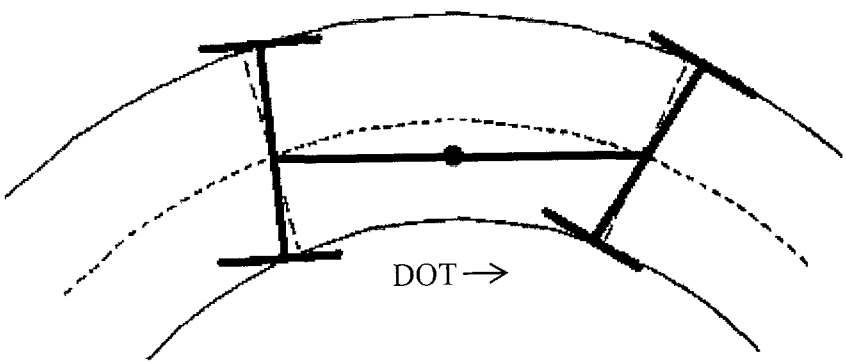

Figure 7 - 33 Axle yaw positions for neutral curving

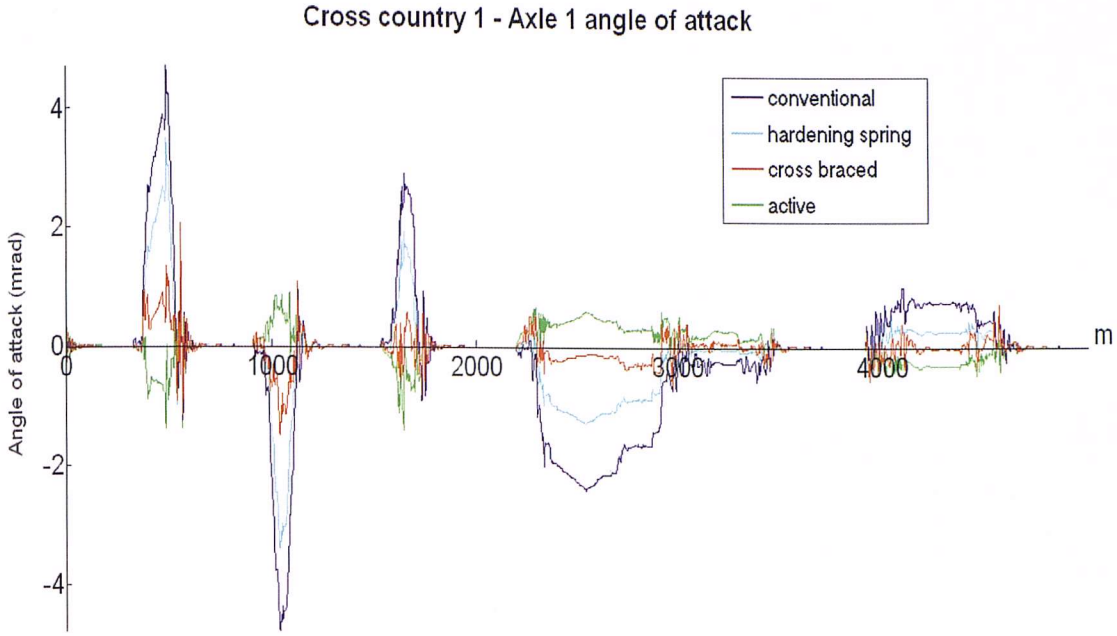

Figure 7 - 34 Axle 1 angle of attack, through cross country 1 test route

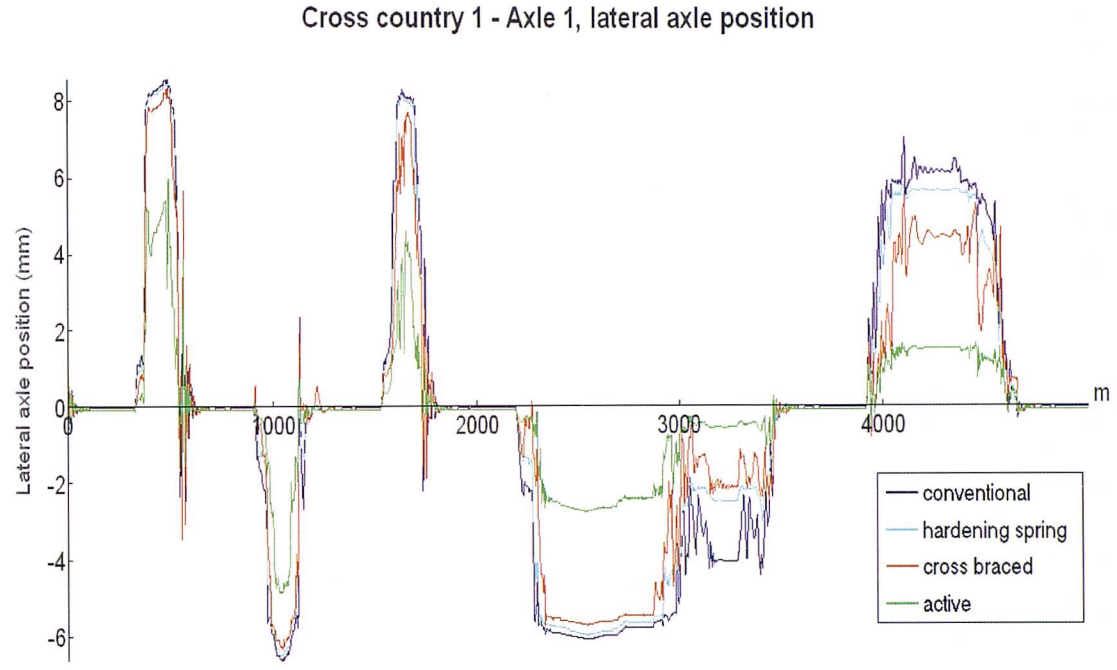

Figure 7 - 35 Axle 1 lateral position through cross country 1 test route

Figures 7 – 36 and 7 – 37 show comparisons of the longitudinal and lateral loading caused at the first axle of a vehicle travelling through the cross country 1 test route, with the different bogie types. The active system, which has achieved the biggest reductions in angle of attack and lateral displacement, is showing significant reductions in longitudinal load through all curves (unsurprisingly, as this is the 'mission' of the active control system). In most cases the mechanical system is more effective at reducing the lateral loads, whilst the passive system tends to give small reductions in both lateral and longitudinal loadings.

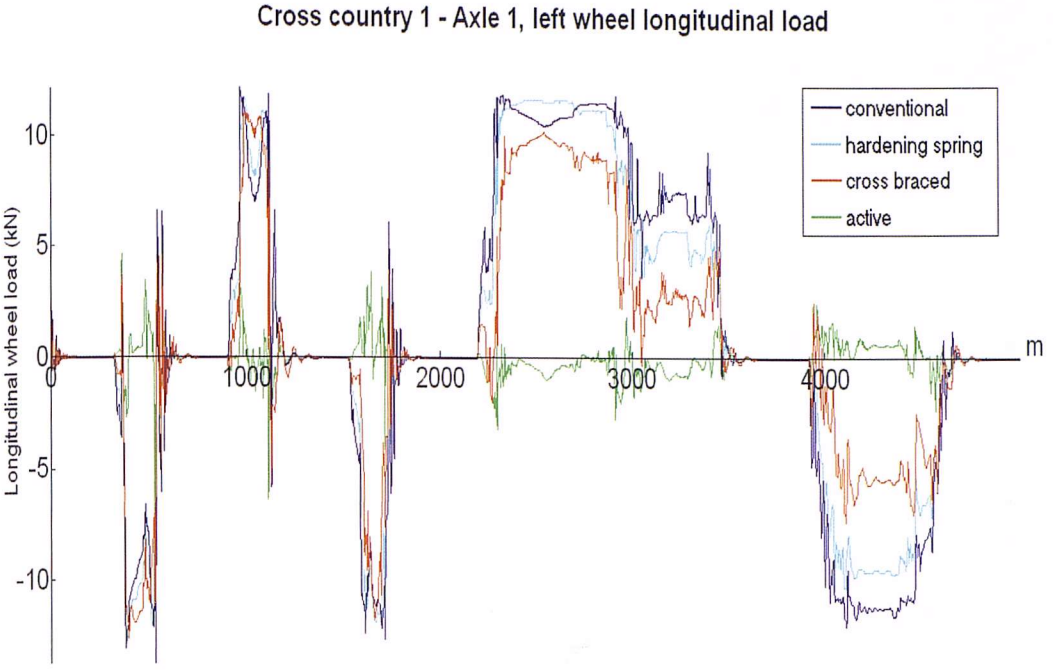

Figure 7 - 36 Axle 1, longitudinal load through cross country 1 test route

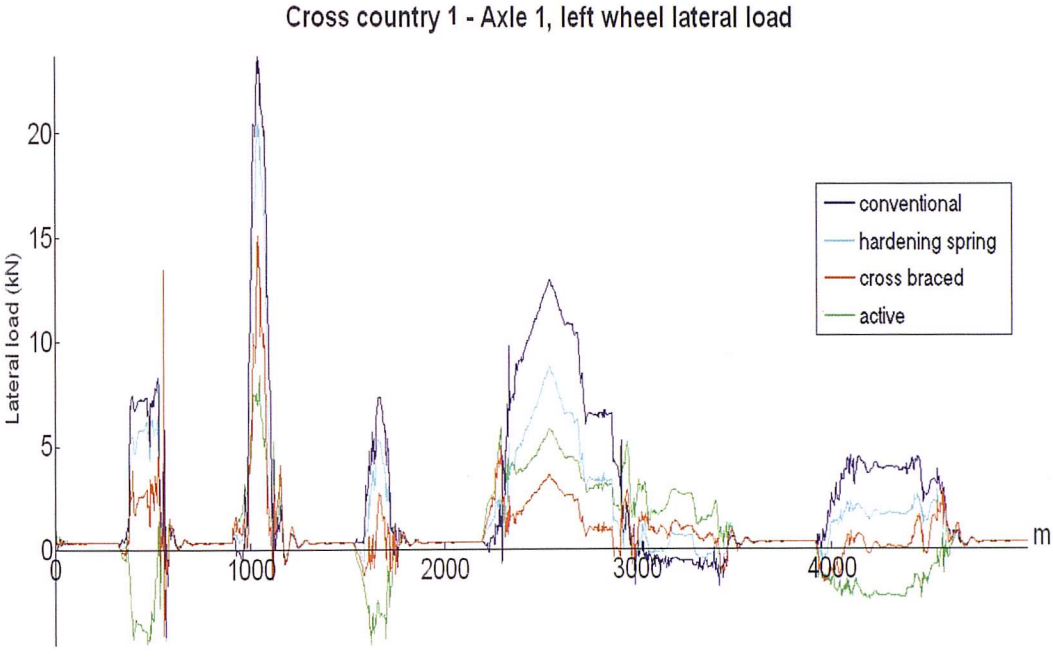

Figure 7 - 37 Axle 1, lateral load through cross country 1 test route

Longitudinal wheel-rail loading is developed as a result of the creep between the wheel and rail. However, the lateral loading is a combination of lateral creep loading (as a result of the lateral creep) and the quasistatic curving loads, as described in Chapter 2.

7.4.2 Rough tracks

Adding in track roughness to the dynamic calculations can make a significant difference to the outputs. Track roughness affects the performance of the different steering bogies to varying degrees. Figure 7 – 38 shows the tangential loading for the front left wheel of a conventional rail vehicle travelling over Mainline 2, with and without track roughness. The track roughness causes an extra high frequency loading on top of the steering loads, causing a significant effect on the overall loading, giving much higher peak loads.

The high frequency longitudinal loads caused by the primary yaw stiffness act to damp out hunting motion. If these loads are inadequate to damp the oscillations, hunting can occur, resulting in repeated flange contact generating significant lateral loads. In this output the combination of longitudinal and lateral is shown.

If a steering bogie gives lower curving loads, but is less stable through rough track, this could still result in higher overall loading, meaning it would not achieve any reduction in track damage.

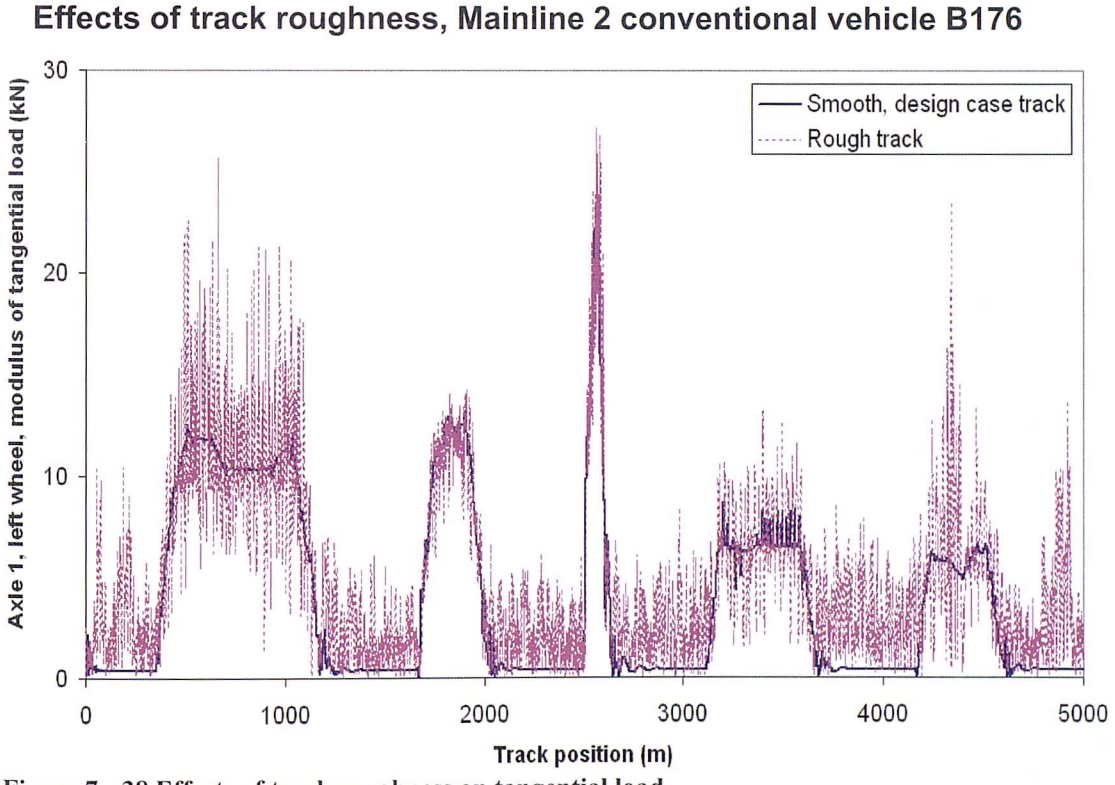

Figure 7 - 38 Effects of track roughness on tangential load

As with the design case track simulations, the same outputs of cumulative load by track position and load distribution were obtained. Figures 7 – 39 to 7 – 43 show comparisons of cumulative load by track position. To give easily interpreted graphical outputs, results have again been smoothed; in this case using worst case loading from 50 m track sections.

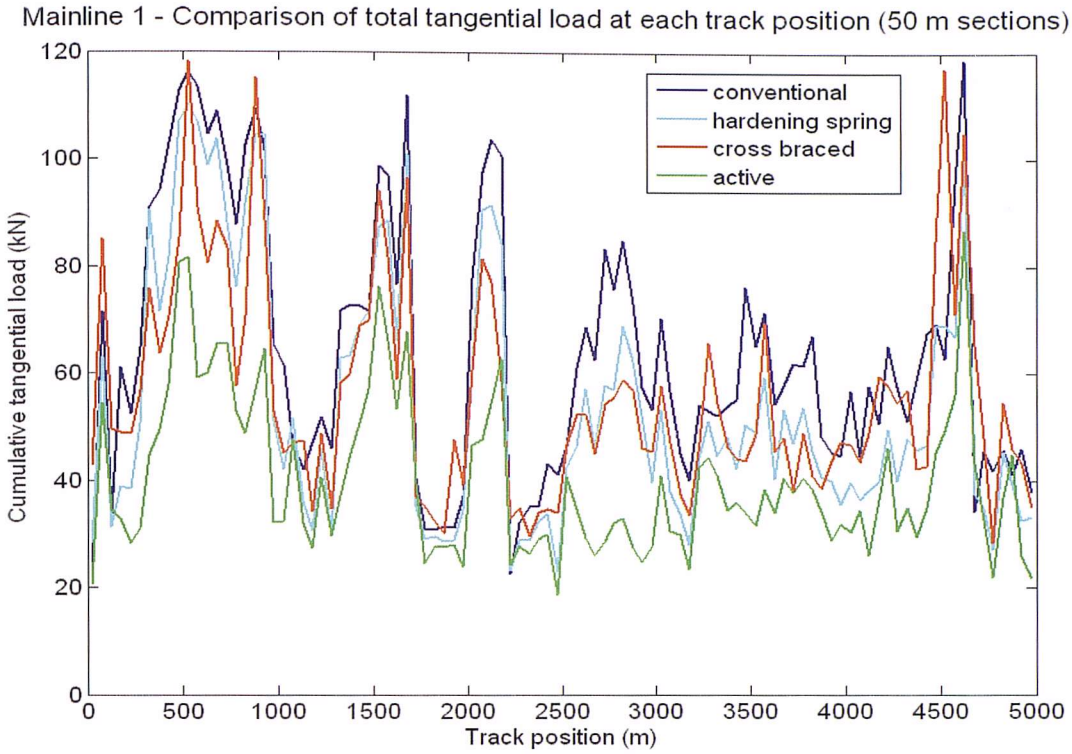

Figure 7 - 39 Loading comparison on Mainline 1, rough track

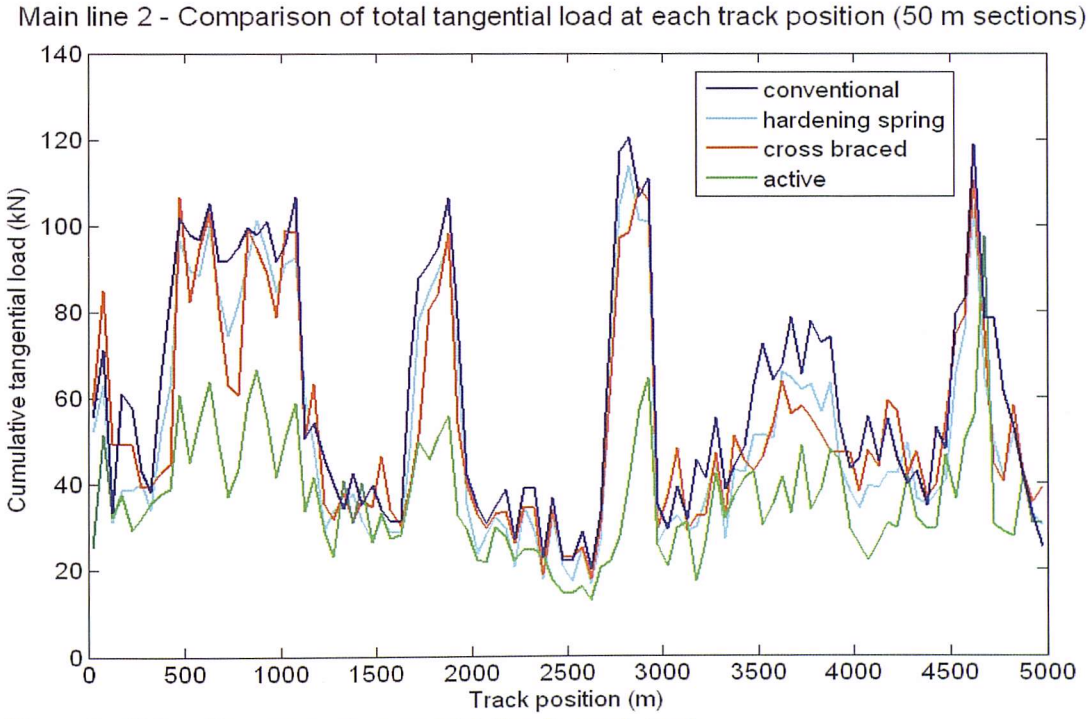

Figure 7 - 40 Loading comparison on Mainline 2, rough track

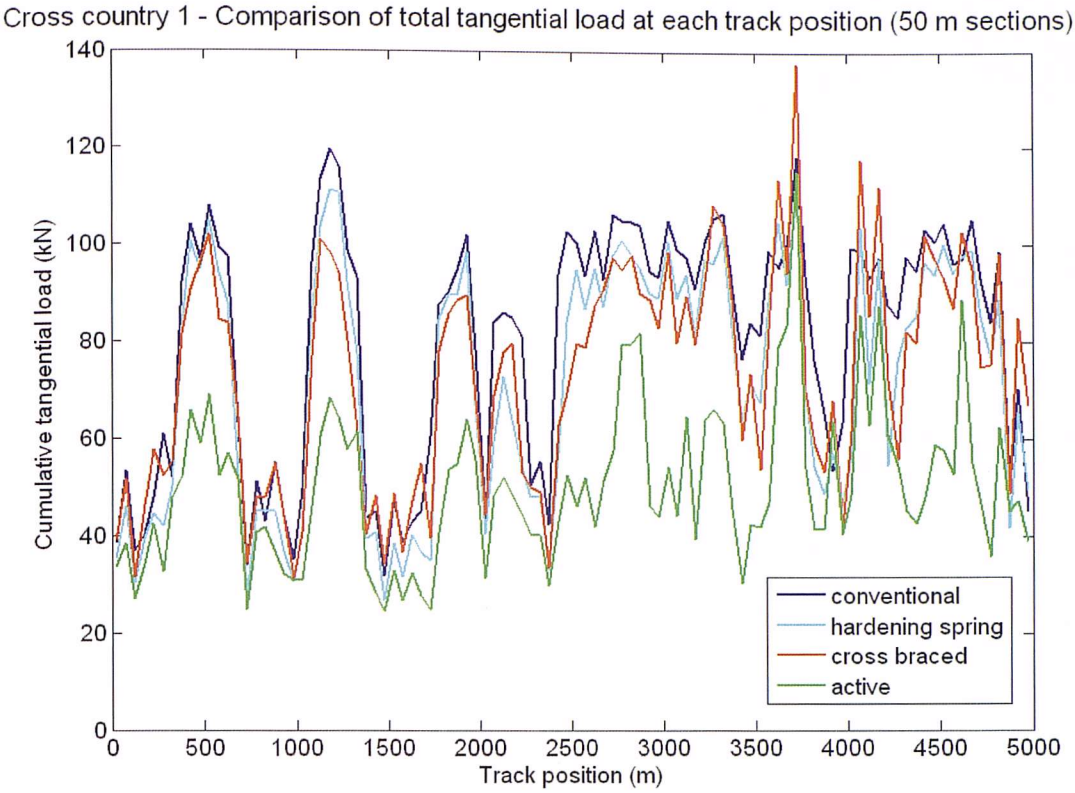

Figure 7 - 41 Loading comparison on Cross country 1, rough track

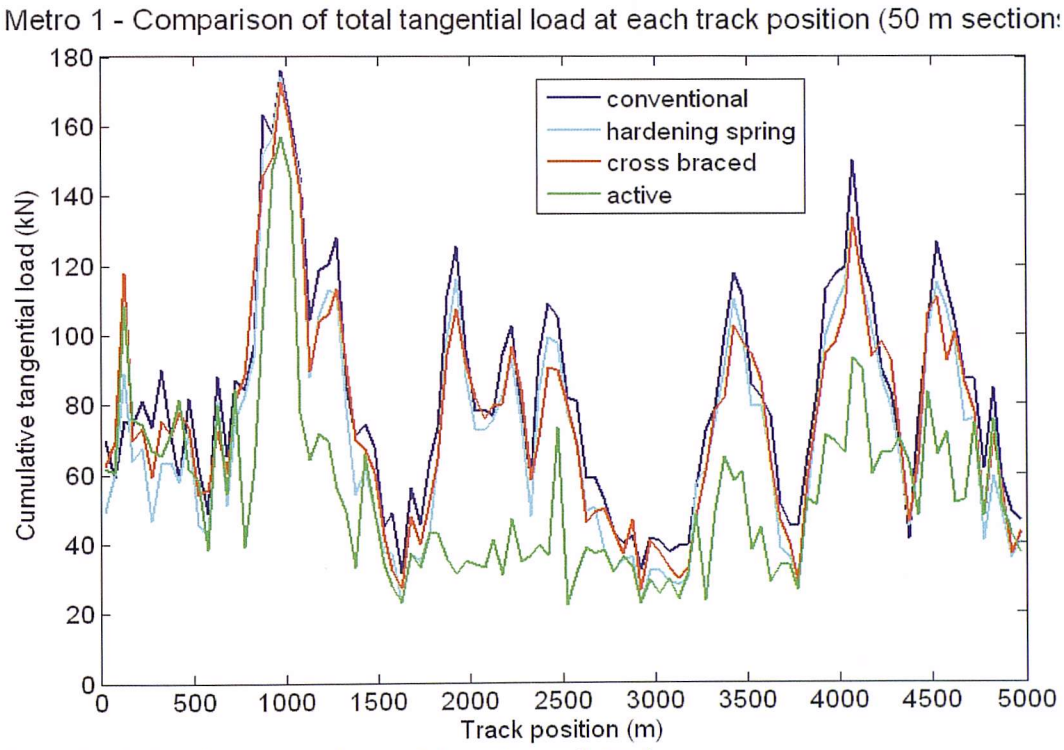

Figure 7 - 42 Loading comparison on Metro 1, rough track

In all cases the percentage load reduction achieved by the steering bogies has been reduced, although they are all still showing significant benefits. This is because the total tangential loads now contain curving loads, stabilising

longitudinal loads and lateral loads as a result of hunting. In certain curves the mechanical and passive steering bogies are now giving peak loads higher than for the conventional bogie. Figures 7 – 43 to 7 – 46 show a comparison of tangential wheel load distributions for the different test routes.

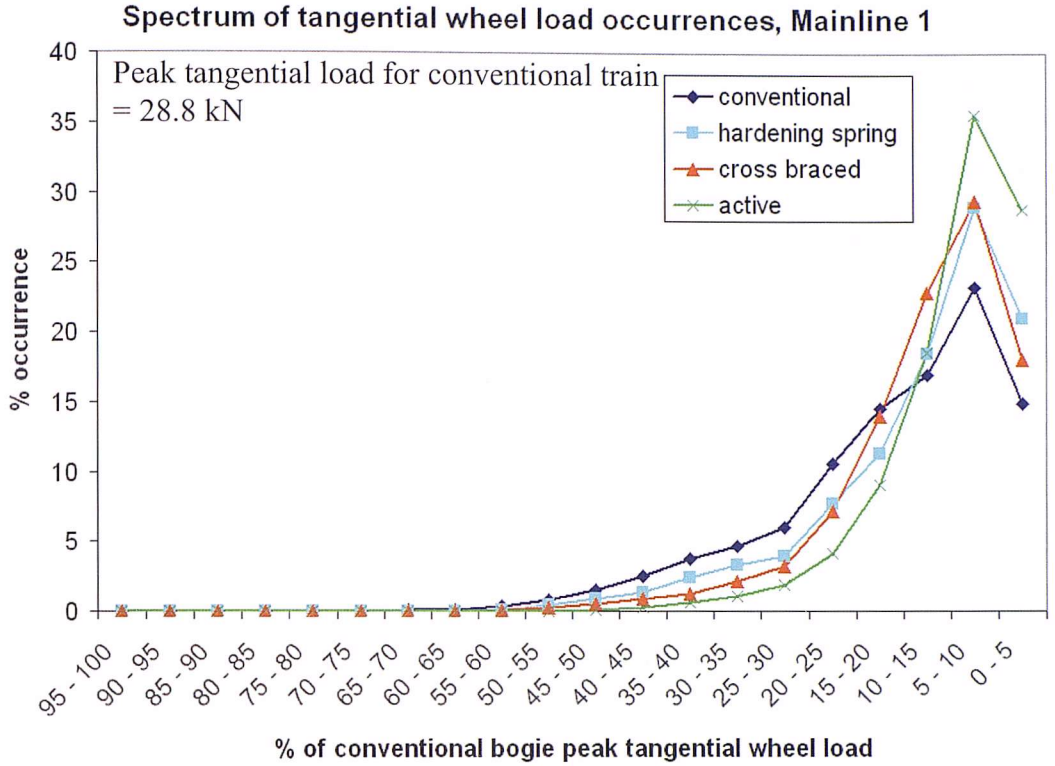

Figure 7 - 43 Comparison of loading distribution caused by the different steering mechanisms on Mainline 1 (rough track)

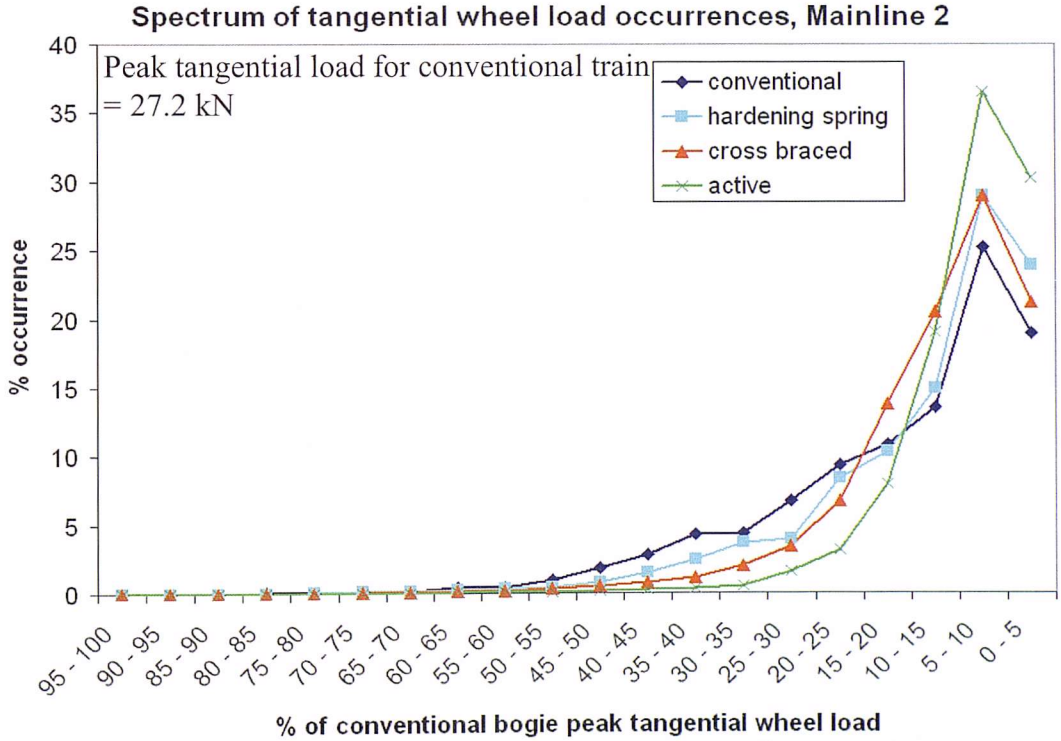

Figure 7 - 44 Comparison of loading distribution caused by the different steering mechanisms on Mainline 2 (rough track)

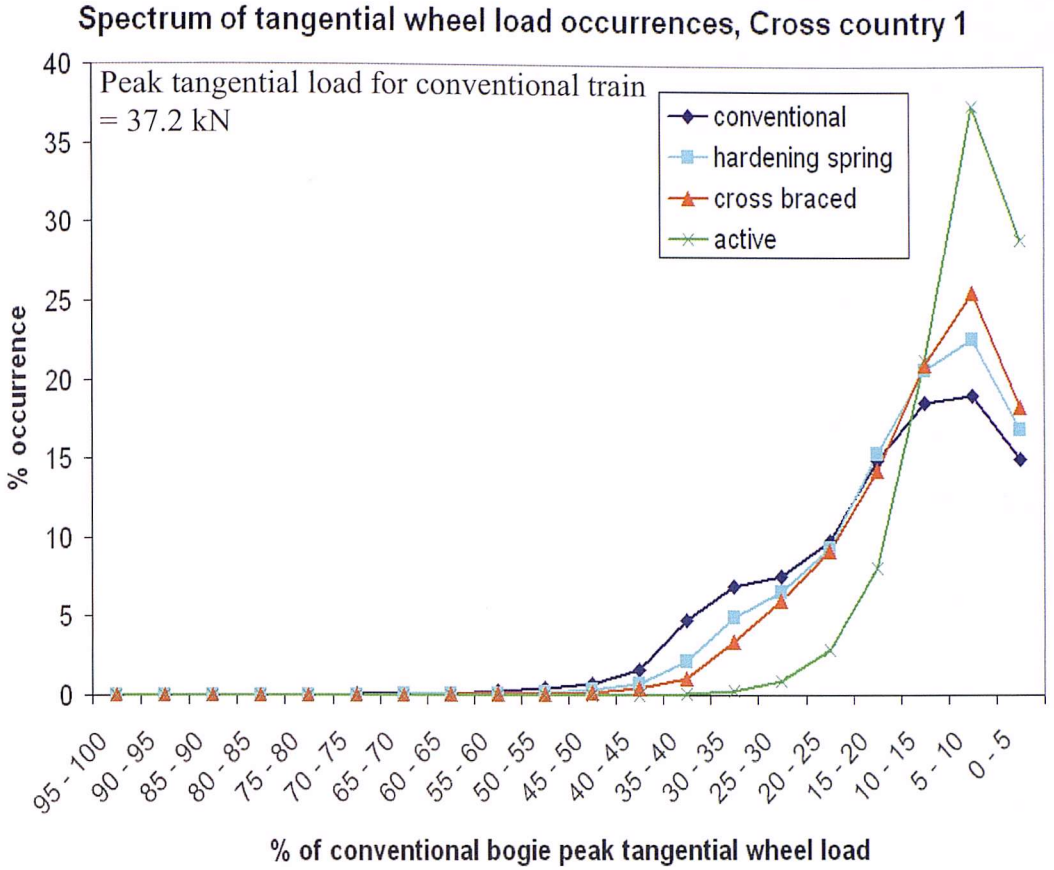

Figure 7 - 45 Comparison of loading distribution caused by the different steering mechanisms on Cross country 1 (rough track)

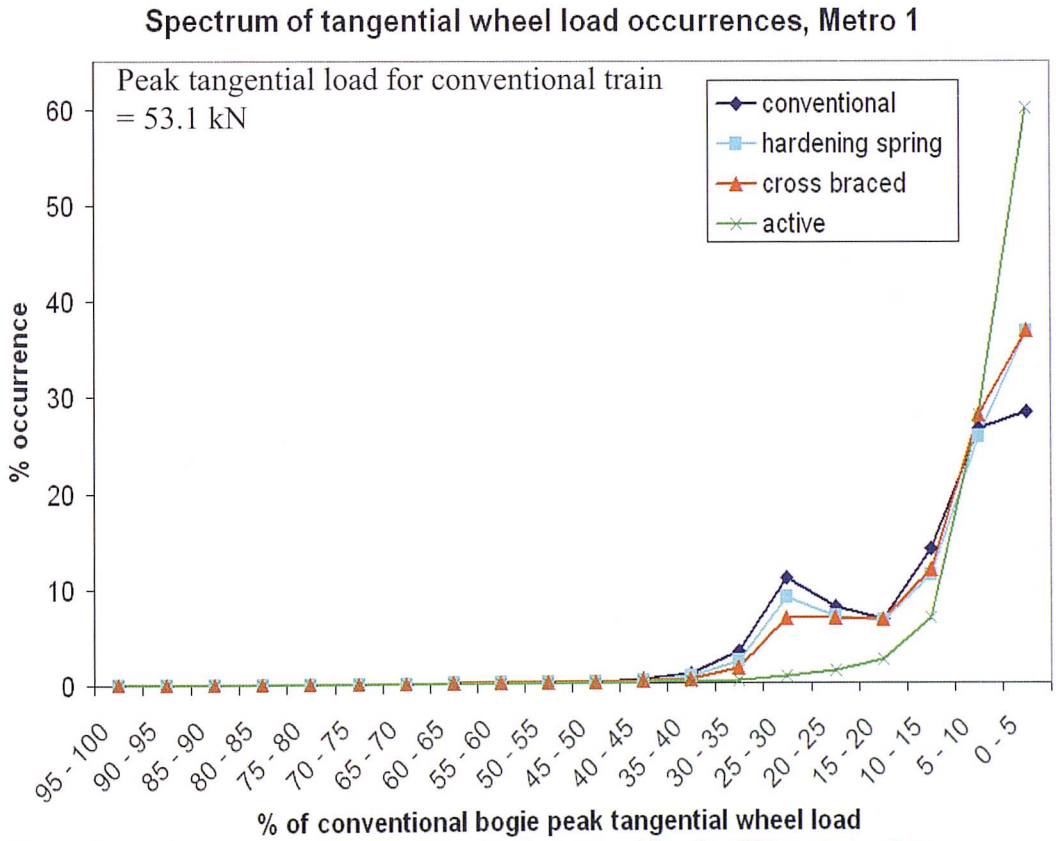

Figure 7 - 46 Comparison of loading distribution caused by the different steering mechanisms on Metro 1 (rough track)

Looking at these loading distributions, the highest loads occur when a section of severe track roughness coincides with a curve. Compared to outputs for design case track, these highest loads occur a lot less frequently. The load reductions achieved with the steering bogies are shown more clearly in the 15 – 65 % loading bracket for mainline and cross country routes, and 10 – 50 % for the metro route.

7.4.3 Summary of results for B187 derivative vehicles

	Design case tracks					Rough tracks				
Mainline 1	peak load	% total load saving	% saving ($load^2$)	% saving ($load^3$)	% saving ($load^4$)	peak load	% total load saving	% saving ($load^2$)	% saving ($load^3$)	% saving ($load^4$)
conventional	20.4	-	-	-	-	28.8	-	-	-	-
hardening spring	19.5	21	33	40	44	24.7	19	31	37	42
cross braced	19.4	38	58	67	70	32.5	23	42	54	59
active	12.9	52	75	85	90	26.0	42	66	79	85
Mainline 2										
conventional	23.4	-	-	-	-	27.2	-	-	-	-
hardening spring	21.5	21	35	42	46	24.9	19	31	37	41
cross braced	22.6	41	63	69	69	28.8	24	44	55	58
active	16.5	58	82	89	92	21.3	54	72	83	88
Cross country 1										
conventional	24.8	-	-	-	-	37.2	-	-	-	-
hardening spring	22.1	13	23	31	38	33.0	13	22	28	34
cross braced	18.2	31	51	64	73	40.3	21	38	50	59
active	11.0	63	87	95	98	32.2	48	74	87	92
Metro 1										
conventional	36.9	-	-	-	-	53.1	-	-	-	-
hardening spring	37.0	10	16	18	17	46.9	13	18	19	17
cross braced	36.9	18	28	32	32	55.0	19	28	32	31
active	34.0	75	88	88	85	39.0	55	76	82	81

Table 7 – 4 Comparison of load reductions achieved with each type of steering bogie

A summary of all results from the analysis using B176 derived vehicles is shown in Table 7 – 4. A comparison of the total tangential load transmitted to the track at every calculation step is shown, along with a comparison of total tangential load squared, to the power three and to the power four. The purpose of these additional comparisons is because the highest loads will make a disproportionately large contribution to track damage. For example the 20.4 kN peak load on Mainline 1, caused by the conventional vehicle, will cause more than twice the damage of two further wheel loads of 10.2 kN. Introducing a power law comparison helps to take this into account. Track damage is assumed to have a power law relationship with load, with a power between 2 and 4.

Looking at the design case results first, all types of steering bogie have achieved an overall load reduction across all test routes. The active bogie significantly outperforms the other two steering types, particularly for the routes containing

higher severity curves. However, the cross braced bogie is also showing good results for the mainline routes.

For both of the passive types of steering bogie (hardening spring and cross braced) the percentage load reductions are actually lower for the curvier routes such as the cross country and metro. They perform best in mid range curves, and are not giving the same benefits for tighter curves. For this analysis the same parameters were used for the steering bogie characteristics across all test routes. It may be possible to improve the results for metro and cross country routes, by 'tuning' the mechanical and passive bogie appropriately.

When taking into account track roughness, the benefits of steering are generally reduced; this is because the conventional bogies are typically more stable, meaning the steering bogies give lower steering loads, but give a higher variance on top of that as the vehicles respond to track roughness. Significant load reductions are still achieved, especially with the active bogie, which gives a reduction in tangential load squared of 66 – 76 % across all track types. Because of the control system filter used in the active bogie, the active elements should not respond to track roughness inputs, maintaining stability through rough track. The cross braced bogie gives reduction in total tangential load squared between 38 and 44 % for cross country and mainline routes, which again could make a significant contribution towards reducing track damage.

All of these results have been derived from a comparison against the same base case vehicle across all test tracks. This is not necessarily a fair comparison, but it should give repeatable results because of the benchmark vehicle chosen. In reality, each type of railway uses a different type of rolling stock, which although not necessarily perfectly optimised, should give a better performance than the standard benchmarking vehicle used for this set of results.

7.5 Representative vehicles

In order to give a fairer assessment of the steering bogies, vehicle models have been created which should give a more accurate representation of the type of vehicle used for each type of route, as described in section 7.3.2.

In this section results are shown for whole trains, rather than individual cars as shown in section 7.4. However, for each test case all the relevant types of car were simulated along the test routes individually. The results were then produced by summing together the output from the calculations for each car, to make up a whole train.

The simulations carried out in the previous section were all carried out assuming no tractive effort at any of the axles. This set of results has been carried out with appropriate torques applied at powered axles to take into account the effects of tractive effort on tangential loading.

Using Jorgensen and Sorenson's train resistance curves[18] the train resistances have been calculated for all vehicles across their range of operational speeds, as shown in Figure 7 – 47.

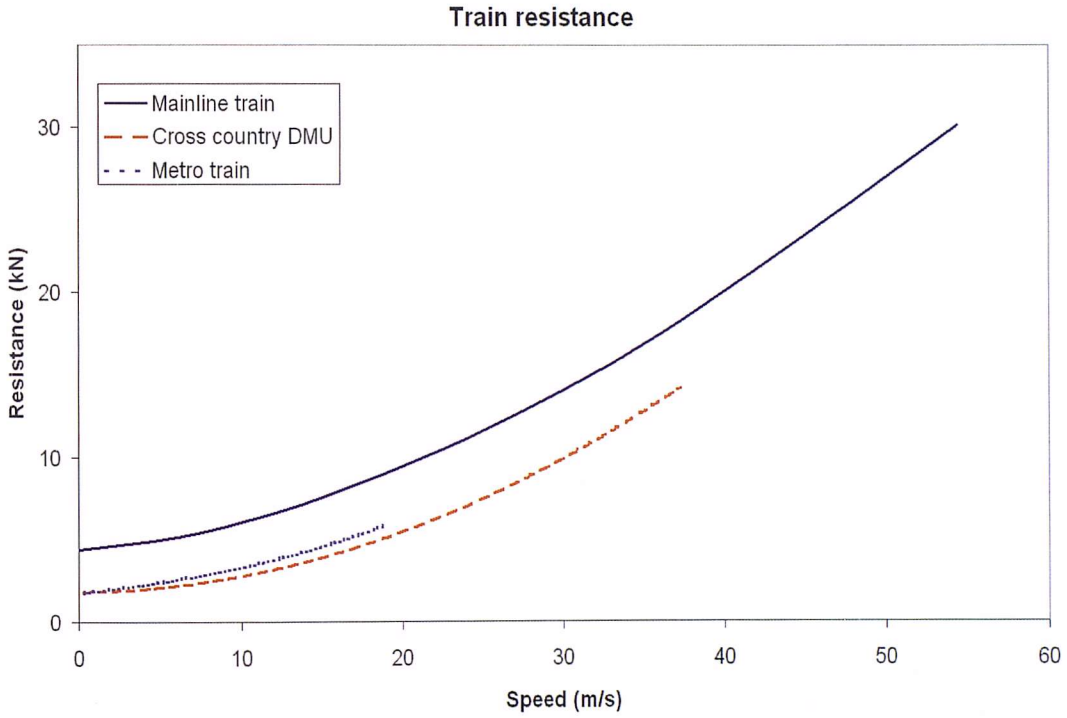

Figure 7 - 47 Train resistance against speed for vehicles used in this study, data from[18]

In all cases, the tangential curving loads are far greater than the tractive force transmitted at the wheel-rail interface. For the multiple unit trains where the tractive effort is spread over a large number of axles, the tractive load gives a very small contribution to overall tangential loading at each wheel. For locomotives, the tractive force is a bigger proportion of total loading. Figure 7 –

48 shows the longitudinal load for the front left wheel of a locomotive travelling along Mainline 1, with and without traction. This graph shows the tractive effort has a small but noticeable impact on the overall loading. This means peak loading is higher, so will cause more damage to the track.

For this study only the tractive effort to maintain a steady speed, i.e. to equal the train resistance has been included. Much higher longitudinal loads are created during acceleration and braking; for a complete picture of wheel-rail loading these would also need to be taken into account. For this study, the purpose is to assess the steering bogie concepts, so this added detail is not deemed necessary.

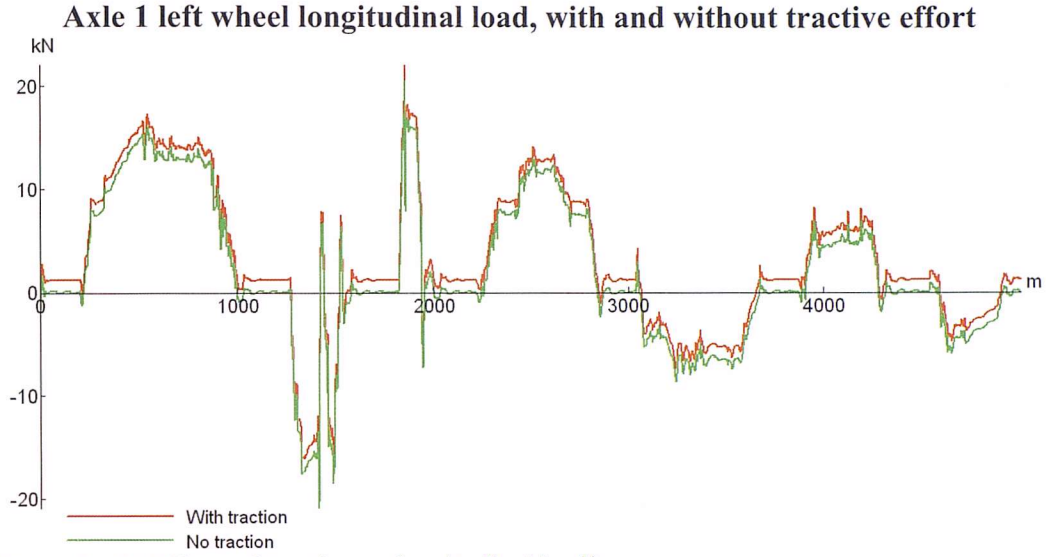

Figure 7 - 48 Effects of traction on longitudinal loading

7.5.1 Summary of results from representative vehicles

A full set of graphical outputs as shown in Section 7.4 for the B176 derivative vehicles are shown in Appendix E. Table 7 – 5 gives a comparison of the overall results.

For this set of results, the base case, conventional vehicles have lower primary yaw stiffnesses than the B176 vehicle. This means they already generate lower curving loads, so the datum for comparison is a lot lower; meaning the percentage load savings achieved by the steering bogies are generally not as high as in the previous set of results. Also as the applied tractive effort is the same

across bogie types on each route, the percentage change in loading will be smaller than if traction were not included.

Again the hardening spring, cross braced and actively steered vehicles in each test case have been derived from the relevant conventional vehicle for that line, with only primary tangential suspension details modified.

	Design case tracks					Rough tracks				
Mainline 1	peak load	% total load saving	% saving ($load^2$)	% saving ($load^3$)	% saving ($load^4$)	peak load	% total load saving	% saving ($load^2$)	% saving ($load^3$)	% saving ($load^4$)
conventional	28.5	-	-	-	-	36.0	-	-	-	-
hardening spring	25.4	1	12	27	39	32.3	0	11	25	37
cross braced	23.4	17	36	52	63	33.5	8	26	43	56
active	24.0	30	53	68	78	31.1	27	49	62	69
Mainline 2										
conventional	37.6	-	-	-	-	42.0	-	-	-	-
hardening spring	35.0	2	13	26	35	40.2	0	11	24	34
cross braced	40.5	16	31	39	38	45.6	7	23	33	35
active	31.9	30	52	63	67	38.2	28	60	81	91
Cross country 1										
conventional	21.0	-	-	-	-	29.7	-	-	-	-
hardening spring	12.0	-9	-15	-19	-21	37.4	-9	-14	-17	-20
cross braced	23.6	8	16	20	20	33.4	-1	4	7	7
active	9.8	53	82	82	96	25.8	40	68	83	90
Metro 1										
conventional	24.0	-	-	-	-	27.8	-	-	-	-
hardening spring	24.4	-7	-9	-10	-10	28.6	-8	-11	-12	-12
cross braced	25.3	0	2	2	-1	36.7	-6	-5	-4	-6
active	22.7	71	86	85	80	26.3	44	67	75	75

Table 7 – 5 Comparison of load reductions achieved with each type of steering bogie, based on representative vehicles

Looking firstly at the results for design case track, the active bogie is still achieving significant load savings, with higher load reductions on the more severe curves in the cross country and metro test routes. The cross braced bogie is also showing reasonable load reductions for the two mainline routes. The hardening spring bogie is however not performing well, showing only minor improvements compared to conventional bogies for the mainline routes, and actually increasing overall tangential loading on the more severely curved cross country and metro routes.

When taking into account track roughness, the benefits of almost all steering types are reduced. Track roughness affects the steering mechanisms to varying extents. The hardening spring and cross braced bogies do not perform well when taking into account track roughness, giving only minor (or negative) improvements in tangential loading. The reduction achieved by the cross braced bogie on the mainline routes may have some benefits in reducing track damage;

inspection of the load squared column indicates 26 and 23 % load reductions. However, the active bogie gives a distinct improvement over the conventional train and the other two steering concepts. Benefits improve with route curvature, although track roughness reduces these benefits, significant savings in tangential loading can still be achieved.

7.6 Active steering: a closer look

In the simulations presented here, no limits were placed on actuator torque or range of motion. In reality the maximum required actuator torque is limited by maximum creep loads which can be generated at the wheels, which is dependent on vehicle weight and the available wheel-rail friction. The actuators only need a small range of motion to work effectively. As shown in Figure 7 – 49 the maximum actuator torque per axle for the cross country route was 15 kNm, with no more than 10 mrad of motion required between the axle and bogie.

Figure 7 – 49 shows a comparison of the angle of attack, bogie-axle angle and longitudinal wheel-rail loading for the front axle of a conventional DMU travelling over the test route cross country 1, compared to the same vehicle fitted with active bogies (the design case track has been used for this example, as the simpler outputs can be more easily compared graphically). As discussed in section 7.4.1.3, the longitudinal load has been greatly reduced through the use of active steering, whilst the angle of attack has been reduced and some minor over-steer has been introduced. Looking at the yaw angle between bogie and axle, the active system has kept this angle a lot more stable for the front axle, and generally reduced bogie-axle yaw. In the tighter curves the conventional bogie shows a yaw oscillation between the wheelset and bogie, which is evidence of 'bogie hunting'[§].

These changes in bogie-axle yaw angle have reduced the axle-track yaw angle (or angle of attack), achieving the wheel-rail load reduction already presented.

[§] As opposed to wheelset hunting, which has already been discussed

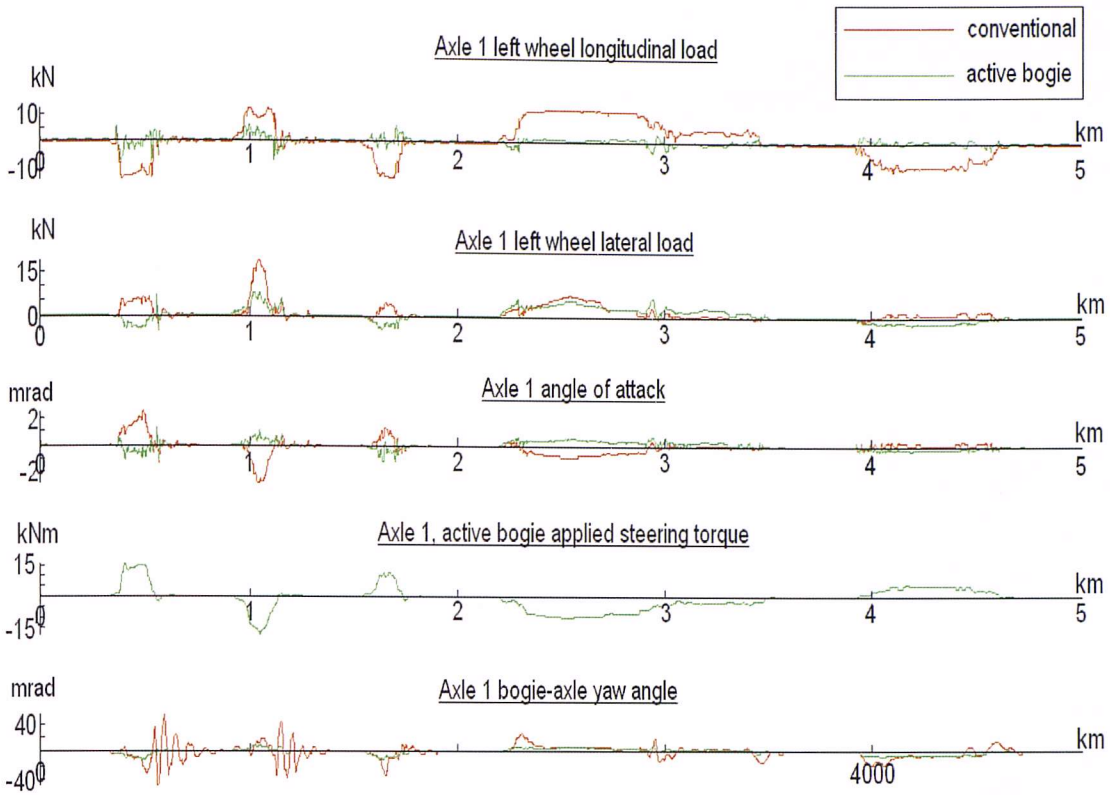

Figure 7 - 49 Comparison of DMU with conventional and active steering bogies, travelling over cross country 1 design case track

For this case, the maximum applied steering torque is 15 kNm occurring at 600 m when the vehicle is exiting the sharpest curve (see Figure 7 – 8 for the route details).

By taking the applied steering torque and the change in position of the wheelsets relative to the bogie, the work done by the steering system can be calculated. Table 7 – 6 shows the mechanical energy used by the active steering system across each route compared against the tractive energy used, for the representative vehicle derivatives travelling over rough track.

Route	Traction Energy (MJ/train km)	Steering Energy (kJ/ train km)	Extra energy requirement due to steering (%)
Mainline 1	29.0	21.8	0.1
Mainline 2	29.2	20.5	0.1
Cross Country 1	2.1	21.4	1.0
Metro 1	1.8	79.6	4.3

Table 7 – 6 Energy used per train km by the steering system, compared against tractive energy used by the train

For both the steering and tractive energies** presented here, the numbers given are mechanical work done (no account has been made for the steering actuator or traction system efficiencies).

For the mainline routes, and even the cross country route, the additional energy required for steering is small compared to that associated with the train's tractive effort (1 % or less). However, the metro route has a higher demand on the steering system, adding 4 % to the train's energy requirements. The cost of this additional energy needs to be offset by the reductions in track maintenance requirement.

7.7 Discussion

Results from the B176 derivative vehicles appear to be very promising, with significant loading reductions achieved. The active bogie achieved overall tangential load reductions between 42 and 55 % across all test routes.

This method gave a comparison of all the steering mechanisms across the different routes against an equal datum (i.e. based on the same vehicle type). However, for a more thorough analysis it was necessary to use more realistic vehicle models, each matched to a different test route.

Results from these more realistic vehicles give a different perspective on the suitability of each steering type. This is because these realistic vehicles have, to a certain extent, already been optimised for the duties required of them. The representative vehicle models used contain lower primary yaw stiffness than the B176 model, so already cause lower curving loads.

Including track roughness in the dynamic simulation had a significant effect on the percentage load reduction; in part because the total loads in all cases contained necessary damping loads created by the suspension in response to track roughness. Adding in the track roughness has caused a significant reduction in the benefits of the steering bogies; this is because the bogies have started to go unstable as a result of the track roughness. This needs to be taken

** These tractive energies have been calculated based on the applied motor torques used in the simulation.

into account before introducing any of these steering bogies into an operational railway. Improving overall track quality would reduce this problem[††]. However, this would require further investment in maintenance. As the purpose of this study is to provide a solution that will help to reduce maintenance requirement, this is not necessarily a recommended course of action. The purpose of introducing a new steering bogie would be to reduce loading for current track conditions. A suitable steering bogie will need to give good loading reductions through curves, whilst maintaining a reasonable stability through the track roughness it is likely to encounter. Results for the active bogie show that this is possible with overall load reductions of 27 to 44 % from the representative vehicle comparisons. Results are even better when comparing load squared, cubed and to the fourth power (as explained in 7.4.3 track damage is expected to be dependent on a power law).

The active bogie shows considerably better load reductions across all route types than the two passive alternatives, demonstrating a resilience and adaptability to the different route characteristics, and achieving a minimum of 27 % total tangential load saving for every route type.

All comparisons in this chapter have been based on total wheel-rail tangential loading, with no account for how this tangential load is made up (i.e. the proportion of longitudinal and lateral loading). This total has been used as a convenient metric for comparing the steering types; however, in reality loading in the two directions causes different degradation modes. Longitudinal load primarily contributes to fatigue and wear, whilst lateral loading causes fatigue and wear, but can also cause gauge spread and lateral shift[‡‡]. How the loading reduction shown in this chapter corresponds to reductions in track damage and cost savings still needs to be analysed before a comment can be made on their likely contribution to reducing maintenance cost. Thus further investigation is carried out in Chapter 8 to analyse how these load reductions affect track damage as well as maintenance and renewals cost.

[††] This would also reduce the track loading for conventional bogies, on straight track section, or allow conventional bogies to be designed with lower stiffness and thus lower curving loads.
[‡‡] As mentioned in Chapter 3, lateral shift can also lead to an increased ballast settlement rate

References

1. DeltaRail, http://www.deltarail.com/products_mech_interaction_vehicle_dynamics.htm, [Accessed, 26/6/08]
2. Iwnicki, S., *Manchester Benchmarks for Rail Vehicle Simulation.* Vehicle System Dynamics, 1998. **30**(3): p. 295 - 313.
3. Iwnicki, S., *The Manchester Benchmarks for Rail Vehicle Simulation.* 1999, Lisse, the Netherlands: Swets & Zeitlinger.
4. Kalker, J.J., *A fast algorithm for the simplified theory of rolling contact.* Vehicle System Dynamics, 1982. **11**(1): p. 1 - 13.
5. Shackleton, P. and S. Iwnicki, *Comparison of wheel-rail contact codes for railway vehicle simulation: an introduction to the Manchester Contact Benchmark and initial results.* Vehicle System Dynamics, 2008. **46**(1): p. 129 - 149.
6. Iwnicki, S., *The results of the Manchester benchmarks, in The Manchester Benchmarks for Rail Vehicle Simulation.* 1999. p. 2 - 12.
7. Evans, J.R., *Rail vehicle dynamic simulation using Vampire*, in *The Manchester Benchmarks for Rail Vehicle Simulation.* 1999. p. 119 - 140.
8. *GC/RT5021 Track System Requirements*, Railway Group Standard, Rail Safety and Standards Board, 2007
9. Storlarski, T.A. and S. Tobe, Rolling Contacts. Tribology in Practice Series. 2000, London: PE Publishing.
10. Office of the Rail Regulator, Track usage price list, http://www.rail-reg.gov.uk/upload/pdf/arev-price_list1_19dec.pdf, [Accessed, 8/8/08]
11. Tunna, J. and R. Joy, TTCI(UK), Methodology to calculate variable usage charges for control period 4, UK NR report No. 08-002, www.networkrail.co.uk/browse%20documents/StrategicBusinessPlan/Update/TTCI%20(UK)%variablecharges%methodology.pdf, [Accessed, 25/6/08]
12. Innotrack, D1.1.1 Database of representative vehicle and characteristics from participant countries; Thematic Priority 6: Sustainable Development, Global Change and Ecosystems; Project TIP5-CT-2006-031415. 2006, Rail Safety and Standards Board.
13. Ding, Y., M. Sterling, and C.J. Baker, An alternative approach to modelling train stability in high cross winds. Proceeding of the IMechE Part F: Journal of Rail and Rapid Transit, 2008. 222(1): p. 85 - 97.
14. London Underground, Rolling stock information sheets, http://www.tfl.gov.uk/assets/downloads/foi/Rolling_stock_Data_Sheet_2nd_Edition.pdf, [Accessed, 10/6/08]
15. Pérez, J., J.M. Busturia, and R. Goodall, Control strategies for active steering of bogie-based railway vehicles. Control Engineering Practice, 2002. 10(9): p. 1005 - 1012.
16. Goodall, R.M. and W. Kortum, Mechatronic developments for railway vehicles of the future. Control Engineering Practice, 2002. 10(8): p. 887-898.

17. Perez, J., J.M. Stow, and S.D. Iwnicki, Application of active steering systems for the reduction of rolling contact fatigue on rails. Vehicle System Dynamics, 2006. 44(Supplement): p. 730 - 740.

18. Jorgensen, M.W. and S.C. Sorenson, Report for the Project MEET: Methodologies for estimating air pollutant emissions from transport. 1997, European Commission Transport RTD, contract ST-96-SC.204, report ET-EO-97-03, Department of Energy Engineering, Technical University Denmark.

Chapter 8: Cost Savings Achievable With Steering Bogies

The previous chapter looked at the possible load savings that different types of steering bogie can achieve. The purpose of attempting to reduce tangential wheel-rail loading is to reduce the rates of wear and fatigue damage to the rail and reduce the spending on maintenance and renewals activities. In this chapter, a study of the possible cost reductions is presented.

8.1 Scope

As discussed in Chapter 7, the benefits of introducing steering bogies will vary depending on the route characteristics. In this study, two costing tools have been used to assess the achievable cost savings for two different sections of track; VTISM, which is a new industry costing model, and the Tunna method for assessing the cost of 'rail surface damage', both of which were introduced in Chapter 5.

Both methods rely on wheel-rail loading outputs from a vehicle dynamics simulation. For this analysis, vehicle-track simulations were carried out over longer routes*, based on measured track data, including cant and curvature profiles as well as full track roughness. Traffic data, giving details of the number of vehicles per annum travelling over each route is based on records from the operational railway. The active and cross braced steering bogies are compared against a conventional bogie. The hardening spring bogie showed less promising results in Chapter 7, and has therefore not been included in this analysis.

The first route is a relatively straight section of mainline, similar to the Great Western Mainline from London to Bristol (111 miles long). The second route is a curvy cross country route, similar to the Trans Pennine Express between Manchester and Leeds (42 miles). The curvature profiles of the two test routes are shown in Figure 8 – 1. Profiles of the short test routes used in the previous

* As opposed to the shorter 'representative routes' used in Chapter 7.

chapter are also included for comparison. The profiles of these two longer test routes are at the extremes of the test routes used in Chapter 7.

The mainline route carries 36 high-speed trains per day, each made up of two locomotives and eight carriages (or 5.7 MGT pa). Whilst the cross country route carries 111, three car DMUs per day (or 5 MGT pa)

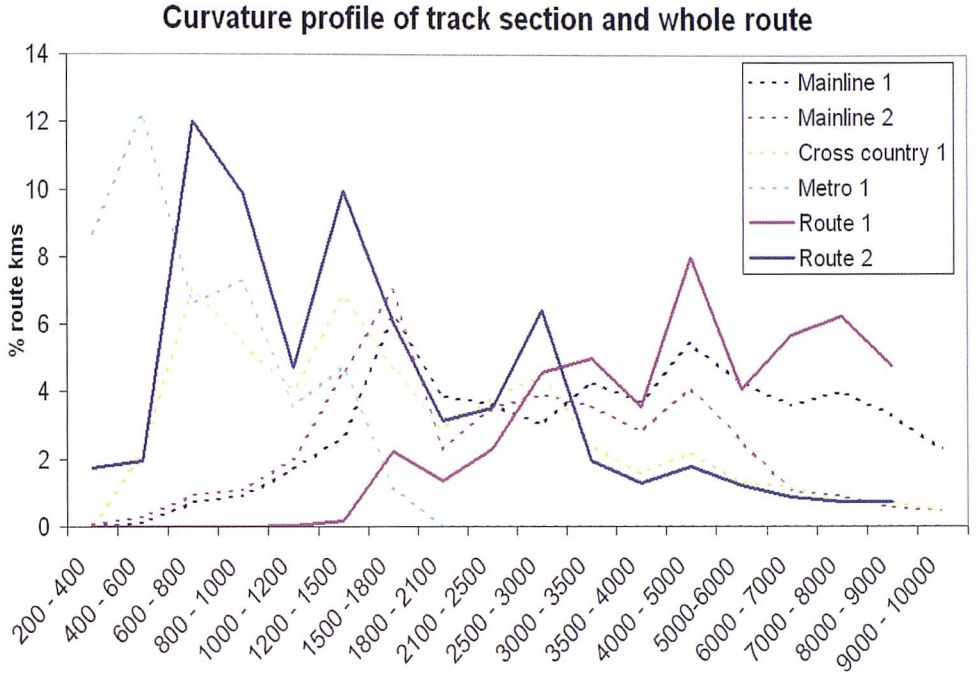

Figure 8 - 1 Curvature profile of test routes

8.2 Costing analysis using VTISM

As described in section 5.5.6, VTISM is a new industry costing model which can be used to take wheel-rail loading data from the vehicle dynamics package, VAMPIRE and include this in a maintenance and renewals cost analysis. It is probably the most complete system available for this type of study, at the present time.

There are a limited number of track sections available within the VTISM database which are available for carrying out costing studies. Rather than the short representative routes used in Chapter 7, longer sections of track based on real measured geometry are used. Details of current traffic and component condition along the route are all provided

VTISM integrates two existing damage models, T SPA which predicts track maintenance requirements (based primarily on vertical train dynamics, and doesn't account for wear and fatigue damage), and WLRM which is used to calculate wear and fatigue rates which are added into the T SPA calculations to be included in maintenance and renewal programmes. T SPA generates a maintenance and renewal programme, based on a set of predefined intervention criteria. From the volumes of work for each type of maintenance and renewal activity an overall cost is calculated.

8.2.1 Vehicle-track VAMPIRE simulation

The WLRM requires an input of $T\gamma$[†] for every wheel of a rail vehicle as it moves along the section of track under investigation. Simulations are carried out using single carriages travelling over the test route (as in the investigation in Chapter 7). Serco, the developers of VTISM, suggest using the loading at the front two axles (i.e. the front bogie) of the rail car, then doubling the predicted damage to give an output for the whole car[1]. This cuts down on processing time, but could introduce inaccuracies, as wheel-rail loading at the back bogie of a rail car will not exactly match that of the front bogie.

In Chapter 7 all calculations were carried out using a new P8[‡] wheel profile; however, over the course of their life, railway wheels wear, which changes the shape of their profile. This in turn affects the steering performance of the wheelset. This can be taken into account in the WLRM by carrying out dynamic simulations for trains with a variety of wheel profiles, using a new wheel profile and worn profiles. Introducing steering bogies will change the amount of wear on the track, as shown in section 8.2.2, but it will also change how the wheels wear. This means a standard worn wheel profile will not necessarily be representative of a wheel that has been worn through use in a steering bogie; the profiles will most likely be different in some way. As no measured data is

[†] i.e. tangential load multiplied by creep ratio, as defined in Chapter 5.
[‡] This is a standard wheel profile, used widely on the UK railways

available for how steering affects wheel wear, a standard worn P8 profile has been included for this study.

When carrying out vehicle dynamics simulations to calculate creep loads that will be used as inputs for the WLRM, Evans suggests using a coefficient of friction between wheel and rail of 0.45[2]. This does not represent a typical value that can be measured at the rail head, although Evans suggests it can be taken as a *'reasonable upper bound of friction conditions'*[2]. RCF damage predictions from the model have shown good correlation with measured results[3]; 0.45 has been used for this analysis rather than 0.3 as used in Chapter 7.

8.2.2 WLRM outputs

Vehicle-track interaction simulations were carried out for two types of steering bogie, along with the conventional bogie for use on trains running on the two different test routes. Wheel-rail loading outputs were then fed into the WLRM model. The track has been split up into sections of 55 metres, and the WLRM used to calculate a wear and RCF damage index for each section. Figures 8 – 2 and 8 – 3 show the outputs for RCF and wear, respectively, for Route 1 (the straighter, mainline route). The outputs shown here are for the average damage index over each track section.

As demonstrated in Figures 8 – 2 and 8 – 3, the active bogie has significantly reduced RCF and achieved moderate reductions in wear. The mechanical bogie achieved some reduction in RCF damage in the first 20 km of the test track. However, on inspection of the wear damage comparison, it is clear this is actually because it has increased track loading and therefore increased the wear to the extent that it is 'rubbing out' cracks before they can develop. This is a very straight section of railway (as shown in Figure 8 – 1); because the mechanical bogie is slightly less stable through track roughness, it has increased the overall track loading compared to the conventional bogie. Because of this the mechanical bogie causes a small overall increase in both wear and RCF damage.

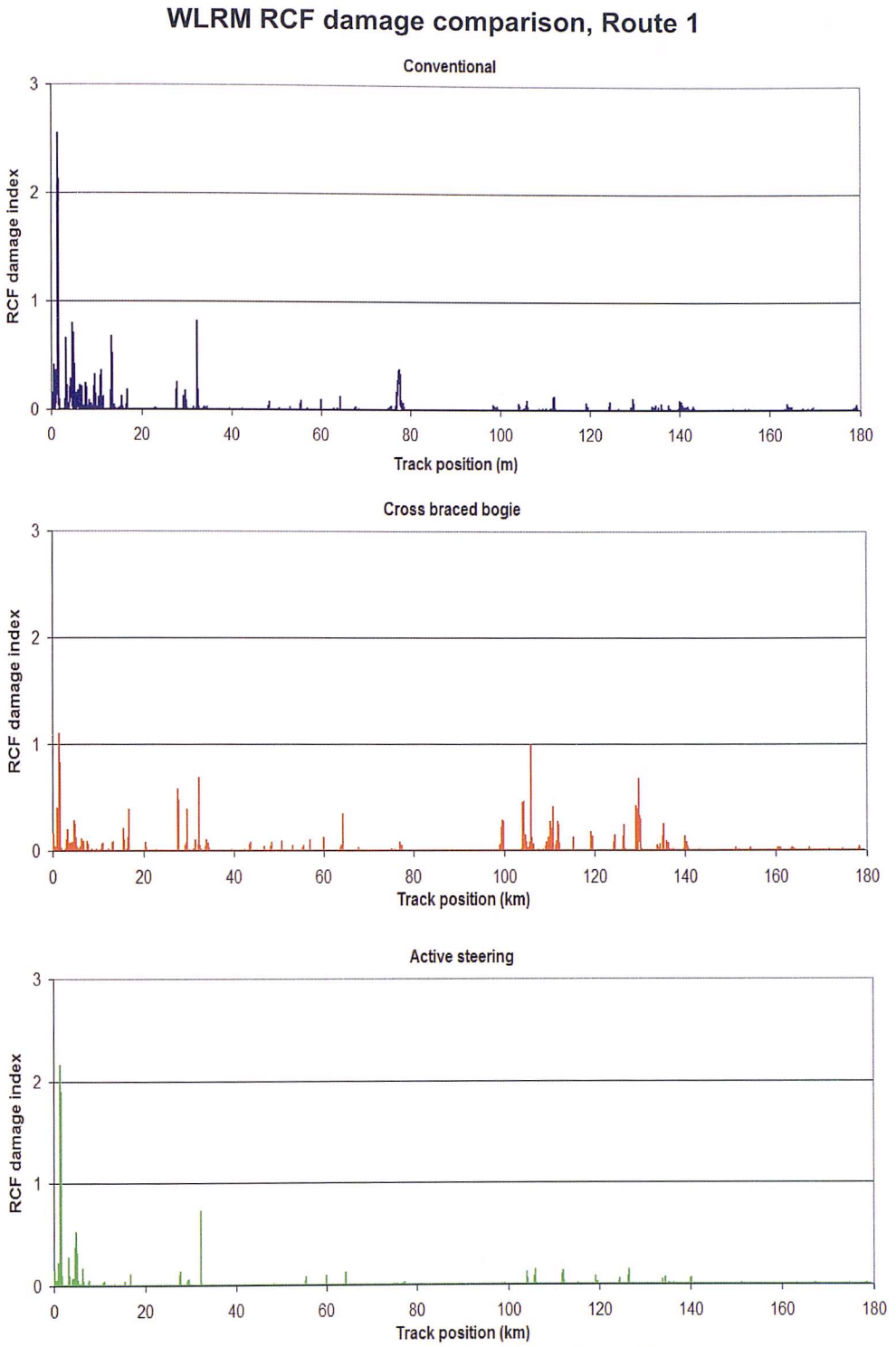

Figure 8 - 2 WLRM output, comparison of RCF damage on Route 1

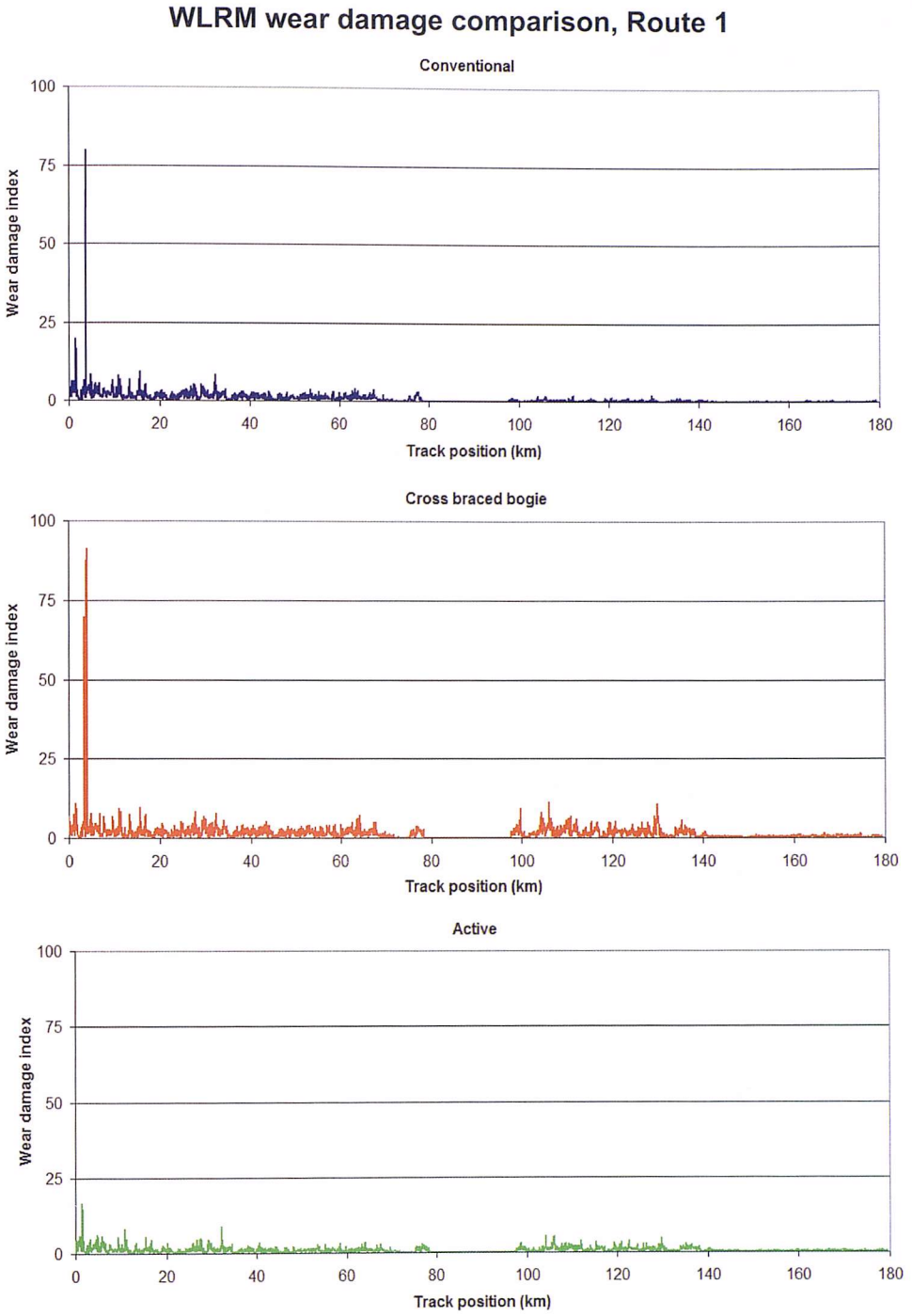

Figure 8 - 3 WLRM output, comparison of wear on Route 1

Route 2 (based on a cross country route), which contains more high severity curves, shows very different results (as demonstrated in Figures 8 – 4 and 8 – 5).

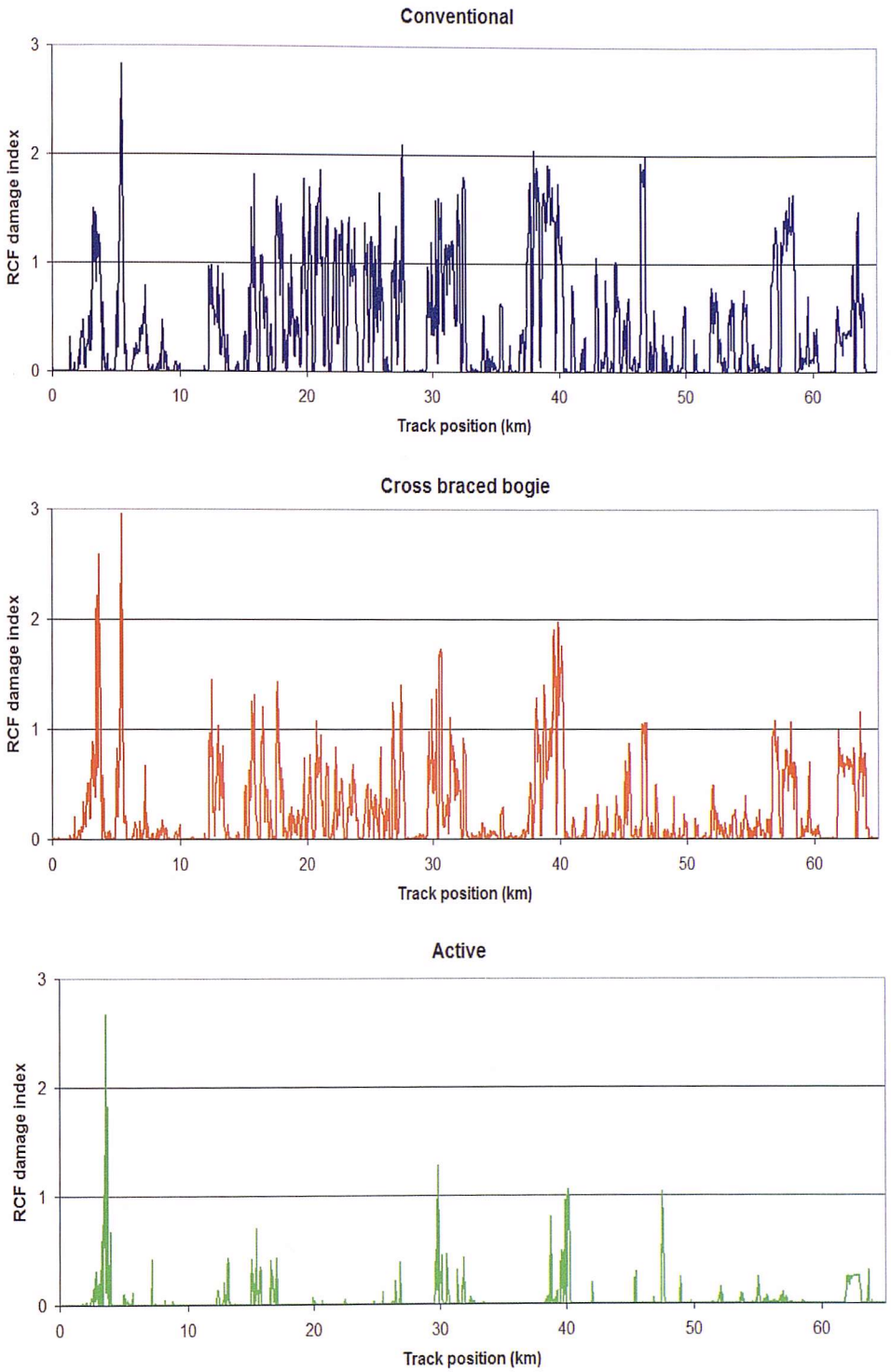

Figure 8 - 4 WLRM output, comparison of RCF damage on Route 2

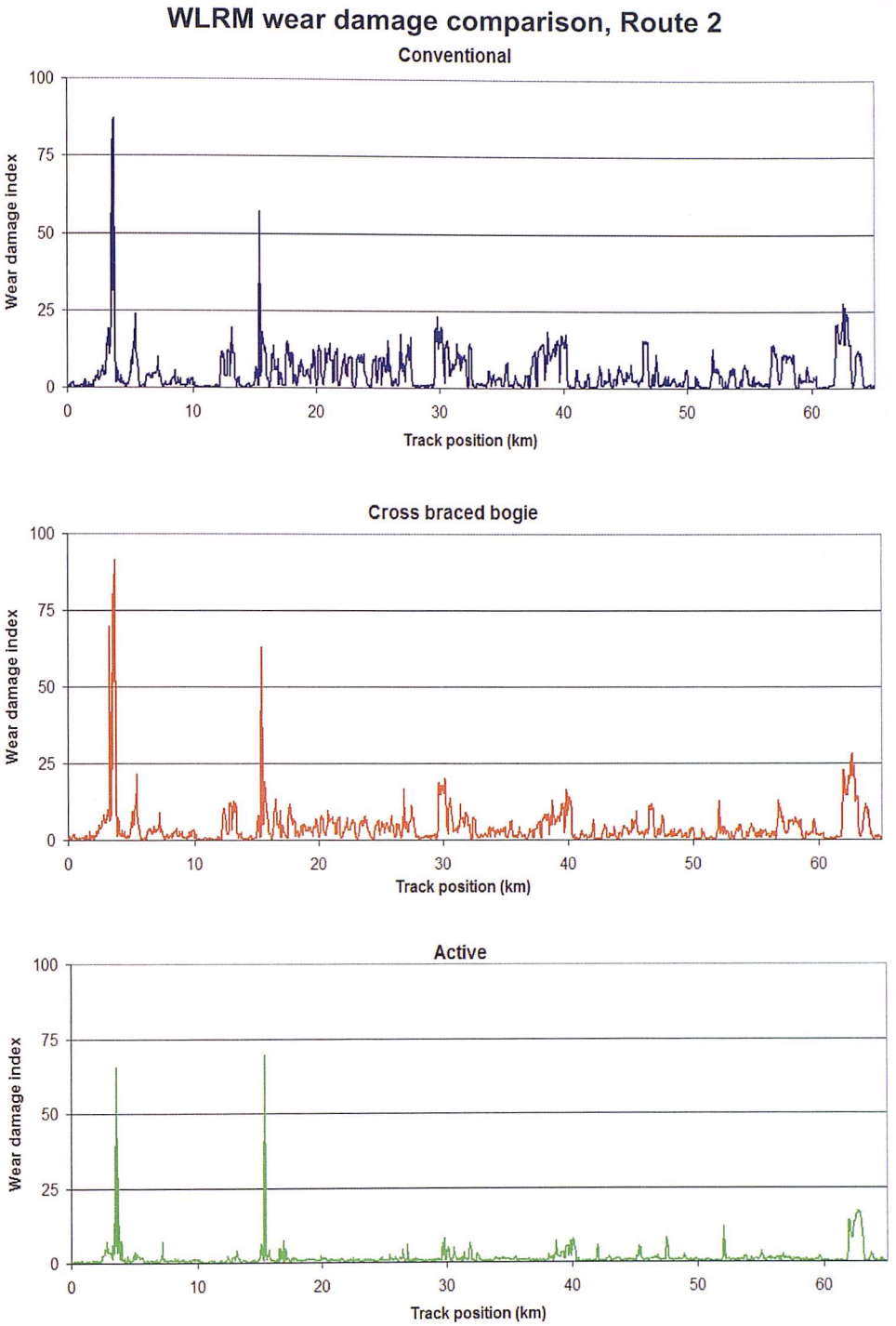

Figure 8 - 5 WLRM output, comparison of wear on Route 2

For both damage mechanisms, the damage indices are significantly higher than for Route 1. Because of the more severe curves experienced along this route, the steering bogies can make a greater contribution towards reducing track damage. In this case the mechanical bogie is showing good reductions over the

conventional bogie, with the active system significantly out-performing both of them.

8.2.3 Comparison with results from 5k test routes

The reductions in WLRM wear and fatigue indices achieved by the steering types appear to be more pronounced than the comparisons of total tangential load used in the earlier analysis presented in Chapter 7. This is partially due to the nature of the damage functions used (i.e. values of $T\gamma$ under 15 are assumed to cause no damage to the track); but also because the creep (γ) is now included in the comparisons.

Using the same outputs[§] as in Chapter 7, results can be compared with those of the shorter 5 km representative route.

Route 1 (Mainline)	% total saving (T)	% saving (T^2)	% saving (T^3)	% saving (T^4)	% saving ($T\gamma$)
cross braced	-6	-4	6	2	8
active	6	15	24	31	81
Route 2 (Cross country)					
cross braced	1	11	22	28	14
active	49	75	85	77	90

Table 8 – 1 Comparison of total load reductions achieved and total reductions in $T\gamma$

Looking at the percentage load savings achieved, and comparing against results show in table 7 – 5, similar loading reductions are being achieved. The two routes used in this chapter are at the extremes of the four test routes used in Chapter 7, and the results achieved reflect this. Results for the active bogie show a very good correlation with results from the shorter routes.

Figure 8 – 6 shows a comparison of total T, T^2, T^3 and T^4 for the active bogie across Routes 1 & 2, compared with results from the earlier test routes (Mainline 1, Mainline 2, Cross country 1 and Metro 1). Results correlate well with Routes 1 and 2, showing comparisons at the extremes of the earlier studies. It is difficult to draw too many conclusions from these comparisons, as results are for a range of different railways types with different types of rolling stock

[§] i.e. relative total tangential load, total tangential load squared, to the power three and to the power four

and levels of track roughness. Also, these total load savings only give a general overview of results, they give no indication of how track loading varies against distance along each route.

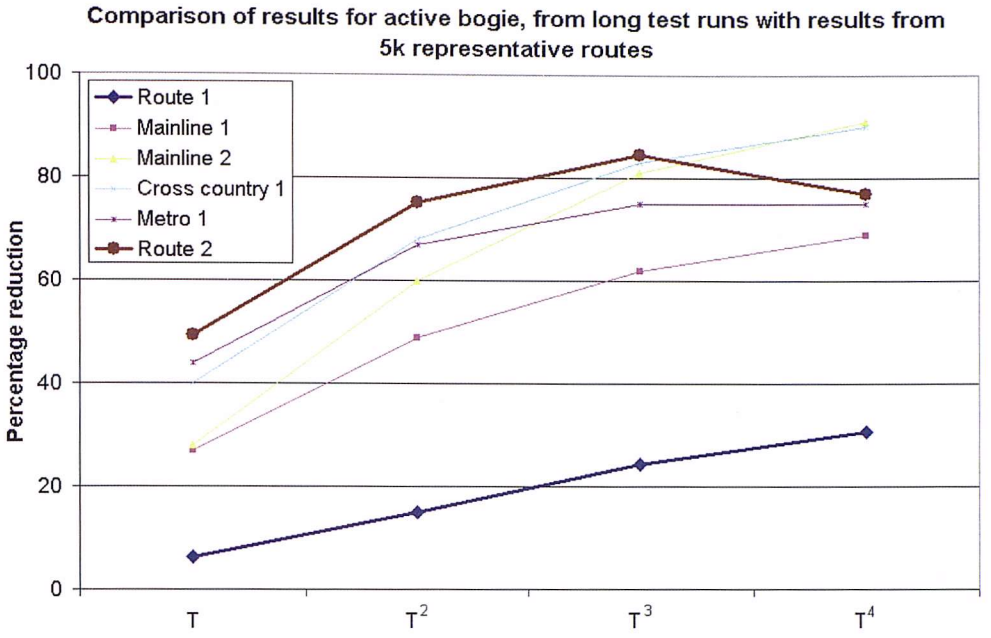

Figure 8 – 6 Comparison of total tangential load outputs for active bogies, based on calculations for short representative routes and longer measured routes

Results from the cross braced bogie correlate less well between the two studies, as shown in Figure 8 – 7.

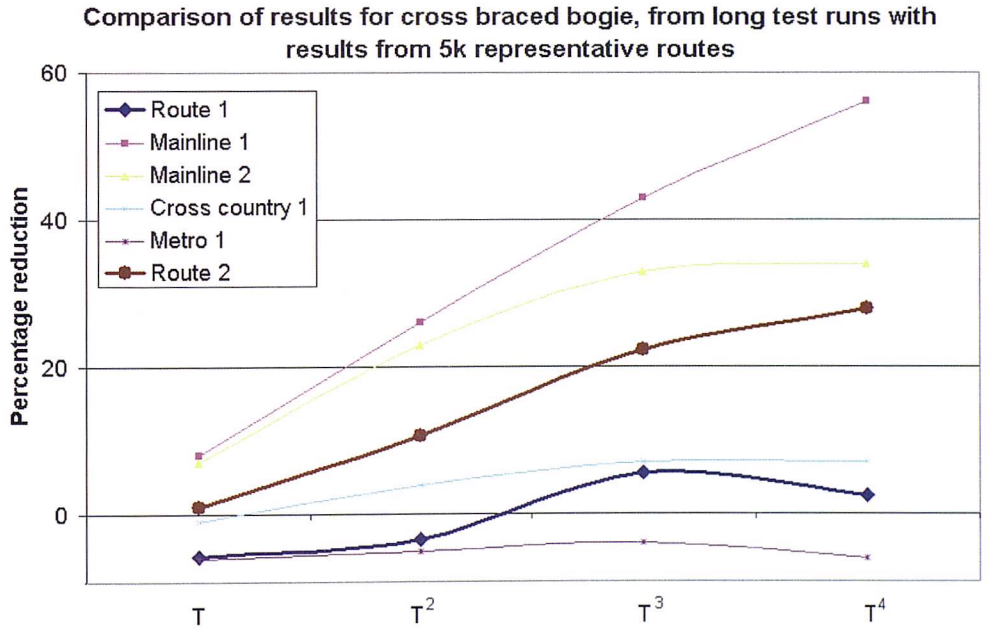

Figure 8 – 7 Comparison of total tangential load outputs for cross braced bogies, based on calculations for short representative routes and longer measured routes

These results do not correlate so well as the active bogie results, because the cross braced bogie is more affected by travelling through track roughness. This means a higher proportion of these total loading figures are made up of loading as a result of track roughness. The two sets of results were calculated using different coefficients of friction; the short routes used in Chapter 7 were simulated using a value of 0.3 (which was taken as a typical measured value from in-service rails), while results from these longer routes were based on a coefficient of friction of 0.45 (as stated in section 8.2.1, this value is suggested by the creators of the WLRM to give the best correlations between predicted wear and fatigue rates and measured values). The track roughnesses applied to the representative routes were based on average profiles within a given standard deviation band, for the appropriate route type. However, the longer routes include full detail of all measured track roughness along the track. The higher coefficient of friction used appears to make the cross braced bogie more stable, and hence less affected by track roughness. This means for the second set of results (Route 1 and Route 2), there are higher savings for the routes containing higher severity curves, i.e. savings from Route 2 are higher than Route 1; whilst in the previous calculations, over representative routes, using 0.3 coefficient of friction, the higher levels of roughness on the cross country and metro routes made the cross braced bogie more unstable and hence caused higher track loads (i.e. achieved less savings).

Looking at the savings in $T\gamma$, the reductions tend to be larger than reduction in tangential load only. This is because, as discussed in section 7.4.1.3, lateral loading makes up a large proportion of the tangential load (i.e. the combined lateral and longitudinal load). However lateral loading through curves is dominated by the lateral quasistatic load, multiplying by the creep ratio (γ) means creep loading dominates the analysis (and not quasistatic loading).

The active bogie is particularly effective at reducing longitudinal creep loading through curves, although it does also make a contribution towards reducing lateral quasistatic load. Because of this the $T\gamma$ comparisons show a much more pronounced saving for active bogies.

8.2.3.1 Steering effort

The applied steering energy for the active steering bogies over Route 1 was calculated at an average of 17.7 kJ/km (an additional 0.1 % on top of the required traction energy). Over Route 2, the applied steering energy is an average of 31.5 kJ/km (1.5 % of the traction energy). This correlated well with results from Chapter 7, where Mainline 2 required a steering energy of 20.5 kJ/km and Cross Country 1 a steering effort of 21.4 kJ/km.

8.2.4 Cost comparison

The WLRM results shown in Figures 8 – 2 to 8 – 5 were fed into T SPA which is the maintenance and renewals planning, and costing module of VTISM. For this analysis a time frame of 30 years was chosen.

The system has a variety of output options, including a breakdown of maintenance and renewal activities. As discussed in Chapter 4, it can be difficult to allocate certain activities to maintenance or renewal. The maintenance and renewal activities included in T SPA are shown in Table 8 – 2.

Renewal	**Description**
Complete renewal with trax	Renewal of rails, sleepers and ballast
Complete renewal and ABC	Renewal of rails and sleepers, with an advanced ballast clean
Rail renewal	Renewal of a full length of rail on both sides
Reballast ABC	Advanced ballast clean
Reballast trax	Replace ballast
Maintenance	
Single rail renewal	Renewal of a full section of rail on one side only
Single rail repair	Renewal of a very small length of track to repair localised damage
Stone blowing	A method of removing accumulated fines from the ballast
Tamping	Mechanically vibrating the ballast to restore geometry

Table 8 – 2 T SPA Maintenance and renewal activities

The 'single rail renewal', 'rail renewal' and 'single rail repair' activities will be affected by tangential loading. The 'rail renewal' and 'single rail renewal'

activities are triggered as the rails reach their wear limit; whilst 'single rail repair' is triggered due to localised fatigue damage. T SPA does not include a rail grinding activity as a method of preventing fatigue damage, but triggers a 'single rail repair' after a section of rail has accumulated a certain amount of damage. This is not a real representation of how infrastructure providers manage RCF. However, the outputs from this give a measure that can be used to compare the effects of different bogie designs on the cost of fatigue damage.

8.2.4.1 Mainline route

As demonstrated in section 8.2.2, the fatigue and wear indices were both reduced using active steering on Route 1 (with a more pronounced reduction shown for fatigue damage). However, fatigue and wear damage contribute only a small proportion of the overall cost of maintaining this route. Tangential damage (i.e. wear and fatigue) contribute £240 /mile/annum out of the total cost of £43.5k /mile/annum for the conventional rail vehicles. Figure 8 – 8 shows a comparison of average cost per track mile, per annum for Route 1, looking at vehicles with, active steering, cross braced bogies and conventional bogies.

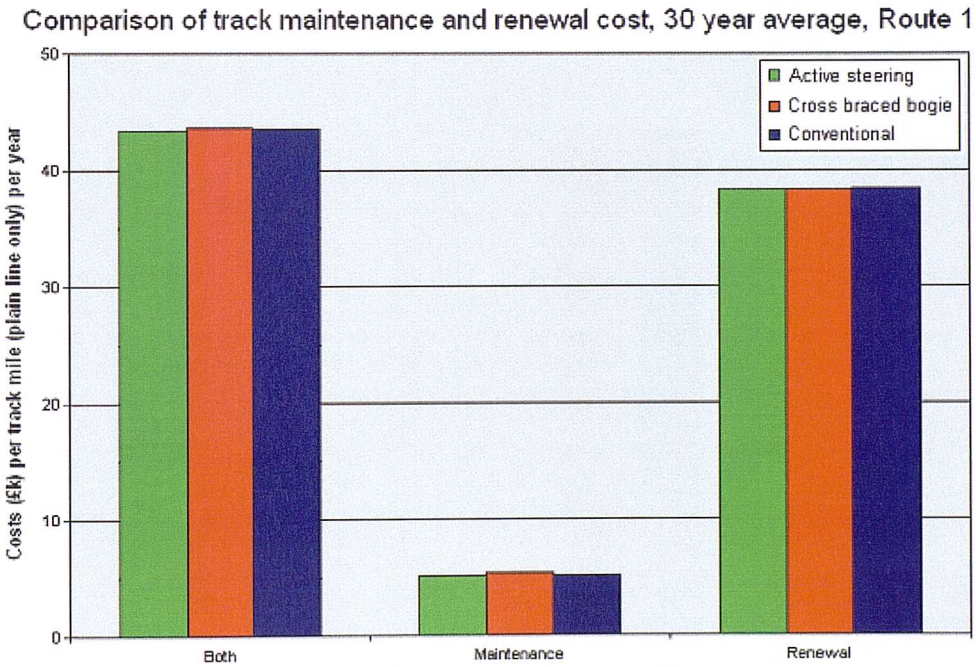

Figure 8 - 8 Route 1 maintenance and renewal costing comparison

The two steering bogies only cause a very small change to the overall track maintenance and renewals costs. Figure 8 – 9 shows a comparison of the costs of tangential damage only. The active bogie has reduced the cost of tangential

damage by £110 /mile/annum, whilst the cross braced bogie caused an increase of £90 /mile/annum.

Results for the cross braced bogie appear to contradict the reduction in total Tγ, presented in Table 8 – 1. However, as explained in Chapter 7, comparisons of total loading reduction over a given route will not directly correlate with changes in track damage.

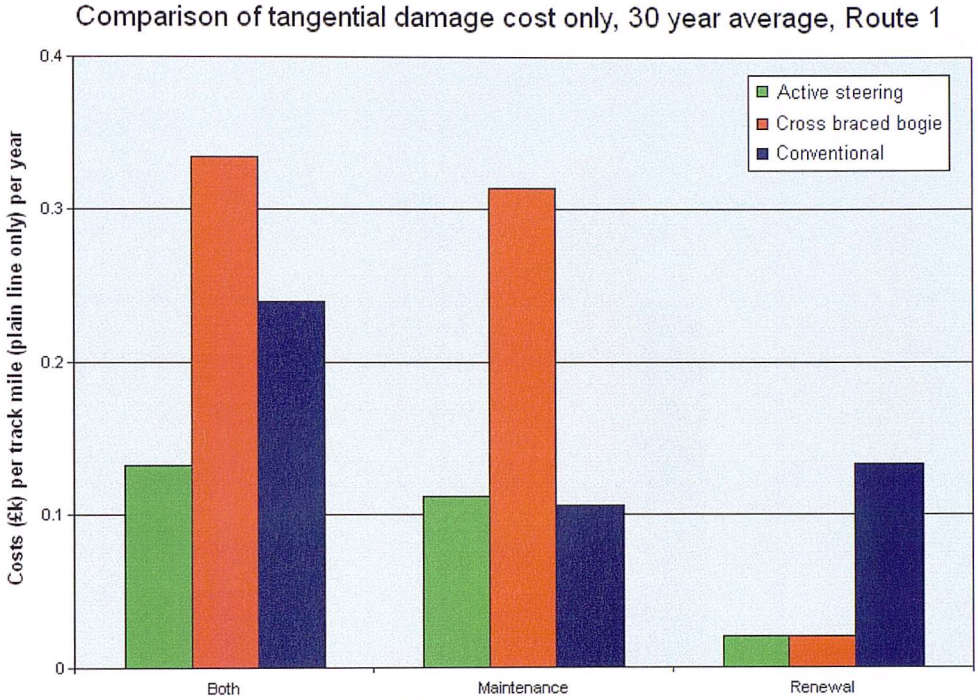

Figure 8 - 9 Route 1 cost of tangential damage only

As this section of track is so straight, with virtually no curves below 1500 m radius, tangential damage is not expected to have a major impact on the overall costs. So although the active bogie has successfully achieved a large percentage reduction in the cost of tangential damage, the contribution to overall track maintenance and renewals cost is very small (a saving of 0.5 %).

Figure 8 – 10 shows a cost breakdown by activity, there are small differences in rail renewals and single rail repair.

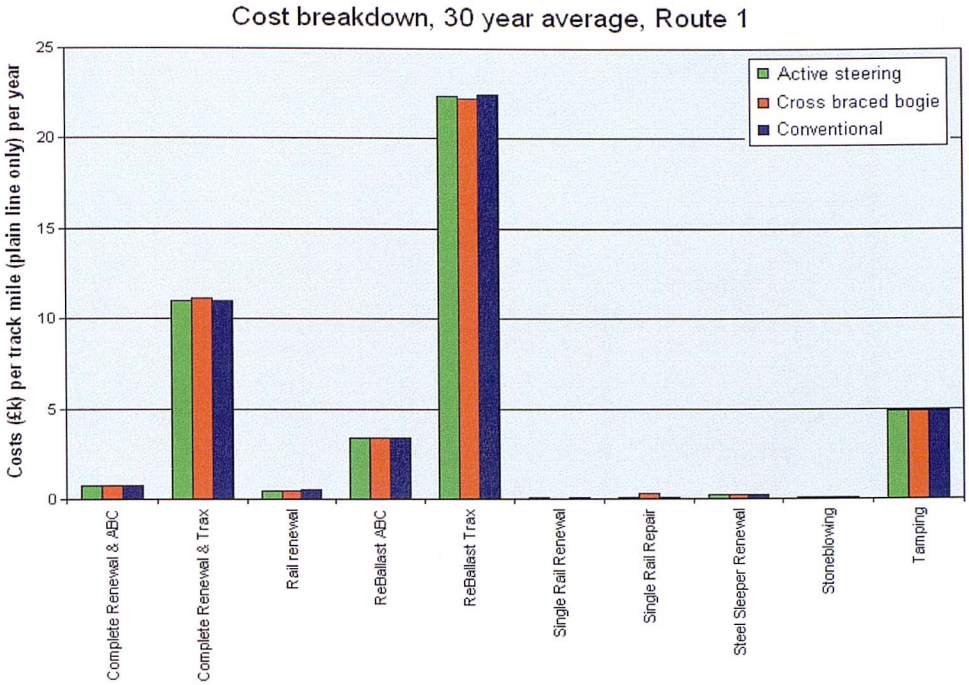

Figure 8 - 10 Route 1 comparison of cost breakdown by activity

8.2.4.2 Cross country route

The cross country route contains many more curves of higher severity (as shown in section 8.1) and, as expected, the tangential damage makes a much bigger contribution to overall costs. Figure 8 – 11 shows the cost savings achievable with the two steering bogie types. The cross braced bogie achieves an 18 % reduction in track maintenance and renewals cost, whilst the active bogie achieves a 35 % reduction.

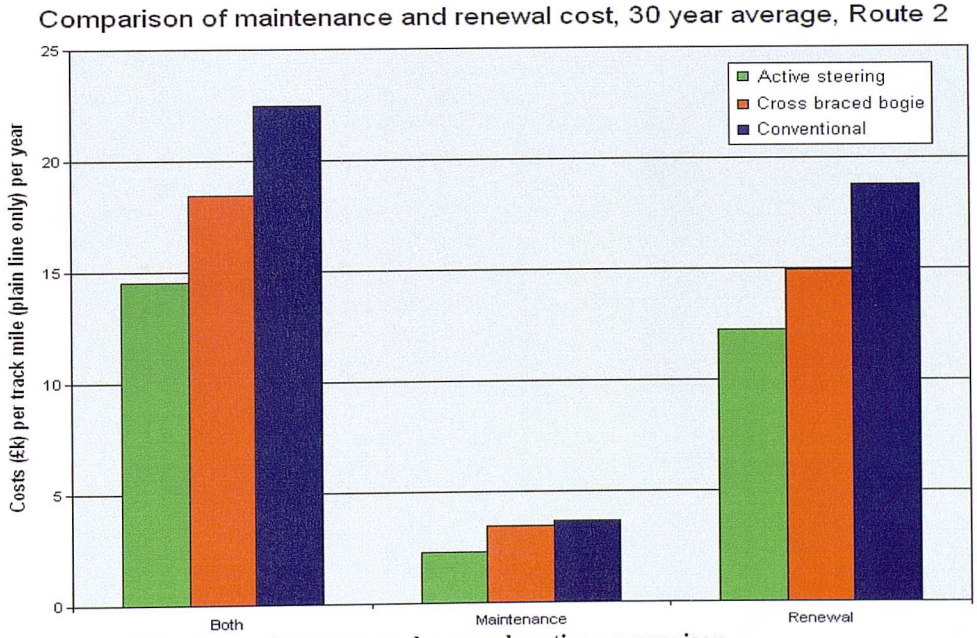

Figure 8 - 11 Route 2 maintenance and renewal costing comparison

Looking at the cost of tangential damage only, the mechanical and active steering bogie have reduced the cost by 46 % and 90 % respectively, as shown in Figure 8 – 12.

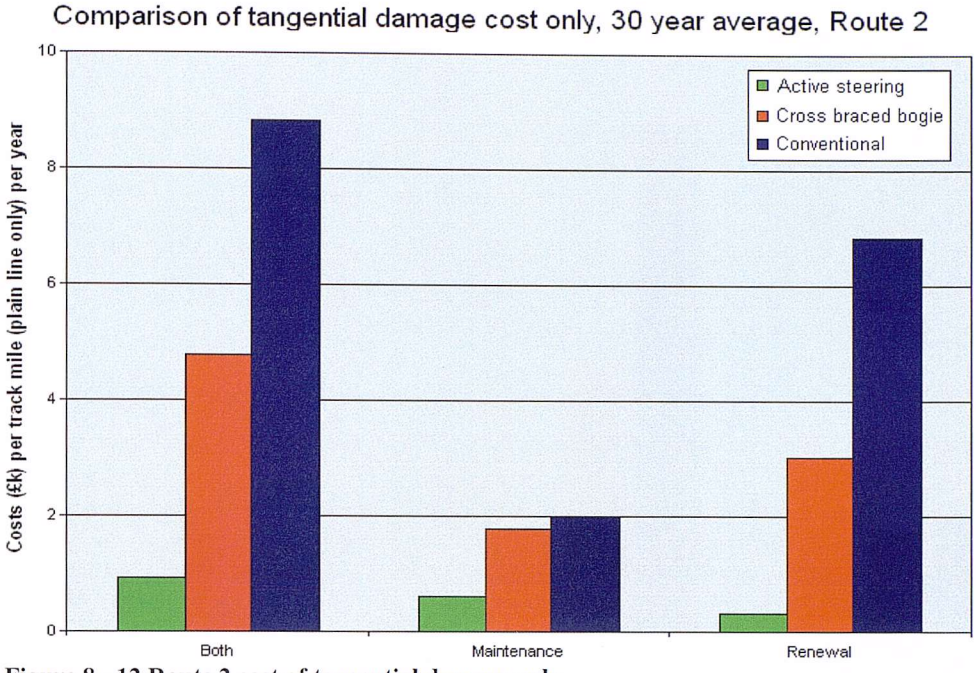

Figure 8 - 12 Route 2 cost of tangential damage only

These savings have been achieved by reducing the requirement for rail renewals (because of the reduced wear) and single rail repair (because of the reduced fatigue damage).

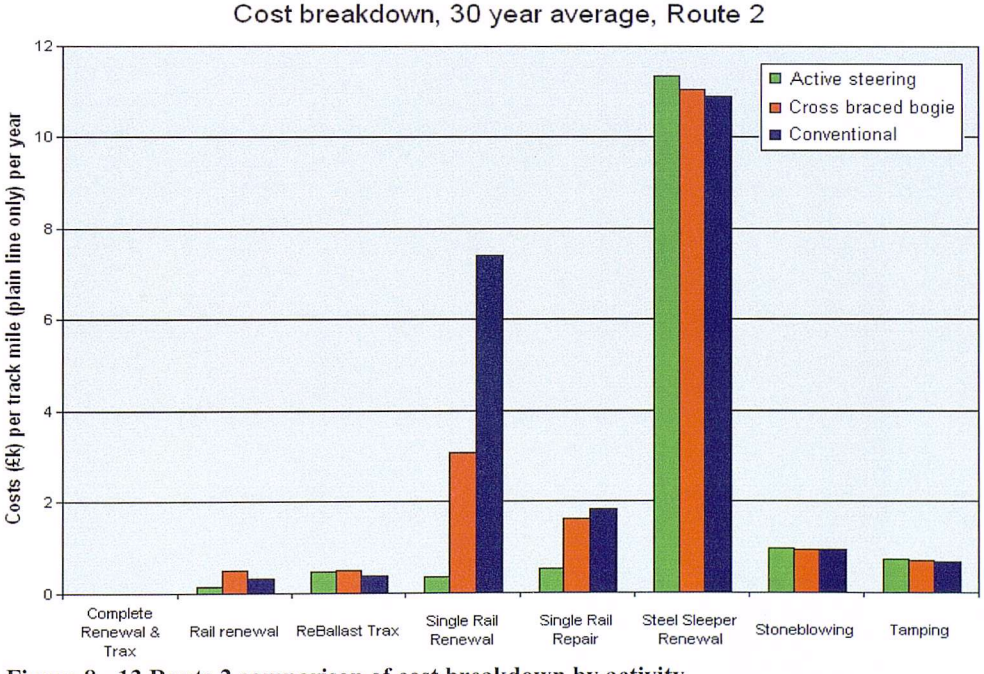

Figure 8 - 13 Route 2 comparison of cost breakdown by activity

8.2.5 Necessary assumptions and limitations of VTISM

The VTISM software gives a good overview of the effects of introducing new vehicles or changing service patterns on track maintenance and renewals cost. It is the most complete model for an investigation of this type that is currently available. The degradation models used are largely based on empirical relationships. As discussed in Chapter 5, empirical models are quick and reliable methods of extrapolating existing data. Providing the models are based on a suitable data range, and the system is not being fundamentally changed, these relationships are a good method of predicting future trends. However, when completely new technologies are being evaluated, a more detailed knowledge of the physical degradation process is required to ensure the empirical based relationships are still valid.

The maintenance planning module of VTISM does not include a grinding activity. This is one of the most important methods of managing RCF and for a complete analysis of the effects of reducing tangential rail loading, this really needs to be included. Because of this, the results may well underestimate the cost benefits of reducing tangential load; not only because of the cost of the grinding itself, but because grinding is effectively increasing the wear rate. Therefore rails need to be replaced more often, hence increasing the rail renewals cost; which is not accounted for in the VTISM model.

Assumptions suggested by the creators of VTISM, for calculating wheel-rail loads with a vehicle-track simulation are: using only the load outputs from the front bogie of a rail vehicle, modelling single carriages rather than whole trains, and not adding tractive forces into the analysis.

When carrying out vehicle dynamic simulations over longer routes with small time steps, especially when using active control systems, the calculations are extremely memory intensive and are at the limits of the capabilities of existing desk top computers. Simplifications such as running single car simulations and only saving results from the front bogie make it possible to carry out longer runs and more accurately model the interactions by using smaller time steps.

However, further analysis is required to evaluate the affects of these simplifications.

As discussed in section 7.5, tractive forces have a small but noticeable effect on the overall tangential loading. In section 7.5 the effect of steady state tractive loading was considered; however, acceleration and braking will cause significantly higher loading. For the purpose of this analysis, the focus is to compare the steering types, which all have the same tractive loads applied. Because of this they have not been taken into account. For a full analysis of track damage the complete loading environment should be included in the calculations.

In VTISM, the analysis of 'vertical damage' using T SPA, such as ballast settlement and sleeper damage is completely isolated from the 'tangential damage' calculations for wear and fatigue which are carried out using the WLRM. However, the curving performance of a rail vehicle can have an effect on the 'vertical damage' mechanisms. As demonstrated in Chapter 7, the steering bogies reduce the 'angle of attack' through curves, which in turn reduced the lateral displacement of the wheelset relative to the track. As explained in Chapter 2, quasistatic curving loads are caused by the displacement of the wheelset relative to the track. By reducing the wheelset lateral displacement, both lateral and vertical loads (at the high rails) through curves are also reduced. Further to this, lateral loads can also cause the track and sleepers to shift relative to the ballast, which can contribute to accelerating ballast settlement. None of this is accounted for in the VTISM calculation; linking outputs from the dynamic vehicle-track simulations directly to all of the degradation modes (as opposed to wear and fatigue only) would give a more thorough analysis.

8.3 Cost comparison using Tunna method

As described in section 5.5.3.1, the Tunna method[4] is an alternative approach to calculating damage costs, based on outputs from the WLRM**. Taking the

** Which only looks at tangential damage

same RCF and wear indices shown in section 8.2.2, the Tunna equations were used to estimate the cost of wear and RCF for vehicles containing the three types of bogie.

Tunna's equations are based on the use of grinding to control RCF, and replacing the rails when they have reached their wear limit.

Tunna suggests using the wear number ($T\gamma$) due to steady-state curving load on the outside rail through curves as the inputs to his damage model. Track roughness has been included for this analysis so the WLRM outputs are not based on steady-state loading but also include responses to track roughness. This is a more accurate representation of the real wheel-rail loading. Outputs from the WLRM give average or maximum damage indices in each track section. The average damage indices will roughly equate to the damage as a result of steady-state curving (because track roughness causes an extra oscillation about this steady-state curving load, as shown in section 7.4.2).

Figure 8 – 14 shows the costing comparison for Route 1. The three bogie types have been ranked in the same order as the VTISM calculations; however, the cost calculated here are significantly higher in all cases, when compared to Figure 8 - 9. The cost of tangential damage for the conventional vehicle calculated using VTISM was £240/mile/annum, whilst here the figure is £10,000/mile/annum.

There are various reasons for the differences between outputs from the two models. VTISM does not specifically include grinding, missing out the cost of the grinding activity and also the extra wear caused by grinding Also for the mainline route, the VTISM maintenance includes a significant amount of 'complete renewal & trax'. This activity has been triggered by vertical geometry deficiencies, and not the tangential load. However, it is removing rail that has been worn and contains RCF damage. When comparing the cost of tangential damage, these cost are not included. Because the track is already being replaced for other reasons this cost cannot be reduced through the use of

steering bogies, in the VTISM analysis. The Tunna method looks only at 'rail surface damage' and does not account for other maintenance activities.

Whilst Tunna has published the base cost data for his model[4], £2000/km for grinding and £250,000/km for renewals, the base cost data for VTISM is largely hidden. So there may be further discrepancies here.

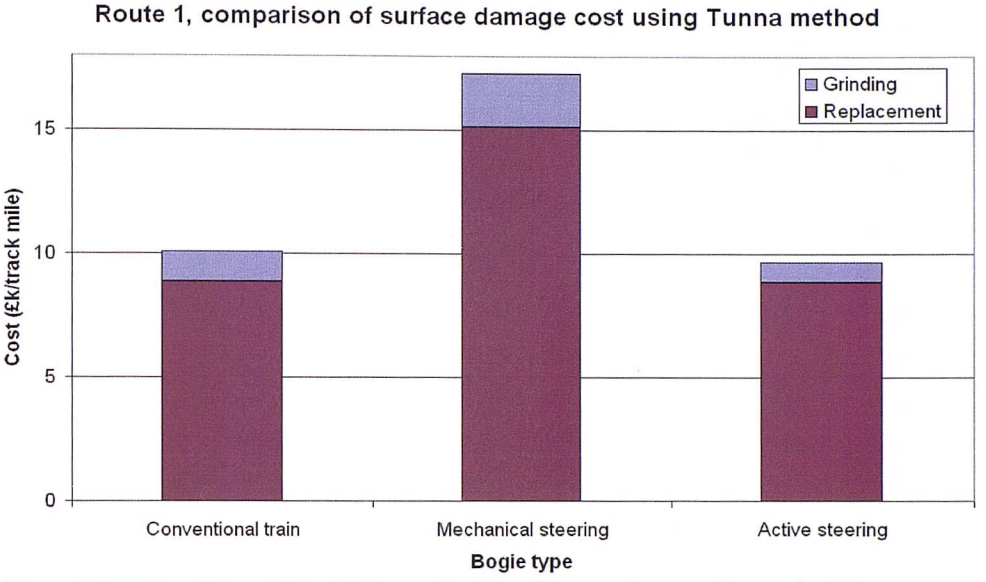

Figure 8 - 14 Route 1 cost of grinding and rail replacement comparison using Tunna method

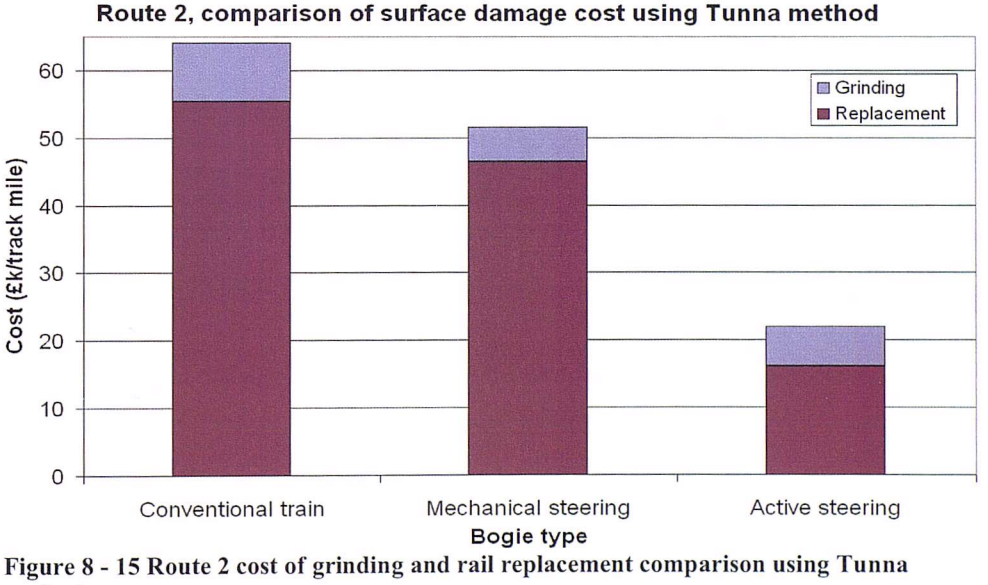

Figure 8 - 15 Route 2 cost of grinding and rail replacement comparison using Tunna method

Figure 8 – 15 shows the cost comparison for Route 2; again, total costs are significantly larger than the VTISM outputs, but showing a similar ranking of

the bogie types. However, the percentage cost reduction of both the mechanical and active bogies appears to be slightly smaller. Table 8 – 3 shows a comparison of results using each method, looking at the percentage reductions in tangential damage.

	Route 1					Route 2				
	Conventional	Mechanical steering		Active steering		Conventional	Mechanical steering		Active steering	
	£/mile	£/mile	% saving	£/mile	% saving	£/mile	£/mile	% saving	£/mile	% saving
VTISM	240	330	-38	130	46	8800	4800	45	910	90
Tunna	10100	17300	-71	9600	5	64000	46000	28	22000	66

Table 8 – 3 Comparison of results from VTISM and Tunna method

Both analyses rank the steering types in the same order, and suggest the active steering gives a significantly higher cost reduction than the cross braced bogie. However, the magnitude of the costs being predicted by the two methods is significantly different and the percentage savings show a significant variance.

An integration of Tunna's grinding cost model into VTISM, along with a verification of the back ground data used by both models, would be a useful exercise to aid the future analysis of new vehicle types.

8.4 Effect of savings on train life cycle cost

The figures presented in the previous sections have all been based on costs per track mile. When comparing the savings over the lifetime of a train, it can be more convenient to use the cost of track damage per train mile (i.e. for every mile travelled by that train).

Using the VTISM outputs, Figure 8 – 16 shows the cost per train mile for each steering type, for a train travelling exclusively over Route 2.

As discussed in section 4.6, the purchase price of a 3 car DMU is £2.62m[6]. The analysis presented in section 4.6 suggested that the lifetime cost of track damage caused by that rail vehicle would be £3.19m. This figure was based on the Network Rail track access charge allocated to that vehicle of 42.6 pence

/vehicle mile[7]. The VTISM analysis calculates a track damage cost of 55 pence/vehicle mile (or £4.12m over the life time of the train)[††]. Based on the same service patterns used in the earlier analysis (250,000 miles per annum, and a service life of 30 years), using the savings calculated by VTISM, the mechanical steering train could save £0.75m in track damage over the lifetime of the train; whilst the active bogie could save £1.45m over the lifetime of a train (roughly half of the purchase price of the conventional vehicle).

Figure 8 - 16 Route 2 comparison of costs per train mile

As stated in section 8.2.3.1, the steering system requires an average of 31.5 kJ/km, increasing the train's energy requirement by 1.5 %. Based on the analysis from section 4.6, this would increase the life time energy cost for this train by £3400; which is a small compared to the considerable saving in track costs.

[††] The track access charge is just a method of dividing up the spending on track maintenance and renewals rather than an attempt to thoroughly investigate the cost per mile of each train. The cost per mile over this very curvy route should be higher than average.

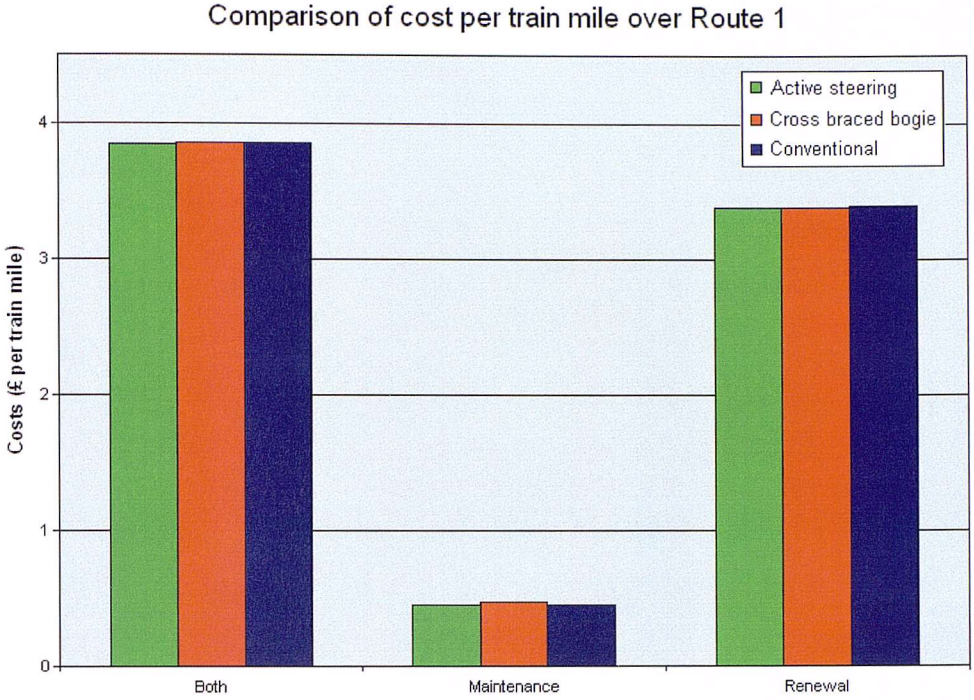

Figure 8 - 17 Route 1 comparison of costs per train mile

Looking at the straighter Route 1, the cost per train mile with conventional bogies is £3.85/train mile. The trains running over Route 2 are lightweight, low speed 3 car DMU's, compared to heavier high speed trains on Route 1 made up of 2 locomotives and 8 carriages. As shown in Figure 8 – 17 (and previously in Figure 8 – 8) there are only small changes around this by introducing steering bogies. The active bogie gives a saving of 2 pence/train mile, or £0.15m over the lifetime of a train[‡‡]; with the mechanical bogie increasing cost by 1 pence/train mile or £0.08m over the lifetime of a train. Compared to the cost of a new high speed intercity train of £31.4m[6], the benefits are very small, and it is unlikely these benefits would outweigh the extra cost of installing these bogies.

8.5 Discussion

On straight sections of track, wear and fatigue occur very slowly compared to other degradation modes such as, ballast settlement and sleeper degradation. Route 1 used in this analysis is a very straight section of mainline, and the benefits of introducing steering bogies to vehicles which operate exclusively on a section of track like this are negligible; the cross braced steering bogie actually

[‡‡] Again assuming 250,000 train miles per annum, and 30 year life cycle

increased wear and fatigue, as it proved to be less stable than the conventional bogie.

However, on the more severely curved Route 2, which is based on a cross country route, wear and fatigue damage make up a significant proportion of the overall cost of track maintenance and renewals. In this case the wear and fatigue made up 40 % of total costs, giving an opportunity for steering bogies to make a significant contribution to reducing the overall cost.

Results from both cost assessment methods give the same ranking of the different steering types on both routes; however, the absolute values given from each method differ dramatically. Both systems are largely empirically based, and an analysis taking into account a closer understanding of the relationship between wheel and rail, as well as the physical process behind wear and fatigue, is required to give more reliable results.

The results do give a significant indication that active steering bogies are capable of giving significant cost saving over routes containing more curves. Using the active bogie over Route 2 the Tunna method predicts a 66 % reduction in tangential damage cost; whereas the VTISM model predicts a 90 % reduction. The cross braced bogie, which would be cheaper to produce and maintain, also appears to show promise, with savings of 28 % and 45 % from the Tunna and VTISM models respectively.

The two routes chosen for this study are at the extremes of the track conditions experienced across the UK network, and no train will realistically operate exclusively on either of these routes. All trains will operate over a curve profile somewhere in between those of these two tracks. Significant cost savings can be achieved at the more severe end of this scale. Each case needs to be looked at individually to assess the costs, depending on the duties required of each train type.

References

1. Ling, D., *VTISM version 2.0 user guide, SA/TSS/17524/R008*. 2007, Serco Assurance.
2. Evans, J., *Whole life rail model application and development for RSSB - dynamic modelling of rolling contact. AEATR-VTI-2003-048*. 2003, AEA Technology.
3. Burstow, M., *Whole Life Rail Model application and development for RSSB - Development of a rolling contact fatigue damage parameter*. 2003, Railway Safety & Standard Board.
4. Tunna, J. and R. Joy, TTCI(UK), Methodology to calculate variable usage charges for control period 4, UK NR report No. 08-002, www.networkrail.co.uk/browse%20documents/StrategicBusinessPlan/Update/TTCI%20(UK)%variablecharges%methodology.pdf, [Accessed, 25/6/08]
5. *GC/RT5021 Track System Requirements*. 2007, Rail Safety and Standards Board.
6. *The Comprehensive Guide to Britain's Railways*. Ninth ed, ed. P. Dunn. 2006, Peterborough: EMAP Active Limited.
7. Office of the Rail Regulator, Track usage price list, http://www.rail-reg.gov.uk/upload/pdf/arev-price_list1_19dec.pdf, [Accessed, 8/8/08]

Chapter 9: Discussion and Conclusions

9.1 Discussion

There are existing published studies looking at the load saving achievable with specific steering bogies over short sections of track or a limited range of curves. For the first time, this thesis has taken a selection of possible steering bogies, assessed the load reduction they can achieve over a range of railway types using a consistent comparison metric, and carried out an analysis of possible reductions in track maintenance and renewals costs.

The results presented in Chapter 7, developed using short representative test routes, showed that steering bogies, particularly the active and cross braced bogies have the potential to reduce tangential track loading across a range of railway types. Unfortunately the hardening spring bogie proved to be unsuccessful; although with some tuning of the design a bogie of this nature may provide some level of loading reduction.

The representative routes made it possible to investigate a wide range of vehicle designs over a variety of different route types. As presented in Chapter 8, results from the short, representative routes correlated well with the outputs from simulations over longer routes (i.e. the two test routes used in Chapter 8, containing track models of 111 and 42 miles long respectively).

The more curvaceous routes tended to show the best loading reductions with steering bogies. However, including track roughness in the analysis can reduce the benefits of the steering bogies. As stated in Chapter 2 the requirements of a bogie for good steering performance and straight line stability are not compatible. Passive types of steering bogie can be used to modify the relationship between steering performance and stability; allowing for reductions in steering loads with some trade off in stability (though improved compared to a low stiffness conventional bogie). However, the use of active systems can isolate the curving performance and stability by filtering the active system to

only respond to low frequency curving loads whilst leaving a conventional parallel suspension to maintain stability through track roughness.

The majority of contemporary research into active steering bogies suggest using a feedback control system based on the position of wheelsets relative to the track. This can not be measured directly, so position data needs to be calculated based on accelerometer measurements taken at the axle box. The method of controlling active steering bogies through the use of force feedback* suggested in this thesis has proven to be a successful control strategy. It should be easier to implement, cope better with changes in wheel-rail adhesion, require fewer sensors and be more robust than the alternative position based systems. This system can be implemented with no requirement for the controller to contain a route map, or any wayside beacons; meaning a train with this type of active bogie could travel anywhere on the network with no additional preparation work.

The Chapter 8 results were based on vehicle-track interaction models, using longer sections of measured track geometry. The routes chosen were at the extremes of the four representative routes analysed in Chapter 7. Unfortunately, using the standard industry costing model VTISM, it is only possible to carry out cost analysis for sections of measured track, rather than short representative routes; this may be something worth adding into the software in future, to allow users to quickly carry out a high level comparison of various options. Track sections were chosen with curvature characteristics at the extremes of the UK network, in order to cover the whole range of possible conditions. Results from a very straight section of mainline (Route 1 in Chapter 8) showed benefits of introducing steering bogies for lines of this type would be virtually zero. While results from the cross country route showed the cross braced and active bogies could reduce the cost of tangential damage by 46% and 90% respectively.

* measuring the applied yaw torque acting on each wheelset because of wheel-rail creep loading and attempting to cancel that out with an opposing applied steering torque

9.2 How can this research be applied?

This work has shown the scope of the savings in track maintenance and renewals cost that can be achieved through the use of steering bogies.

As discussed in Section 4.4, the cost of 'rail surface damage', i.e. wear and fatigue, costs the railways in the order of £100 million per annum. This is small compared to the £9 billion per annum which is suggested to be the total operational cost of the railways (as described in section 4.1.1). The introduction of steering bogies in order to reduce tangential load, and consequently wear and fatigue damage rates, cannot on its own create a step change in the economic performance of the rail system. However, any contribution towards improving the efficiency of the railways is helpful to the overall system. When viewed as a proportion of the traffic dependent track damage, rail surface damage is 40 % of the total. In this frame of reference, steering bogies can make a big contribution towards reducing costs. Savings will vary depending on the routes a particular type of train needs to travel on. In some cases, such as the cross country route used in Chapter 8, the cost savings appear to be considerable. As stated in section 8.4, a conventional 3 car DMU costs £2.62m; simulation results suggest the active bogie could save £1.45m in track damage over the lifetime of that train, and the mechanical bogie £0.75m (if that train operates exclusively on the route in question). The practicalities of implementing the two steering types and how they might affect the achievable cost reductions needs to be investigated further. The cost of manufacturing and maintaining steering bogies needs to be assessed, as does the achievable reductions in wheel wear and fatigue, to give a full cost assessment.

Presuming these further costing comparisons still suggest significant savings can still be achieved, the next step would be to begin some physical testing of the two steering types.

For a railways system that is not vertically integrated[†], which is now common in Europe, it can be difficult to encourage separate private companies to modify

[†] i.e. track and trains are owned and operated by separate companies

their assets to cause less damage to the assets of (and hence save money for) a separate private company. A clear method needs to be defined in order to share out any cost savings appropriately. In the UK the track access charge could be used to incentivise train operators and manufacturers to use and produce trains which cause lower tangential loading. This has already been suggested by Tunna, as discussed in section 5.5.3.1. If this method of including tangential load in the costing scheme is taken on board, it may well encourage a further interest in steering bogies.

9.3 Further work

As suggested in the previous section, further work needs to be carried out looking at the practical design of the steering bogies suggested; however there are also a range of other possible options for reducing tangential rail loading. There are other types of steering bogie not included in this analysis, including those mentioned in Chapter 6; as well as the steer**ed** bogies mentioned in section 6.4.1.

Further to this, some yaw control of the inter-car connections could well be a good method of reducing tangential wheel loading, by improving tangential alignment of the car bodies, as already briefly mentioned in section 7.3.2. This would however, not help loading at the front bogie of a train, which is generally assumed to cause the highest track loading.

Simpler bogie modifications may also achieve small reductions in tangential loading with minimal implementation costs. A form of variable primary yaw stiffness, as opposed to actively controlled steering, may prove a suitable option. i.e. Using a low yaw stiffness bogie that can travel through curves with minimal loading, but with an addition stiffness element that can be switch in, between axles and bogie on straight sections (or above a certain speed). NB This would not have the same isolating effect of improving curving without impairing stability, as the active bogie investigated in this thesis does.

Other than these alternative methods of reducing tangential loading, the costing tools also need to be improved. The VTISM software used as part of this study has proved to be a very useful method of comparing the different steering types. However, it has its limitations as discussed briefly in section 8.2.4, and costing outputs were considerably different to outputs from the Tunna model. Work needs to be carried out to include (or at least assess the effects of) all wheel-rail forces which make up the loading environment. Grinding really needs to be explicitly included in the maintenance planning to give a more representative picture of how RCF is managed. In parallel with this, an RCF damage model, which has a more theoretically sound base, may prove to be useful.

9.4 Conclusion

Railway systems are expensive to build and operate. There are a variety of opportunities to improve the efficiency and effectiveness of how they are run, particularly through improvement of the system interfaces.

Can the whole life cost of railway track be reduced through the effective management of tangential wheel-rail loading? The use of steering bogies can reducing tangential wheel-rail loading; however the level of loading reduction, and savings in track maintenance and renewals depend on the route characterises each train is operated on. Used in an appropriate fashion steering bogies can make a contribution to reducing costs, and moving towards a more economically sustainable railway.

APPENDIX A:– Hertzian contact area, F_1 constant

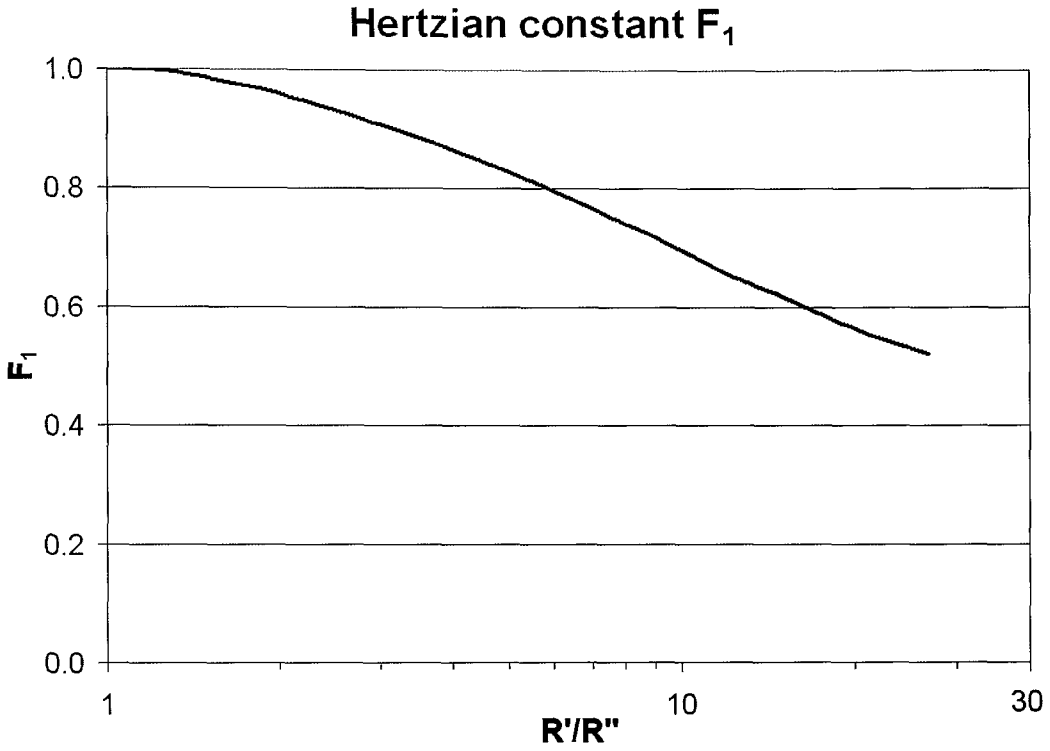

Figure A-1 F_1 constant used for Hertzian contact area calculation[1]

1. Johnson, K.L., *Contact Mechanics*. 1985: Cambridge University Press.

APPENDIX B: Change in wheel rail contact shape due to lateral displacement of the wheelset

Numbers in the centre column show displacement of the left contact patch (top), and right contact patch (bottom), movement to the left is taken as positive.

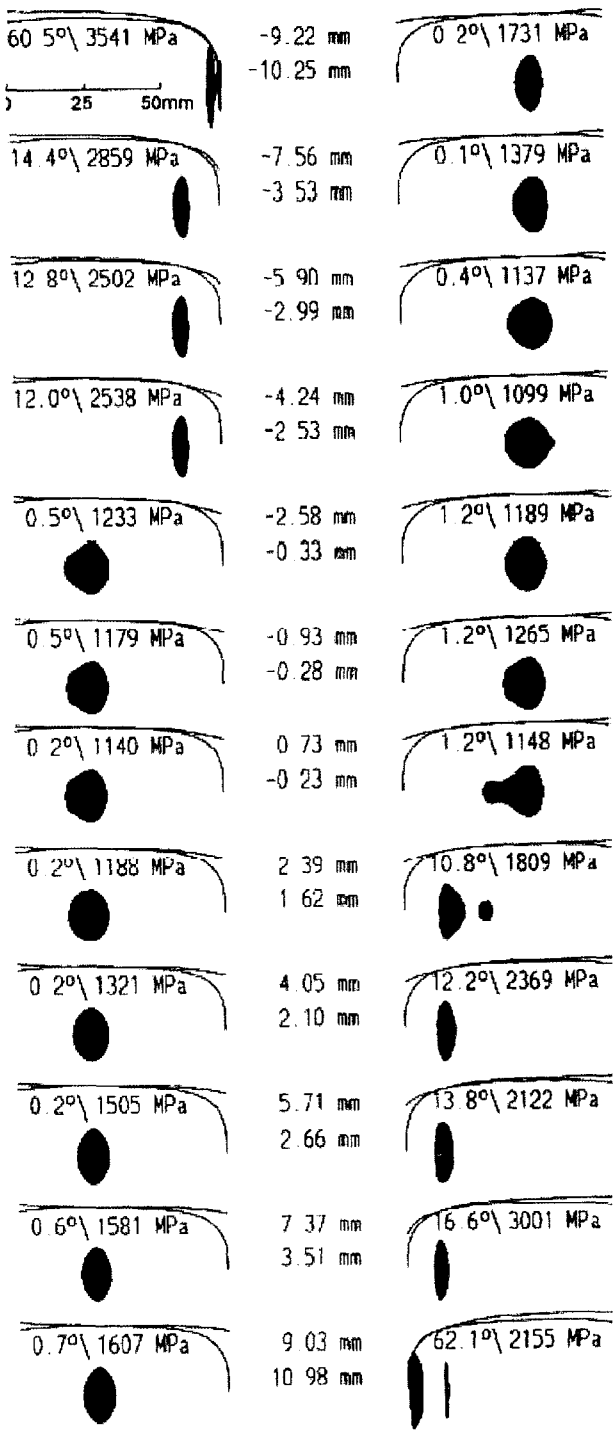

Figure B – 1 Variation in contact patch shape and size due to lateral displacement of the wheelset[1]

1. Knothe, K., *History of wheel/rail contact mechanics: from Redtenbacher to Kalker.* Vehicle System Dynamics, 2008. **46**(1): p. 9 - 26.

APPENDIX C: Derivation of Tunna costing equation

Tunna shows the derivation of his costing equation in Appendix B of his report, 'Methods to calculate variable usage charges of control period 4'[1]

The annual cost of tangential damage for a mile of track will be the grinding cost plus the annualised renewal cost:

$$\frac{Cost}{Year} = \frac{GrindingCycles}{Year} \times GrindingCost + \frac{\mathrm{Re}newalCost}{RailLife} \qquad \textbf{(eqn C.1)}$$

Using the wear index (WI) and RCF index (RI) calculated, based on Tγ using the WLRM, assuming grinding is triggered when RI = I:

$$\frac{GrindingCycles}{Year} = \frac{RI}{axle} \times \frac{axles}{year} \qquad \textbf{(eqn C.2)}$$

Assuming rail is replaced, when it reaches a certain wear limit:

$$RailLife = \frac{WearLimit}{Wear/Year} = \frac{WearLimit}{Wear/axle \times axles/Year} \qquad \textbf{(eqn C.3)}$$

$$\frac{Cost}{Year} = \frac{Cost}{axle} \times \frac{axles}{Year} \qquad \textbf{(eqn C.4)}$$

Substituting Equations 2,3 and 4, into equation 1 gives:

$$\frac{Cost}{axle} = \frac{RI}{axle} \times GrindingCost + \frac{Wear}{axle} \times \frac{\mathrm{Re}newalCost}{WearLimit} \qquad \textbf{(eqn C.5)}$$

$$\frac{Wear}{axle} = \frac{DepthGround}{axle} + \frac{DepthWorn}{axle} \qquad \textbf{(eqn C.6)}$$

Where:

$$\frac{DepthGround}{axle} = \frac{DepthGround}{GrindingCycle} \times \frac{GrindingCycles}{Axle}$$

$$= \frac{DepthGround}{GrindingCycle} \times \frac{RI}{axle} \qquad \textbf{(eqn C.7)}$$

For $15 < T\gamma \leq 175$

$$\frac{\text{DepthWorn}}{\text{DepthGround}} = \frac{WI}{RI} \qquad \textbf{(eqn C.8)}$$

Thus:

$$\frac{DepthWorn}{Axle} = \frac{WI}{RI} \times \frac{DepthGround}{axle}$$

$$= \frac{DepthGround}{GrindingCycle} \times \frac{WI}{axle} \qquad \textbf{(eqn C.9)}$$

Substituting Equations 6, 7 and 9 into 5, gives:

For $15 < T\gamma \leq 175$

$$\frac{Cost}{axle} = \frac{RI}{axle} \times GrindingCost + \frac{DepthGround}{GrindingCycle} \times \left(\frac{RI}{axle} + \frac{WI}{axle} \right) \times \frac{\text{Re}newalCost}{WearLimit} \qquad \textbf{(eqn C.10)}$$

So:

$$Cost = RI \times GrindingCost + \frac{DepthGround}{GrindingCycle} \times (RI + WI) \times \frac{\text{Re}newalCost}{WearLimit} \qquad \textbf{(eqn C.11)}$$

For $T\gamma > 175$

$$\frac{DepthWorn}{axle} = \frac{DepthGround}{GrindingCycle} \times \frac{WI}{axle} \qquad \textbf{(eqn C.12)}$$

Substituting Equation 6 and 12 into Equation 1, gives:

$$\frac{Cost}{axle} = \frac{DepthGround}{GrindingCycle} \times \frac{WI}{axle} \times \frac{\text{Re}newalCost}{WearLimit} \qquad \textbf{(eqn C.13)}$$

So:

$$Cost = \frac{DepthGround}{GrindingCycle} \times WearDamage \times \frac{\text{Re}newalCost}{WearLimit} \qquad \textbf{(eqn C.14)}$$

Using the values:

Grinding Cost = £2,000/km

Renewal Cost = £250,000/km

Depth Ground/Grinding Cycle = 0.5 mm

Wear Limit = 10 mm

The following equations can be used to give a cost per track km:

For $15 < T\gamma \leq 175$

$$\text{Cost} = 14500 \times \text{RI} + 12500 \times \text{WI} \qquad \textbf{(eqn C.15)}$$

And for $T\gamma > 175$

$$\text{Cost} = 12500 \times \text{WI} \qquad \textbf{(eqn C.16)}$$

1. Tunna, J. and R. Joy, TTCI(UK), Methodology to calculate variable usage charges for control period 4, UK NR report No. 08-002, www.networkrail.co.uk/browse%20documents/StrategicBusinessPlan/Update/TTCI%20(UK)%variablecharges%methodology.pdf, [Accessed, 25/6/08]

APPENDIX D: Allowable vertical and lateral standard deviations in the rail head, depending on line speed

As presented in Railway Group Standard GC/RT5021[1], the allowable standard deviations in track geometry depending on line speed as shown in the table below

Speed (mph)	Vertical profile standard deviation (mm)			Lateral alignment standard deviation (mm)		
	35 m filter		70 m filter	35 m filter		70 m filter
	Maximum (eighth mile)	Very poor (eighth mile)	Very poor (quarter mile)	Maximum (eighth mile)	Very poor (eighth mile)	Very poor (quarter mile)
10-20	8.3	N/A	N/A	9.3	5.6	N/A
25-30	7.7	N/A	N/A	8.6	5.2	N/A
35-40	7.2	N/A	N/A	7.9	4.7	N/A
45-50	6.7	N/A	N/A	7.3	4.5	N/A
55-60	6.3	N/A	N/A	7.0	4.2	N/A
65-70	6.0	5.4	N/A	6.7	3.6	N/A
75-80	5.7	4.8	6.3*	6.3	3.1	5.7*
85-95	5.3	4.0	5.6	6.0	2.7	5.0
100-110	5.0	3.4	5.0	5.7	2.3	4.3
115-125	4.7	3.0	4.4	5.0	2.0	3.7
130-140	4.4	2.6	3.8	4.7	1.8	3.1

1. *GC/RT5021 Track System Requirements*. 2007, Rail Safety and Standards Board.

APPENDIX E: Full graphical results for representative vehicles

E.1 Design case tracks

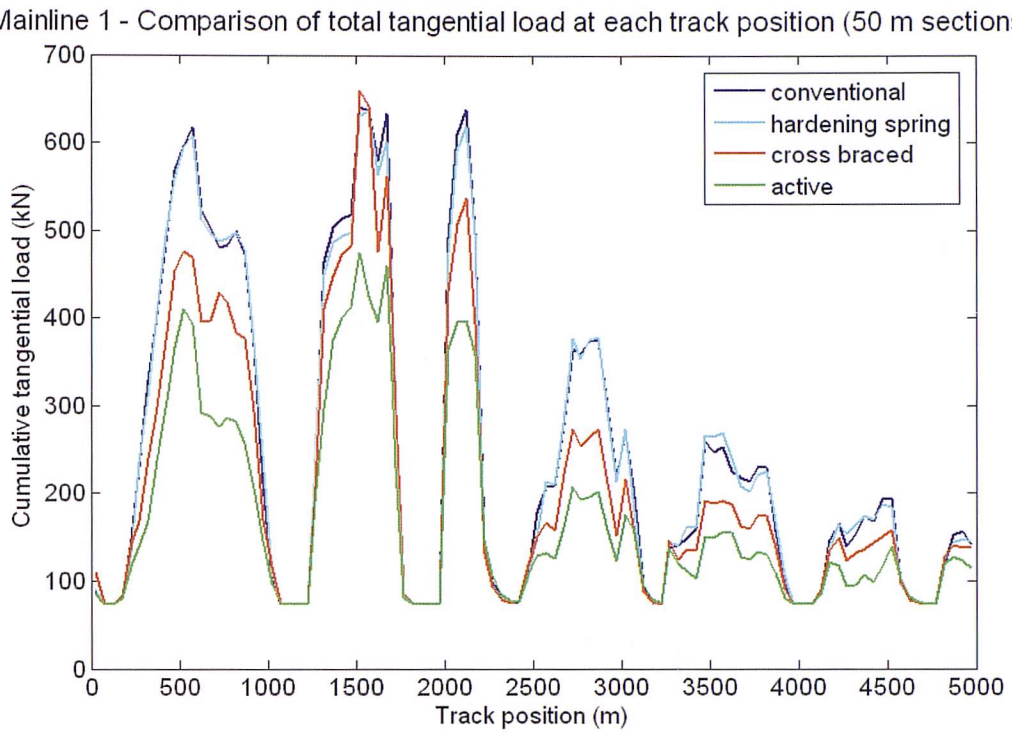

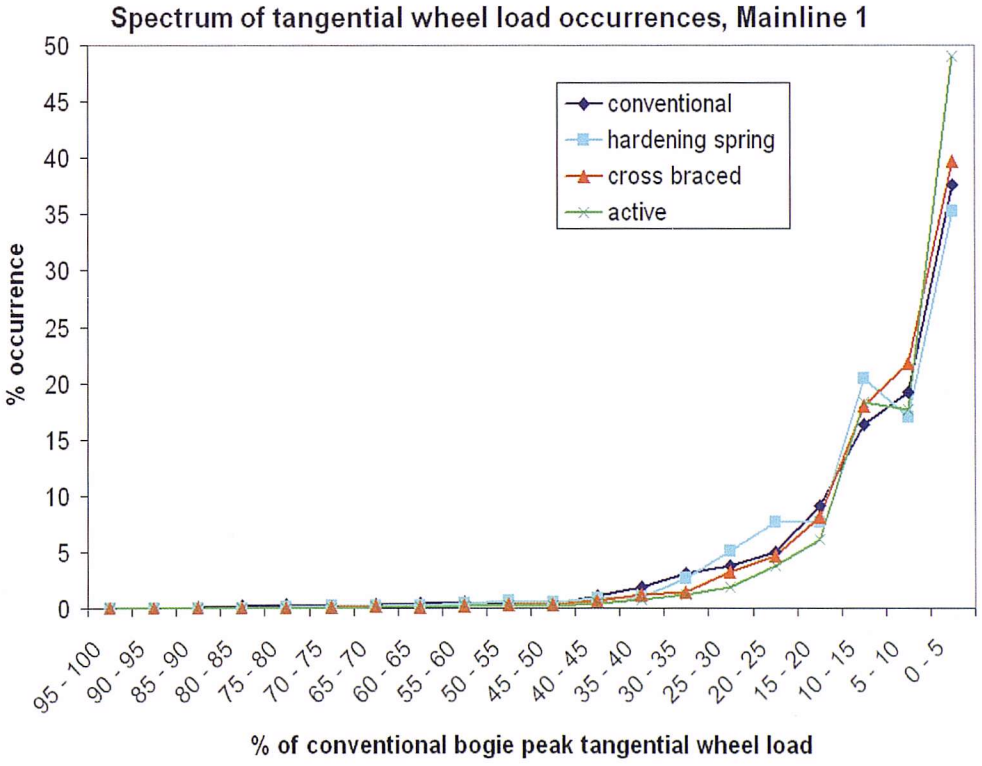

Mainline 2 - Comparison of total tangential load at each track position (50 m sections)

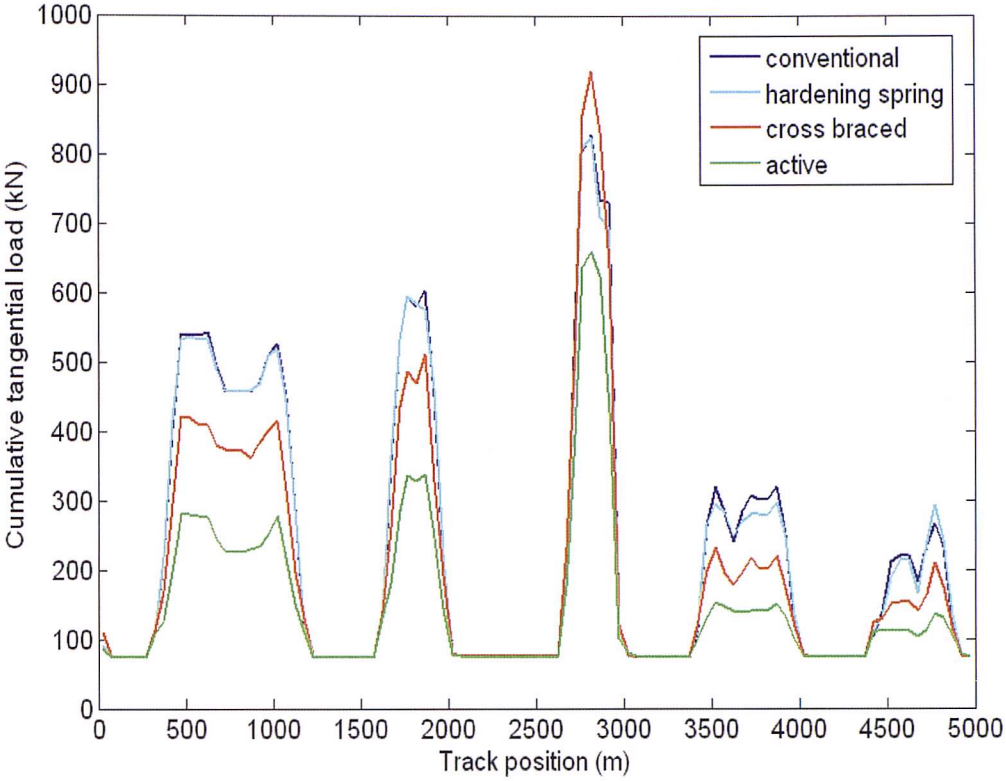

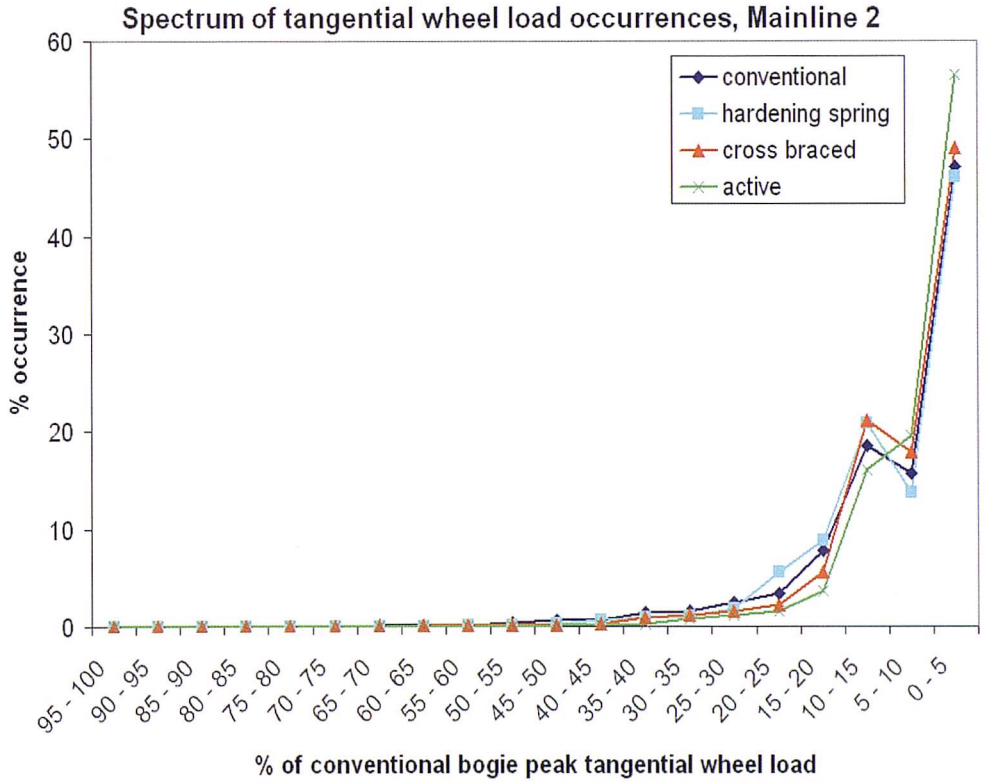

Cross country 1 - Comparison of total tangential load at each track position (50 m sections)

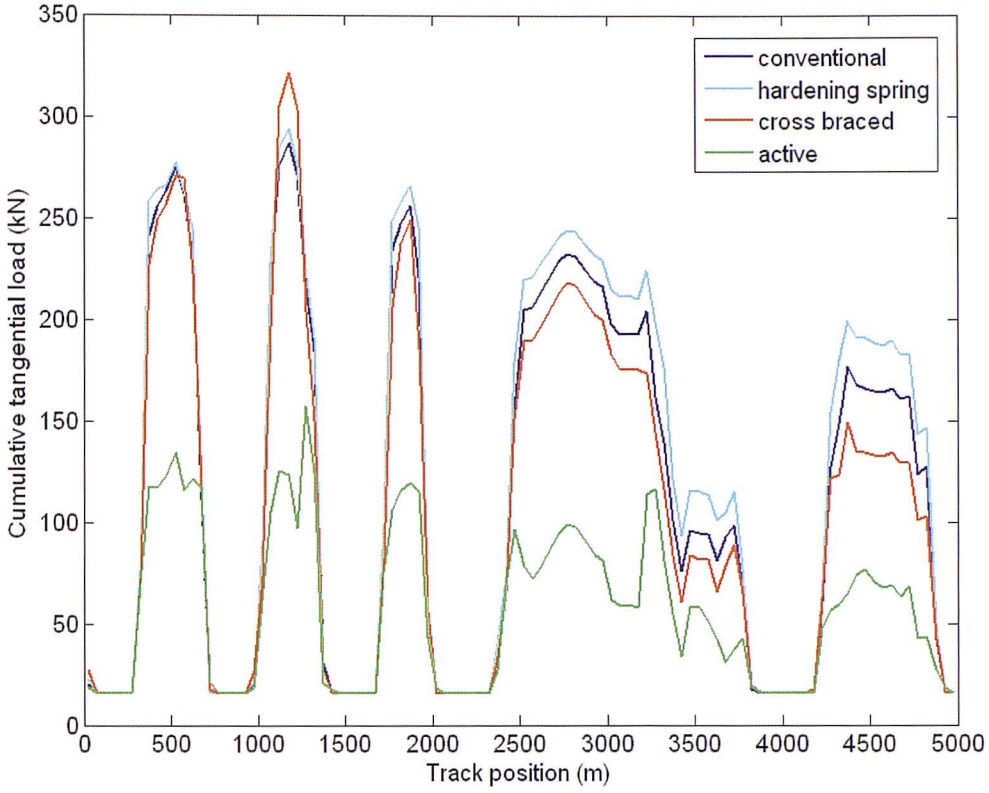

Spectrum of tangential wheel load occurrences, Cross country 1

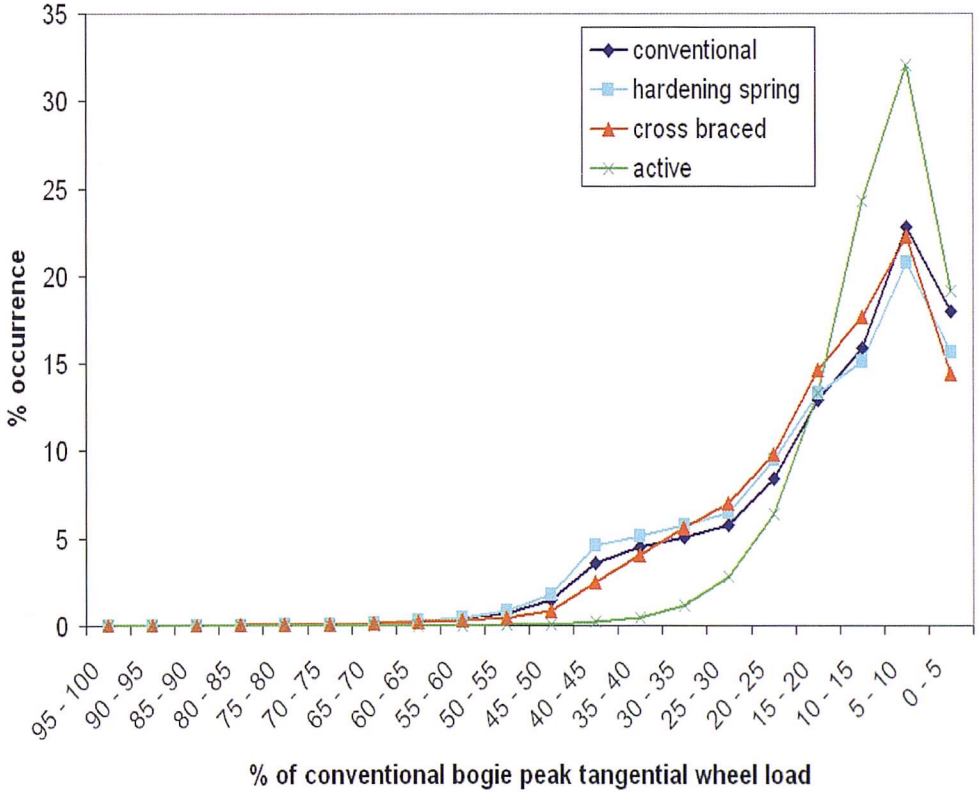

Metro 1 - Comparison of total tangential load at each track position (50 m sections)

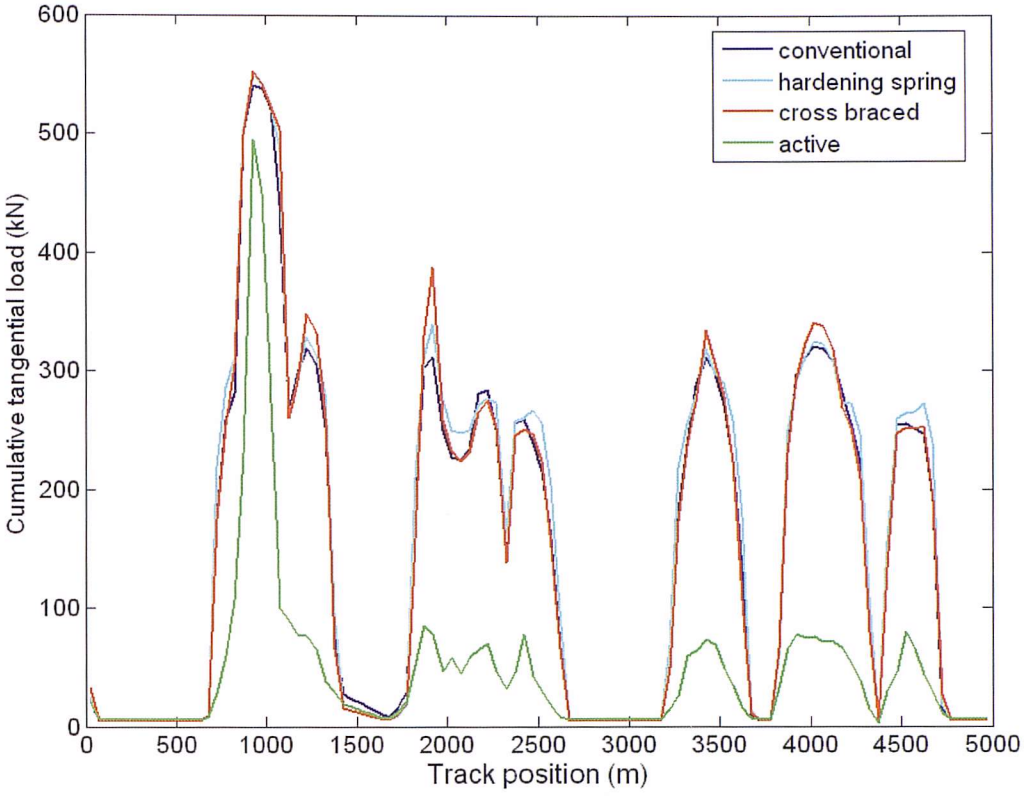

Spectrum of tangential wheel load occurrences, Metro 1

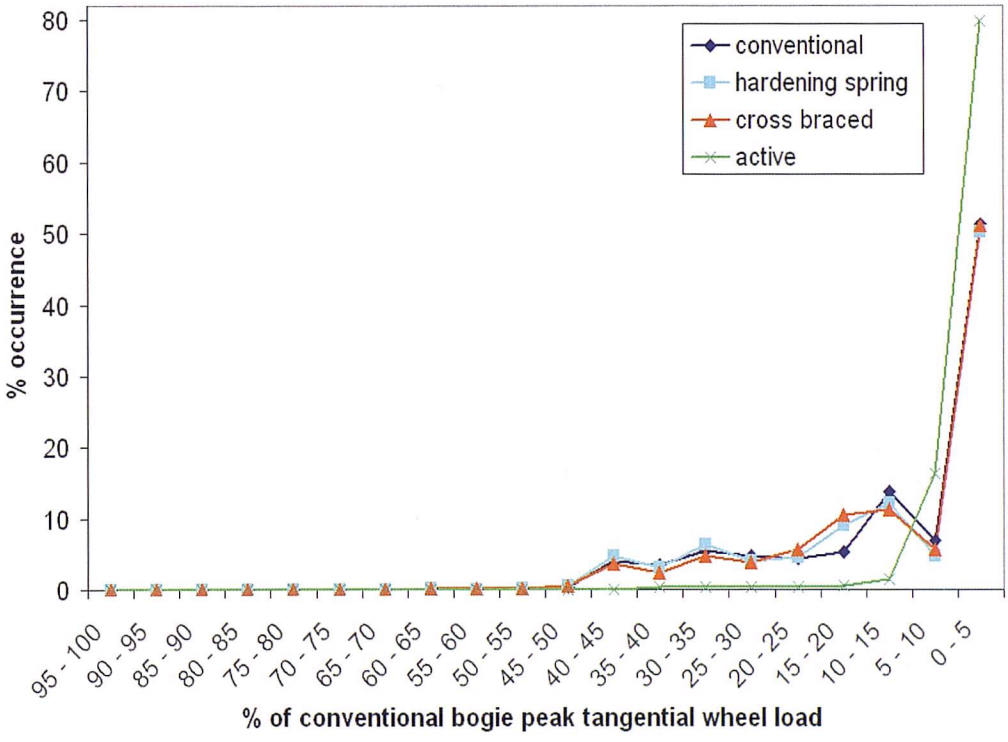

E.2 Rough track

Mainline 1 - Comparison of total tangential load at each track position (50 m sections)

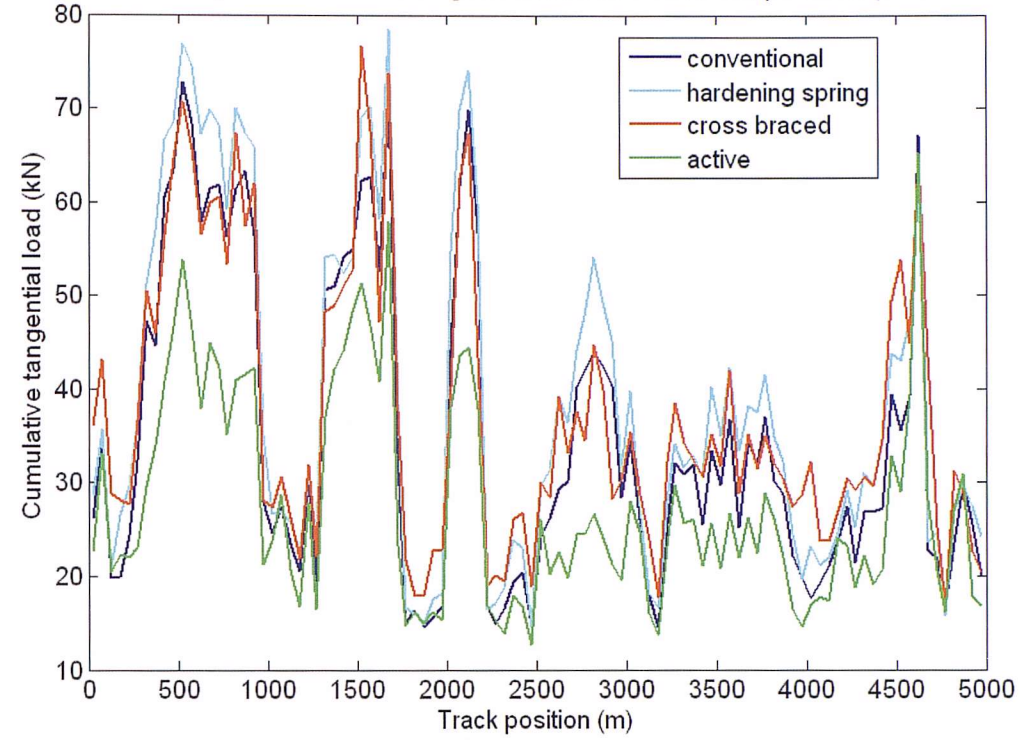

Spectrum of tangential wheel load occurrences, Mainline 1

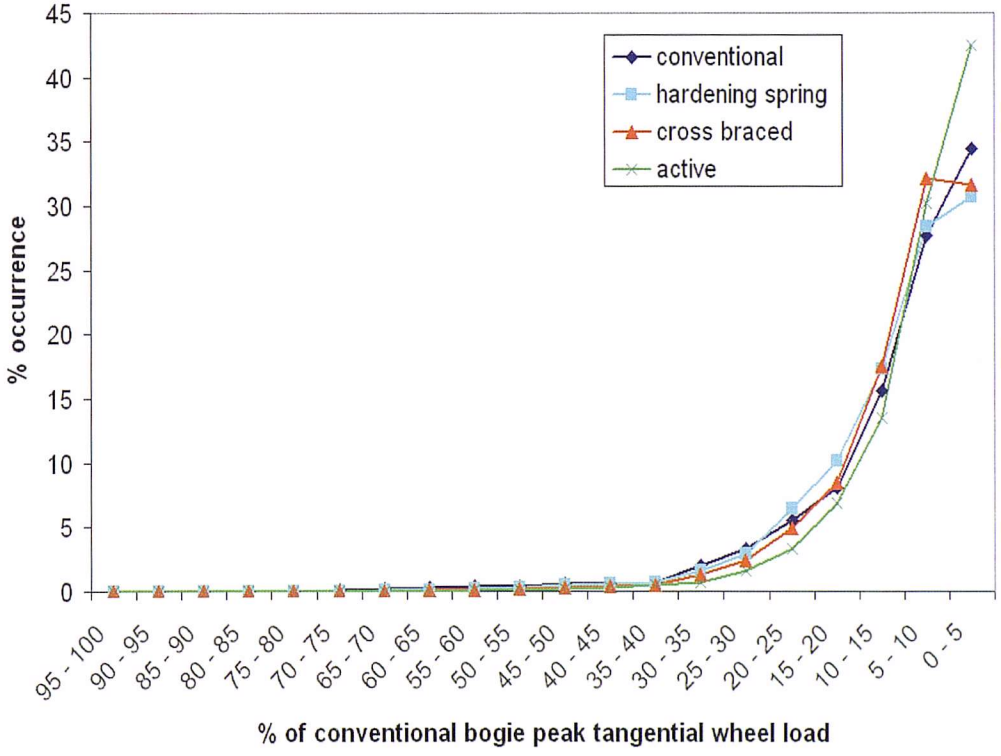

Mainline 2 - Comparison of total tangential load at each track position (50 m sections)

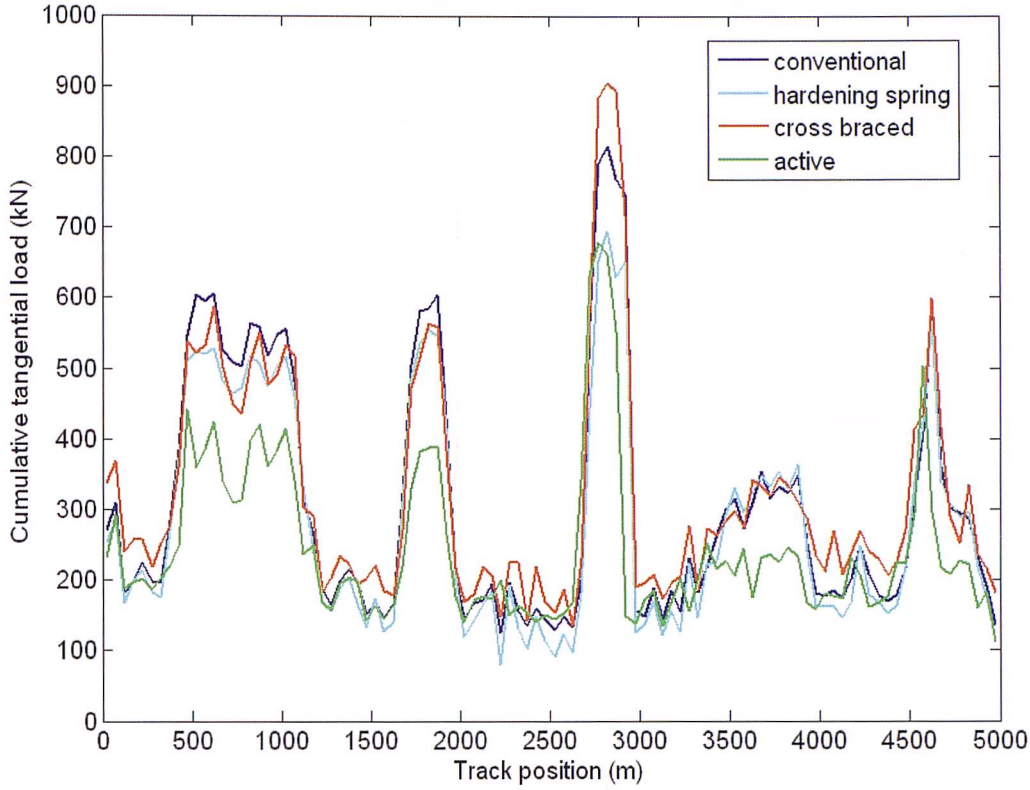

Spectrum of tangential wheel load occurrences, Mainline 2

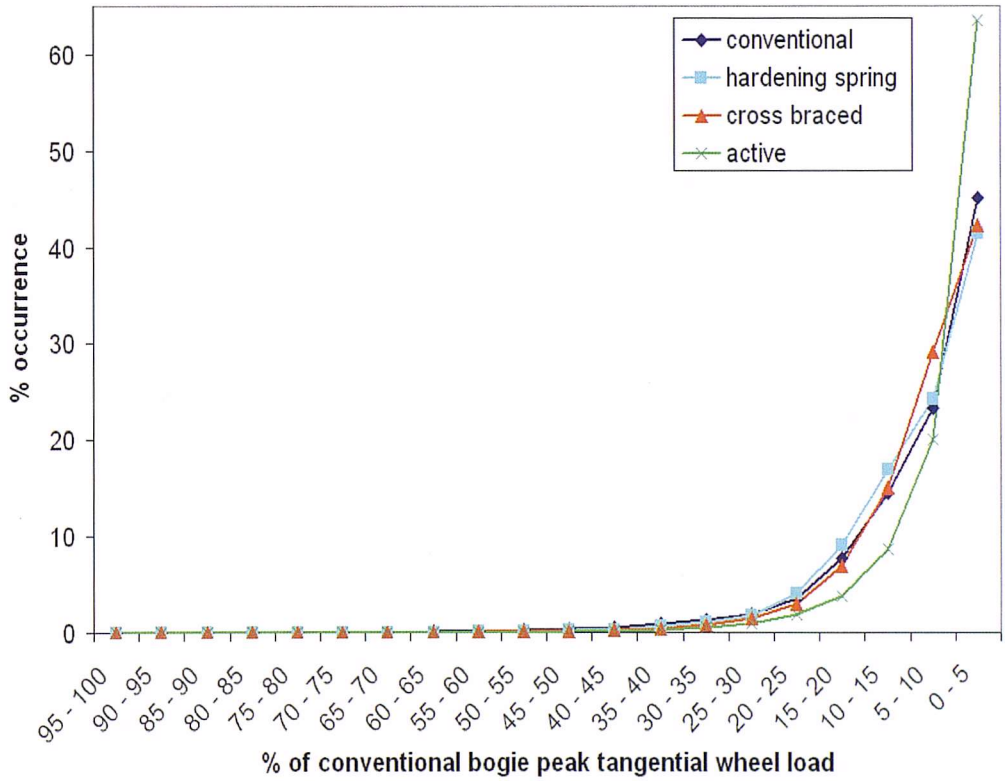

Cross country 1 - Comparison of total tangential load at each track position (50 m sections)

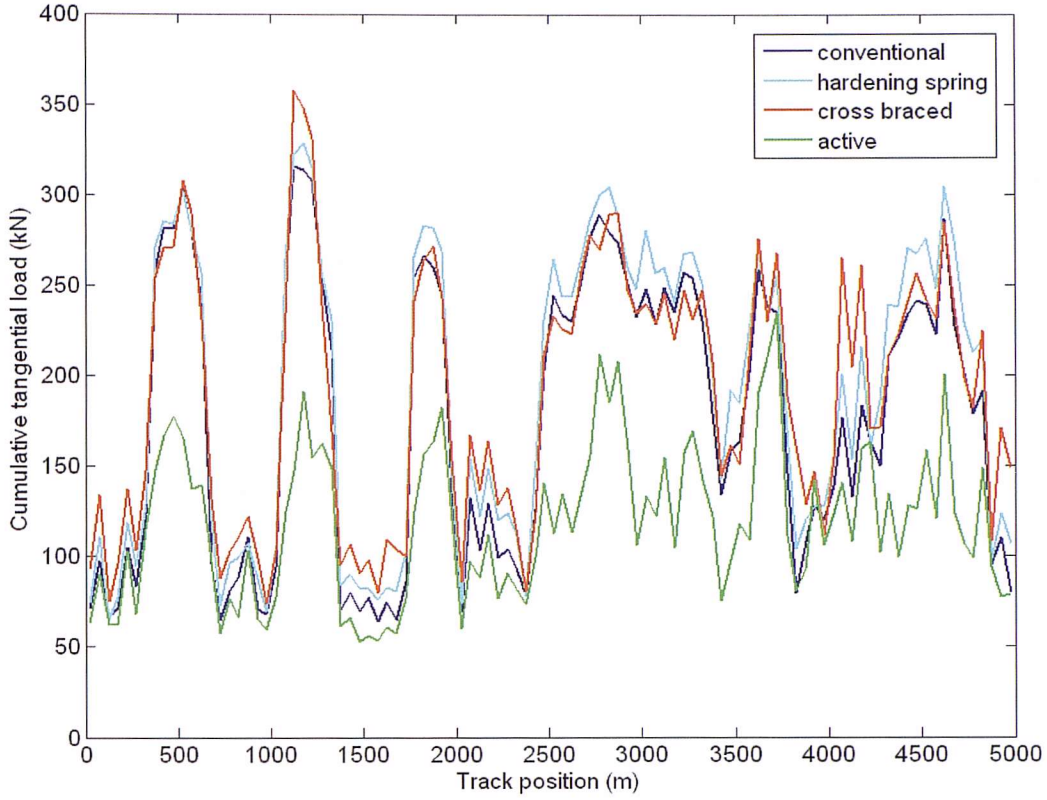

Spectrum of tangential wheel load occurrences, Cross country 1

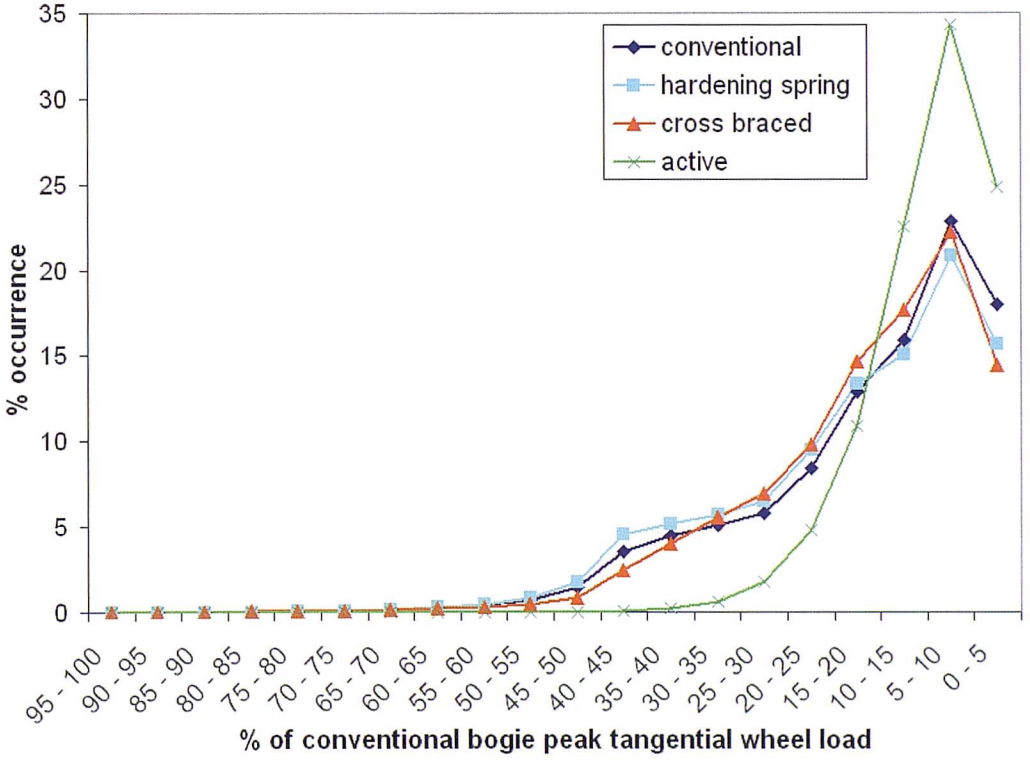

Metro 1 - Comparison of total tangential load at each track position (50 m sections)

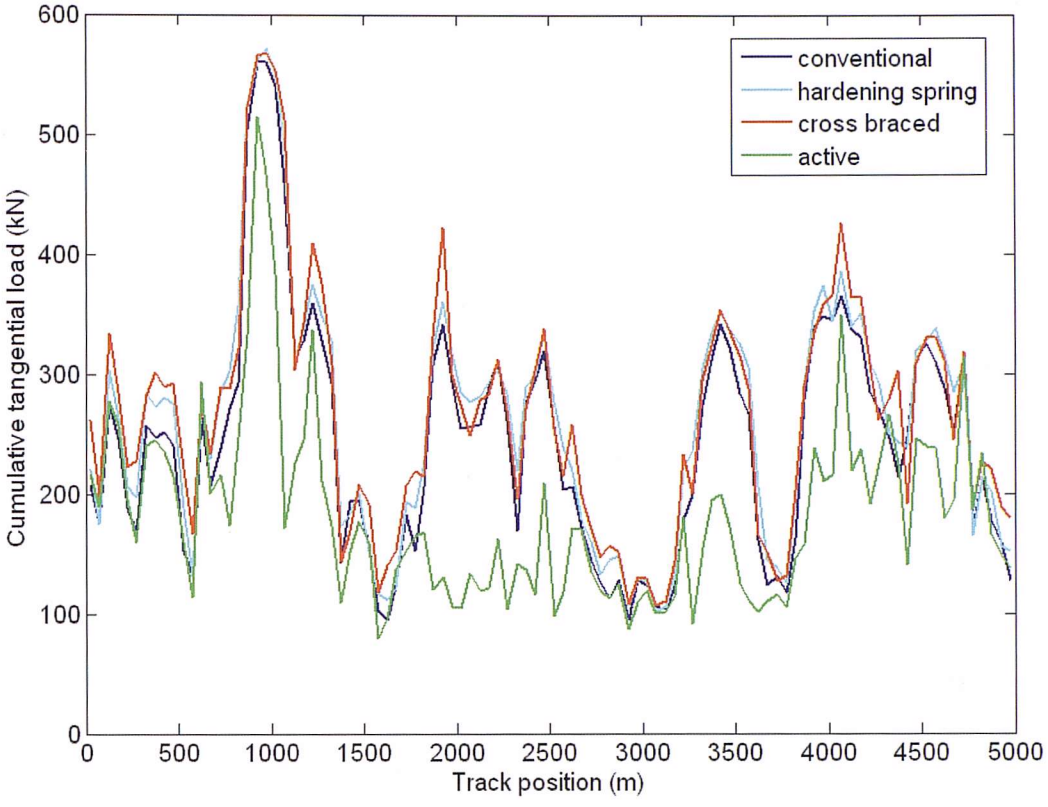

Spectrum of tangential wheel load occurrences, Metro 1